DRY POWDER INHALATION OF PNEUMOCOCCAL VACCINE USING POLYMERIC NANOPARTICLES AS CARRIERS

NITESH KUMAR KUNDA

Thesis submitted in partial fulfillment of the requirements of Liverpool John Moores University for the degree of Doctor of Philosophy

November 2014

Acknowledgements

I would like to thank my supervisor Dr Imran Saleem for giving me the opportunity to work on this project in his lab. He has given me constant support, guidance, motivation and encouragement throughout my PhD. I am very grateful to him for his continuous supervision during the PhD and writing this thesis. In addition, I would also like to thank my co-supervisors Dr Gillian Hutcheon and Professor Stephen Gordon (Liverpool School of Tropical Medicine) for their suggestions and feedback during my PhD. Further, I would like to express gratitude to Dr Satyanarayana Somavarapu (School of Pharmacy, University College London) for his recommendations during my PhD that helped in a great way.

I am thankful to Dr Eliane Miyaji and Dr Vivianne Goncalves (Instituto Butantan, Brazil) for providing us the pneumococcal surface protein A and guiding me with the molecular biology techniques involved in the project. I am also grateful to Dr Sarah Rachel-Dennison (University of Central Lancashire) for performing and analysing the circular dichrosim experiments. I would also like to thank University of Liverpool and University of Central Lancashire for letting me use the ultracentrifuge. I am thankful to all the technicians in School of Pharmacy and Biomolecular Sciences (PBS, LJMU) especially Dr Nicola Dempster and Dr Cheryl Waring for their support in conducting some crucial experiments. I would also like to acknowledge the staff in Formulation and Drug Delivery Research Group for sharing their knowledge with me. I would like to thank Dr Daniela Ferriera from Liverpool School of Tropical Medicine for her valuable suggestions during the PhD.

I thank all my lab colleagues especially Iman Al-fagih for their support and care. I would also like to thank all my friends for their love and support. I am very grateful to my parents and brother for their unconditional love, support, motivation and encouragement in successfully completing my project and achieving my goal.

Table of Contents

List of Tables

List of Figures

List of Schemes

List of Abbreviations

Ab	Antibody
ACN	Acetonitrile
Adr	O-acetyl transferase
Ag	Antigen
ALRI	Acute Lower Respiratory Infections
AM	Alveolar Macrophage
ANOVA	Analysis of Variance
APC	Antigen Presenting Cell
ATCC	American Type Culture Collection
BAL	Bronchoalveolar Lavage
BCA	Bicinchoninic Acid
BCG	Bacillus Calmette-Guérin
BgaA	b-Glucosidase
BSA	Bovine Serum Albumin
CAP	Community-Acquired Pneumonia
CbpA	Choline-Binding Protein A
CBP	Choline-Binding Protein
CD	Circular Dichroism
CD4	Cluster of Differentiation 4
CD8	Cluster of Differentiation 8
C_e	Concentration in Equilibrium
CLSM	Confocal Laser Scanning Microscopy
cm	centimetre
CP	Cryoprotectant
CTL	Cytotoxic T-lymphocytes
d_{ae}	Aerodynamic Diameter
DCM	Dichloromethane
DC	Dendritic Cell
d_g	Geometric Diameter
DMAB	Didodecyldimethylammonium Bromide
DMPC	Dimyristoyl Phosphatyl-Choline
DMSO	Dimethyl Sulfoxide

DNA	Deoxyribonucleic Acid
DoE	Design of Experiment
DOTAP	Dioleoyltrimethylammoniumpropane
DPIs	Dry Powder Inhalers
DSC	Differential Scanning Calorimeter
ELISA	Enzyme-Linked Immunosorbent Assay
ER	Endoplasmic Reticulum
EU	Endotoxin Units
FCS	Foetal Calf Serum
FD	Freeze-Drying
FITC-BSA	Fluorescein Isothyocyanate-Bovine Serum Albumin
FM	Freundlich Model
FMDV	Foot and Mouth Disease Virus
FPD	Fine Particle Dose
FPF	Fine Particle Fraction
FPM	Fine Particle Mass
FT-IR	Fourier Transform Infrared Spectroscopy
g	gram
GM-CSF	Granulocyte Macrophage Colony-Stimulating Factor
GPC	Gel Permeation Chromatography
GUS	β-Glucuronidase-Enzyme
h	hour
HA	Hemagglutinin
HAP	Hospital Acquired Pneumonia
HBsAg	Hepatitis B Surface Antigen
HLA	Human Leukocyte Antigen
HPLC	High Performance Liquid Chromatography
HPMC	Hydroxypropyl Methylcellulose
ICH	International Conference on Harmonisation
IFN	Interferon
IgA	Immunoglobulin A
IgG	Immunoglobulin G
IL	Interleukin

IPD	Invasive Pneumococcal Diseases
kDa	kilo daltons
K_F	Freundlich Constant
kg	kilogram
K_L	Langmuir Constant
l	litre
L-leu	L-Leucine
LM	Langmuir Model
LMICs	Low and Middle Income Countries
LN	Lymph Node
LOD	Limit of Detection
LOQ	Limit of Quantification
LPS	Lipopolysaccharide
LPXTG	Leu-Pro-X-Thr-Gly
LTA	Lipoteichoic Acid
Mbar	Megabar
mDC	Myeloid Dendritic Cell
MDI	Metered Dose Inhaler
mg	milligram
MHC	Major Histocompatibility Complex
min	minute
mm	millimetre
mM	millimolar
MMAD	Mass Median Aerodynamic Diameter
mmol	millimole
MP	Microparticle
Mtb	*Mycobacterium tuberculosis*
MTT	3-4,5-Dimethylthiazol-2-yl-2,5-Diphenyl Tetrazolium Bromide
mV	millivolt
MW	Molecular Weight
Nan	Neuraminidase
NCMP	Nanocomposite Microparticle
NCSP	Non-Classical Surface Protein

NGI	nanogram
NGI	Next Generation Impactor
NIH	National Institutes of Health
nm	nanometre
NPA	4-Nitrophenyl Acetate Esterase Substrate
NP	Nanoparticle
NR	Nile Red
ρ	Mass Density of the Particle
ρ_a	Unit Density
PAFr	Platelet-Activating Factor Receptor
PBS	Phosphate Buffered Saline
PBS-T	Phosphate Buffered Saline-0.5% Tween 20
PCho	Phosphorylcholine
PCM	Peptide Cross-linked Micelle
PCV	Pneumococcal Conjugate Vaccine
pDC	Plasmacytoid Dendritic Cell
PdgA	N-Acetylglucosamine-deacetylase A
PDI	Poly Dispersity Index
PEG	polyethylene glycol
PEI	Polyethyleneimine
PGA-co-PDL	Polyglycerol Adipate-co-ω-Pentadecalactone
pI	Isoelectric Point
PiaA	Pneumococcal Iron Acquisition A
PLA	Poly-L-Lactic Acid
PLGA	Poly Lactic-co-Glycolic-Acid
Ply	Pneumolysin
pNPP	Alkaline Phosphatase Yellow Liquid Substrate Buffer
PPV	Pneumococcal Polysaccharide Vaccine
PsaA	Pneumococcal Surface Antigen A
PspA	Pneumococcal Surface Protein A
PspC	Pneumococcal Surface Protein C
PVA	Polyvinyl Alcohol
Q_e	Amount of Protein Adsorbed

Q_m	Maximum Adsorption Capacity
rHBsAg	Recombinant Hepatitis B Surface Antigen
RPM	Revolutions per Minute
RPMI	Roswell Park Memorial Institute
RSD	Relative Standard Deviation
s	second
S/N	Signal-to-Noise Ratio
SD	Spray-Drying
SD	Standard Deviation
SDS-PAGE	Sodium Dodecyl Sulfate-Polyacrylamide Gel Electrophoresis
SEM	Scanning Electron Microscopy
SFD	Spray-Freeze-Drying
sIgA	Secretory Imuunoglobulin A
siRNA	Small Interfering RNA
SrtH	b-N-Glucosaminidase
TA	Teichoic Acid
TEM	Transmission Electron Microscopy
TFA	Tri-fluoroacetic Acid
T_g	Glass Transition Temperature
TGA	Thermo Gravimetric Analysis
Th1	T helper cell 1
Th2	T helper cell 2
THF	Tetrahydrofuran
T_m	Metling Point Temperature
TNF	Tumor Necrosis Factor
µg	microgram
µl	microlitre
µm	micrometre
w/v	weight/volume
w/w	weight/weight
WGA	Wheat Germ Agglutinin
α-MEM	Alpha Minimum Essential Medium
^{1}H-NMR	Proton Nuclear Magnetic Resonance

Abstract

Streptococcus pneumoniae is the leading bacterial cause of pneumococcal diseases, of which pneumonia is the main cause of death amongst the immunocompromised, elderly over the age of 50 and children under the age of 5. Although vaccines such as pneumococcal polysaccharide vaccine 23, pneumococcal conjugate vaccine 7, 10 and 13 are available, they are expensive to produce and distribute. Moreover, the variation in serotype distribution across geographical locations and rise in dominance of disease due to non-vaccine serotype coverage has led to significant attention towards the development of alternate vaccine candidates such as pneumococcal surface protein A (PspA). A potential dry powder vaccine formulation containing polymeric nanoparticles (NPs) adsorbed with PspA4Pro and formulated into nanocomposite microparticles (NCMPs) using L-leucine (L-leu) to be delivered via inhalation was developed.

Poly(glycerol adipate-co-ω-pentadecalactone), PGA-co-PDL, NPs with either anionic or cationic surface charge of optimum size (~200-250 nm) to be effectively taken up by the lung dendritic cells (DCs) were successfully produced. The NPs were then surface adsorbed with PspA4Pro (~20 µg of PspA4Pro per mg of NPs) and spray-dried using L-leu as a microcarrier to produce NCMPs with a product yield of 55.55±6.64% for the PspA4Pro adsorbed anionic NPs/NCMPs and 53.98±2.23% for the PspA4Pro adsorbed cationic NPs/NCMPs. The NCMPs produced had a corrugated and wrinkled surface morphology. The aerosol properties of anionic NPs/NCMPs determined using a Next Generation Impactor

displayed a fine particle fraction (FPF) of 74.31±1.32% and mass median aerodynamic diameter (MMAD) of 1.70±0.03 μm indicating that the majority of the dose would be deposited in the respirable airways of the lungs. The anionic and cationic PGA-co-PDL NPs upon incubation with DCs for 1 h showed an effective uptake as visualised using confocal microscopy. Furthermore, the anionic NPs/NCMPs were well tolerated by the A549 cell line with a cell viability of 87.01±14.11% at 1.25 mg/ml concentration, whereas the cationic NPs/NCMPs showed a cell viability of 75.76±03.55% at 156.25 μg/ml concentration upon 24 h exposure. The PspA4Pro released from the optimised formulations largely maintained its structure as determined using SDS-PAGE and circular dichroism, and the relative antigenicity measured using ELISA was 0.97±0.20 and 0.85±0.05 for anionic and cationic formulations, respectively. Overall, the results obtained indicate the use of these NPs as novel carriers for pulmonary vaccine delivery against pneumococcal diseases.

1. General Introduction

1.1 Pneumococcal Diseases

Pneumococcal diseases are infections caused by *Streptococcus pneumoniae* (*S. pneumoniae*) bacterium, also known as pneumococcus [1]. Pneumococcal diseases are classified into non-invasive pneumococcal diseases (occur outside the major organs or blood, e.g. otitis media, sinusitis) or invasive pneumococcal diseases (IPD) (occur inside the major organs or blood e.g. septicemia, meningitis, pneumonia) [2]. Amongst all the pneumococcal diseases, pneumonia is the leading cause of death especially amongst the immunocompromised, elderly over the age of 50 and children under the age of 5. Moreover, it is often referred to as *'The Forgotten Killer of Children'* as it is known to kill more children every year than any other illness; more than measles and malaria combined [3,4].

Any part of the respiratory system from middle ear to nose to lungs can be the site of acute respiratory infections [3]. Acute lower respiratory infections (ALRI), such as pneumonia and bronchiolitis, severely affect the lungs and are a leading cause of death in young children under the age of 5, and annually cause 1.6 million deaths in adults aged >59 years [5,6]. The lungs are composed of several thousands of bronchioles that end in small sacs called alveoli. The alveoli have an abundance of capillaries that exchange gases such as oxygen and carbon dioxide, wherein the oxygen thereafter enters the blood stream [3,7]. However, when infected with pneumonia the alveoli are filled with pus and fluid in one or both of the lungs interfering with the absorption of oxygen into the blood thereby making breathing extremely difficult [3,7].

1.1.1 Causes of Pneumonia

Streptococcus pneumoniae (Figure 1-1) is the bacterial cause of pneumonia worldwide [3,8–11]. The words uttered by Sir William Osler, nearly a century ago, that pneumococcus as *''the captain of all the men of death''*, still holds true today [11]. However, we are now able to control many pathogens of respiratory infections such as tuberculosis, pertussis and influenza. The current vaccine is very effective against pneumococcal sepsis and meningitis but many challenges persist with pneumococcus such as an effective vaccine against mucosal disease [2,11].

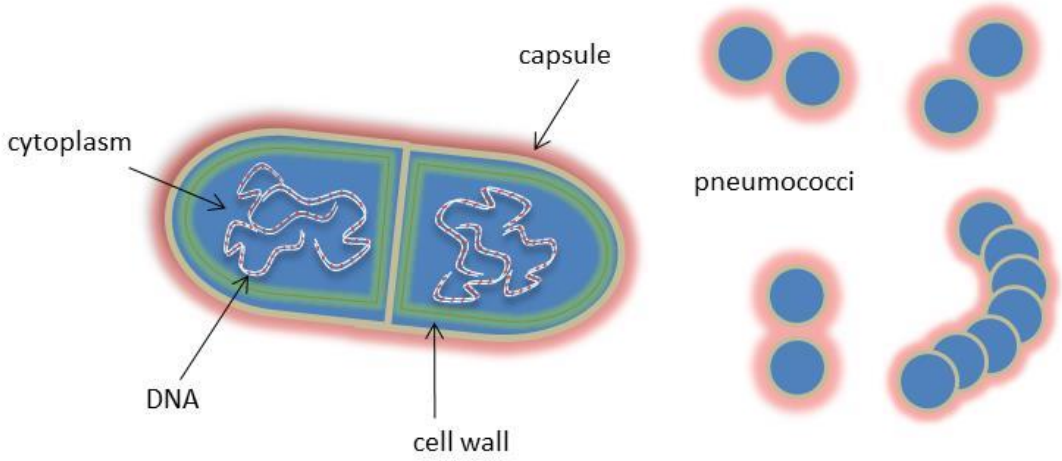

Figure 1-1 Cross-section of *Streptococcus pneumoniae*

Pneumonia can be classified as either community-acquired pneumonia (CAP) or hospital-acquired pneumonia (HAP). CAP is pneumonia acquired outside of hospitals or health care settings, and is the most prevalent type, whereas HAP is acquired in a hospital or health care setting [12,13]. People get infected by CAP by inhalation of pathogens [12] and pneumococcus was identified as the most common pathogen, accounting for up to 35% of CAP cases [14].

1.1.2 Statistics for Pneumonia

Streptococcus pneumoniae is a common bacterial agent that can cause or progress to respiratory tract mucosal infections such as sinusitis and otitis media or even more serious diseases such as pneumonia, septicaemia and meningitis [10,15,16]. Although we have been successful in reducing the number of child deaths worldwide, under the age of 5, due to various infectious diseases from 12.6 million in 1990 to 6.6 million in 2012 where pneumonia accounts for about 18-20% of deaths [17], much work still remains with regards to the elderly over the age of 50 [18]. The vast majority of these deaths are observed in the sub-Saharan African and South Asian countries, accounting for nearly 85-90% [19–21]. The IPD accounted for 36,000 cases in the USA in the year 2011 and incidence was strongly age related with 38% occurring in children under the age of 2 and 54% in adults above the age of 50 years [14].

Walker *et al.* estimated that, in 2011, nearly 74% of the total burden of diarrhoea and pneumonia mortality was observed in 15 countries, namely - Afghanistan, Angola, Burkina Faso, China, Democratic Republic of the Congo, Ethiopia, India, Indonesia, Kenya, Mali, Niger, Nigeria, Pakistan, Tanzania and Uganda [20]. Patterson *et al.* estimated the incidence of CAP in the UK to be about 5-11 per 1,000 adults with hospital admissions indicated for 22-42% of the overall CAP patients [12]. Moreover, in the UK, case-fatality rates of 5.6% for <65 years of age and 47.2% for ≥85 years of age have been reported indicating the burden of CAP in aging populations [22]. In addition, a growing concern is that the population aged >65 years is expected to triple globally from 673 million in 2005 to 2 billion in 2050 [14].

Various studies indicate an incidence for CAP ranging from 1.6 to 9 cases per 1,000 general adult population with the financial burden worldwide estimated to be US $4.8 billion for patients aged ⩾65 years and US $3.6 billion for patients aged <65 years [6,23–25]. A study by Broulette *et al.* showed that the incidence rate (10.6 per 1,000-person years) and economic burden ($20,961 for patients) of CAP in a working age population ranging from 18-64 years underlies the importance of effectively tackling CAP [26]. Estimates show that in Europe, the cost incurred for pneumonia is approximately €10.1 billion annually with indirect costs due to lost work days amounting to €3.6 billion [22].

1.1.3 The Bacteria

The bacterium, *S. pneumoniae*, is a Gram-positive, α-haemolytic and aerotolerant member of the streptococcus family [1]. It is observed as diplococcus with oval cocci arranged end to end in pairs [1]. The bacterium produces a range of colonisation and virulence factors such as the polysaccharide capsule, surface proteins and enzymes, and toxins (as shown in Figure 1-2) which play an important role in its function in targeting the host cells. A brief summary of some of these factors is described below to understand the mechanism of colonisation and invasion of the pneumococci into host cells.

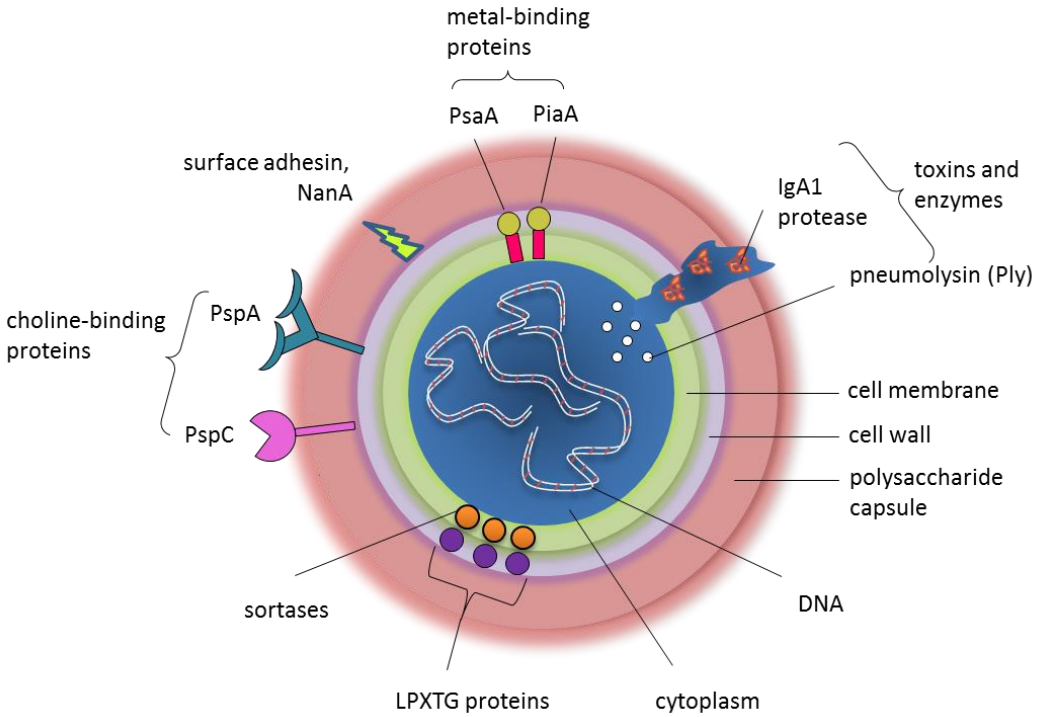

Figure 1-2 The various virulent factors of pneumococcus (redrawn from [11,27]); Note: Pneumococcal surface protein A (PspA), pneumococcal surface protein C (PspC), neuraminidase A (NanA), pneumococcal surface antigen A (PsaA), pneumococcal iron acquisition A (PiaA)

1.1.3.1 The Capsule

The outer surface of the pneumococci is covered with a negatively charged polysaccharide capsule which is highly heterogeneous and is approximately 200-400 nm thick [15,28,29]. Nearly 94 different serotypes of the capsule have been identified so far and the capsule is one of the important virulent factors of pneumococci providing its anti-phagocytic activity, i.e. protecting the bacteria from phagocytosis [11,15,30]. The capsule also helps to prevent the clearance or entrapment by mucus, restricts autolysis and aids in migration to the surface of epithelium [11,31]. Moreover, the pneumococci have the potential to regulate the

amount of capsular material from transparent (thin) to opaque (thick) to aid in colonisation and invasion resisting phagocytosis, respectively [11].

1.1.3.2 The Cell Wall

The cell wall of pneumococci is composed of multi-layered peptidoglycans covalently attached to teichoic acid (TA) and is membrane-bound to lipoteichoic acid (LTA) by a lipid moiety [30]. The chemical structures of the TA and LTA are identical in nature and so far this is a unique feature observed in pneumococci [30]. In addition, the TA and LTA present choline as phosphorylcholine (PCho), essential for binding to choline-binding receptors on host cells [30,31].

1.1.3.3 Surface Proteins

The cell surface proteins have been classified into three major groups, namely, (i) choline-binding proteins, CBPs (approximately 16), (ii) lipoproteins (approximately 50), and (iii) LPXTG proteins (approximately 18) (Leu-Pro-X-Thr-Gly, X = any amino acid) that are covalently linked to the peptidoglycan cell wall of the pneumococci by a carboxy-terminal sortase motif [27,30]. In addition, the cell wall also has a cluster of proteins lacking a leader peptide and therefore are named non-classical surface proteins (NCSPs) [30]. Of these three groups, CBPs are of prime importance for their potential to be used as candidates in vaccine development [29].

1.1.3.4 Pneumolysin

Pneumolysin (Ply), a 53 kDa protein, is an important virulent factor of the pneumococcus and is produced during the late log phase of growth by all clinical isolates of pneumococci [29,31]. This cytoplasmic enzyme is mainly released

when cells undergo autolysis [29]. It is also referred to as a pore forming toxin for its ability to form pores of up to 30 nm in diameter upon binding to the cholesterol membrane of the host cells [16,27,31]. This enzyme mainly interacts with the ciliary beating of the epithelial cells, slowing the beating and disrupting the tight intercellular junctions and the integrity of the monolayer [16,29]. This therefore hinders the clearance mechanism of the mucus and aids in facilitating the spread of pneumococcal infection [16]. In addition, Ply disrupts the alveolar-capillary boundary resulting in alveolar flooding. This leads to the availability of nutrients for bacterial growth facilitating the migration of pneumococci into the interstitium and finally into the blood stream [29,32].

1.1.4 Colonisation and Invasion

Nasopharyngeal colonisation, the main reservoir, is a prerequisite for pneumococcal infections and is believed to spread from person to person through airborne droplets, aerosols, drinking bottles and nasal secretion [16,28]. Pneumococci can be found in many healthy individuals (5 to 40%) depending on their age; however, the disease process begins only after aspirating the colonising bacteria [1,10,15]. Figure 1-3 shows plausible routes and infections that occur due to pneumococcus.

Once the bacterium contacts the nasal mucosa, the capsule aids in escaping mucus entrapment and helps reach the surface of the epithelium (Figure 1-4A) [11,28]. The evasion of mucus entrapment and clearance by pneumococcus occurs in three ways: a) the negative charge of the capsule repulses the sialic acid residues of the mucus restricting the chances of entrapment, b) the enzymes expressed by the

pneumococcus such as NanA and NanB (neuraminidase), BgaA (b-glucosidase), and SrtH (b-N-glucosaminidase) cleave the terminal sugars from the glycoconjugates of the mucus decreasing the viscosity of the mucus thus reducing entrapment and aiding adherence to receptors of the host cells, and c) the presence of toxin, Ply, in pneumococcus decreases the beating of cilia on the epithelial cells aiding the binding to receptors of the host cells hence making it difficult for mucus clearance (as explained above in section 1.1.3.4) [11,16,28].

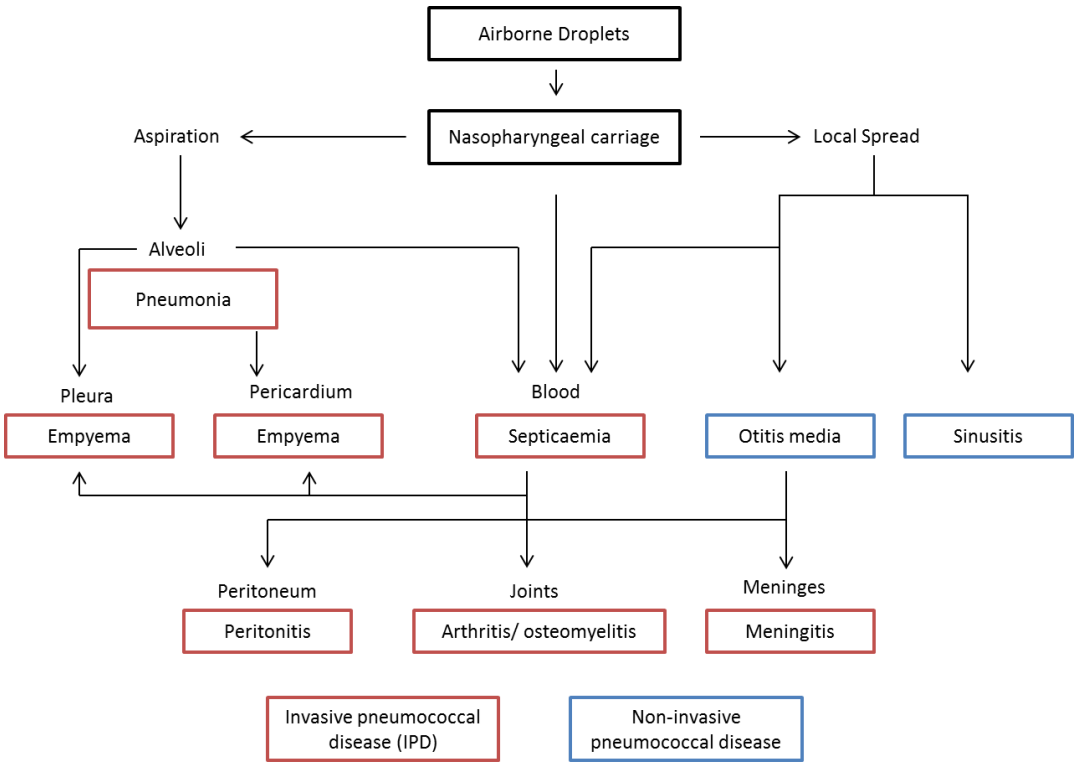

Figure 1-3 Pathogenesis of pneumococcal infection (redrawn from [10,15])

Lysozyme destruction is another barrier to successful colonisation and invasion of pneumococci [28]. Lysozyme is a muramidase that cleaves the peptidoglycans and acetylated peptidoglycans present in the cell wall of many pathogens, including pneumococci [28,33]. However, pneumococcus has two enzymes; peptidoglycan N-acetylglucosamine-deacetylase A (PdgA) and an O-acetyl

transferase (Adr), that deacetylate the peptidoglycans from the bacterial cell wall thereby resulting in resistance to lysozyme destruction (Figure 1-4B) [28,33].

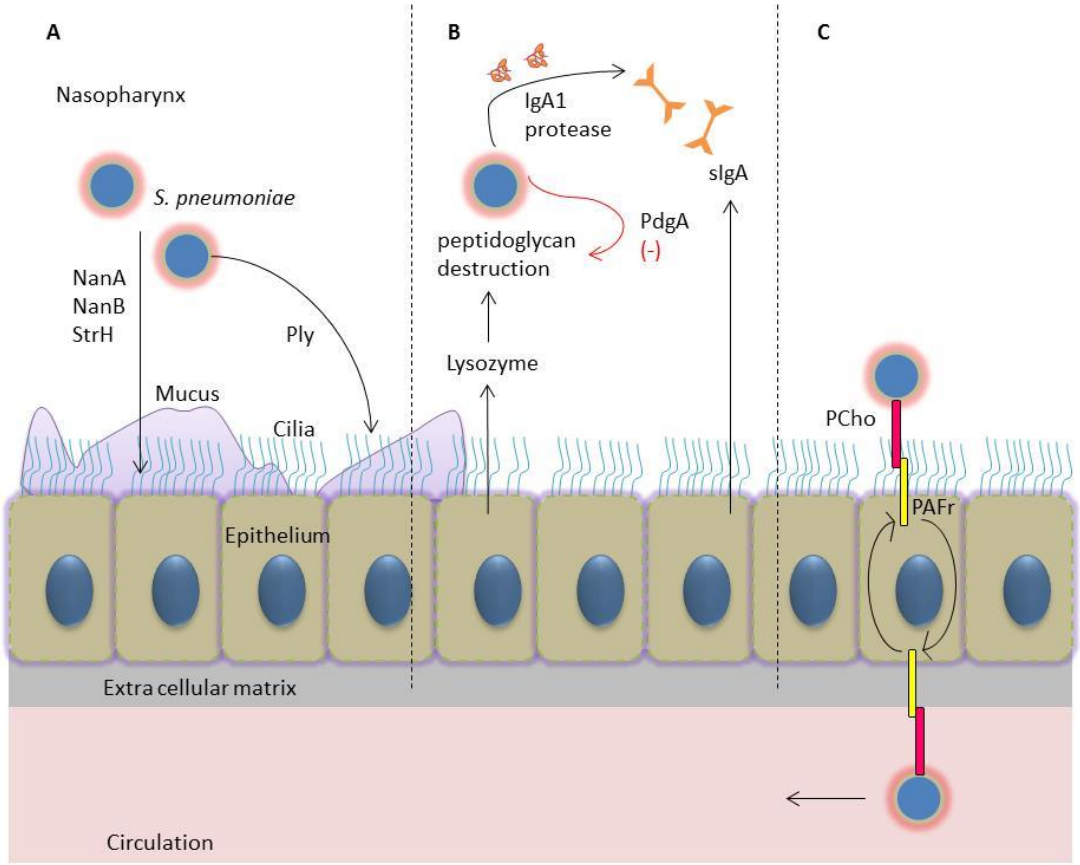

Figure 1-4 Pneumococcal colonisation and invasion. (A) Colonisation of the nasopharynx facilitated by the mucus degradation by NanA, NanB and StrH enzymes, (B) Evasion of lysozyme destruction of peptidoglycan cell wall of the pneumococcus by PdgA, and degradation of sIgA by IgA1 protease enzyme, and (C) Intracellular translocation followed by invasion into bloodstream facilitated by binding of PCho with PAFr (redrawn from [28]); Note: Neuraminidase A, B (NanA, B), platelet-activating factor receptor (PAFr), phosphorylcholine (PCho), peptidoglycan N-acetylglucosamine-deacetylase A (PdgA), secretory IgA (sIgA)

Secretory immunoglobulin A (sIgA) interferes with the invasion of pneumococci by facilitating opsonisation and enabling phagocytosis by antigen presenting cells (APCs) [15,28]. However, Weiser *et al.* have shown that pneumococcus overcomes this problem by releasing IgA1 protease [34]. In addition to the capsule protecting the pneumococci from sIgA, the pneumococcal IgA1 cleaves the sIgA at the hinge region preventing opsonisation and increasing binding to the mucus (Figure 1-4B) [15,28,34].

For invasive disease to occur, inflammatory factors such as interleukin 1 and tumour necrosis factor are generated affecting the presence of receptors on the surface of host cells [15]. One of the most important receptors that is up-regulated is platelet-activating factor receptor (PAFr) [10,15,16]. The surface decoration of PCho on the cell wall of pneumococci immediately binds to PAFr thereby facilitating internalisation and uptake of live bacteria, resulting in migration from respiratory epithelium into vascular endothelium and the bloodstream (Figure 1-4C) [15,16]. Moreover, other surface proteins such as choline-binding protein A (CbpA) and pneumococcal surface protein A (PspA) help binding to host cells and invasion [15,28]. PspA, a choline-binding protein expressed on the surface of pneumococci, interacts with apolactoferrin, a bactericidal compound that disrupts the bacterial cell leading to lysis, at its active site leading to inhibition of apolactoferrin mediated bacterial killing [28,35].

1.1.5 Treatments and Current Vaccine Strategies

From the 1940's, penicillin was the obvious choice for treating CAP until the mid-1970s, when resistant strains of pneumococci were widely reported [11]. The

resistant strains are now widespread and although they can be overcome by using high level doses of β-lactam antibiotics (penicillin or cephalosporins) this only has limited success [9,11,15]. Moreover, antimicrobial drugs such as fluoroquinolones, macrolides, vancomycin and trimethoprim can be used but resistance to these is also widely reported worldwide [11]. A combination of β-lactam antibiotics and antimicrobials is also recommended in some cases for an effective treatment [11]. The treatment guidelines vary between the UK [36], continental Europe [37] and the US [38], and are tailored for each population in the region. However, with growing resistance to antibiotics and very few new antibiotics being reported, vaccines are proving to be the choice for prevention rather than cure. Currently, there are two types of vaccines available against *S. pneumoniae*: pneumococcal polysaccharide vaccine (PPV) and pneumococcal conjugate vaccine (PCV, serotype conjugated to a carrier protein). These are designed to generate antibodies against capsular polysaccharides and immunise against IPD [39–41]. Table 1-1 lists the availability of different pneumococcal vaccines.

Pneumovax23®, (PPV23), an unconjugated and non-adjuvanted pneumococcal polysaccharide vaccine, developed by Merck & Co, is administered either by intramuscular or subcutaneous injection [39,41]. This 23-valent vaccine is composed of the 23 most common serotypes prevalent in developed countries [42], accounting for 85–90% of pneumococcal diseases [9]. It is usually recommended for people older than 65 years of age and children ≥ 2 years of age at high-risk for pneumococcal disease (individuals with conditions such as HIV, sickle-cell anaemia etc.) [40]. This vaccine induces T-cell independent B-cell

responses, leading only to a temporary protection [41]. Moreover, it is not conjugated to a protein and does not induce a memory immune response resulting in poor immunogenic responses in populations that are at a greater risk of pneumococcal diseases [11,43].

Prevenar7®, (PCV7) was developed and licensed by Wyeth Pharmaceuticals Inc. (now Pfizer Inc.) in 2000 to address the immunogenicity problem faced by PPV23. This 7-valent vaccine is composed of 7 different pneumococcal polysaccharides conjugated to a protein carrier CRM-197™, a cross-reactive mutant of a diphtheria toxin. It contains an alum-bound adjuvant and is administered by intramuscular injection. It is recommended, in the US, for children at the age of 2, 4 and 6 months with a booster at the age of 2. The capacity of the vaccine to induce both T-cell and B-cell responses makes it highly immunogenic in young children. However, there is growing evidence to suggest that non-vaccine serotypes have become more dominant and have been significantly contributing to the carriage and IPD [40]. Recently, Synflorix10®, (PCV10) from GlaxoSmithKline and Prevenar13®, (PCV13) from Pfizer Inc. both administered by intramuscular injection, were developed to cover more serotypes that have been recognised to be contributing to the spread of the disease [40,41,44]. The chief trait of the PCVs has been to generate a herd immunity thereby resulting in an overall reduction of IPD [11,39].

Table 1-1 Currently available pneumococcal vaccines (adapted from [41])

Vaccine (Valency)	Type	Brand Name	Company	Year (available since)	Serotypes
PPV23	pneumococcal polysaccharide vaccine	Pneumovax23®	Merck	1983	1, 2, 3, 4, 5, 6B, 7F, 8, 9V, 9N, 10A, 11A, 12F, 15B, 17F, 18C, 19A, 19F, 20, 22F, 23F, 33F
PCV7	pneumococcal conjugate vaccine	Prevenar7®	Wyeth	2000	4, 6B, 9V, 14, 18C, 19F, 23F
PCV10		Synflorix10®	GlaxoSmithKline	2009	1, 4, 5, 6B, 7F, 9V, 14, 18C, 19F, 23F
PCV13		Prevenar13®	Pfizer Inc (formerly Wyeth)	2010	1, 3, 4, 5, 6A, 6B, 7F, 9V, 14, 18C, 19A, 19F, 23F

Note: PPV – pneumococcal polysaccharide vaccine, PCV – pneumococcal conjugate vaccine, serotype – distinct variations within a species of bacteria

1.1.6 The Need for New Vaccines

The main challenge to the PCVs is the prevalence of non-vaccine serotypes and consequently re-emergence of the diseases associated with *S. pneumoniae* [9,40,41]. A classic example of the above scenario was observed in Alaskan natives wherein a steady increase in the cases of pneumococcal disease by non-vaccine serotypes was reported, following the introduction of PCV7 [45]. In addition, the variation in serotype distribution across geographical locations coupled with the cost and complexity of manufacturing PCVs raises the need for the development of new vaccines [9,39,40].

The requirements are to develop a low-cost and effective vaccine against pneumococcus to prevent hospital admissions, reduce costs associated with treatment, reduce loss in income, remove the requirement for cold-chain and trained medical personnel, and that can be successfully employed in the low and middle income countries (LMICs). This generated much scientific attention within institutes such as the US National Institutes of Health (NIH) and PATH, an international non-profit organisation, who organised a symposium dedicated for this purpose in 2010 [46].

Pneumococcal protein vaccines have the potential to cover and protect against all serotypes of pneumococcus leading to prevention of the prevalence of certain types of serotypes or serotype replacements [39,46]. The pneumococcal proteins can be used alone, as a carrier protein for PCVs or in combination with PCVs. However, due to the cost and complexities associated with the manufacture of PCVs, the use of pneumococcal proteins as a stand-alone vaccine has gained

major importance [46,47]. Over the years, researchers have identified nearly 20 proteins that offered protection against pneumococcal disease when evaluated in animal models [47,48].

1.1.7 Pneumococcal Surface Protein A

PspA is an important virulent factor present on the surface of all clinically isolated pneumococci [49]. The molecular weight of PspA ranges from 67 to 99 kDa in various strains of pneumococci [29,50]. The protein has been identified to have four distinct regions (Figure 1-5A) [29,30,51]: an N-terminal region (composed of 288 amino acids in strain Rx1), a proline rich region (60-80 amino acids), a choline binding region composed of ten 20-amino acid repeats and a C-terminal tail of 17 hydrophobic residues. By interacting with the choline in LTA, the choline binding domain helps the attachment of the PspA to the cell wall surface of pneumococci [51]. The N-terminal is understood to be highly helical and extends from the cell wall protruding outside the capsule [29,30]. The N-terminal region is highly charged and polar, whilst the C-terminal end anchors the protein to the cell surface [29,50]. Moreover, the proline-rich region allows for greater flexibility and movement of the N-terminal region [27]. PspA is a highly variable protein and based on the sequences of the N-terminal can be classified into three families that are further subdivided into six different clades. Family 1 (Fam1) is composed of clades 1 and 2, Fam 2 of clades 3, 4 and 5, and Fam 3 of clade 6 [49,52].

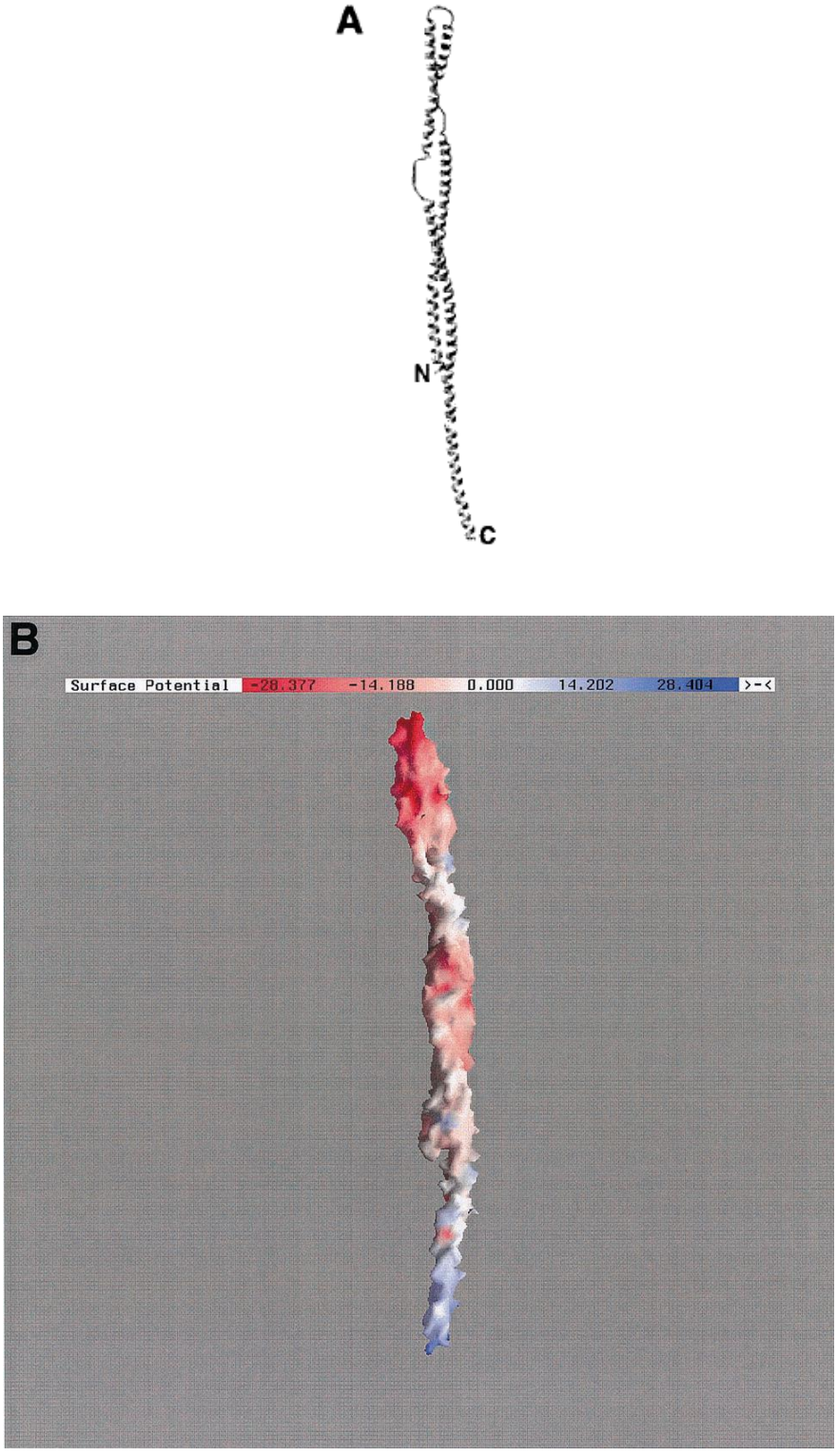

Figure 1-5 (A) Structural model of pneumococcal surface protein A (PspA), (B) the charge distribution on the surface of PspA based on the model of a PspA molecule containing amino acids 1 to 303 (adopted from [29])

The main function of PspA is protection against the host complement system [29]. The electropositive C-terminal interacts and stabilises the capsular electronegative polysaccharide whereas the electronegative end of the protein points away due to the repulsive interactions from the capsule (Figure 1-5B). This electronegative end is exposed outside the capsule and prevents the C3-mediated binding of the host complement to pneumococci thereby preventing lysis of the bacteria [29]. Moreover, PspA has a lactoferrin-binding region within 168-288 amino acid residues that is thought to protect the pneumococcus from the bactericidal activity of apolactoferrin [30]. It is also observed that PspA plays a role in restricting or decreasing the clearance of pneumococci from the blood of infected mice [53]. With these important functions associated with the pneumococci much attention has been recently focused on PspA, a well characterised protein, for its potential as a vaccine candidate against pneumonia [54–60].

1.2 Lungs

1.2.1 Anatomy of the Human Lung

The human lung, weighing about 1 kg, is divided by the pleural membranes into three lobes on the right and two lobes on the left [61]. Once inhaled, air passes through the nose and mouth, from the larynx to the trachea and thereafter to a series of approximately 16 generations of conductive bronchi and bronchioles [61,62]. From the 17th generation of bronchioles, alveoli begin to appear in the walls (respiratory airways) and by the 20th generation of airways, the entire wall is composed of alveoli, commonly referred to as alveolar ducts. At the 23rd generation, the alveolar ducts end in blind sacs lined with alveoli referred to as

alveolar sacs (Figure 1-6) [61–63]. It is estimated that on an average a human lung consists of about 300 million alveoli providing a surface area of exchange of 80-90 m^2 [61,64].

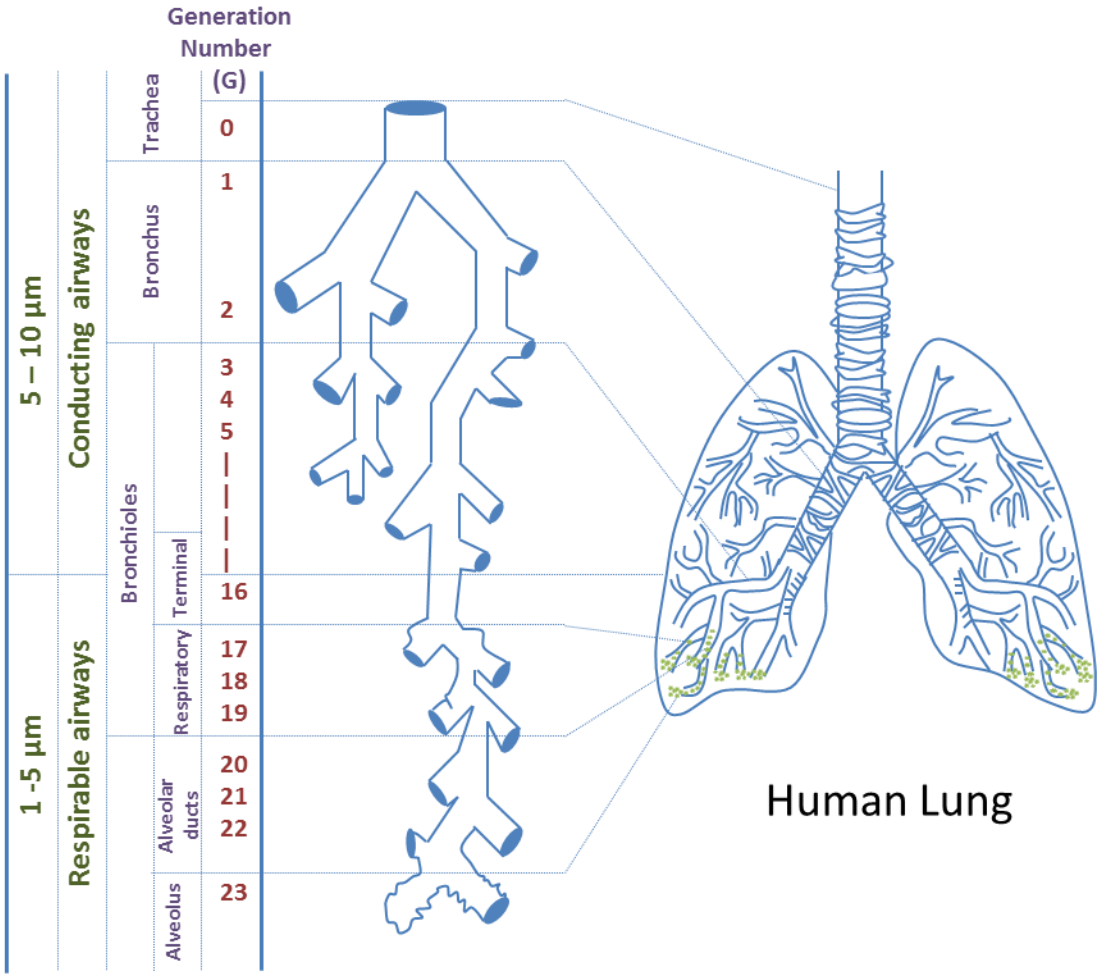

Figure 1-6 Diagram of the lung and size dependent particle deposition (adopted from [65])

Submucosal glands and the goblet cells, present on the bronchial surface, secrete mucus onto the bronchial surfaces. The submucosal glands also help by producing an electrolyte solution on which the mucus rests. The mucus covering the airways is transported towards the mouth with the coordinated movement of cilia present on top of the ciliated columnar cells and this mucus is then swallowed. This

process of mucus movement is mainly responsible for removing any foreign material that lands on the bronchial surfaces [61].

The alveoli and the pulmonary capillaries are separated by a barrier composed of endothelial cells, interstitial space, and pneumocytes (pulmonary epithelial cells). The pneumocytes are divided into two types; type I and type II cells. Type I (~93% surface area coverage) cells are very flat and cover the alveolar surface. They provide a barrier of minimal thickness facilitating the gaseous exchange between the alveoli and blood [61]. Type II (~7% surface area coverage) cells are irregularly shaped, and contain lamellar bodies and secretory organelles that serve as pulmonary surfactant. Moreover, in alveoli they can further divide and produce type I and type II cells [61,66].

1.2.2 The Lung as a Delivery Site

The lung is an excellent choice for the delivery of macromolecules for the treatment of both local and systemic disorders [67]. With regards to the delivery of vaccines, a high density of APCs including alveolar macrophages (AMs), dendritic cells (DCs) and B-cells represent an ideal target to induce a strong immune response [68]. The major benefit of a mucosal vaccine delivery system is the production of protective B and T-cells in mucosal and systemic environments aiding the induction of mucosal and systemic immunity [69]. The mucosal membranes produce sIgA that is more stable, has higher avidity for mucosal surfaces and acts as a first line of defence against invading pathogens. In addition, the T-cells in the mucus have special ‘homing’ receptors that facilitate travel to other mucosal tissues leading to systemic immunity [70]. Recent research has

confirmed that the induction of an immune response at one mucosal site elicits an immune response at distant mucosal sites leading to both mucosal and systemic immunisation including $CD4^+$ Th1 and Th2, $CD8^+$ cytotoxic T-lymphocytes (CTLs), and Ab responses in the bloodstream [69,71,72]. There is some evidence that mucosal immunisation may also reduce the dosage required to achieve a desired immunity compared to liquid formulations administered via the parenteral route [73,74].

1.2.2.1 Pulmonary Delivery of Macromolecules

The lung as a delivery route for macromolecules offers several advantages [65,67,75]; a large surface area for drug absorption (80-90 m^2); a thin alveolar epithelium (approximately 0.1-0.5 μm) providing transport across the air/blood barrier; dense vasculature for systemic circulation; a high capacity for solute exchange; less enzymatic activity than the gut which is likely to reduce degradation of the active; and it is a non-invasive route of administration, thereby potentially increasing patient compliance and therapeutic outcome. Within the pulmonary lymphatic system, lymphatic vessels are present in the interstitium near the small airways and blood vessels but not in the alveolar walls [76]. The leaky lymphatic endothelia allow micron-sized particles (lipoproteins, plasma proteins, bacteria and immune cells) to pass freely into the lymph fluid [77] and this can be utilised as a mechanism for the transport of macromolecules and polymeric particles into the lymphatic system for systemic delivery.

Soluble macromolecules are absorbed into the body from the lung by two mechanisms; absorptive transcytosis (through the cells) or paracellular transport (between the cells) [77,78]. Absorption from the lung to the blood is highly

dependent on the molecular weight of the macromolecule [77]; the larger the macromolecule, the longer it takes for absorption to occur and this relationship holds over the range of 1-500 kDa [77,79]. Inhaled peptides and proteins with molecular weights < 40 kDa rapidly appear in the blood whereas those > 40 kDa (> 5-6 nm in diameter) are absorbed over many hours [77,78].

1.2.2.2 Barriers to Macromolecule Absorption

There are several challenges to using the lung for the delivery of macromolecules. In the trachea, the airway epithelium is 50-60 μm thick and though leakier than alveoli, is a significant barrier to the absorption of inhaled drugs; whereas in the alveoli, this barrier is reduced to 0.1-0.5 μm supporting absorption [79]. The presence of different cell types in the trachea, bronchi, bronchioles and alveoli also modifies absorption [80] and factors such as respiratory mucus, mucociliary clearance, pulmonary enzymes, macrophages, and basement membranes have been identified as limiting the absorption of macromolecules. The alveolar epithelium, though permeable to water, gases and lipophilic molecules, restricts the absorption of hydrophilic substances, such as many therapeutic macromolecules. In addition, upon reaching the alveoli, proteins are cleared by macrophages or DCs [75]. However, this clearance process can be advantageous for vaccine delivery where the antigen-containing carrier can be taken up by macrophages or DCs thereby aiding the initiation of an immune response.

1.3 Vaccine Delivery

Vaccination refers to the induction of an immune response using antigens to generate protective immunity against infections [81,82]. Traditional vaccines are

often administered via the parenteral route requiring infrastructure such as cold-chain, sterilised water for reconstitution of dry powder vaccines and trained medical personnel. Lack of these facilities in LMICs is leading to many eligible children and adults not receiving vaccination [65]. Moreover, the majority of the potential vaccines under development employ purified subunits or recombinant proteins that are often poorly immunogenic thus needing adjuvants and effective delivery systems to generate an optimal immune response [81,82]. To address these issues, particulate delivery systems and non-invasive routes of delivery are being investigated. The pulmonary route has gained significant attention for the delivery of vaccines as it is one of the main entry portals for pathogens (e.g. pneumococcus, tuberculosis) and can address some of the challenges such as invasiveness, cold-chain requirement, and stability of the antigen by delivering the antigen as a dry powder [65].

1.3.1 Pulmonary Vaccine Delivery

Pulmonary delivery as a route of drug administration can be traced back 4000 years to India where people suffering from cough suppressed it by inhaling the leaves of *Atropa belladonna* [83]. Later in the 19th and 20th centuries, people suffering from asthma smoked cigarettes containing tobacco and stramonium powder to alleviate their symptoms [83]. The first inhalation apparatus for dry powder delivery was patented in London in 1864 [84]. Since then, much progress has been made in developing devices such as nebulisers, metered dose inhalers (MDIs) and dry powder inhalers (DPIs) for delivery of therapeutics. With recent advancements in pulmonary delivery devices and recombinant protein technology,

the first peptide DPI formulation, Exubera (Nektar/Pfizer), was approved and released into the market in January 2006. This was soon withdrawn for several reasons including bulkiness of the device, complicated administration, contraindication in smokers and insufficient evidence regarding the patients preference of Exubera (inhaled dosage form) compared to other dosage forms [85]. This led to further research and development of DPI of macromolecules, and currently many new investigations are being pursued by the pharmaceutical industry such as the Technosphere system AFREZZA® (Mannkind, approved June 2014) [78]. This has been followed by research into DPI of vaccines [86–90].

1.3.2 Pulmonary *vs.* Parenteral Vaccine Delivery

During the development of novel anti-tuberculosis vaccines, Ballester *et al.* demonstrated that inhaled vaccination compared favourably to an intradermal route of delivery [91]. In particular, vaccination with nanoparticle-Ag85B and immune-stimulatory oligonucleotide CpG as a Th1-promoting adjuvant via the pulmonary route modified the pulmonary immune response and provided significant protection following a *Mycobacterium tuberculosis (Mtb)* aerosol challenge [91].

Muttil *et al.* successfully prepared poly(lactic-co-glycolic-acid) (PLGA) NPs entrapping diphtheria CRM-197 antigen (CrmAg) with a size of 200±50 nm by the emulsification solvent diffusion and double-emulsion methods. The NPs were then spray-dried with L-leucine (L-leu) and the resulting spray-dried powders of formalin-treated/untreated CrmAg nanoaggregates were delivered to the lungs of guinea pigs. This study evaluated the immune response elicited in guinea pigs

following pulmonary and parenteral immunisations with the dry powders. The highest titer of serum IgG antibody was observed in guinea pigs immunised by the intramuscular route whereas high IgA titers were observed for dry powder formulations administered by the pulmonary route. This demonstrates that pulmonary immunisation with dry powder vaccines leads to a high mucosal immune response in the respiratory tract and sufficient neutralising antibodies in the systemic circulation to provide protection against diphtheria [92].

An ideal vaccine formulation for mass vaccination would induce the desired immunity upon administration of a single dose. Moreover, it is important to target APCs like DCs to illicit a strong and durable immune response with a single dose aimed at both systemic and mucosal immunity [93]. In addition, the size, shape and aerodynamic properties of the delivery vehicle, and the delivery device also contribute to improving the treatment [80].

1.3.3 Dendritic Cells

DCs were first identified in 1868 by Paul Langerhans in the basal layer of the epidermis [94]. However, it took more than a century to properly identify them as white blood cells related to macrophages and monocytes, and to understand their importance in the role of immunity [94,95]. In 2011, the Nobel Prize in Physiology or Medicine was awarded to Ralph M. Steinman for his discovery of DCs and their role in adaptive immunity, paving the way for more research in the field of immunity and vaccines [96]. Adaptive immunity, also known as acquired immunity, is a subset of the overall immune system and is responsible for creating an immunological memory after an initial response to a specific pathogen [82,95].

Moreover, adaptive immunity includes both humoral (immunity mediated by macromolecules in extracellular fluids such as antibodies, complement proteins) and cellular (immunity involving the activation of phagocytes, antigen-specific CTLs and release of cytokines) immunity [95,97]. It has become evident over the years that DCs are APCs, 'true professionals' [98] with exceptional capability to internalise, process and present antigens through major histocompatibility complex (MHC) class I and II pathways. DCs induce a strong immune response by activating naïve T-cells which are produced in the bone marrow and have the capability to respond to novel pathogens that have not been processed before [97,99]. The role of DCs in initiating a primary immune response has now been shown to be greater than the role played by macrophages and the B-cells [100].

The lung is armed with an intricate network of DCs that can be found throughout the conducting airways, lung interstitium, lung vasculature, pleura, and bronchial lymph nodes [101,102]. It is now apparent that there are at least five different subsets of DCs in the murine lung; resident DCs, plasmacytoid DCs, alveolar DCs, inflammatory DCs and interferon-producing killer DCs [101,102]. Data for the subsets of DCs present in the human lung is rare [103] owing to the need to obtain lung tissue, as they are not found in the bronchoalveolar lavage (BAL) fluid. However, studies on human AMs are common as they are readily obtained from BAL [104]. The AMs are primarily phagocytes with poor APC function that live in the air space, whereas immature DCs have high APC function but lower phagocytic function and live mainly in the interstitium [105]. In the human lung, the mucosal surface in the conducting airways consists of ciliated epithelial cells, interspersed goblet cells, macrophages and DCs [106]. The DC population in this

region is mainly composed of myeloid DCs (mDCs), however, a small fraction of plasmacytoid DCs (pDCs) can be found [106]. These mDCs have a high capability for antigen uptake but less ability to stimulate the T-cells [106]. Moreover, the human DCs are generated from haematopoietic stem cells, mDCs from bone marrow–derived monocytic precursors and pDCs from lymphoid progenitors [94]. The mDCs and pDCs are activated by a different set of pathogenic stimuli, making them functionally distinct which is reflected by the different expression of cell surface receptors such as Toll-like receptors [94,106]. The lung parenchyma consisting of lung interstitium, respiratory and terminal bronchioles, and alveoli is mainly composed of 80% macrophages with rest being DCs and T-cells. The 'immature' resident DCs are highly capable of detecting, capturing and processing the encountered antigen [94,106].

Human DCs are identified by over expression of human leukocyte antigen (HLA) DR (MHC class II) with the absence of monocyte, lymphocyte, natural killer cell and granulocyte lineage markers [103]. In addition, the specific markers for identifying mDCs include $CD11c^{+}$, $CD1a^{+}$, BDCA-1^{+}, BDCA-3^{+}, HLA-DR^{+} whereas for pDCs they are $CD11c^{-}$, HLA-DR^{+}, BDCA-2^{+} and $CD123^{+}$ [103,106,107].

Inhaled antigens or antigen particulates are believed to encounter the widespread DC network that lines the bronchiolar and alveolar epithelium and are subsequently taken up by cellular processes extending into the alveolar lining fluid [93]. Antigens are then processed and fragments of antigenic peptides are presented on the surface through MHC class I and II pathways for recognition by the T-cell receptors present on T-cells [100]. This process is often referred to as

antigen presentation and typically takes place in the regional lymph node after chemokine dependent migration of the antigen-loaded DC. Also, APCs perceive danger signals from cells and offer co-stimulatory signals [108] through co-stimulatory molecules present on their surface for recognition by receptors on recirculating T-cells to initiate an immune response in the lymph node [100]. Upon encountering danger signals, immature DCs change to a mature stage where they present the antigen on their surface. This step is usually concurrent with the migration of DCs from peripheral tissue to the lymph node for T-cell activation (Figure 1-7). It is believed that soon after antigen presentation, DCs undergo apoptosis in the lymph nodes [100].

Antigen uptake by DCs occurs by macro-pinocytosis, receptor-mediated endocytosis (macrophage mannose receptor) and/or phagocytosis [109–112]. Recent research by Foged *et al.* has shown that both particle size and surface charge of the material to be delivered plays an important role in determining the uptake by human DCs derived from blood. Furthermore, it was recognised that for optimal uptake by DCs the preferred particle size was 0.5 µm (diameter). Uptake of large particles (~ 1 µm) was greatly enhanced when they displayed a positive surface charge [113].

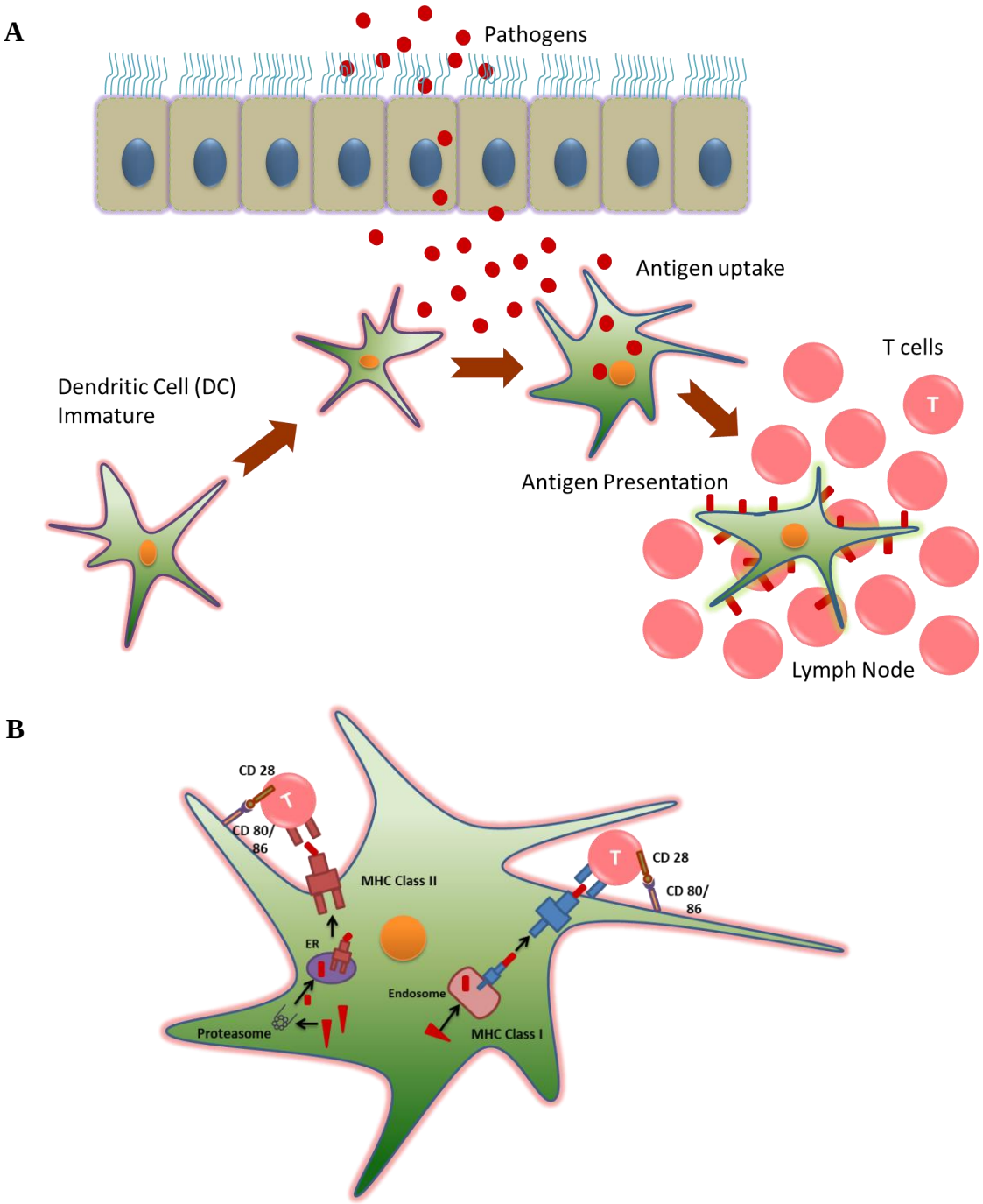

Figure 1-7 Antigen uptake and presentation by dendritic cells (DCs) in the airways. (A) Upon a pathogen attack the immature DCs are recruited from the blood circulation and migrate towards the site of attack. DCs at this stage express a wide variety of receptors (Fc, C-type lectin receptors etc.) and uptake the antigen. After antigen uptake and activation, high amounts of peptide-loaded major histocompatibility complex (MHC) molecules and T-cell co-stimulatory receptors appear on the surface of DCs. The DCs then

migrate to the lymph nodes and activate the antigen specific T-cells. (B) After antigen uptake, the antigen is either processed through MHC class I (either through endogenous or exogenous pathway) or MHC class II (the antigen is degraded in endosomes and the obtained polypeptide is transported and loaded onto MHC II molecules) and DCs present it on their surface for specific T-cell activation. *ER – Endoplasmic reticulum (adopted from [65])

Antigen can be targeted to DCs, for enhanced immune response, by making particles that bind to the specific receptors expressed on the DC surface [109–111]. Effective targeting of vaccines to the DCs results in the possibility of delivering a reduced vaccine dose, less side effects, improved efficacy and an enhanced immune response [100]. Vaccines can be targeted to DCs in different ways (for example via mannose, glucan, anti-DEC205 or anti-CD11c receptors) [100,114–117]. There is currently no literature that describes or reports the targeting of pulmonary DCs through pulmonary delivery of dry powder vaccines.

1.4 Nanoparticles for Inhalation

Nanoparticles (NPs) are referred to as particles in the size range of 1-1000 nm with one dimension ≤ 100 nm and have been used in drug delivery for the last 40 years [118]. NPs have been shown to pass rapidly (within 1 h) into the systemic circulation from the lungs after aerosol inhalation in humans [119]. NPs are used as drug carriers either by encapsulating, dissolving, surface adsorbing or chemically attaching the active substance [118].

NPs have a large surface area-to-volume ratio and also an increased saturation solubility thus favouring application in the field of drug delivery. In delivery of NPs to the lung by inhalation, deposition takes place through impaction,

sedimentation, interception or diffusion (Table 1-2) depending on particle size, density, airflow, breathing rate, respiratory volume and the health of the individual [80,120]. These are discussed in greater detail by Smyth *et al.* [121] and relevant definitions are summarised in Table 1-2.

The deposition of particles in the lungs is evaluated using the aerodynamic particle size (d_{ae}), which is defined as the diameter of a sphere (density – 1 g/cm^3) in air that has the same settling velocity as the particle in consideration [118]. This is defined by the equation 1-1:

$$d_{ae} = \sqrt{(\rho/\rho_{a)}}\ d_g \qquad \text{(eq. 1-1)}$$

where ρ is the mass density of the particle, ρ_a is the unit density (1 g/cm^3) and d_g is the geometric diameter.

Particles greater than 10 µm (d_{ae}) in size are commonly impacted in the throat or sedimented in the bronchial region whereas particles less than 1 µm (d_{ae}) in size are exhaled and not likely to be deposited in the alveolar region. It is expected that particles in the size range of 1-5 µm (d_{ae}) avoid deposition in the throat and reach the respirable airways and the periphery of the lung [120]. Particles less than 1 µm (referred to as NPs) are driven by diffusion and are most likely to be exhaled due to low inertia hence they are therefore often delivered within microparticles (MPs). In addition, upon long term storage NPs tend to aggregate due to high particle-particle interactions [118]. Nanocomposite microparticles (NCMPs) prepared from NPs are typically about 1-5 µm in size (aerodynamic diameter) and usually also encompass inert pharmaceutical excipients (sugars, amino acids etc.)

that act as carriers. The excipients dissolve upon encountering the respiratory environment thereby releasing the NPs.

Table 1-2 Broad descriptions of impaction, sedimentation, interception and diffusion (adopted from [65])

Impaction	The delivered particles, due to inertia, do not change their path and as the airflow changes with bifurcations they tend to get impacted on the airway surface. This is mostly experienced by large particles and is highly dependent on the aerodynamic properties of the particles.
Sedimentation	The settling down of the delivered particles. This is generally observed in the bronchioles and alveoli.
Interception	This occurs when particles, due to their shape and size, interact with the airway surface and is experienced when the particles are close to the airway wall.
Diffusion	Is the transport of particles from a region of higher concentration to lower concentration, is observed for particles that are less than 0.5 μm in diameter and occurs in the regions where the airflow is low. This is highly dependent on the geometric diameter of the particles.

Over the past few decades, NPs have gained increasing attention and polymeric NPs have been tested for delivery via different delivery systems and routes, such as oral [122], intravenous [123], transdermal [124], ocular [125], and pulmonary [126,127]. Different types of NPs have been explored for vaccine delivery where antigenic peptides or proteins can be either surface adsorbed or encapsulated within the NPs. In addition, both antigen and materials that augment the immune response (adjuvants) can be encompassed together in NCMPs, resulting in their

simultaneous delivery [128]. Table 1-3 outlines some types of NPs evaluated for vaccine delivery.

Table 1-3 Examples of nanoparticles currently being evaluated for vaccine delivery (adopted from [65])

Nanoparticles	Description	Size	Vaccine	Ref
Micelles (Peptide Cross-linked micelles – PCMs)	PCMs are composed of block copolymers and encapsulate immuno stimulatory DNA in the core and bind peptide antigens through disulphide linkages. In the presence of a high concentration of glutathione they deliver antigenic peptides and immunostimulatory DNA to APCs	50 nm	HIV peptide vaccine	[129]
Liposomes	Dimyristoyl phosphatyl-choline (DMPC):cholesterol-(7:3) liposomes were prepared by dehydration-rehydration followed by freezing-thawing method. The enzyme, GUS, was successfully encapsulated and showed encouraging activity following aerosolisation	~ 6.4 µm (with 1:4 liposome: mannitol)	β-Gluc-uronidase – enzyme (GUS)	[130]
Polymersomes	poly(g-benzyl-L-glutamate)-K polymersomes were prepared by the solvent removal method and influenza hemagglutinin (HA) was surface adsorbed. When tested *in vivo*, polymersomes acted as an immune adjuvant and showed an improved immunogenicity	250 nm	influenza HA – subunit vaccine	[131]
Polymer-based	Porous poly-L-lactic acid (PLA) and PLGA NPs were prepared by a double-emulsion-solvent evaporation method encapsulating HBsAg and were tested for pulmonary delivery in rat spleen homogenates. The study demonstrated enhanced immune responses	474-900 nm	hepatitis B surface antigen (HBsAg)	[90]

1.4.1 Polymeric Delivery Systems

A drug delivery system can be defined as a formulation or device that assists the introduction of a therapeutic substance into the body, improving the efficacy and safety of the substance [132]. Various polymeric carriers such as dendrimers, micelles, and nano- and micro-particles have been developed for the deposition of macromolecules in various regions of the lung [133]. The role of the polymeric carrier includes: transportation, protection, controlled release, targeting and maximising cellular uptake [133].

Natural polymers such as: chitosan, gelatin, alginate, cyclodextrin, collagen, and albumin; and synthetic polymers such as: polyesters, polyacrylates and polyanhydrides, have been used for the preparation of biodegradable delivery systems [134–137]. Natural polymers tend to have a comparatively short duration of therapeutic release but the properties of synthetic polymers can be tailored to provide sustained release of the encapsulated drug over a period of days to several weeks [138].

Biodegradable polymers have gained significant attention for the preparation of NPs for drug delivery and are often favoured as they offer several advantages such as controlled or sustained drug release, biocompatibility with the surrounding tissues and cells, low toxicity, are nonthrombogenic and are more stable in the blood [139,140].

1.4.2 Polymeric Nanoparticles for Macromolecule Delivery

Polymeric particles are solid colloidal structures in which the active therapeutic is either physically adsorbed or chemically bonded to the polymer, or encapsulated inside the particle [141]. They have been extensively investigated for the delivery of a wide variety of drugs [133] and macromolecules [90,134–137,142–149] due to their generally good biocompatibility. Moreover, these particles have demonstrated a significant effect in enhancing the therapeutic index of macromolecules via increased stability, targeted deposition, sustained release and reduced dosing frequency [138]. There is also the potential to modify polymeric particles to provide different chemical compositions (e.g. by attachment of a ligand), altering the surface properties (e.g. by adsorption or coating with chitosan [150] or mannan [151]), and improve their circulation time (e.g. by addition of polyethylene glycol, PEG [152]). However, for pulmonary delivery, the potential toxicity for chronic use must be carefully investigated and this should include monitoring the accumulation of polymeric particles, and their decomposition products, which can hinder the surfactant function in the lung.

Biodegradable polymer-based NPs offer an additional advantage for vaccine delivery systems by acting as adjuvants and aiding in activating both cellular and humoral immune responses [153]. It has been reported that upon phagocytosis by APCs, such as DCs, these NPs release the antigen intercellularly and elicit $CD8^+$ and $CD4^+$ T cell responses [154].

In a study performed by Bivas-Benita *et al.* (2004), the potential of enhanced immunogenicity upon pulmonary delivery of DNA encapsulated in chitosan NPs

was evaluated [155]. Chitosan-DNA NPs were prepared by the complexation-coacervation method and the resultant DNA-loaded NPs had an average size of 376±59 nm (*n*=5), zeta-potential of 21±4 mV (*n*=5) and a loading efficiency of 99%. Pulmonary administration of the chitosan-DNA NPs was shown to induce increased levels of interferon-γ (IFN-γ) secretion compared to pulmonary delivery of the plasmid in solution and the intramuscular immunisation route. This indicates the plausibility of achieving pulmonary delivery of DNA vaccines with increased immunogenicity against tuberculosis compared to immunisation through the intramuscular route [155].

The polyesters PLA and PLGA are broadly investigated synthetic polymers in the field of drug delivery [138,139,156]. They are rapidly hydrolysed upon introduction into the body and are eventually removed by the citric acid cycle. The hydrolysed products form at very slow rate and include lactic acid and glycolic acid which are biologically compatible and easily metabolised making them safe and non-toxic [139,157]. However, the acidic degradation products can cause problems by eliciting inflammation and also a reduction in pH within the micro and nanoparticles and the environment resulting in the hydrolysis of the macromolecules [158].

Muttil *et al.* prepared novel NP-aggregate formulations using PLGA and rHBsAg and showed that the dry powder formulations elicited a high mucosal immune response after pulmonary immunisation of guinea pigs without the need for adjuvants [149]. They prepared three different formulations of dry powders by spray-drying with leucine, (1) rHBsAg encapsulated within PLGA/PEG NPs (antigen NPs, AgNSD), (2) a physical mixture of rHBsAg and blank PLGA/PEG

NPs (antigen NP mixture (AgNASD), and (3) rHBsAg encapsulated in PLGA/PEG NPs with free rHBsAg (antigen NPs plus free antigen). All the particles had mass median aerodynamic diameter of around 4.8 µm and a fine particle fraction of 50%. After immunisation the highest titre of serum IgG antibodies was observed in the control group immunised with alum adsorbed with rHBsAg (Alum Ag, intramuscular route) whereas the highest IgA titres were observed for animal groups immunised with powder formulations via the pulmonary route. It was also noteworthy that guinea pigs immunised with AgNASD dry powder exhibited IgG titers above 1,000 mIU/ml in the serum (required 10 mIU/ml) suggesting the potential of administering novel dry powder formulations via the pulmonary route [149].

An alternative biodegradable polyester, poly(glycerol adipate-co-ω-pentadecalactone), PGA-co-PDL, has been extensively studied for the delivery of both small molecule drugs (dexamethasone phosphate, ibuprofen, sodium fluorescein), and large molecule drugs (α-chymotrypsin, DNase I) [159–163]. In this project, PGA-co-PDL will be utilised for developing an alternate particulate delivery system employing NPs for vaccine delivery.

1.4.3 Preparation of Polymeric Nanoparticles

The incorporation of macromolecules into polymeric particles can be achieved by encapsulation or adsorption using various methods, e.g. single or double emulsion solvent evaporation, salting out, solvent displacement, and coacervation [65]. The technique that is utilised depends on the physicochemical activity and stability of

the macromolecule to be delivered and the proposed application requirements such as: solubility, release and elimination [164].

1.4.3.1 Emulsification Solvent Evaporation

The emulsification solvent evaporation technique is the most commonly used method of preparing NPs. It involves the emulsification of an organic phase into an aqueous phase which is then subjected to organic solvent removal. The polymer (with or without the drug) is solubilised in an organic solvent, e.g. dichloromethane, ethyl acetate, chloroform, or acetone and then poured into an aqueous phase (often containing an emulsifier) and either sonicated or homogenised under high pressure [165]. The organic solvent is then evaporated by continuous stirring to form NPs (Figure 1-8). The particle size and distribution can be adjusted by varying the type, viscosity and amount of organic and aqueous phases, stirring rate, pressure, and temperature [164]. This technique can be used to encapsulate water soluble and water insoluble molecules; however, agglomeration of nanodroplets during the evaporation phase is a drawback. Moreover, for encapsulation of macromolecules the double emulsion solvent evaporation technique must be employed wherein the macromolecule is initially dissolved in an aqueous medium which is emulsified in an organic solution followed by emulsification in a second aqueous phase. HBsAg has previously been encapsulated using this method in PLA and PLGA NPs of size ~774 and 474 nm, respectively [90].

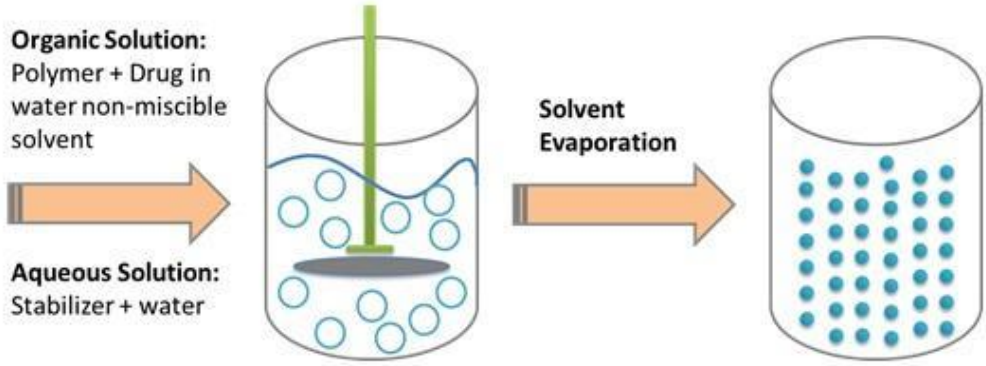

Figure 1-8 Schematic representation of the emulsification/solvent evaporation technique (modified from [65])

1.4.4 Encapsulation or Adsorption

A high loading capacity is one of the most desired qualities of NP-based vaccines. The main advantage of having a high loading capacity is that the amount of polymer required to carry the drug or vaccine is reduced [166] hence minimising any toxic effects from the polymer. Drugs can be loaded into or onto NPs using two approaches (Figure 1-9) [167]. The first is encapsulation where the drug is incorporated into the NP at the time of preparation; the second is adsorption where the drug is either chemically or physically adsorbed onto the NP after preparation.

It is important to note that the chemical structure of the drug, the polymer and the conditions of drug loading all influence the amount of drug bound to the NPs and the type of interactions that occur between them [166]. In addition, the encapsulation or adsorption of a drug depends on the disease to be treated or prevented, route of administration, manufacturing feasibility and economic challenges.

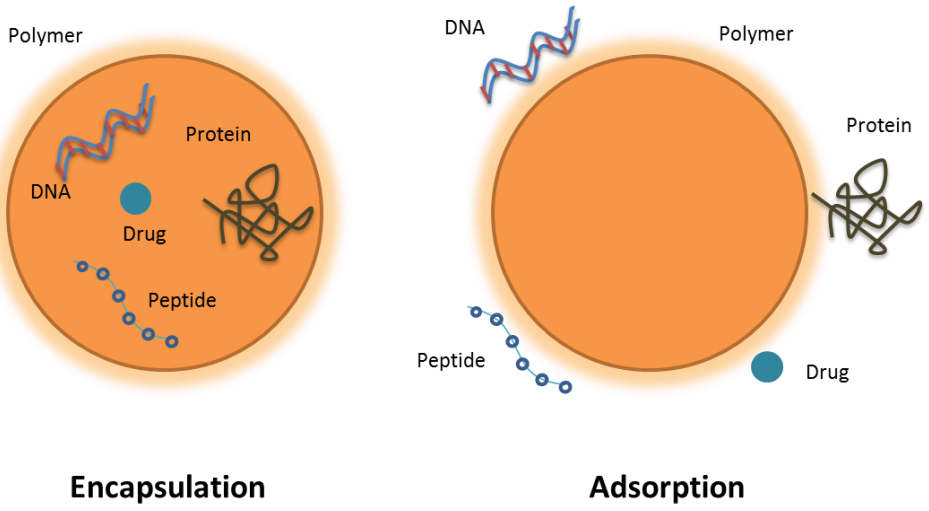

Figure 1-9 The molecule of interest (DNA/Drug/Peptide/Protein) is either encapsulated *(Left)* within or surface adsorbed *(Right)* onto the polymer-based nanoparticle (adopted from [65])

Bivas-Benita *et al.* prepared PLGA–polyethyleneimine (PEI) NPs by an interfacial deposition method [168]. The resultant NPs were loaded with *Mtb* Ag85B by adding the NP suspension to 25 µg/ml DNA plasmid solution. The characterisation studies revealed that the particle size increased from 235 to 275 nm upon re-suspension in water with the mean zeta-potential increase from +38.8 mV to +40.6 mV, respectively. The NPs greatly stimulated human DCs resulting in the secretion of interleukin-12 (IL-12) and tumour necrosis factor-α (TNF-α) at comparable levels to that observed after stimulation using lipopolysaccharide (LPS) [169].

Biodegradable polymer-based NPs have been widely explored and appear to be well tolerated when administered into the body. These NPs have gained significant attention and are being accepted as effective delivery systems with the development of NP-based vaccines [170,171]. In addition, the NP-based vaccines

need to be formulated appropriately, as dry powders and at low cost to help achieve effective mass vaccination.

1.4.5 Adjuvants

Modern day vaccines contain pure recombinant or synthetic antigens that are less immunogenic than live or inactivated whole organism vaccines. Thus, in order to obtain a strong immune response upon administration of antigen and provide long term protection against the infection, adjuvants are included within the formulation [172]. Adjuvants are substances used in combination with an antigen to produce a stronger and more robust immune response than the antigen alone [173]. Adjuvants also; provide a depot for the antigen favouring a slow release, reduce the dose of antigen required to generate a strong immune response, modulate the immune response, aid in targeting the APCs and provide danger signals helping the immune system respond to the antigen [172–174]. The selection of an adjuvant depends on the antigen, delivery system, route of administration and possible side-effects. However, an ideal adjuvant should have a long shelf-life and be safe, stable, biodegradable, economical and should not induce an immune response against themselves [172].

Despite massive efforts over nearly 90 years into the research and development of adjuvants, the list of adjuvants that are clinically approved is short [175]. Alum salts have a well-established safety record, are the most widely used human adjuvants and are used as standards to assess other adjuvants [172,173,175,176]. Despite this wide use their mechanism is poorly understood [172]. The main hurdle in the development of new adjuvants is safety [177]. However, research is

now focused on delivering antigens via particulate carriers acting as delivery systems [173,177].

Recently, antigen-loaded polymeric NPs have shown to possess a significant potential as effective vaccine delivery systems and adjuvants [82,139,178–183]. It is observed that the uptake by DCs is enhanced and a more efficient immune response generated for particulate antigen delivery systems compared to soluble antigen. The adjuvant effect observed for particulate antigen delivery systems is largely a result of their uptake by DCs [82,180,181].

1.5 Dry Powder Preparation Techniques

The use of liquid suspensions of NPs is often accompanied by several disadvantages such as particle aggregation and sedimentation leading to physico-chemical instability, reduced or loss of biological activity of the drug, contamination and hydrolysis leading to degradation of the polymer [184]. To overcome these problems, preparations can be stored and transported in a dry form [184]. In addition, for vaccines, the delivery of a dry powder by inhalation has the potential benefits of a) increased stability during transport and administration with no cold-storage and trained medical personnel required, b) increased safety by eliminating contamination risks and c) improved cost-effectiveness [185]. The most commonly used methods for converting liquid preparations into dry powders are freeze-drying (FD), spray-drying (SD), spray-freeze-drying (SFD) and the use of super critical fluid technologies. Each of these methods has advantages and disadvantages and selection is dependent on the desired attributes such as narrow particle size distribution, improved

bioavailability, enhanced stability, improved dispersibility and controlled release [133,186].

1.5.1 Spray-Drying

Spray-drying (SD) is a one-step preparation of dry powders. It is a process that converts liquid feed (solution, suspension or colloidal dispersion) into dry particles [187]. The process can be divided into four parts [188]: (1) atomisation, (2) spray-air contact, (3) drying and (4) separation. The liquid feed is atomised *(1)* to break the liquid into droplets and this spray form comes into contact with a hot gas *(2)*, causing rapid evaporation of the droplets to form dry particles *(3)*. The dry particles are then separated from the hot gas with the help of a cyclone *(4)* [186]. Compared to particles obtained from micronisation using milling, spray-dried particles are more spherical and have a homogenous size-distribution resulting in a higher respirable fraction which is advantageous for pulmonary delivery [186]. In addition, SD has the advantage of being; simple, easily scalable, cost-effective, suitable for heat-sensitive products and enables high drug loading [188]. An economically acceptable yield can now be achieved with the fourth and newest generation of laboratory-scale spray dryer developed by Büchi, the Nano Spray Dryer B-90. This nano spray dryer can generate particles of size ranging from 300 nm to 5 μm for milligram sample quantities at high yields (up to 90%) [189]. However, there is a chance of degradation of macromolecules during the process due to high shear stress in the nozzle and thermal stress while drying [186]. Fourie *et al.* formulated a dry powder TB vaccine for delivery to the lung by preparing *Mycobacterium bovis* Bacillus Calmette-Guérin (BCG) spray-dried

particles which, when administered into *M. tuberculosis* infected guinea-pigs, resulted in enhanced immunogenicity levels compared to an equal dose injected subcutaneously into control animals [87].

Table 1-4 highlights some recent studies that have employed various dry powder preparation techniques and the subsequent evaluation for vaccine delivery.

Table 1-4 Dry powder particle-based vaccine delivery (adopted from [65])

Disease	Antigen	Carrier / Stabiliser	Dry Powder Preparation	Size (μm)	Model	Ref
Bacterial Infections	Bacteriophages	Trehalose, Leucine	SD	2.5 – 2.8	NA	[190]
Diptheria	Diptheria Toxoid	Chitosan	SCF	3 – 4	GP	[134]
Diptheria	Diphtheria CRM-197 antigen	L-leu	SD	~ 5	GP	[91]
Hepatitis B	rHBsAg	Leucine	SD	4.8	GP	[149]
Influenza	Influenza monovalent	Inulin	SD, SFD	2.6 (SD), 10.5 SFD)	M	[191]
Influenza	Influenza subunit	Inulin	SFD	~ 10	M	[89]
Tuberculosis	Ad35-vectored tuberculosis (TB) AERAS-402	mannitol-cyclodextrin-trehalose-dextran, MCTD	SD	3.2 – 3.5	NA	[192]
Tuberculosis	BCG	Leucine	SD	2 – 3	GP	[193]
Tuberculosis	rAg85B	NA	SD	2.8	GP	[194]

Note: SD – Spray-drying, SFD – Spray-freeze-drying, SCF – Supercritical Fluid; M – Mice, GP – Guinea Pigs; NA – Not Available

Optimal delivery of macromolecules to the lungs depends on the interaction between the inhaler device, the properties of the formulation and the inhalation manoeuvre [83]. In animal studies the site of lung deposition was shown to be strongly related to the method of delivery. The aerosol inhalation method resulted in a more uniform lung distribution, compared to liquid instillation, and produced more pronounced distribution into the alveolar region [195,196].

Present-day inhalation devices can be divided into three categories, nebulisers, MDIs and DPIs. Macromolecules are very unstable in aqueous solutions at room temperature; thus limiting their usage by nebulisers. Furthermore, the shear stress exerted on the proteins during nebulisation can result in denaturation. MDIs, on the other hand, use propellants such as hydrofluoroalkanes for atomising the drug that can result in protein denaturation. DPIs are a better alternative as they can deliver the macromolecule in a more stable, dry powder form with little requirement for hand-mouth co-ordination; however care must still be taken to address the stability of the macromolecule of interest [83].

1.6 Aims

The purpose of this study was to design, formulate, characterise and evaluate dry powder NCMPs incorporating PGA-co-PDL NPs with surface adsorbed PspA4Pro for pulmonary vaccine delivery against pneumococcal disease.

This was accomplished using the following specific objectives:

1. To investigate and optimise single emulsion solvent evaporation processing parameters for the preparation of PGA-co-PDL NPs.

   a) Use a design of experiment to obtain optimum NP size for uptake into DCs by evaluating different formulation and process parameters.

   b) Study the effect of surface charge of NPs on protein surface adsorption.

   c) Evaluate NPs cytotoxicity and uptake by DCs in vitro.

   d) Optimise bovine serum albumin (BSA) surface adsorption onto optimum NPs (concentration, time and amount of NPs) and apply the optimum conditions for PspA4Pro surface adsorption.

2. To successfully incorporate optimum protein adsorbed PGA-co-PDL NPs into NCMPs by SD using L-leu as a microcarrier.

   a) Produce optimum NCMPs with high yield and low moisture content.

   b) Investigate BSA and PspA4Pro release and aerosol properties from optimum NCMPs carriers in vitro.

   c) Investigate BSA and PspA4Pro stability and integrity after release from optimum formulations and then evaluate the activity of released BSA and relative antigenicity of released PspA4Pro.

   Figure 1-10 depicts a graphical representation of the aim of the project.

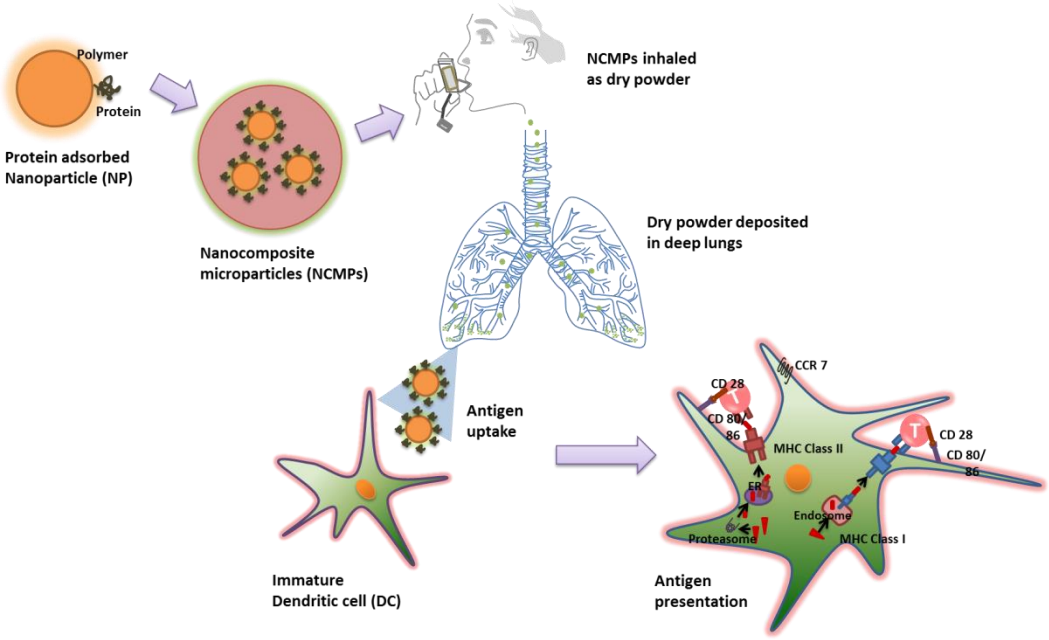

Figure 1-10 Graphical representation showing the pulmonary delivery of pneumococcal vaccine

2. Materials and General Methods

2.1 Materials

Acetonitrile (ACN, HPLC grade), ammonium molybdate, ω-pentadecalactone, bovine serum albumin (BSA, MW 67 kDa), dichloromethane (DCM), didodecyldimethylammonium bromide (DMAB), fluorescein isothyocyanate-BSA (FITC-BSA), glycerol, mannitol, 3-(4,5-dimethylthiazol-2-yl)-2,5-diphenyl tetrazolium bromide (MTT), nile red dye (NR), phosphate buffered saline (PBS) tablets, poly(vinyl alcohol) (PVA, MW 9-10 kDa, 80% hydrolysed), trehalose, tri-fluoroacetic acid (TFA, HPLC grade), Roswell Park Memorial Institute (RPMI-1640) medium with L-glutamine and $NaHCO_3$, Tween 80®, sucrose and antibiotic/antimycotic (100X) solution were obtained from Sigma-Aldrich, UK. Novozyme 435 was purchased from Biocatalytics, USA. L-leucine (L-leu) was purchased from BioUltra, Sigma, UK. Tissue culture flasks (25 and 75 cm^2) with vented cap, 96-well flat bottom and 'U' shaped plates, acetone, chloroform, dimethyl sulfoxide (DMSO), methanol and tetrahydrofuran (THF) were purchased from Fisher Scientific, UK. Alpha minimum essential medium (α-MEM) and granulocyte macrophage colony-stimulating factor (GM-CSF) was purchased from Life Technologies, UK. Divinyladipate was obtained from Fluorochem, UK. Heat inactivated foetal calf serum (FCS) was purchased from Biosera UK. Micro BCA™ protein assay kit was purchased from Thermo Scientific, UK. Adenocarcinomic human alveolar basal epithelial cell line, A549 (CCL-185™) and dendritic cell line, JAWS II (CRL-11904™) were purchased from American Type Culture Collection (ATCC). The human bronchial epithelial, 16HBE14o- cell line was a kind gift from Dr Dieter Gruenert from the University of California San

Francisco, USA. Recombinant PspA4Pro was a gift from Dr Eliane Miyaji and Dr Viviane Gonçalves from the Insituto Butantan, Brazil

2.2 General Methods

2.2.1 Polymer Synthesis

PGA-co-PDL was enzymatically synthesised by a combination of ring opening polymerisation and polycondensation (scheme 2-1) as described by Namekawa *et al.* and Thompson *et al.* [197,198]. Briefly, equimolar concentrations (125 mmol) of ω-pentadecalactone, divinyl adipate and glycerol were added to a dry round bottomed flask, followed by the addition of 15 ml of THF. The flask was then immersed into a water bath maintained at 50 °C. The system was fitted with an open top condenser, acting as an outlet for the acetaldehyde produced, and a central mechanical stirrer paddle (Heidolph RZR1 type mechanical stirrer, mounted horizontally and set at #6) was attached via a teflon shaft, which was placed through a quick-fit thermometer adapter, to a 75 mm teflon paddle. The mixture was stirred for 15-20 min to allow the temperature to equilibrate and then 1.25 g of Novozyme 435 (a lipase derived from *Candida antartica* and immobilised on an acrylic macroporous resin) was added and the reaction was left to proceed for 6 h (to obtain a MW of 14.7 kDa) or 24 h (to obtain a MW of 24.0 kDa). Upon completion, DCM (~ 100 ml) was added to the reaction mixture and the contents were filtered through grade 1 filter paper (Whatman, UK) by standard Büchner filtration to remove the residual immobilised enzyme and stop any further reaction. The solvent was then removed (with little DCM left) through rotary evaporation (60 °C, Heidolph Laborota 4000). To the obtained highly

viscous mixture 150 ml of methanol was added to precipitate the polymer and leave unreacted monomers and oligomers in solution which were filtered using Büchner filtration. The resultant precipitated polymer was transferred to a jar and left at room temperature for 48 h to remove any traces of solvent, then sealed and stored in a desiccator until further use.

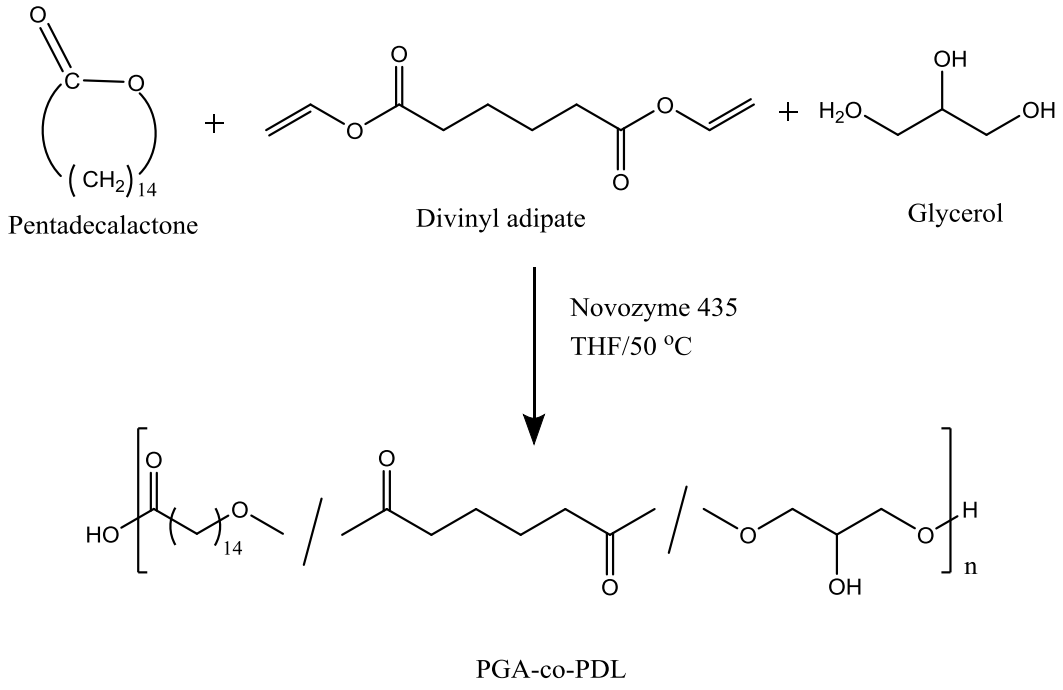

Scheme 2-1 Enzymatic synthesis of poly(glycerol adipate-co-ω-pentadecalactone), PGA-co-PDL

2.2.2 Polymer Characterisation

The synthesised linear polyester, PGA-co-PDL, was analysed using the following techniques:

2.2.2.1 Gel Permeation Chromatography

Gel permeation chromatography (GPC, Viscotek TDA Model 300 using OmniSEC3 operating software) was used to determine the molecular weight of

the obtained polymers. The system was fitted with two PLgel 5 µm MIXED-D 300x7.5 mm columns (Varian, Polymer Laboratories, UK), stored in the detector oven at 40 °C, operated at a flow rate of 1 ml/min using chloroform as a solvent. The system was pre-calibrated with polystyrene standards of different molecular weights (polystyrene standards kit, Supelco, USA).

2.2.2.2 Fourier Transform Infrared Spectroscopy

The chemical structure of PGA-co-PDL was analysed using a Perkin Elmer Spectrum BX Fourier transform infrared (FT-IR) spectrometer (Perkin Elmer, USA). The spectra was collected from 400 to 4000 cm^{-1} at a resolution of 4 cm^{-1}, analysed using the Perkin Elmer Spectrum software (Perkin Elmer, USA). Each sample was measured with 32 scans.

2.2.2.3 Proton Nuclear Magnetic Resonance

The chemical structure of the synthesised PGA-co-PDL was characterised using proton nuclear magnetic resonance (^{1}H-NMR). The ^{1}H-NMR spectra was recorded on a Bruker Avance 300 MHz spectrometer, inverse probe with B-ACS 60 and auto sampler with gradient chemming. The obtained spectra were analysed using MestReNova software.

2.2.2.4 Differential Scanning Calorimeter

The differential scanning calorimeter (DSC) data was obtained using a Perkin Elmer DSC 8000 controlled by Pyris software. The system had previously been calibrated using an indium reference standard. The polymer sample, 3-5 mg, was hermetically sealed in standard aluminium pans and scanned at heating and cooling rates of 10 °C min^{-1} under nitrogen. The T_m (melting point) and T_g (glass

transition temperature) were recorded from the second heating scan after previously heating to 75 °C followed by cooling to −90 °C, before commencing data collection.

2.2.3 Preparation of Nanoparticles

The PGA-co-PDL NPs were fabricated using an oil-in-water (o/w) single emulsion solvent evaporation method (Figure 2-1).

2.2.3.1 Negatively Charged Nanoparticles (Anionic NPs)

PGA-co-PDL (200 mg) was dissolved in 2 ml DCM and upon addition to 5 ml of 10% w/v PVA (1st aqueous solution) was probe sonicated (20 microns amplitude) for 2 min under ice to obtain an emulsion. This emulsion was immediately added drop wise to 20 ml of a 2nd aqueous solution (0.75% w/v PVA) under magnetic stirring at a speed of 500 RPM and stirred at room temperature for 3 h to facilitate the evaporation of the DCM.

A Taguchi L_{18} orthogonal array design of experiment (DoE) was used to optimise the formulation parameters to achieve NPs of optimum size for targeting lung DCs.

2.2.3.2 Positively Charged Nanoparticles (Cationic NPs)

The same method as in section 2.2.3.1 was used with some modifications. Briefly, 200 mg PGA-co-PDL and DMAB (0, 1 and 2% w/w of polymer) were dissolved in 2 ml DCM and upon addition to 5 ml of 5% w/v PVA (1st aqueous solution) was probe sonicated (20 microns amplitude) for 2 min under ice to obtain an emulsion. This was immediately added drop wise to 20 ml of a 2nd aqueous

solution (0.75% w/v PVA) under magnetic stirring at a speed of 500 RPM and stirred at room temperature for 3 h to facilitate the evaporation of DCM.

The NPs were collected by centrifugation (Type 70.1 Ti rotor, Beckman L-80 Ultracentrifuge, UK) at 78,000 *g* for 40 min, 4 °C, washing twice with distilled water (~ 4 ml) to remove excess surfactant.

For confocal microscopy, nile red (NR, 0.5 mg) was added to the initial DCM polymer solution. The NPs were then collected by centrifugation as mentioned in section 2.2.3.2. Figure 2-2 represents an illustrative picture of the production of negatively and positively charged NPs.

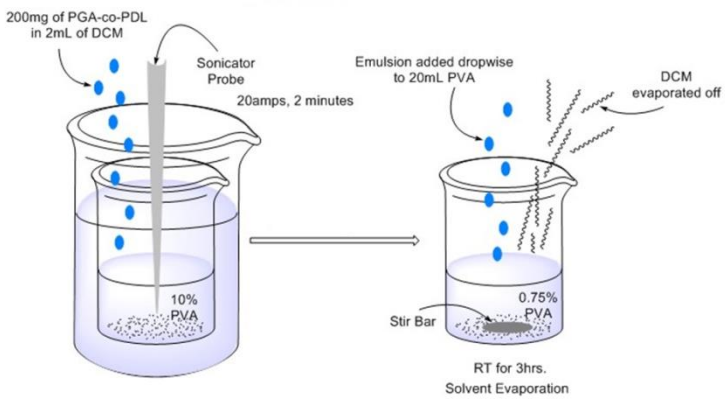

Figure 2-1 Schematic picture of nanoparticle preparation

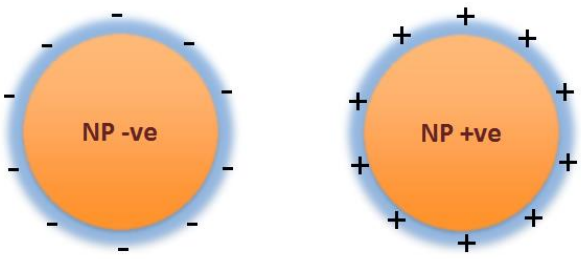

Figure 2-2 Illustrative picture of surface of negatively and positively charged nanoparticles

2.2.4 Characterisation of Nanoparticles

2.2.4.1 Particle Size and Zeta-potential

Particle size, poly dispersity index (PDI, a number between 0 and 1 describing the homogeneity of the sample) and zeta-potential were measured by dynamic light scattering using a particle size analyser (Zetasizer Nano ZS, Malvern Instruments Ltd, UK). An aliquot of 100 µl of the NP suspension was diluted with 5 ml of deionised water, loaded into a cuvette and the measurements were recorded at 25 °C (n=6).

2.2.4.2 Morphology

Morphological analysis of NPs was performed by transmission electron microscopy (TEM) using a FEI Morgagni Transmission Electron Microscope (Philips Electron Optics BV, The Netherlands) using acceleration voltage 100.0 kV. Approximately 50 µl of the NP suspension was negatively stained with 2% ammonium molybdate and placed on a carbon coated copper grid. Digital images were taken at 44,000 and 110,000 times magnification.

2.2.5 Protein Adsorption onto Nanoparticles

Protein was directly adsorbed onto the NPs in the suspension obtained after centrifugation following removal of excess surfactant. The NP suspension (1.25 ml equal to 10 mg of NPs by weight) was then transferred into vials and the volume made up to 4 ml with distilled water, washing twice by centrifugation. The obtained pellets were re-suspended in 4 ml of protein solutions at ratios of NP:Protein (500 µg/ml concentration for anionic NPs and 100 µg/ml

concentration for cationic NPs). The resultant suspension was left rotating for 1 h at 20 RPM on a HulaMixer™ sample mixer (Life Technologies, Invitrogen, UK) at room temperature. The protein adsorbed NP suspensions were transferred into ultracentrifuge tubes and centrifuged (as in section 2.2.3.2). The supernatant was then collected and analysed for protein content as described in section 2.2.6.1.

2.2.5.1 Characterisation

Particle size, PDI and zeta-potential of NPs with and without protein adsorption were characterised as described in section 2.2.4.1. Briefly, 2 mg of NPs were re-suspended in 5 ml of deionised water, loaded into a cuvette and the measurements were recorded on a Malvern Zetasizer Nano ZS at 25 °C (n=3).

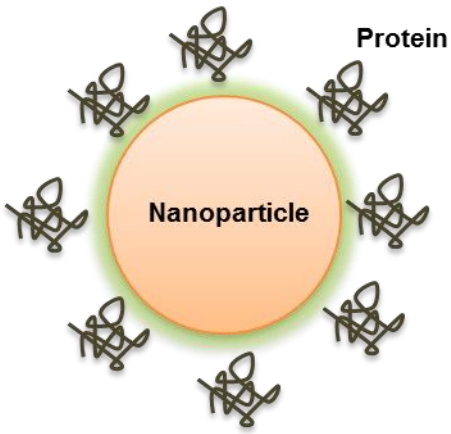

Figure 2-3 Illustrative picture of nanoparticle after protein adsorption

2.2.6 Protein Quantification

Micro BCA protein assay and high performance liquid chromatography (HPLC) were employed to quantify the protein adsorbed onto NPs or released from formulations.

2.2.6.1 Micro BCA Protein Assay

The Micro BCA protein assay is based on colorimetric detection and was employed as a protein quantitation technique [199]. BSA standards or protein samples (150 µl) were loaded as triplicates onto a 96-well plate. To each well, 150 µl of working reagent was added and the plate was placed in an incubator at 37 ºC for 2 h. Following this, the plate was cooled to room temperature and the absorbance was measured at 562 nm using a plate reader (Epoch, BioTek Instruments Ltd, UK).

The amount of protein adsorbed in µg per mg of NPs (n=3) was calculated using equation 2-1:

$$\text{Adsorption (µg per mg of NPs)} = \frac{\text{(Initial protein conc-Supernatant protein conc)}}{\text{Amount of NPs}} \quad \text{(eq. 2-1)}$$

2.2.6.2 High Performance Liquid Chromatography

HPLC is an analytical technique used to quantify the amount of a substance in a given sample. Here, a HPLC method was developed, based on literature [199,200], to quantify the amount of protein, either BSA or PspA4Pro, present in a given sample. The optimal chromatographic conditions employed were as follows: HPLC system Agilent 1100 series (Santa Clara, USA) equipped with a column (Aeris 3.6 µm C4 200A^{o} Wide Pore 4.6 mm i.d. x 150 mm length), security cartridge of the same material (Phenomenex, UK); mobile phase was composed of (A) 0.1% w/v TFA in water and (B) 0.1% w/v TFA in ACN with a gradient flow of A/B from 80:20 to 35:65 in 25 min, post-time 6 min; flow rate of 0.8 ml/min; injection volume of 100 µl; run temperature 40 °C; UV detection at 214 nm and BSA retention time of 14.4 min, PspA4Pro retention time of 14.9

min. Respective protein calibration curves were prepared by accurate dilution of a previously prepared stock solution (1 mg/ml) in HPLC water and PBS (pH 7.4) to obtain the following concentrations: 0.5, 1, 2.5, 5, 10, 25, 50, 100 and 200 µg/ml of protein (n = 9, R^2 = 0.999). All solutions used in the process were filtered using 0.45 µm filters prior to use.

The method was validated based on the international conference on harmonisation (ICH) guidelines for validation of analytical procedures. Parameters such as accuracy, precision, limit of detection (LOD) and limit of quantification (LOQ) were used for validation (appendix-1).

2.2.7 Preparation of Nanocomposite Microparticles

Spray-drying was used to incorporate the NPs into NCMPs using L-leu as a microcarrier at nanoparticle-to-carrier ratio of 1:1.5 w/w. Blank NPs or protein-adsorbed NPs (NP/BSA or NP/PspA4Pro) were dispersed in 20 ml solution of L-leu dissolved in distilled water and spray-dried using a Büchi B-290 mini spray-dryer (Büchi Labortechnik, Flawil, Switzerland) with a nozzle atomiser and nozzle orifice diameter of 0.7 mm. The final conditions used were: pump rate of 10%, an atomising air flow of 400 L/h, aspirator capacity of 100% and an inlet temperature of 100 °C (corresponding outlet temperature of approximately 45-47 °C). The dry particles (NCMPs) were separated from the air stream using a high-performance cyclone (Büchi Labortechnik), collected and stored in desiccator until further use. Figure 2-4 shows an illustration of NCMPs containing protein adsorbed NPs.

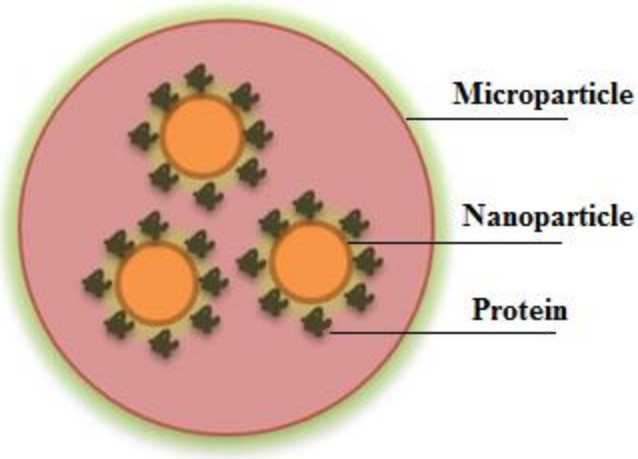

Figure 2-4 Illustrative picture of nanocomposite microparticle containing protein adsorbed nanoparticles

2.2.8 Characterisation of Nanocomposite Microparticles

2.2.8.1 Yield, Particle Size and Morphology

The dry powder yield was determined as the difference in the weight of the sample vial before and after product collection. The weight difference was compared to the initial total dry mass and the yield in % (w/w) was calculated (n=3).

The particle size and PDI of NPs following re-dispersion of blank and loaded NCMPs in distilled water were measured to confirm the NPs recovered were within an appropriate size range for cellular uptake. Particle size and PDI of NPs after re-dispersion were measured as described in section 2.2.4.1. Briefly, 5 mg of NCMPs were dispersed in 2 ml of deionised water, loaded into a cuvette and the measurements were recorded on a Malvern Zetasizer Nano ZS at 25°C (n=3).

Spray-dried NCMPs samples were mounted on aluminium stubs (pin stubs, 13 mm) layered with a sticky conductive carbon tab and coated with palladium (10-

15 nm) using a sputter coater (EmiTech K 550X Gold Sputter Coater, 25 mA for 3 min). The particles were then visualised using scanning electron microscopy (SEM, FEI Quanta™ 200 ESEM, The Netherlands).

2.2.8.2 Moisture Content

Thermo gravimetric analysis (TGA) was used to determine the moisture content in the spray-dried samples. Measurements were carried out in triplicate using a TA Instruments TGA Q50, UK equipped with TA Universal Analysis 2000 software. Solid samples (4-15 mg) analysed in triplicate were loaded on an open platinum TGA pan suspended from a microbalance and heated from 25 to 650 °C at 10 °C min^{-1}. The water content was analysed for data collected between 25 to 120 °C.

2.2.9 Characterisation of Protein Nanoparticle Associations

Confocal laser scanning microscopy (CLSM) was used to confirm the adsorption of protein onto NPs. FITC-BSA (green) was adsorbed onto the surface of NR (red) containing NPs as described in section 2.2.5, followed by SD into NCMPs. The obtained powders were then observed under the confocal microscope to visualise the adsorption of BSA onto the NPs. Confocal imaging was performed using our previously published method [160]. Briefly, a Zeiss 510 META laser scanning microscope mounted on an Axiovert 200 M BP computer-controlled inverted microscope was used to obtain the images. A tiny amount (~1-2 mg) of spray-dried NCMPs were placed in a single well of 8-well chamber slide (Fisher Scientific, UK) and imaged by excitation at a wavelength of 488 nm (green channel for FITC-BSA) and 543 nm (red channel for NR/NPs) using a Plan

Neofluar 63X/0.30 numerical aperture objective lens. Image analysis was carried out using the Zeiss LSM software.

2.2.10 In vitro Release Studies

The optimum formulations (20 mg) were transferred into eppendorfs and dispersed in 2 ml of PBS, pH 7.4. The samples were incubated at 37 °C and left rotating for 48 h at 20 RPM on a HulaMixer^{TM} sample mixer (Life Technologies, Invitrogen, UK). At pre-determined time intervals up to 48 h, the samples were centrifuged (accuSpin Micro 17, Fisher Scientific, UK) at 17,000 g for 30 min and 1 ml of the supernatant removed and replaced with fresh medium. The supernatant was analysed for protein content using the method described in section 2.2.6. Each experiment was repeated in triplicates and the result was the mean value of three different samples (n=3).

The percentage cumulative protein released was calculated using equation 2-2:

$$\% \text{ Cumulative protein released} = \frac{\text{Cumulative protein released}}{\text{BSA loaded}} \times 100 \quad \text{(eq. 2-2)}$$

2.2.11 Investigation of Protein Structure

2.2.11.1 Sodium Dodecyl Sulfate-Polyacrylamide Gel Electrophoresis

The primary structure of the protein (BSA and PspA4Pro) released from the NCMPs after SD was determined by sodium dodecyl sulfate-polyacrylamide gel electrophoresis (SDS-PAGE). The SDS-PAGE was performed on a CVS10D omniPAGE vertical gel electrophoresis system (Geneflow Limited, UK) with 9% stacking gel prepared using ProtoGel stacking buffer (Geneflow Limited, UK)

containing 0.4% SDS. Protein molecular weight markers in the range 10–220 kDa (Geneflow Limited, UK) and respective protein standards were used as controls. The protein loading buffer blue (2X) (0.5 M Tris-HCl (pH 6.8), 4.4% w/v SDS, 20% v/v glycerol, 2% v/v 2-mercaptoethanol and Bromphenol blue in distilled/deionised water) was added to the samples in a 1:1 (v/v) buffer-to-sample ratio. After loading the samples (25 µl per well), the gel was run for approximately 2.5 h at a voltage of 100 V with Tris-glycine-SDS PAGE buffer (10X) (Geneflow Limited, UK) containing 0.25 M Tris base, 1.92 M glycine and 1% w/v SDS. The gel was stained with colloidal Coomassie blue G and then destained overnight in distilled water. An image of the gel was scanned on a gel scanner (GS-700 Imaging Densitometer, Bio-Rad) equipped with Quantity One software.

2.2.11.2 Circular Dichroism

The secondary structure of standards and released proteins (BSA and PspA4Pro) was determined by recording the circular dichroism (CD) spectra. All CD experiments were performed using a J-815 spectropolarimeter (Jasco, UK) at 20 °C as previously described [201]. Five scans per sample using a 10 mm path-length cell were performed over a wavelength range 260 to 180 nm at a data pitch of 0.5 nm, band width of 1 nm and a scan speed 50 nm/min. Far-UV CD spectra were collated for all samples. For all the spectra, the baseline acquired in the absence of sample was subtracted [202]. The secondary structure of the samples was estimated using using the CDSSTR method [203] from the DichroWeb server [203–205].

2.2.12 In vitro Aerosolisation Studies

A next generation impactor (NGI) was employed to assess the aerosol performance of spray-dried NCMPs. The protein containing NCMPs (BSA adsorbed NPs/NCMPs or PspA4pro adsorbed NPs/NCMPs) were weighed (4 or 5 capsules, each corresponding to 12.5 mg spray-dried powder and equivalent to 5 mg of NPs) and manually loaded into a hydroxypropyl methylcellulose, HPMC, capsule (size 3), and placed in a Cyclohaler® (Teva Pharmaceutical Industries Ltd.). The samples were drawn through the induction port into the NGI using a pump (Copley Scientific, Nottingham, UK) operated at a flow rate of 60 L/min for 4 s. The plates were coated with 1% Tween 80:acetone solution and samples collected using a known volume of distilled water or 2% SDS for NCMPs containing anionic NPs or cationic NPs, respectively. The samples collected were left on a roller-shaker for 24-48 h for the BSA/PspA4Pro to be released from the NCMPs and then centrifuged using an ultracentrifuge (as described in section 2.2.3.2). The supernatants were then analysed using the Micro BCA protein assay (section 2.2.6.1) or HPLC method (section 2.2.6.2) for NCMPs containing cationic NPs or anionic NPs, respectively, to determine the amount of BSA/PspA4Pro deposited in each stage. The emitted dose was defined as the amount of drug exiting the inhaler. The fine particle fraction (FPF, %) was determined as the fraction of emitted dose deposited in the NGI with $d_{ae} < 4.46$ μm, the mass median aerodynamic diameter (MMAD) was calculated from log-probability analysis, and the fine particle mass (FPM) was expressed as the mass of drug deposited in the NGI with $d_{ae} < 4.46$ μm (n=3) in one actuation. Additionally, the percentage deposition (%) of protein in each stage was

calculated as the percentage of ratio of amount of protein collected in each stage to that of total amount of protein collected in all stages.

2.2.13 Cell Viability Studies

The in vitro cytotoxicity of the anionic NPs and NPs/NCMPs, and cationic NPs and NPs/NCMPs on different cell lines were evaluated using the 3-(4,5-dimethylthiazol-2-yl)-2,5-diphenyltetrazolium bromide (MTT) assay [206].

Three cell lines, namely, (i) adenocarcinomic human alveolar epithelial cell line, A549, (ii) the human bronchial epithelial cell line, 16HBE14o-, and (iii) DCs, JAWS II (ATCC® CRL 11904™) mouse immature dendritic cell; monocyte, were used to assess the cytotoxicity of NPs and NCMPs with the MTT assay.

Cell lines (i) and (ii) were grown in RPMI-1640 medium supplemented with 10% FCS and 1% antibiotic/antimycotic solution (complete growth medium 1) in an incubator at 37 °C supplemented with 5% CO_2 in either 25 or 75 cm^2 tissue culture flasks. Cell line (iii) was grown in α-MEM containing ribonucleosides, deoxyribonucleosides, 4 mM L-glutamine, 1 mM sodium pyruvate supplemented with 20% FCS, 5 ng/ml murine GM-CSF and 1% antibiotic/antimycotic solution (complete growth medium 2) in an incubator at 37 °C supplemented with 5% CO_2 in either 25 or 75 cm^2 tissue culture flasks.

For the MTT assay, cells were seeded in 100 µl (1.25×10^5-2.5×10^5 cells/ml) of their respective complete growth medium in 96-well plates and placed in an incubator at 37 °C for 24 h supplemented with 5% CO_2. Then, 100 µl of freshly prepared NP or NCMP dispersions in complete growth medium were added to the

wells to an appropriate concentration (0-2.5 mg/ml) (n = 3), using 10% dimethyl sulfoxide (DMSO) as a positive control. The NPs were assayed for toxicity over 4 h (DCs) and 24 h (A549) and the NCMPs over 24 h (A549 and 16HBE14o-) of incubation, followed by the addition of 40 µl of a 5 mg/ml MTT solution in PBS to each well. After 2 h of incubation at 37 °C, the culture medium was gently removed (for cell line (iii), the 96-well plate is centrifuged at 1300 *g* for 7 min at 4 °C to pellet the suspended cells) and replaced by 100 µl of DMSO in order to dissolve the formazan crystals. The absorbance of the solubilised dye, which correlates with the number of living cells, was measured at 570 nm using a plate reader (Epoch, BioTek Instruments Ltd, UK). The percentage of viable cells in each well was calculated as the absorbance ratio between treated and untreated control cells.

2.2.14 Statistical Analysis

All statistical analysis was performed using Minitab® 16 statistical software. One-way analysis of variance (ANOVA) with the Dunnett's multiple comparison test employed for comparing each formulation with the control formulation and Tukey's comparison employed for comparing the formulations with each other. Statistically significant differences were assumed when $p < 0.05$. All values are expressed as their mean ± standard deviation.

3. Bovine serum albumin adsorbed onto anionic PGA-co-PDL nanoparticles for vaccine delivery via dry powder inhalation

3.1 Introduction

Advancements in biotechnology in the last decade have led to the development of new therapeutics such as peptides, proteins and other macromolecules. However, the therapeutic application of these macromolecules is hugely impacted due to lack of effective and specific delivery strategies [207]. In addition, the presence of strong acids and proteases in the stomach limit their use via the oral route [208].

Biodegradable polymeric NPs have gained significant attention and are largely being explored as delivery vehicles for the delivery of peptides, proteins, antigens, DNA etc. [65,89,90]. Biodegradable polymers offer controlled or sustained drug release, biocompatibility with surrounding cells and tissues, degrade into low molecular weight non-toxic products and act as adjuvants helping to generate cellular and humoral immune responses [65,81,139]. In this current investigation, PGA-co-PDL, a biodegradable polyester, is to be employed that has previously been studied extensively for the delivery of both small molecule and model drugs (dexamethasone phosphate, ibuprofen, sodium fluorescein), and macromolecules (α-chymotrypsin, DNase I) [159–163].

In these biodegradable polymeric NP formulations, the vaccine antigens (i.e. proteins, peptides etc.) are either adsorbed onto the surface or encapsulated within the particles [65]. Encapsulated antigens are protected by polymeric NPs and their release can be modified by tailoring the properties of the polymers. Adsorbed antigen can offer enhanced stability and activity over the encapsulated antigen by avoiding contact with organic solvents employed during particle preparation [209–211].

NPs in the lungs can be up taken by APCs thereby generating an immune response. Recent strategies for effective vaccine delivery have included targeting the DCs, the true professional APCs [73]. DCs have the exceptional ability to internalise, and in LNs they process and present antigens through MHC class I and II pathways thereby activating naïve T-cells resulting in the induction of a strong immune response [65,73,212]. A study conducted by Manolova *et al.* indicated the importance of particle size in determining uptake by DCs, where it was shown that upon intracutaneous injection of polystyrene beads of varying sizes, large particles (500-2000 nm) associated with DCs from the site of injection whereas small particles (20-200 nm) drained freely to the LNs and were present in LN resident DCs [212]. In addition, Kim *et al.* also showed that uptake of 200 nm sized NPs by bone marrow DCs was greater than that of 30 nm sized NPs [213]. Furthermore, Foged *et al.* has shown that particles of size 500 nm or below were preferred and demonstrated fast and efficient uptake by human DCs derived from blood [113]. The above literature suggests that smaller particles of 200 to 500 nm size could effectively be up taken by DCs thus generating a stronger immune response compared to antigen alone. However, these studies cannot be directly compared to lung DCs as DCs from different parts of the body behave differently. However, due to the lack of information available on the effect of NP size on uptake by lung DCs a similar response can be assumed.

The Taguchi L_{18} orthogonal array DoE was used to optimise formulation parameters to achieve NPs of the desired size for targeting the lung DCs without the need to prepare a large number of different formulations. Literature suggests that factors such as molecular weight (MW) of the polymer, organic solvent,

surfactant concentration, i.e. the aqueous phase, sonication time and stirrer speed all have an influence on the size of the resultant NPs [214–216] and these parameters can be readily evaluated using experimental design.

As a dry powder, nanosized particles cannot be directly used for inhalation as they are too small and it is expected that the majority of the inhaled dose will be exhaled with a very minimal amount deposited in the lung [217]. Thus, NPs can be formulated into NCMPs using additives such as lactose [22], L-leu [218,219], trehalose [220], mannitol [220] by various manufacturing techniques such as FD, SD, SFD or supercritical fluid technologies [65,221]. The NCMPs in the size range of 1-5 μm in diameter are reported to be deposited in the respirable airways and periphery of the lung [120]. Moreover, the additives used to form NCMPs dissolve upon encountering the respiratory environment thereby releasing the NPs [167].

The aim of this chapter was to produce negatively charged PGA-co-PDL NPs (referred to as anionic NPs) of optimum size to be effectively up taken by the DCs, surface adsorb a model protein, BSA onto the surface of NPs and formulate the NPs by SD into NCMPs using L-leu as a carrier for delivery via dry powder inhalation.

3.2 Materials and Methods

3.2.1 Polymer Synthesis and Characterisation

The PGA-co-PDL was synthesised and characterised as described in section 2.2.1 and 2.2.2 respectively.

3.2.2 Preparation and Characterisation of Nanoparticles

The PGA-co-PDL NPs were prepared as described in section 2.2.3.1. The NPs were characterised for particle size, PDI, zeta-potential and morphology as described in section 2.2.4.

3.2.3 Optimisation of NP Size by Taguchi L_{18} Design

In order to evaluate the influence of formulation parameters and minimise the number of experiments, Taguchi DoE was employed through Minitab® 16 statistical software. Seven factors (polymer MW, organic solvent, internal aqueous phase concentration and volume, sonication time, stirrer speed and external aqueous phase concentration) were evaluated by constructing and using a L_{18} orthogonal array design with 1 factor, MW, at two levels and the remaining 6 factors at three levels (Table 3-1).

The design was applied to identify the significant factors that would affect the size of PGA-co-PDL NPs. The optimum conditions were indicated by high signal-to-noise (S/N) ratios, where signal factor (S) is the outcome, i.e. the particle size, and noise factors (N) are parameters such as humidity, temperature, experience of the experimenter etc.

A greater S/N ratio corresponds to minimum variance of the outcome, the particle size, i.e. a better performance. In other words, the experimental parameter having the least variability is the optimal condition [222]. The optimisation of size was carried out using the Taguchi's 'smaller-is-better' criterion, i.e. to achieve a particle size as small as possible.

Table 3-1 Taguchi's experimental design L_{18} for producing PGA-co-PDL nanoparticles

Levels	Units	1	2	3
A - MW of Polymer	kDa	14.7	24.0	-
B - Org Sol (DCM)	ml	1	1.5	2
C - Aq. Vol (PVA)	ml	3	4	5
D - 1st Aq. Conc (PVA)	% w/v	2.5	5	10
E - Sonication Time	min	1	2	5
F - Stirrer Speed	RPM	400	500	600
G - 2ndAq. Conc (PVA)	% w/v	0.5	0.75	1

3.2.4 Freeze-drying of Nanoparticle Suspensions

Sucrose, mannitol and trehalose were employed as cryoprotectants (CPs) for the FD of NP suspensions. Initially, stock solutions (10% w/v in distilled water) of the CPs were prepared. Following centrifugation, the NPs were re-suspended in the CP stock solutions at three different ratios of CP:NP (1.25:1, 2.5:1 and 5:1) and frozen at -80 °C for 24 h. The frozen CP:NP suspensions were then transferred into a freeze-dryer (Lyotrap, LTE Scientific Ltd, UK) operated at -50±5 °C and 0.054±0.002 Mbar for 48 h. Then, the freeze-dried powders were transferred into glass vials, tightly sealed and stored in a desiccator until further use. The optimum concentration of CP was found by evaluating the increase in particle size (nm) (see section 2.2.4.1) after the FD process.

3.2.5 Optimisation of BSA Adsorption

The NP suspensions were collected by centrifugation (78,000 g, 40 min, 4 °C) and surface adsorbed with BSA (Figure 3-1).

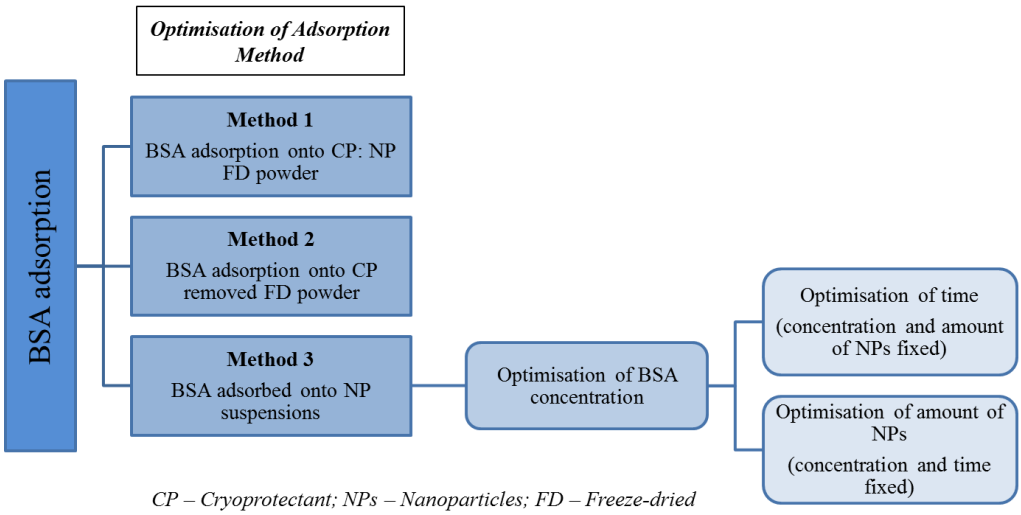

Figure 3-1 Flow chart depicting the steps for optimisation of bovine serum albumin (BSA) adsorption

3.2.5.1 Optimisation of Adsorption Method

Optimisation of the BSA adsorption method was performed as described below:

Method (1): Protein was directly adsorbed onto the CP:NP freeze-dried powders by adding 4 ml of protein solutions at different ratios of 100:4, 100:10 and 100:20 (NP:BSA) corresponding to 100, 250 and 500 µg/ml BSA to 10 mg of NP equivalent freeze-dried powder. The resultant suspension was left rotating for 1 h at 20 RPM on a HulaMixer^{TM} sample mixer (Life Technologies, Invitrogen, UK) at room temperature.

Method (2): The CP was removed by centrifugation (as in section 2.2.3.2) from the CP:NP freeze-dried powders followed by adsorption. Initially, 10 mg of NP equivalent freeze-dried powder was weighed and transferred into 4 ml of distilled water then centrifuged to separate the CP. The supernatant was removed, the pellets re-suspended in 4 ml of protein solution at different ratios of 100:4, 100:10

and 100:20 (NP:BSA) corresponding to 100, 250 and 500 µg/ml BSA and the adsorption process described in method (1) was followed.

Method (3): Protein was directly adsorbed onto the NP suspension obtained after centrifugation following removal of excess surfactant. The NP suspension (1.25 ml equal to 10 mg of NP by weight) was transferred into vials and the volume made up to 4 ml with distilled water, washing twice by centrifugation. The obtained pellets were re-suspended in 4 ml of protein solution at different ratios of 100:4, 100:10 and 100:20 (NP:BSA) corresponding to 100, 250 and 500 µg/ml BSA and the adsorption process described in method (1) was followed.

In addition, further optimisation studies to achieve effective adsorption and to assess the influence of time and amount of NPs on BSA adsorption were undertaken.

3.2.5.2 Optimisation of BSA Concentration

The NP suspension (equivalent to 10 mg, i.e. 1.25 ml of suspension) was centrifuged (as in section 2.2.3.2) and the resultant pellet was re-suspended in vials containing 4 ml of BSA at different ratios of 100:4, 100:7, 100:10, 100:12, 100:16 and 100:20 (NP:BSA) corresponding to 100, 175, 250, 300, 400 and 500 µg/ml BSA, respectively. The resultant suspension was left rotating for 1 h at 20 RPM on a HulaMixer^{TM} sample mixer (Life Technologies, Invitrogen, UK) at room temperature.

3.2.5.3 Optimisation of Time

The NP suspension (equivalent to 10 mg, i.e. 1.25 ml of suspension) was centrifuged (as in section 2.2.3.2) and the resultant pellet was re-suspended in

vials containing 4 ml of BSA at NP:BSA ratio of 100:20, corresponding to 500 µg/ml BSA. The resultant suspension was left rotating for 30 min, 1, 2 and 24 h at 20 RPM on a HulaMixer™ sample mixer (Life Technologies, Invitrogen, UK) at room temperature.

3.2.5.4 Optimisation of Amount of NPs

The NP suspension (corresponding to 10, 20 and 40 mg of NPs) was centrifuged (as in section 2.2.3.2) and the resultant pellet was re-suspended in vials containing 4 ml of 500 µg/ml BSA. The resultant suspension was left rotating for 1 h at 20 RPM on a HulaMixer™ sample mixer (Life Technologies, Invitrogen, UK) at room temperature.

For all the scenarios stated above, at the respective time points, the protein adsorbed NP suspensions were transferred into ultracentrifuge tubes and centrifuged (as in section 2.2.3.2). The supernatant was then collected and analysed for protein content as described in section 2.2.6.1. Furthermore, Langmuir (LM) and Freundlich (FM) models were employed to understand the relationship between the amount of BSA effectively adsorbed onto the NPs and the BSA concentration in the solution at equilibrium.

The particle size, PDI and zeta-potential of the NPs with and without BSA adsorption were characterised as described in section 2.2.5.1.

3.2.6 Preparation and Characterisation of Nanocomposite Microparticles

The NCMPs were prepared by SD as described in section 2.2.7. The resultant NCMPs were characterised for yield, particle size, PDI, morphology and moisture content as described in section 2.2.8.

3.2.7 Characterisation of BSA Nanoparticle Associations

The association of BSA with NPs was characterised using CLSM as described in section 2.2.9.

3.2.8 In vitro Release Studies

The in vitro release studies were performed as described in section 2.2.10.

3.2.9 Investigation of BSA Structure and Activity

The released BSA was evaluated for stability of primary structure (SDS-PAGE) and secondary structure (CD) as described in section 2.2.11.

The activity of BSA was investigated using 4-nitrophenyl acetate esterase substrate (NPA, Sigma Aldrich, UK) as described by Abbate *et al.* [223]. Briefly, 1.2 ml of released BSA sample (50 µg/ml) in PBS was added to freshly prepared NPA solution (15 µl of a 5 mM solution in ACN) and incubated for 1 h using HulaMixer™ Sample Mixer. Thereafter, the solution was transferred to a plastic cuvette and absorbance measured at 405 nm. As a positive control, standard BSA (50 µg/ml) was treated exactly the same as the released sample whereas for a

negative control, PBS buffer alone was treated as the sample. The relative residual esterolytic activity of the samples was calculated as the ratio of absorbance of the released BSA and standard BSA, with the esterolytic activity obtained for standard BSA considered to be 100%.

3.2.10 In vitro Aerosolisation Studies

The aerosol properties of the BSA adsorbed anionic NPs/NCMPs were determined as described in section 2.2.12.

3.2.11 Cell Viability Study

The cytotoxicity of anionic NPs after 24 h exposure to A549 cell line, and anionic NPs/NCMPs after 24 h exposure to A549 cell line and 16HBE14o- cells were determined as described in section 2.2.13.

3.3 Results

3.3.1 Polymer Synthesis and Characterisation

The PGA-co-PDL (monomer ratio, 1:1:1) synthesised at 6 and 24 h was a white powder with a MW of 14.7 and 24.0 KDa, respectively, as determined by the GPC. The structure of the co-polymer was confirmed by FTIR spectroscopy (Figure 3-2) and ^{1}H-NMR spectroscopy (Figure 3-3), (δH $CDCl_3$, 300 MHz): 1.3 (s, 22 H, H-g), 1.64 (m, 8 H, H-e, e′, h), 2.32 (m, 6 H, H-d, d′, i), 4.05 (q)-4.18 (m) (6 H, H-a, b, c, f), 5.2 (s, H, H-j). The T_m (melting point) of the co-polymer was determined by DSC and was found to be ~55 ºC which is similar to previous reports [160].

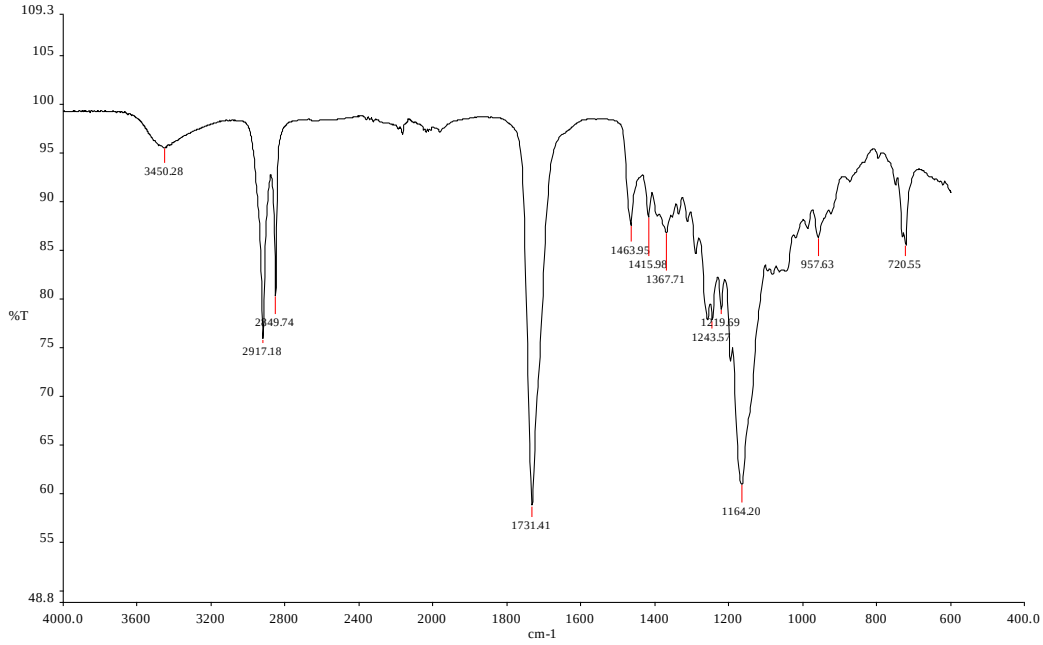

Figure 3-2 Fourier transform infrared spectra of PGA-co-PDL

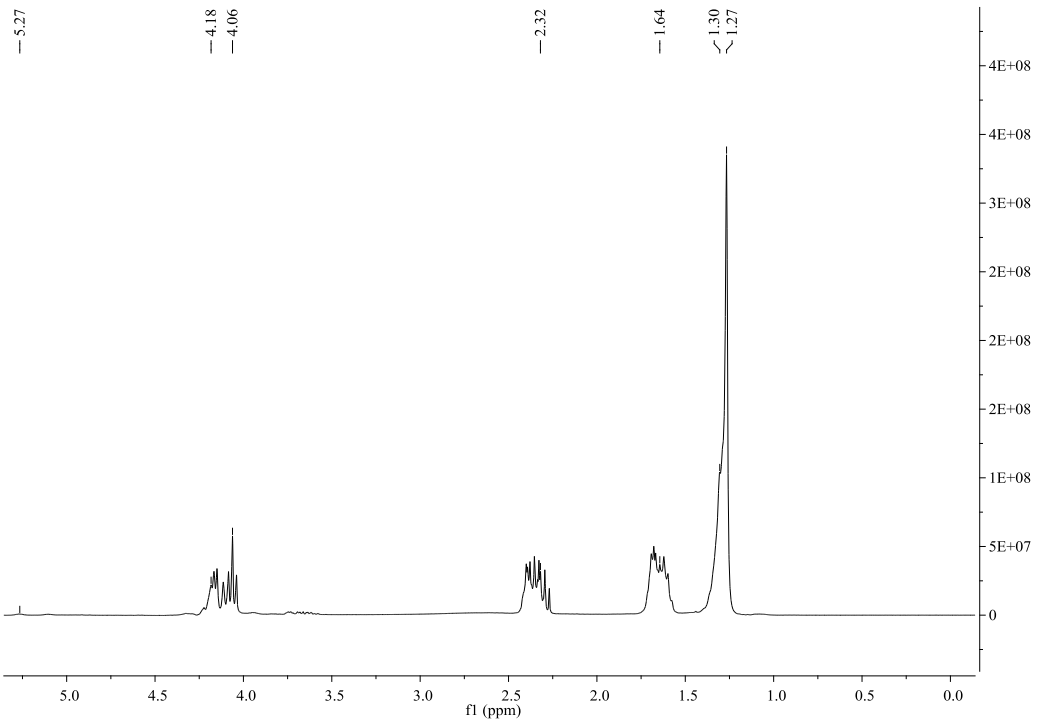

Figure 3-3 Nuclear magnetic resonance spectra of PGA-co-PDL

3.3.2 Optimisation of NP Size by Taguchi L_{18} Design

The Taguchi design was applied in this study to identify the significant factors that would influence the size of PGA-co-PDL NPs. Investigating seven factors (1 factor at 2 levels and 6 factors at 3 levels) without the usage of experimental design would have resulted in 1458 ($2*3^6$) individual experiments to be performed which would be an arduous and inefficient task.

The Taguchi L_{18} orthogonal array design required 18 runs to be performed to yield the optimum conditions for each factor to achieve the smallest PGA-co-PDL NP size. Table 3-2 illustrates the structure of the L_{18} orthogonal array, the corresponding results and S/N ratios.

The results obtained from 18 runs indicated particle sizes ranging from 138.7±6.4 (run 3) to 459.4±69.5 (run 11). Figure 3-4 shows the mean S/N graph of the particle size for each parameter level. The parameter with the largest range and corresponding rank (indicating the relative importance compared to other parameters) was considered as the critical factor affecting that particle size.

Analysis of the particle size from the 18 runs using the Taguchi's 'smaller-is-better' criterion in Minitab® 16 statistical software, indicated the optimum conditions inferred from the range, rank and the S/N response graph were A1B3C3D3E2F2G2.

The optimum formulation made using these conditions yielded anionic NPs with a size of 128.50±6.57 nm lower than the minimum size of 138.7±6.4 nm obtained using run 3, with a PDI of 0.07±0.03 and zeta-potential of -10.2±3.75 mV.

Table 3-2 Structure of Taguchi's L_{18} orthogonal array, corresponding particle size and signal-to-noise (S/N) ratios *(Mean±SD, n=3)*

Runs	Parameters							Particle Size (nm)	PDI	S/N Ratio (dB)
	A	B	C	D	E	F	G			
Run 1	1	1	1	1	1	1	1	315.5±6.90	0.151±0.05	-49.979
Run 2	1	1	2	2	2	2	2	186.5±4.30	0.097±0.03	-45.412
Run 3	1	1	3	3	3	3	3	138.7±6.40	0.093±0.01	-42.843
Run 4	1	2	1	1	2	2	3	210.1±18.7	0.116±0.04	-46.449
Run 5	1	2	2	2	3	3	1	208.7±49.9	0.123±0.06	-46.389
Run 6	1	2	3	3	1	1	2	182.0± 3.20	0.075±0.04	-45.199
Run 7	1	3	1	2	1	3	2	192.9±9.30	0.077±0.04	-45.705
Run 8	1	3	2	3	2	1	3	149.3±2.50	0.075±0.01	-43.481
Run 9	1	3	3	1	3	2	1	192.9±23.0	0.050±0.03	-45.704
Run 10	2	1	1	3	3	2	2	269.1±68.9	0.205±0.04	-48.598
Run 11	2	1	2	1	1	3	3	459.4±69.5	0.233±0.02	-53.243
Run 12	2	1	3	2	2	1	1	242.5±19.1	0.188±0.06	-47.694
Run 13	2	2	1	2	3	1	3	253.2±47.3	0.155±0.10	-48.069
Run 14	2	2	2	3	1	2	1	217.3±18.9	0.116±0.01	-46.742
Run 15	2	2	3	1	2	3	2	240.5±35.1	0.133±0.05	-47.622
Run 16	2	3	1	3	2	3	1	169.3±7.60	0.144±0.04	-44.573
Run 17	2	3	2	1	3	1	2	235.9±29.6	0.119±0.08	-47.453
Run 18	2	3	3	2	1	2	3	221.7±11.0	0.150±0.04	-46.915

Note: A - MW of Polymer, B - Org Sol (DCM), C - Aq. Vol (PVA), D - 1st Aq. conc (PVA), E - Sonication time, F - Stirrer Speed and G - 2nd Aq. conc (PVA)

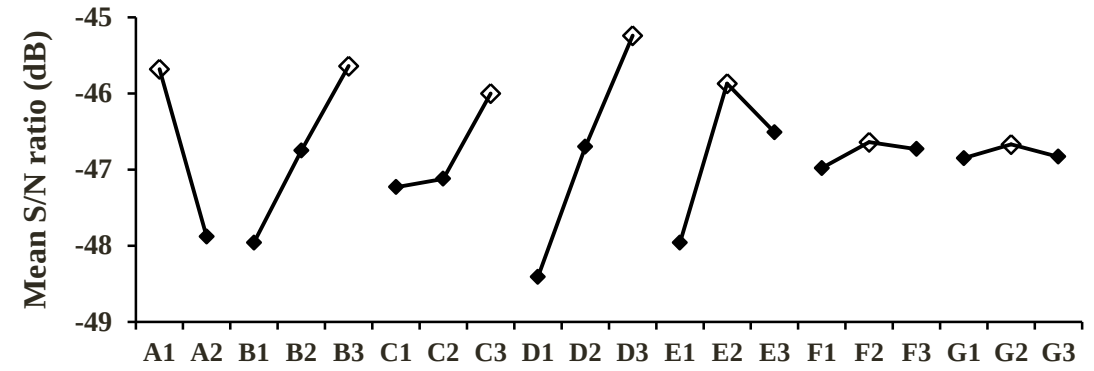

Range	2.19	2.32	1.23	3.17	2.09	0.34	0.18
Rank	3	2	5	1	4	6	7

Parameter Levels

Figure 3-4 Mean signal-to-noise (S/N) graph for particle size response. Letters (A–E) denote the experimental parameters and numeric values denote the parameter levels (◇ indicates maximum S/N value) *(Mean±SD, n=3);* Note: A - MW of Polymer, B - Org Sol (DCM), C - Aq. Vol (PVA), D - 1st Aq. conc (PVA), E - Sonication time, F - Stirrer Speed and G - 2nd Aq. conc (PVA)

The microscopic images (Figure 3-5) show that the NPs appeared to be smooth and spherical in shape with no visible aggregation.

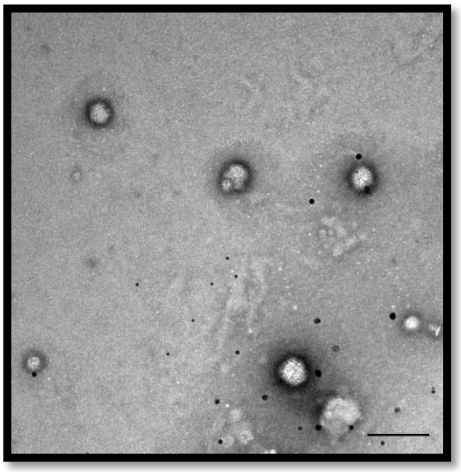

Figure 3-5 Transmission electron microscope image of anionic nanoparticles at 44,000X (scale bar – 200 nm)

3.3.3 Freeze-drying of Nanoparticle Suspensions

The optimum PGA-co-PDL anionic NPs were freeze-dried with and without the use of CPs (i.e. S-Sucrose, M-Mannitol and T-Trehalose at 1.25:1, 2.5:1 and 5:1/CP:NP ratios). In the absence of any CP, reconstitution of freeze-dried NPs resulted in a significant increase ($p < 0.05$, ANOVA/Dunnett's comparison) in size (Figure 3-6) and PDI (Table 3-3). The FD of NPs was considered successful if the S_f/S_i (S_f-Size after FD, S_i-Size before FD) remained close to 1 with low PDI values. In most cases in presence of CP, the increase in size, although significant, was relatively small. The highest S_f/S_i ratio (Table 3-3) was observed for mannitol at M:NP/1.25:1 (S_f/S_i = 5.45) and 2.5:1 (S_f/S_i = 4.08) with a particle size increase of 662 nm and 459 nm, from emulsions, respectively. The lowest S_f/S_i ratio was observed for sucrose at S:NP/5:1 (S_f/S_i = 1.38) suggesting successful FD with a minimal size increase of 58 nm from emulsion. This shows that the presence of CP stabilised the anionic NPs and maintained the particle size and PDI. Additionally, in the presence of CPs (S, M and T) the aggregation of NPs after FD was minimised. In general, higher PDI values were obtained after FD; however, there was no significant difference in PDI between any of the freeze-dried samples indicating similar size distributions. In addition, better size retention was observed with sucrose above S:NP/2.5:1, trehalose above T:NP/1.25:1 and mannitol above M:NP/5:1. Sucrose was the best at S:NP (5:1) ratio with a minimum increase in size, and such similar results were also reported by Anhorn *et al.* and others [224,225].

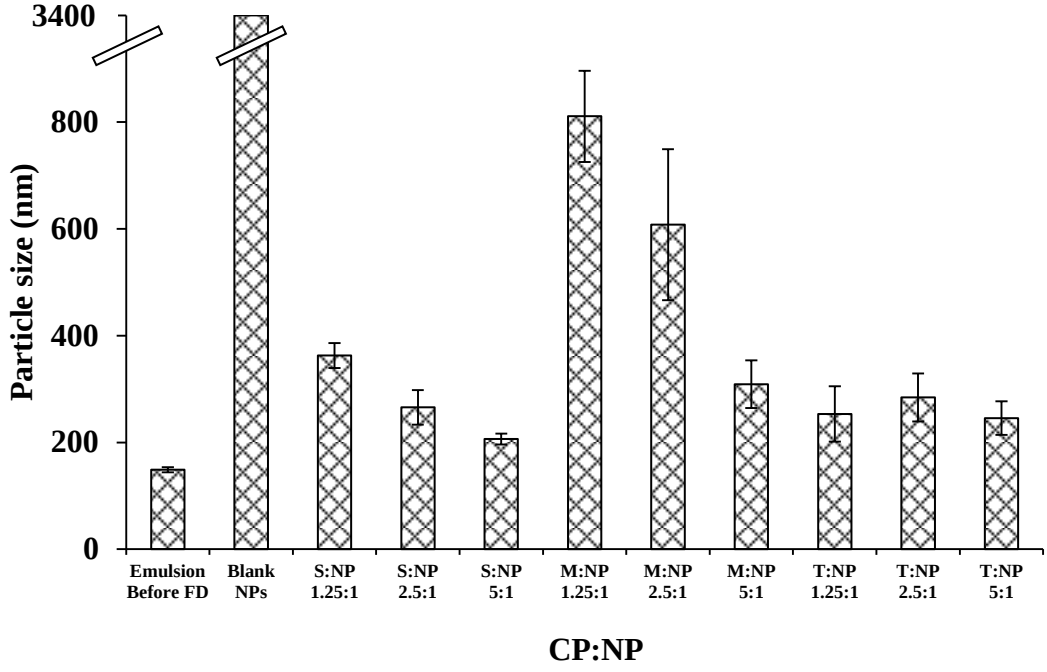

Figure 3-6 Particle size (nm) for different cryoprotectant:nanoparticle (CP:NP) ratios; Note: S-Sucrose, M-Mannitol, T-Trehalose *(Mean±SD, n=6)*

Table 3-3 S_f/S_i and PDI values of freeze-dried powders for different cryoprotectant:nanoparticle (CP:NP) ratios *(Mean±SD, n=6)*

Cryoprotectant:Nanoparticle (CP:NP)	S_f/S_i	PDI
S: NP (1.25:1)	2.44	0.43±0.11
S:NP (2.5:1)	1.78	0.41±0.10
S:NP (5:1)	1.39	0.36±0.11
M:NP (1.25:1)	5.45	0.46±0.09
M:NP (2.5:1)	4.08	0.55±0.15
M:NP (5:1)	2.08	0.35±0.10
T:NP (1.25:1)	1.70	0.46±0.15
T:NP (2.5:1)	1.91	0.39±0.14
T:NP (5:1)	1.65	0.39±0.11

Note: S-Sucrose, M-Mannitol, T-Trehalose, PDI-Polydispersity index, S_f-Size after freeze-drying, S_i-Size before freeze-drying

3.3.4 Optimisation of BSA Adsorption

Initially, protein adsorption was carried out utilising three different methods as described in section 3.2.5.1. Figure 3-7 shows the amount of BSA adsorbed in µg per mg of NPs at different NP:BSA ratios for three different methods.

For method (1), the average adsorption of BSA increased significantly from a NP:BSA ratio of 100:4 (1.50±0.25 µg per mg of NPs) to 100:20 (6.46±1.97 µg per mg of NPs) ($p < 0.05$, ANOVA/Tukey's comparison). However, there was no significant difference in adsorption from 100:10 (3.97±1.38 µg per mg of NPs) to 100:20 ($p > 0.05$, ANOVA/Tukey's comparison).

For method (2), the average adsorption of BSA increased significantly from a NP:BSA ratio of 100:4 (3.19±0.38 µg per mg of NPs) to 100:10 (5.01±1.18 µg per mg of NPs) to 100:20 (9.71±0.71 µg per mg of NPs) ($p < 0.05$, ANOVA/Tukey's comparison). In addition, there was a significant difference in BSA adsorption of 9.71±0.71 µg per mg of NPs for (2) compared to 6.26±1.97 µg per mg of NPs for method (1) at 100:20 (NP:BSA) ratio ($p < 0.05$, ANOVA/Tukey's comparison).

For method (3), the average adsorption of BSA increased significantly from a NP:BSA ratio of 100:4 (4.75±0.39 µg per mg of NPs) to 100:10 (6.59±1.28 µg per mg of NPs) to 100:20 (10.23±1.87 µg per mg of NPs) ($p < 0.05$, ANOVA/Tukey's comparison). Moreover, the average adsorption of BSA at 100:20 (NP:BSA) ratio (10.23±1.87 µg per mg of NPs) was not statistically different from that with 9.71±0.71 µg per mg of NPs for method (2) ($p > 0.05$, ANOVA/Tukey's comparison).

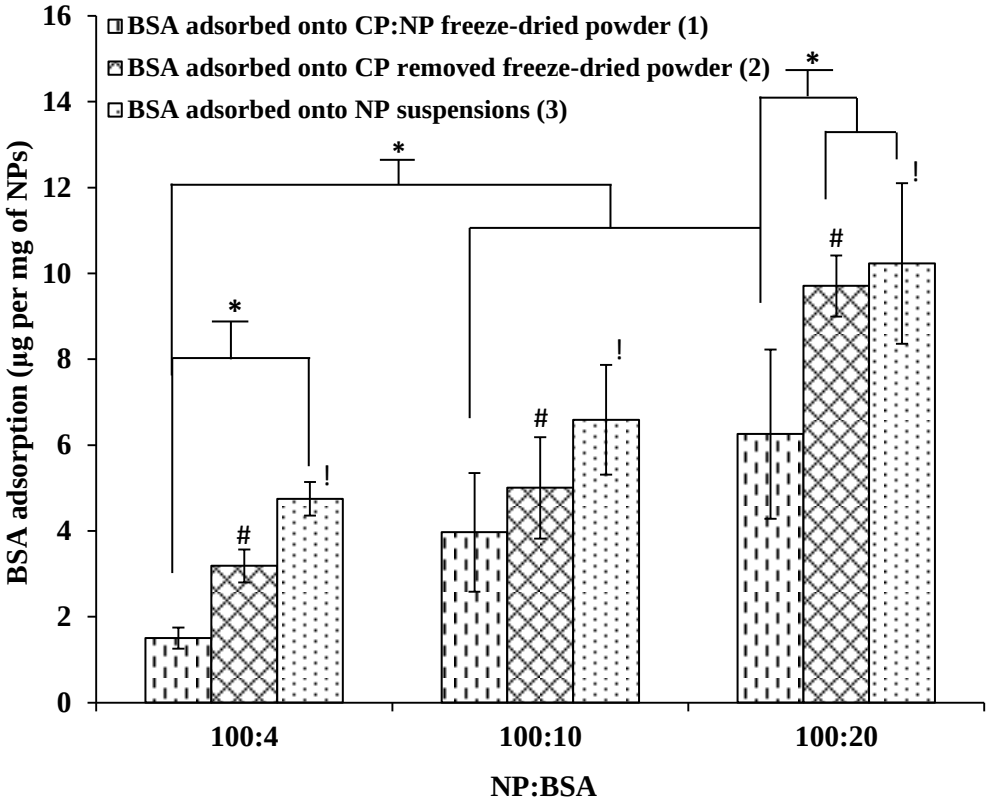

Figure 3-7 Amount of bovine serum albumin (BSA) adsorbed in µg per mg of nanoparticles (NPs) at different NP:BSA ratios by three different methods, # and ! (100:4 vs 100:10 vs 100: 20), * is p < 0.05, ANOVA/Tukey's comparison ***(Mean±SD, n=3)***

Further optimisation of BSA adsorption was achieved by direct adsorption onto NP suspensions. Figure 3-8 shows the amount of BSA adsorbed in µg per mg of NPs for different NP:BSA ratios. The average adsorption of BSA increased significantly ($p < 0.05$, ANOVA/Tukey's comparison) from a NP:BSA ratio of 100:4 (4.75±0.39 µg per mg of NPs) to 100:7 (5.89±1.14 µg per mg of NPs), 100:10 (6.59±1.28 µg per mg of NPs), 100:12 (7.73±0.62 µg per mg of NPs) and 100:16 (7.75±0.5 µg per mg of NPs) with no significant difference between 100:7 vs 100:10 and 100:10 vs 100:12 vs 100:16. However, the adsorption increased

significantly at 100:20 (10.23±1.87 µg per mg of NPs) compared to other NP:BSA ratios ($p < 0.05$, ANOVA/Tukey's comparison).

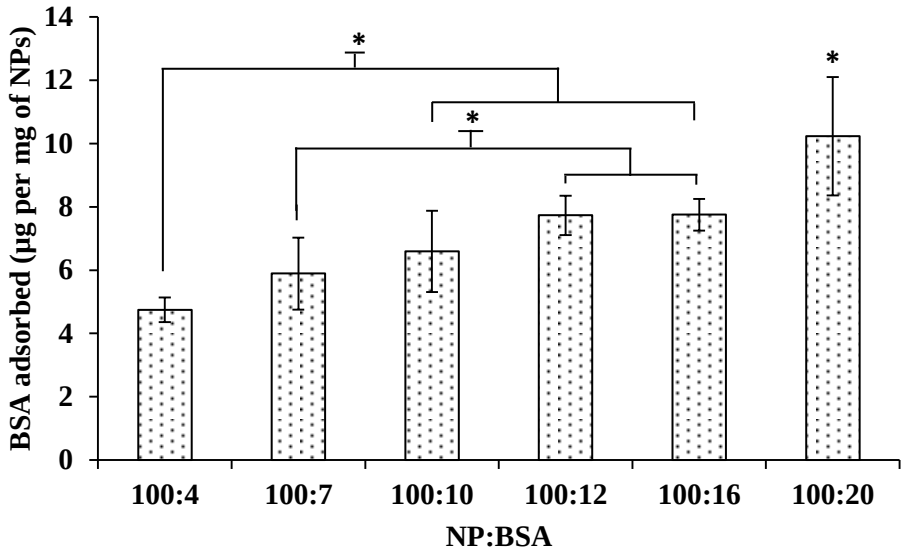

Figure 3-8 Amount of bovine serum albumin (BSA) adsorbed onto NP suspensions in µg per mg of nanoparticles (NPs) for different NP:BSA ratios, * is $p < 0.05$, ANOVA/Tukey's comparison *(Mean±SD, n=3)*

Figure 3-9 shows the amount of BSA adsorbed in µg per mg of NPs at different time points for 100:20 (NP:BSA) ratio. The average adsorption increased significantly from 30 min (1.84±0.82 µg per mg of NPs) to 1 h (10.23±1.87 µg per mg of NPs) ($p < 0.05$, ANOVA/Tukey's comparison) with no significant difference beyond 1 h compared to that of 2 h (8.76±0.34 µg per mg of NPs) and 24 h (8.95±0.39 µg per mg of NPs) ($p > 0.05$, ANOVA/Tukey's comparison) indicating maximum adsorption was achieved at 1 h.

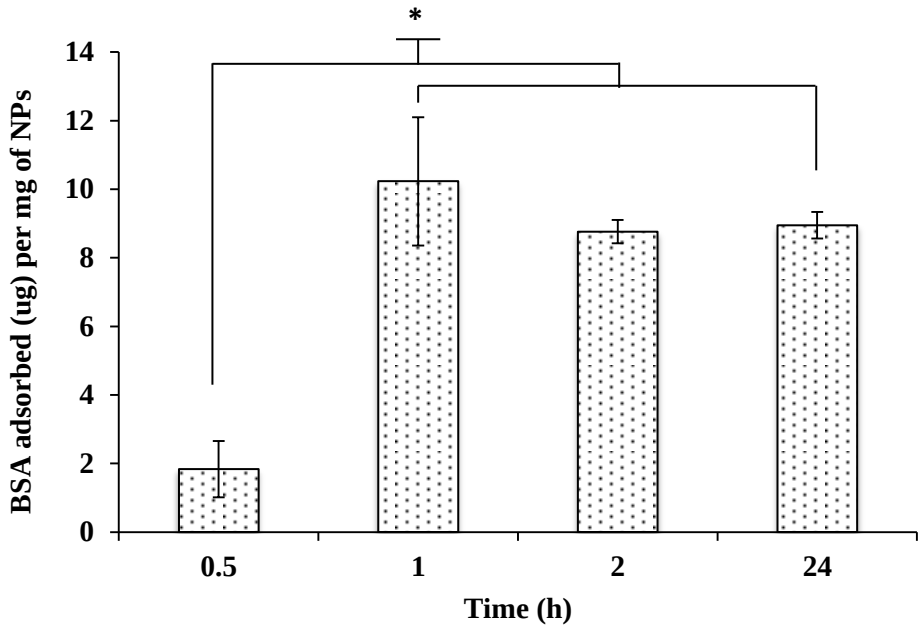

Figure 3-9 Amount of bovine serum albumin (BSA) adsorbed in µg per mg of nanoparticles (NPs) at different time points for 100:20 (NP:BSA) ratio, * is p < 0.05, ANOVA/Tukey's comparison *(Mean±SD, n=3)*

Figure 3-10 shows the amount of BSA adsorbed in µg per mg of NPs for different amounts of NPs used at 500 µg/ml BSA concentration. The average adsorption after 1 h decreased significantly from 10 mg of NPs (10.23±1.87 µg per mg of NPs) to 20 mg (3.18±0.54 µg per mg of NPs) and 40 mg (1.82±0.48 µg per mg of NPs) ($p < 0.05$, ANOVA/Tukey's comparison) indicating maximum adsorption for 10 mg of NPs.

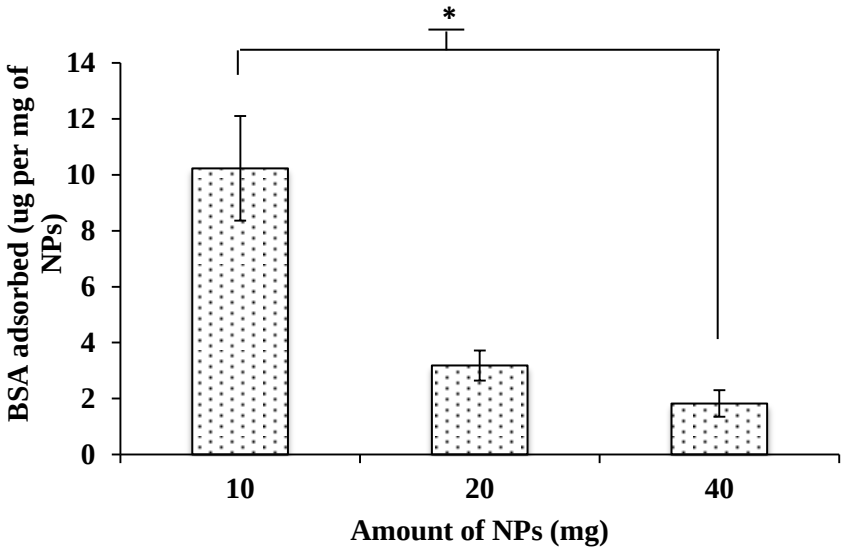

Figure 3-10 Amount of bovine serum albumin (BSA) adsorbed in µg per mg of nanoparticles (NPs) for different amounts of NPs used at 500 µg/ml BSA concentration, * is $p < 0.05$, ANOVA/Tukey's comparison *(Mean±SD, n=3)*

Models such as LM and FM have been used by several authors to characterise the adsorption of protein onto the surface of MPs or NPs [226–229]. The LM is expressed by equation 3-1:

$$\frac{C_e}{Q_e} = \frac{C_e}{Q_m} + \frac{1}{Q_m K_L} \qquad \text{(eq. 3-1)}$$

where C_e is the concentration in equilibrium (µg/ml), Q_e is the amount of protein adsorbed (µg/mg), Q_m is the maximum adsorption capacity (µg/mg) and K_L is a Langmuir constant related to the adsorption capacity. The LM assumes that the adsorption is a monolayer and that all sites are energetically equivalent with no lateral interactions between the protein molecules. For LM (Figure 3-11), the regression coefficient (r^2) was ≥ 0.898, Q_m was 13.28 µg/mg and K_L was $0.4x10^{-2}$.

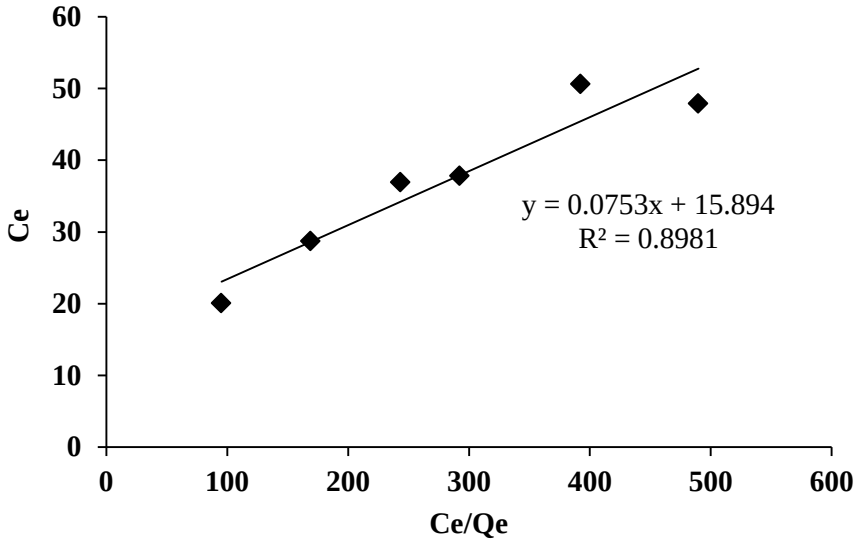

Figure 3-11 Langmuir model (LM) indicating adsorption of bovine serum albumin (BSA) onto nanoparticles; Note: LM (C_e vs C_e/Q_e) where C_e is the concentration in equilibrium (µg/ml) and Q_e is the amount of protein adsorbed (µg/mg)

The FM addresses the deviations from the LM theory and assumes that the adsorption is not necessarily a monolayer and that interactions between protein molecules are possible. The FM is expressed by equation 3-2:

$$\text{Log } Q_e = \log K_F + \frac{1}{n} \log C_e \qquad \text{(eq. 3-2)}$$

where K_F is a Freundlich constant and n is a number usually < 1 that signifies the increase in adsorption is less rapid with increasing concentration. For FM (Figure 3-12), the regression coefficient (r^2) was ≥ 0.969, K_F was 0.591 and n was 2.22 (greater than 1). So, although the r^2 is approaching 1, the n value suggests that more data points at higher concentrations of protein need to be collected before the relation between the protein molecules and NPs can be fully determined.

However, this was not performed as the adsorption achieved using 100:20 (NP:BSA) ratio will be sufficient for dosage purposes when the protein of interest, PspA, is formulated and thus has been left for future studies.

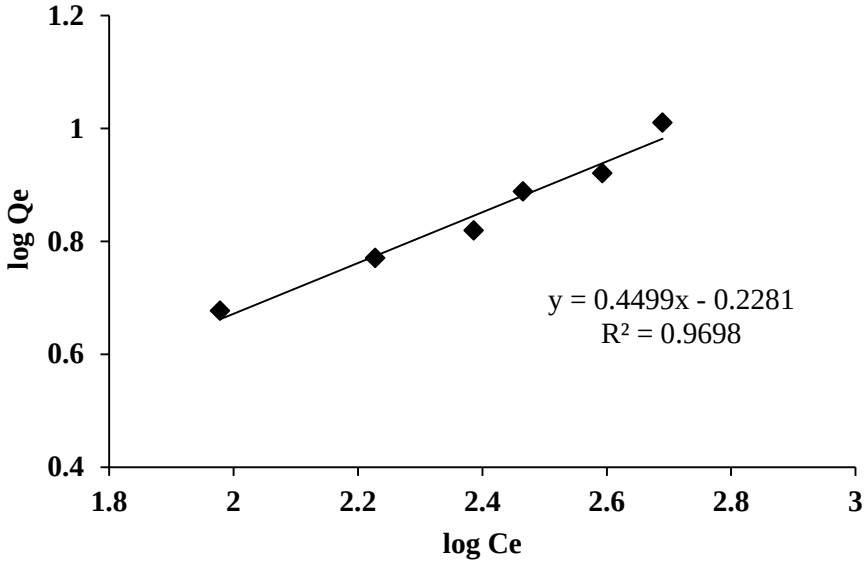

Figure 3-12 Freundlich model (FM) indicating adsorption of bovine serum albumin (BSA) onto nanoparticles; Note: FM (log C_e vs log Q_e) where C_e is the concentration in equilibrium (µg/ml) and Q_e is the amount of protein adsorbed (µg/mg)

Table 3-4 lists the particle size, PDI and zeta-potential of PGA-co-PDL anionic NPs with and without BSA adsorbed. As seen, there is a significant increase ($p < 0.05$, ANOVA/Tukey's comparison) in size which is attributed to the adsorption of BSA onto NPs as confirmed using confocal microscopy (section 3.3.5.3). The difference in zeta-potential could be due to the different orientation the BSA molecules assume on the surface of NPs thereby exposing differently charged amino acids.

Table 3-4 Particle size, PDI and zeta-potential of PGA-co-PDL anionic nanoparticles (NPs) with and without bovine serum albumin (BSA) adsorption *(Mean±SD, n=3)*

	NP suspension[a]	Without BSA adsorption[b]	With BSA adsorption[c]
Particle Size (nm)	128.50±06.57	203.90±02.55*	299.03±32.02*
PDI	0.070±0.030	0.205±0.007	0.322±0.060
Zeta-potential (mV)	-10.20±03.75	-24.56±00.50	-07.56±00.85

[a] NPs characterised immediately after preparation without centrifugation, [b] NPs characterised after centrifugation but without adsorption of BSA, [c] NPs characterised after centrifugation and BSA adsorption, * $p < 0.05$, ANOVA/Tukey's comparison

3.3.5 Characterisation of Nanocomposite Microparticles

3.3.5.1 Yield, Particle Size and Morphology

A reasonable yield of SD, 40.36±1.80% for the empty anionic NPs/NCMPs and 42.35±3.17% for BSA adsorbed anionic NPs/NCMPs was obtained.

The size of NPs after recovery from spray-dried empty anionic NPs/NCMPs in distilled water was 210.03±15.57 nm and PDI 0.355±0.067, and for BSA adsorbed anionic NPs/NCMPs was 222.46±2.17 nm and PDI 0.360±0.008, which is in the required range of 200 to 500 nm for uptake by DCs [16-18].

The shape and surface texture of the anionic NPs/NCMPs were investigated using SEM (Figure 3-13). Photomicrographs of the anionic NPs/NCMPs showed irregular and corrugated NCMPs with a diameter of 1.90±0.34 µm.

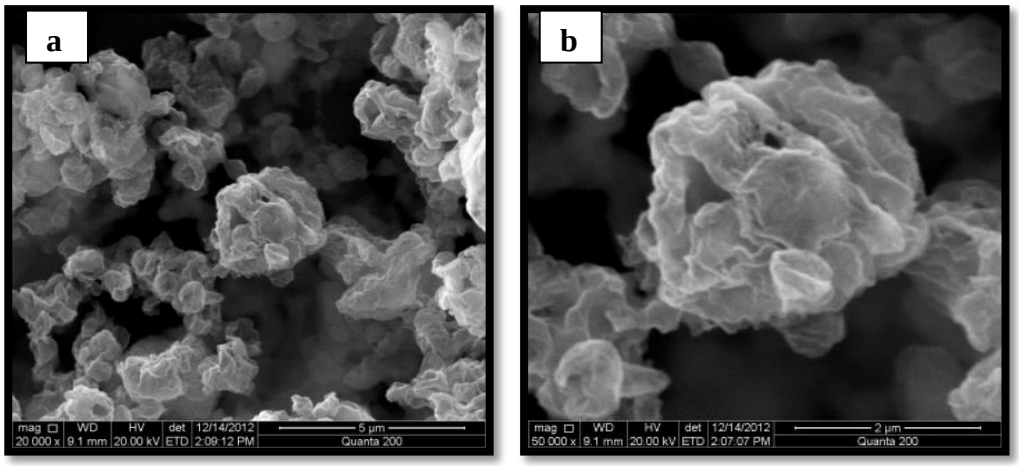

Figure 3-13 Scanning electron microscope pictures of anionic nanocomposite microparticles (a) 5 µm and (b) 2 µm

3.3.5.2 Moisture Content

The moisture content in anionic NPs/NCMPs was determined using TGA and the thermograms (Figure 3-14) show that the spray-dried formulation contained a residual moisture content of 0.47±0.01% w/w.

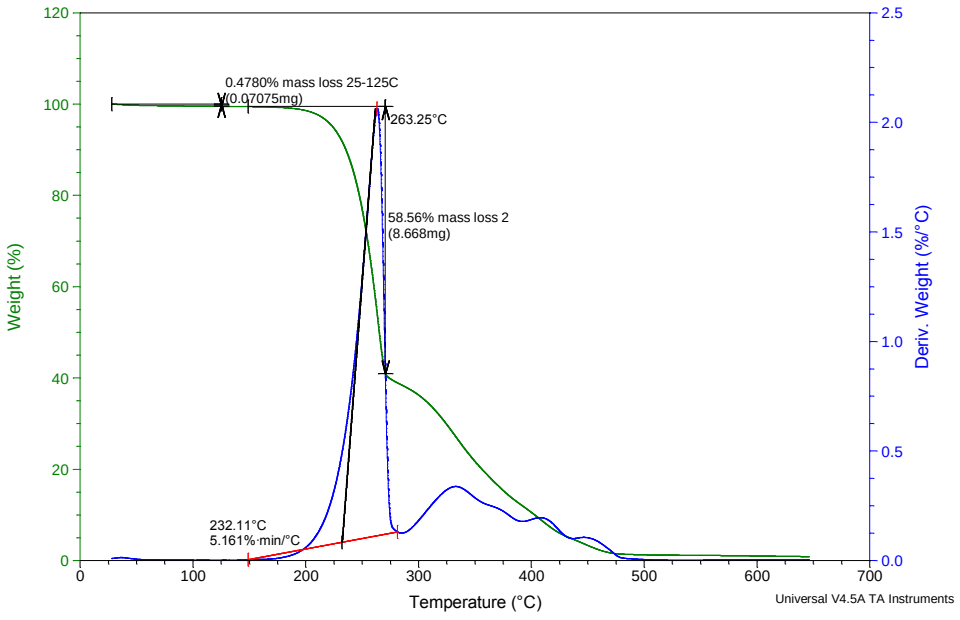

Figure 3-14 Thermogram of anionic nanocomposite microparticles obtained using thermal gravimetric analysis

3.3.6 Characterisation of BSA Nanoparticle Associations

The association of BSA with NPs was visualised using CLSM. The microscopic images in Figure 3-15a (split view) and 3-15b (orthogonal view) shows the spray-dried NCMPs containing the fluorescent NPs (red, labelled using NR dye) adsorbed with FITC-BSA (green). The image shows that FITC-BSA was evidently only present where the NPs were present, indicating their association. Moreover, the increase in size observed after adsorption also confirms the adsorption of BSA onto PGA-co-PDL NPs (Table 3-4).

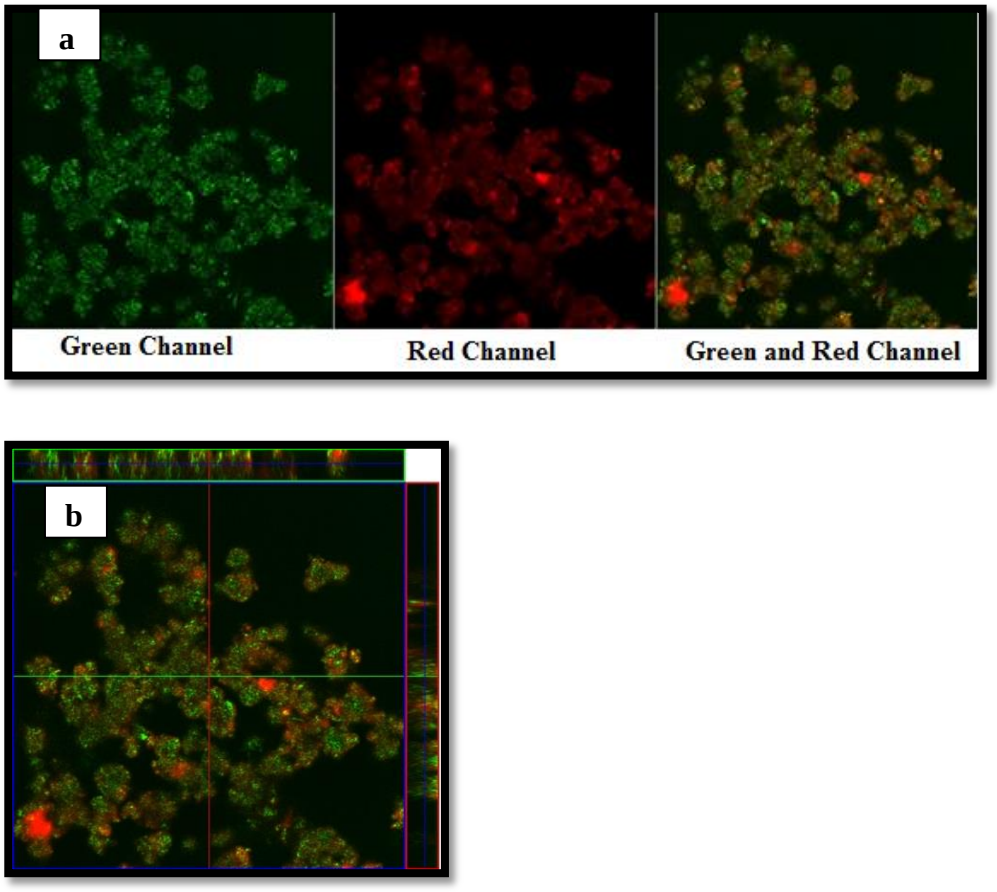

Figure 3-15 Confocal microscopic image of spray-dried nanocomposite microparticles containing the fluorescent nanoparticles (red) adsorbed with FITC-BSA (green) (a) Split view and (b) Orthogonal view

3.3.7 In vitro Release Studies

In vitro release studies were performed on BSA adsorbed anionic NPs/NCMPs and reported as cumulative percentage of BSA released over time (Figure 3-16). An initial burst release of 30.15±2.33% BSA was observed followed by continuous release up to 5 h, with a BSA release of 86.07±0.95%. After this time period, a slow continuous release of BSA was observed with a release of 95.15±1.08% over 48 h, for the BSA adsorbed anionic NPs/NCMPs.

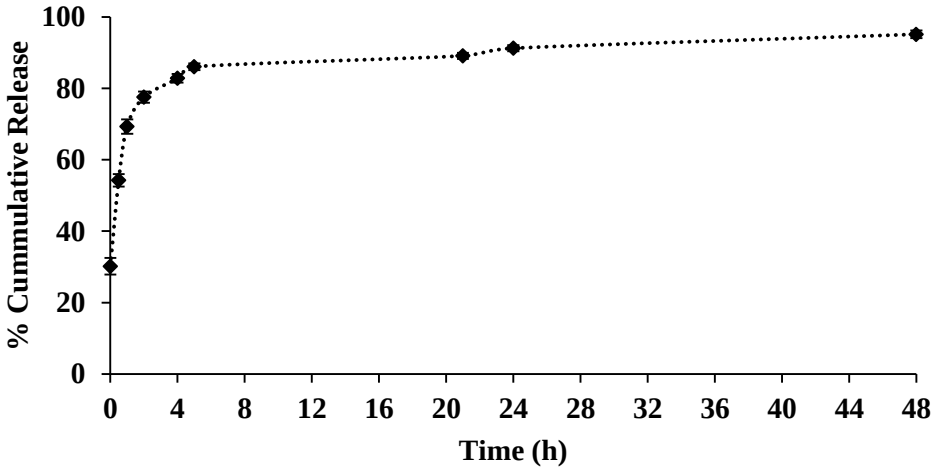

Figure 3-16 In vitro release profile for bovine serum albumin (BSA) from anionic nanocomposite microparticles in phosphate buffer saline, pH 7.4 ***(Mean±SD, n=3)***

3.3.8 Investigation of BSA Structure and Activity

The primary structure of BSA released from the BSA adsorbed anionic NPs/NCMPs was investigated using SDS-PAGE analysis. Figure 3-17 reveals identical bands for the standard BSA and the BSA released from NCMPs without any noticeable new bands of high or low MW BSA.

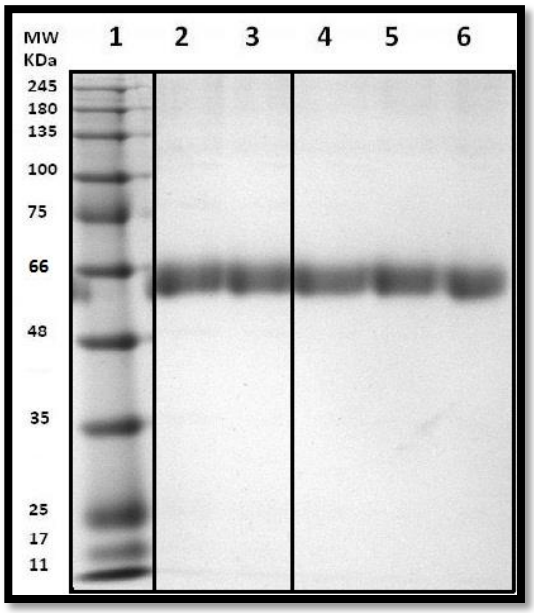

Figure 3-17 SDS-PAGE of Lane 1: MW standards, broad range (Bio-Rad Laboratories, Hercules CA, USA), Lane 2, 3: bovine serum albumin (BSA) standards, Lane 4, 5, 6: Released from BSA adsorbed anionic nanocomposite microparticles after 48 h

The secondary structure analysis was performed using CD. Figures 3-18a and 3-18b show the CD spectra of standard BSA, BSA supernatant and BSA released. In Figure 3-18a, the CD spectra show minima at 221-222 nm and 209-210 nm and a maximum at about 195 nm for both samples which is characteristic of α-helical structure. Further structural analysis showed that the predominant structure was helical displaying 51 and 62.5% helicity, respectively (Table 3-5). Moreover, the experimental data obtained for the standard BSA are in good agreement with previous reports [230]. Figure 3-18b shows that BSA released displayed double minima at 208 and 222 nm and further spectra analysis indicated that this sample adopted a reduced level helical conformation (*circa* 36% helical) (Table 3-5). Comparing the CD results of BSA released with that of standard BSA, the α-helical content decreases by 15%, the β-sheet content increases by 8.9%, the turns

content increases by 1%, and the random coils' content increases by 3% respectively.

The residual esterolytic activity of the released BSA sample was calculated to be 77.73±3.19% relative to standard BSA.

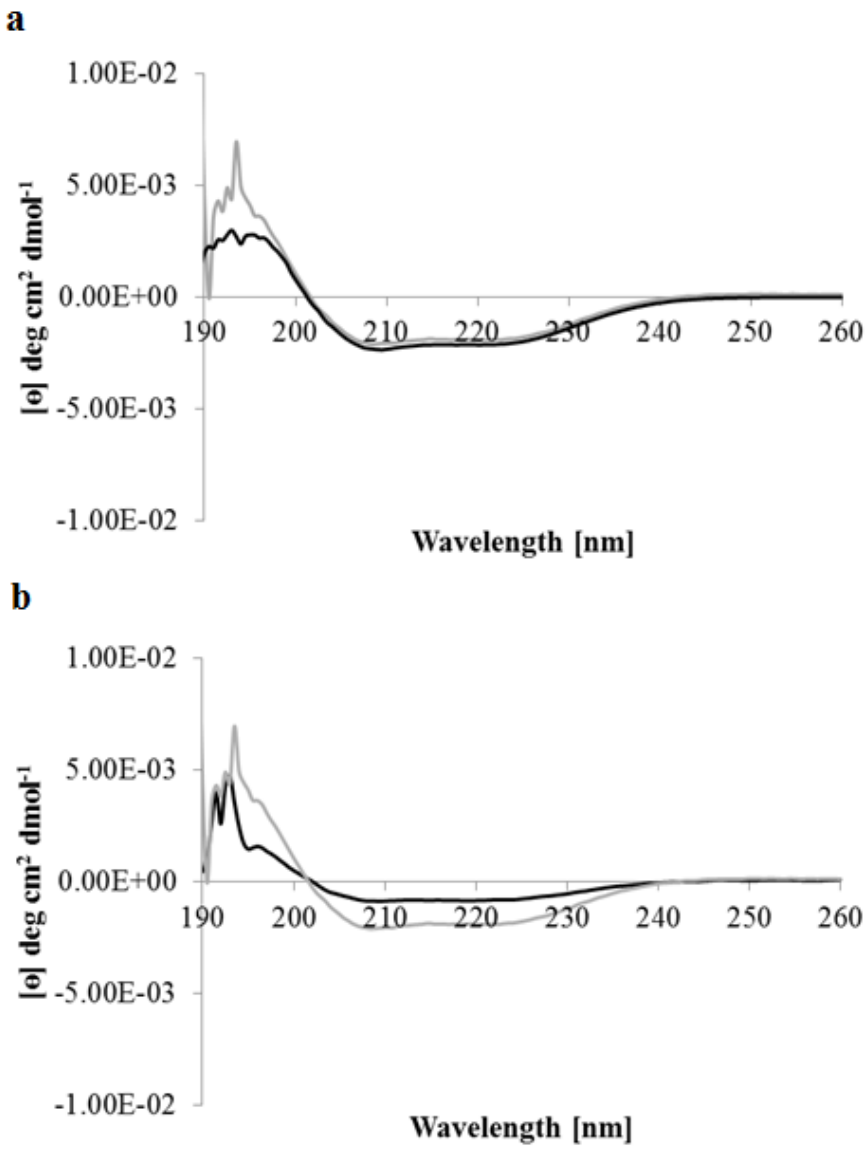

Figure 3-18 Circular dichroism spectra of standard bovine serum albumin (BSA) (grey) (a) supernatant BSA (black) and (b) BSA released (black)

Table 3-5 The percentage of the secondary structure of standard, supernatant and released bovine serum albumin (BSA) samples

Sample	Helix	Strand	Turns	Unordered
Standard BSA	51.0±0.007	21.1±0.070	6.0±0.010	18.0±0.007
BSA Supernatant	62.5±0.035	22.0±0.021	5.5±0.050	9.5±0.060
BSA Released	36.0±0.000	30.0±0.000	7.0±0.000	21.0±0.007

3.3.9 In vitro Aerosolisation Studies

The percentage mass of BSA recovered from the NGI was approximately 77%. The deposition data (Figure 3-19) obtained from optimum spray-dried formulations displayed a FPM (per capsule) of 28.21±8.41 µg, FPF of 76.95±5.61% and MMAD of 1.21±0.67 µm. This suggests that the BSA adsorbed anionic NPs/NCMPs were capable of delivering BSA to the lungs, and are expected to deposit the majority of the emitted dose to the bronchial-alveolar region of the lungs [65].

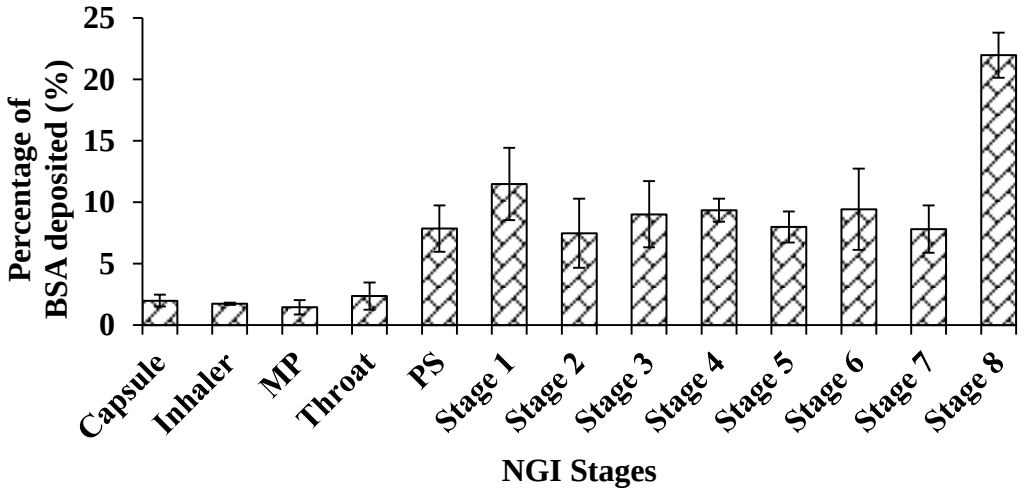

Figure 3-19 Percentage of bovine serum albumin (BSA) deposited stage-wise in a Next Generation Impactor *(Mean±SD, n=3)*

3.3.10 Cell Viability Study

The anionic NPs showed a cell viability of 70.84±6.99 % (A549 cell line) at 1.25 mg/ml concentration (Figure 3-20a). The anionic NPs/NCMPs appear to be well tolerated by both the cell lines, with a cell viability of 87.01±14.11% (A549 cell line) and 106.04±21.14% (16HBE14o- cell line) (Figure 3-20b) at a concentration of 1.25 mg/ml after 24 h exposure indicating a good toxicity profile with no significant difference in cell viability between particle loadings. This provides an indication of the feasibility of using PGA-co-PDL particles as safe carriers for pulmonary drug delivery.

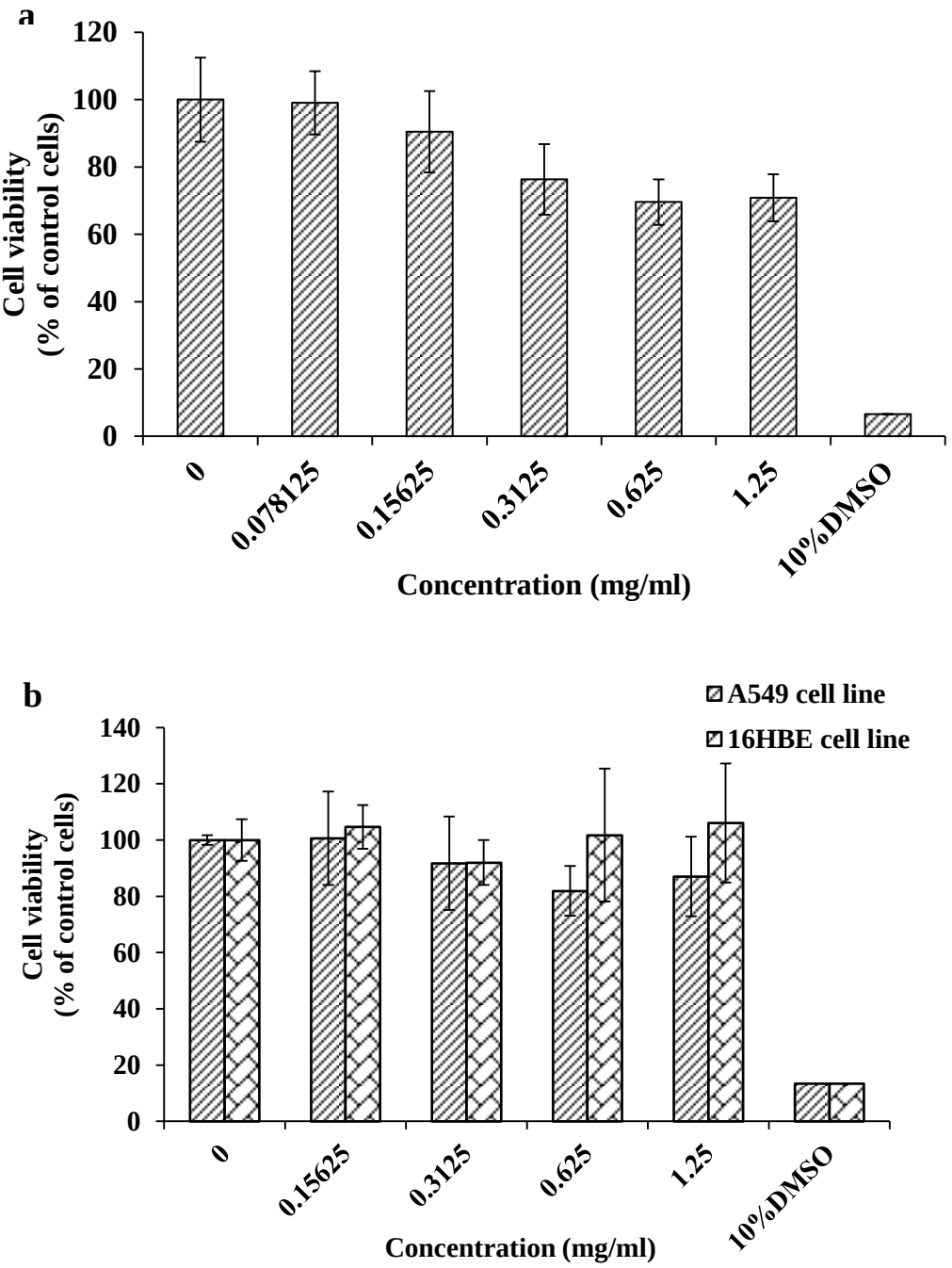

Figure 3-20 Cell viability measured by MTT assay after 24 h exposure to (a) A549 cell line to anionic nanoparticles (NPs) and (b) A549 & 16HBE14o- cell lines to anionic nanocomposite microparticles *(Mean±SD, n=3)*

3.4 Discussion

3.4.1 Preparation and Characterisation of Nanoparticles

The PGA-co-PDL NPs were prepared using a modified o/w single emulsion solvent evaporation method [165]. The optimum outcome of 18 runs, suggested by Taguchi's L_{18} orthogonal array, was NPs of size lower than 150 nm. However, this increased to about 200-300 nm after centrifugation (due to aggregation upon removal of surfactant) and BSA adsorption. According to the literature, particles of this size will be effectively uptaken by DCs [113,212,213]. The effect of each factor is discussed in detail below:

The PVA concentration (range = 3.17, rank = 1), factor D, was the most important factor affecting the particle size. The S/N ratios at three levels indicated that particle size linearly decreased with an increase in surfactant concentration from 2.5 to 10% w/v (S/N ratio, r^2 = 0.997). The particle size decreased because, at lower concentrations, there is an inadequate amount of surfactant to cover all the surfaces of the PGA-co-PDL NPs [231]. The uncovered NPs then tend to aggregate until a point where there is adequate amount of surfactant to cover the total surface area of the aggregated NPs, forming a stable system and leading to larger particles. However, with an increase in surfactant concentration it was possible to efficiently cover the surfaces of all individual NPs thereby stabilising the system, avoiding aggregation and resulting in smaller PGA-co-PDL NPs [231]. This effect of a decrease in particle size with an increase in surfactant concentration, PVA, was also observed by Mitra and Lin [232].

The S/N ratios of MW of the polymer (range = 2.19, rank = 3), factor A, at two levels suggested a directly proportional relationship with MW of polymer, i.e. the particle size decreases with a decrease in the MW. This was also evident from the lower particle sizes observed using 14.7 kDa MW polymer (runs 1-9) relative to 24 kDa MW polymer (runs 10-18). As the MW of a polymer increases, the viscosity of the polymeric solution also increases, thereby imposing difficulty in breaking the suspension into smaller emulsion droplets compared to a lower MW polymer that requires lower efficiency to breakdown under similar conditions. This increase in size of the particles has also been observed by others and is reported to be associated with high MW polymers [90,233,234]

The S/N ratios of volume of organic solvent (DCM, range = 2.32, rank = 2), factor B, at three levels indicated that particle size almost linearly decreased with an increase in volume from 1 to 2 ml (S/N ratio, $r^2 = 0.999$). This decrease in particle size is attributed to the decrease in viscosity of the polymer solution (keeping the amount and MW of polymer constant). This makes it easier to break the suspension into smaller emulsion droplets, resulting in a decreased particle size as explained above. This effect could also be observed with factor C, volume of 1st aqueous phase (range = 1.23, rank = 5), where a decrease in volume increased the viscosity, thereby resulting in an increase in particle size.

The S/N ratios for sonication time (range = 2.09, rank = 4), factor E, did not follow any particular trend; however, the second level was found to be the optimum for achieving smaller particle size. The S/N ratios for stirrer speed, factor F, (the speed at which the magnetic bar was rotating for evaporation of

DCM in the external phase) and G, 2nd PVA concentration have a low range of 0.34 and 0.18 respectively indicating that they have a minimal influence over the size of NPs produced. Therefore, the optimum conditions inferred resulted in NPs of size suitable for cellular uptake into DC as established in the literature [113,212,213,235,236].

FD was employed to obtain the NPs as a dry powder facilitating the use of NPs at a later stage for BSA adsorption. Suitable CPs such as sucrose, trehalose and mannitol were used as stabilisers to ensure good reconstitution after FD. Sucrose at S:NP (5:1) ratio was found to be the best at retaining the size of NPs after FD compared to other CPs.

At a ratio of 100:20 (NP:BSA) there was no significant difference in adsorption whether the BSA was adsorbed onto freeze-dried NPs with CPs, after removal of CPs or directly onto NP suspensions. The overall data (Figure 3-7) suggests that BSA can be effectively adsorbed onto NP suspensions without the need for a FD process, saving time and making the process more economical. Consequently, all the further optimisation was performed with BSA adsorption directly onto NP suspensions.

The adsorption of BSA onto NPs was confirmed by both an increase in particle size after adsorption (Table 3-4) and visually under the confocal microscope (Figure 3-14). In addition, the adsorption of protein onto NPs was expected to be mainly driven by hydrophobic and electrostatic (ionic) interactions, and hydrogen bonding [228]. However, in this study the NPs are negatively charged (evident from zeta-potential values) and BSA in distilled water is also highly negatively

charged [237] suggesting that electrostatic interactions will be minimal and the adsorption process is dominated by hydrophobic interactions and hydrogen bonding. The BSA adsorption onto NPs increased with an increase in the NP:BSA ratio from 100:4 to 100:20, which was expected as the amount of BSA available for adsorption increased. Figure 3-9 indicates that the surface of the NPs was saturated with BSA after 1 h suggesting a maximum adsorption with a ratio of 100:20 (NP:BSA).

3.4.2 Characterisation of Nanocomposite Microparticles

The NCMPs were produced by SD using L-leu as a carrier and a dispersibility enhancer. The SEM pictures (Figure 3-13) showed an irregular or wrinkled surface morphology which is due to an excessive build-up of vapour pressure during water evaporation in the SD process and typically occurs with hydrophobic amino acids, such as L-leu [160,238,239]. Moreover, the size of NPs after dispersing the NCMPs in deionised water confirmed the recovery of NPs with a suitable size for uptake by DCs.

A high residual moisture content can induce particle aggregation and lead to a variation in size distribution [56]. The low moisture content determined from the TGA thermograms indicates a good overall drying efficiency and thus the spray-dried formulations are expected to display higher storage stability [240].

The release profile showed that more than 90% of the BSA was released within 48 h probably because of the weak hydrophobic interactions between BSA and NPs. Moreover, the identical bands (Figure 3-17) observed for BSA standard and BSA

released from the NCMPs suggests that BSA maintained its primary structure and was neither degraded nor affected by the adsorption and SD procedure.

The secondary structure of BSA in the formulation was analysed using CD spectroscopy, a valuable technique in analysing the protein structure [201]. The BSA released samples confirmed the presence of α-helix and β-sheets, although this did decrease compared to standard BSA. However, in protein secondary structure, it is believed that the β-sheet structure is sometimes observed as a special α-helix with only two amino acid residues through stretching resulting from the breakage of hydrogen bond [230,241].

It is established that BSA possesses an enzyme-like activity with the ability to hydrolyse substrates such as p-nitophenyl esters [223,242,243]. In this study, the released BSA sample retained approximately 77% of relative residual esterolytic activity compared to standard BSA. A reduction in BSA activity to 60% was also observed by Abbate *et al.* when released from biohybrid hydrogels [223]. The adsorption and desorption process of BSA could have influenced the structure (evident from a decreased helicity determined by CD) and thus the activity. However, the retention of 77% ester hydrolysis activity would encourage the exploration of the delivery system for further usage.

The FPF value suggests an excellent aerosolisation performance and deep lung deposition profile. The surface activity of the relatively strong hydrophobic alkyl side chain of L-leu accumulating at the particle surface during SD reduces the surface free energy of the dry powder and cohesive inter-particulate interactions resulting in enhanced dispersibility [160,219]. In addition, the dispersibility

enhancing property of L-leu resulting from the corrugated particle surface reduces the contact points between particles leading to improved aerosolisation characteristics of powders [218,239,244]. Similar reports have also demonstrated an enhanced aerosol performance with L-leu containing formulations [218,239,244,245]. Moreover, the MMAD values show an efficient delivery of NCMPs containing BSA to the deep lungs; mainly to the bronchial-alveolar region [65]. A study by Todoroff *et al.* showed that more intense specific immune responses could be achieved by targeting the antigen to the deep lungs rather than to the upper airways [246]. Also, Menzel *et al.* have shown that upon inhalation of Pneumovax®23, a pneumococcal polysaccharide vaccine, by healthy volunteers the vaccine deposited in the alveolar region displaying increased serum antibody levels compared to that deposited in the larger airways [247]. Thus, this deposition to the deep lungs may generate stronger immune responses.

The NGI data suggests a deposition mainly in the bronchial-alveolar region of the lungs [65], thus cell viability studies were performed on A549 and 16HBE14o- cell lines. The results show that both the cell lines were tolerant to the NCMPs containing NPs up to 1.25 mg/ml concentration which is encouraging.

3.5 Conclusions

The PGA-co-PDL anionic NPs of appropriate size to target DCs were successfully produced using Taguchi L_{18} orthogonal array DoE. The BSA adsorption onto NPs in the ratio of 100:20 (NP:BSA) for 1 h at room temperature produced a maximum adsorption of BSA of 10.23±1.87 µg per mg of NPs. The BSA adsorbed NPs were successfully spray-dried using L-leu into NCMPs with a yield

of 42.35±3.17% and the NCMPs had irregular and corrugated morphology. The BSA released from the NCMPs was shown to maintain its structure under SDS-PAGE and CD analysis with 77% of relative residual esterolytic activity. Moreover, a FPF of 76.49±6.26% and MMAD of 1.21±0.67 μm indicate deep lung deposition with NCMPs showing a low toxicity profile.

4. Pulmonary delivery of nanocomposite microparticles containing bovine serum albumin loaded cationic PGA-co-PDL nanoparticles

4.1 Introduction

NPs with a large surface area to volume ratio have reportedly been used as carriers in drug delivery for nearly 40 years [118]. Natural (e.g. albumin, alginate and chitosan) and synthetic (polyesters, polylactides, polyacrylates, polylactones and polyanhydrides) polymers have been exploited to produce these NPs [89,140]. Moreover, biodegradable NPs, made of biodegradable polymers, are being explored for delivery of macromolecules as they offer improved bioavailability, solubility, controlled or sustained release and biocompatibility [140]. The biodegradable polyester, PGA-co-PDL, has been used to produce NPs as described in section 2.2.3.2. In addition to factors such as polymer properties, size and charge of NPs, the surfactants employed in the preparation of NPs also play a vital role in determining their uptake, biodistribution, drug loading and fate after administration, all of which affect the therapeutic efficacy [248,249].

The particle size and surface charge of the NPs are known to play an important role in determining the cellular uptake and cationic NPs (positively charged), compared to either anionic NPs (negatively charged) or neutral NPs, have better interactions with the negatively charged cell membrane thereby improving their cellular uptake [248,250]. Recently, Peetla and Labhasetwar have shown that DMAB-modified polystyrene cationic NPs had better interactions with a model cell membrane demonstrating a greater cellular uptake in vitro [249]. In addition, cationic NPs have the potential to be used for vaccine delivery for their superior interaction with the proteoglycans on the surface of phagocytes such as macrophages and DCs [251,252]. Jensen *et al.* have shown that incorporation of a cationic lipid dioleoyltrimethylammoniumpropane (DOTAP) into the PLGA

matrix during the NP preparation process rendered NPs with a positive surface charge and observed that the surface charge increased with an increase in the concentration of DOTAP from 0 to 20% w/w of PLGA. They further demonstrated the use of these polymeric NPs loaded with small interfering RNA (siRNA) formulated as a dry powder for pulmonary delivery of siRNA [240]. Gupta *et al.* have shown that stable cationic NPs could be produced by coating poly-(ε-caprolactone) NPs with chitosan. These cationic NPs encapsulated H1N1 HA protein which upon intranasal administration induced both Th1 and Th2 responses [253]. Wang *et al.* recently showed that intranasally delivered cationic PLGA particles loaded with foot and mouth disease virus (FMDV) DNA vaccine encoding IL-6 elicited protective immunity against the FMDV challenge [254]. Saljoughian *et al.* demonstrated that upon administration of cationic particles containing a DNA vaccine against *Leishmania donovani* and *L. infantum*, protective immunity associated with high levels of IFN-γ leading to a strong Th1 immune response was observed [255].

Herein, a cationic quaternary ammonium salt, DMAB, was used as a surfactant to produce positively charged NPs. It was previously established that the cationic surfactant, DMAB, produces small and stable NPs and prevents particle agglomeration [248,250,256,257]. Chen *et al.* [250], Hariharan *et al.* [256] and Kwon *et al.* [257] have all reported the use of DMAB to prepare small and stable polymeric cationic NPs. The use of DMAB for pulmonary delivery purposes has not yet been reported till date.

The aim of this chapter was to produce PGA-co-PDL NPs of positive charge and investigate the surface adsorption of a model protein, BSA. The BSA adsorbed NPs were formulated into NCMPs via SD using L-leu as a carrier and characterised for in vitro release profile, aerosol properties, cytotoxicity, and stability and activity of released protein.

4.2 Materials and Methods

4.2.1 Preparation and Characterisation of Nanoparticles

The PGA-co-PDL NPs were prepared as described in section 2.2.3.2. The NPs were characterised for particle size, PDI, zeta-potential and morphology as described in section 2.2.4.

4.2.2 BSA Adsorption and Quantification

The NP suspensions were collected by centrifugation (78,000 g, 40 min, 4 °C) and surface adsorbed with BSA. The adsorption of BSA onto NPs was performed as described in section 2.2.5. The particle size, PDI and zeta-potential of the NPs with and without BSA adsorption were characterised as described in section 2.2.5.1.

4.2.3 Preparation and Characterisation of Nanocomposite Microparticles

The NCMPs were prepared by SD as described in section 2.2.7. The resultant NCMPs were characterised for yield, particle size, PDI, morphology and moisture content as described in section 2.2.8.

4.2.4 Characterisation of BSA Nanoparticle Associations

The association of BSA with NPs was characterised using CLSM as described in section 2.2.9.

4.2.5 In vitro Release Studies

The in vitro release study was performed as described in section 2.2.10.

4.2.6 Investigation of BSA Structure and Activity

The released BSA was evaluated for stability of primary structure (SDS-PAGE) and secondary structure (CD) as described in section 2.2.11. The esterolytic activity of BSA was determined as described in section 3.2.9.

4.2.7 In vitro Aerosolisation Studies

The aerosol properties of the BSA adsorbed cationic NPs/NCMPs were determined as described in section 2.2.12.

4.2.8 Cell Viability Study

The cytotoxicity of cationic NPs and NPs/NCMPs after 24 h exposure to A549 cell line were determined as described in section 2.2.13.

4.3 Results

4.3.1 Preparation and Characterisation of Nanoparticles

The addition of the cationic surfactant, DMAB, at 1% w/w to the organic phase showed no significant difference ($p < 0.05$, ANOVA/Tukey's comparison) in particle size and PDI compared to no cationic surfactant whereas the surface charge changed from negative to positive, as shown in Table 4-1. Moreover, with an increase in the concentration of DMAB, from 1 to 2% w/w, the particle size of NPs decreased significantly ($p < 0.05$, ANOVA/Tukey's comparison) accompanied by an increase in surface charge. However, it was observed that after two washes (by centrifugation) the surface charge decreased with an increase in particle size (Table 4-1) for all concentrations of DMAB.

Table 4-1 The average particle size and surface charge of nanoparticles prepared using different concentrations of surfactant *(Mean±SD, n=3)*

Concentration of DMAB (% w/w)	0	1	2
Before Centrifugation			
Z-Average size (nm)	162.23±06.80*	175.74±15.46*	128.64±06.01*
Surface Charge (mV)	-10.28±01.00	+13.24±08.00	+42.32±02.70
After Centrifugation			
Z-Average size (nm)	463.52±23.69*	710.71±152.66*	223.08±05.60*
Surface Charge (mV)	-19.14±01.08	-10.86±00.84	+35.94±01.36

Note: The PDI values of all samples were in the range of 0.1-0.2 (before centrifugation) and 0.2-0.3 (after centrifugation); * is $p < 0.05$, ANOVA/Tukey's comaprison

The microscopic images of NPs shown in Figure 4-1 indicate that the NPs appeared to be smooth and spherical in shape with no visible aggregation or adhesion between NPs.

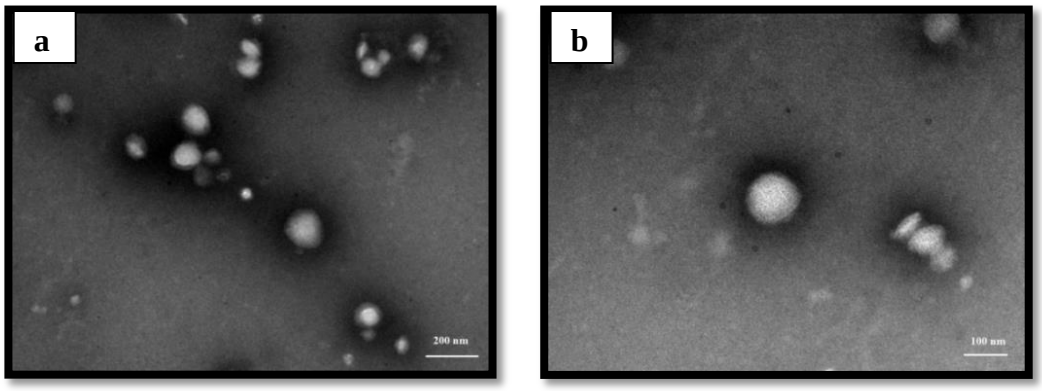

Figure 4-1 Transmission electron microscope image of cationic nanoparticles formulated with 2% w/w DMAB stabiliser (a) 44,000X (scale bar – 200 nm) and (b) 110,000X (scale bar – 100 nm)

4.3.2 BSA Adsorption and Quantification

The average amount of BSA adsorbed onto cationic NPs, as shown in Figure 4-2, increased significantly from a NP:BSA ratio of 100:4 (10.01±1.19 µg per mg of NPs), 100:7 (33.70±3.25 µg per mg of NPs), 100:10 (54.04±1.66 µg per mg of NPs), 100:12 (64.10±4.05 µg per mg of NPs), 100:16 (79.54±0.57 µg per mg of NPs) to 100:20 (91.29±3.66 µg per mg of NPs) ($p < 0.05$, ANOVA/Tukey's comparison; all the values are significantly different to each other).

Table 4-2 lists the particle size, PDI and zeta-potential of PGA-co-PDL cationic NPs with and without BSA adsorption. The significant increase ($p < 0.05$, ANOVA/Tukey's comparison) in particle size of NPs accompanied with a change

in the surface charge was ascribed to the adsorption of BSA onto NPs as confirmed using confocal microscopy (section 4.3.5).

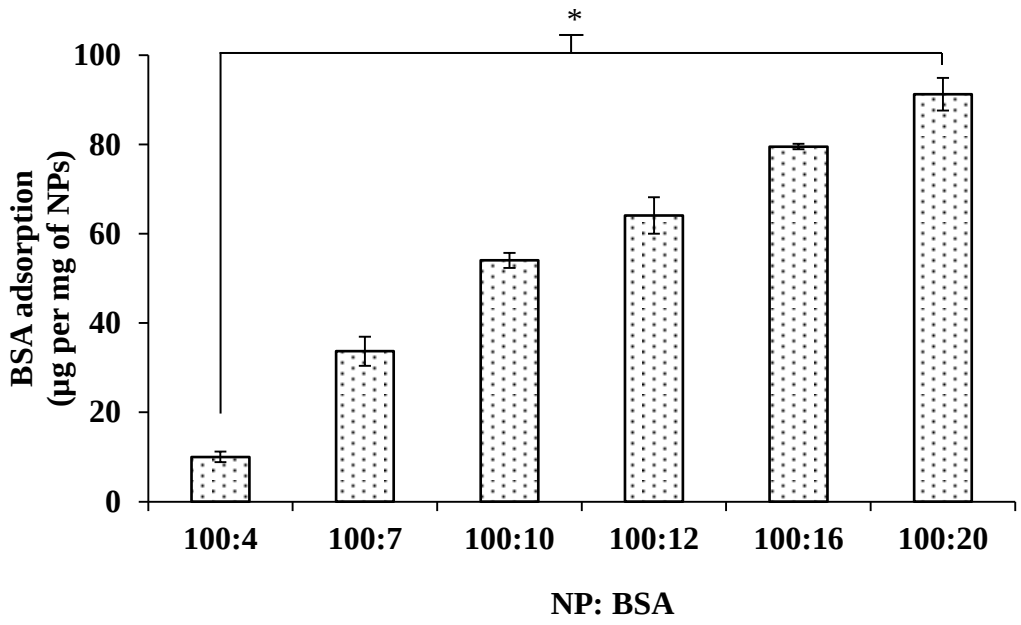

Figure 4-2 Amount of bovine serum albumin (BSA) adsorbed in µg per mg of nanoparticles (NPs) for different ratios of NP:BSA, * is $p < 0.05$, ANOVA/Tukey's comparison *(Mean±SD, n=3)*

Table 4-2 Particle size, PDI and zeta-potential of PGA-co-PDL cationic nanoparticles (NPs) with and without bovine serum albumin (BSA) adsorption *(Mean±SD, n=3)*

	NP suspensions[a]	Without BSA adsorption[b]	With BSA adsorption[c]
Particle Size (nm)	128.64±06.01*	234.65±10.25*	348.36±04.02*
PDI	0.099±0.016	0.200±0.010	0.266±0.006
Zeta-potential (mV)	+42.32±02.70	+20.50±00.17	-01.44±00.18

[a] NPs characterised immediately after preparation without centrifugation, [b] NPs characterised after centrifugation but without adsorption of BSA, [c] NPs characterised after centrifugation and BSA adsorption, * $p < 0.05$, ANOVA/Tukey's comparison

4.3.3 Characterization of Nanocomposite Microparticles

4.3.3.1 Yield, Particle Size and Morphology

A reasonable yield of spray drying, 44.82±4.12% for the empty cationic NPs/NCMPs and 48.00±5.66% for BSA adsorbed cationic NPs/NCMPs was obtained.

The size of NPs after re-dispersion in deionised water for spray-dried empty cationic NPs/NCMPs was 216.50±25.45 nm and PDI 0.276±0.034, and for BSA adsorbed cationic NPs/NCMPs was 356.73±33.83 nm and PDI 0.467±0.116, confirming the recovery of NPs from spray-dried formulations *(Mean±SD, n=3)*.

The scanning electron pictures (Figure 4-3) of NCMPs revealed their irregular shape and corrugated surface texture. In addition, the size of the NCMPs calculated from the SEM pictures was found to be approximately 2.09±0.16 µm.

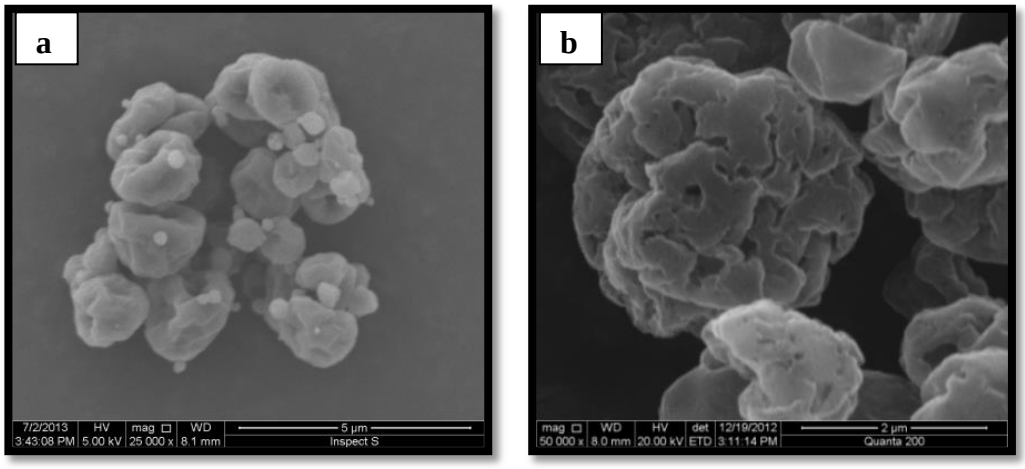

Figure 4-3 Scanning electron microscope pictures of cationic nanocomposite microparticles (a) 5 µm and (b) 2 µm

4.3.3.2 Moisture Content

The analysis of thermograms (Figure 4-4) obtained using TGA showed that the dry powder formulation had a residual moisture content of 0.46±0.01% w/w indicating the drying efficiency employed during the SD process.

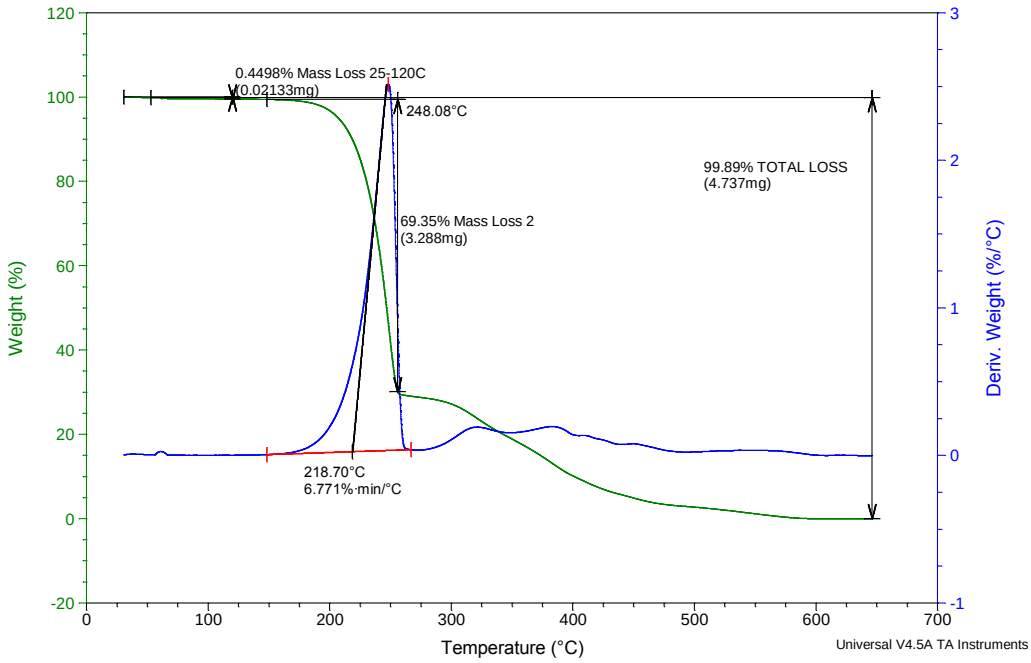

Figure 4-4 A representative thermogram of cationic nanocomposite microparticles obtained using thermal gravimetric analysis *(Mean±SD, n=3)*

4.3.4 Characterisation of BSA Nanoparticle Associations

The association of BSA with NPs was visualised using the confocal microscope. The confocal images (Figure 4-5) obtained, the red and green colours representing NR/NPs and FITC-BSA, respectively, were present simultaneously indicating their association. In addition, the increase in particle size observed after adsorption of BSA onto PGA-co-PDL cationic NPs also confirms their association (Table 4-2).

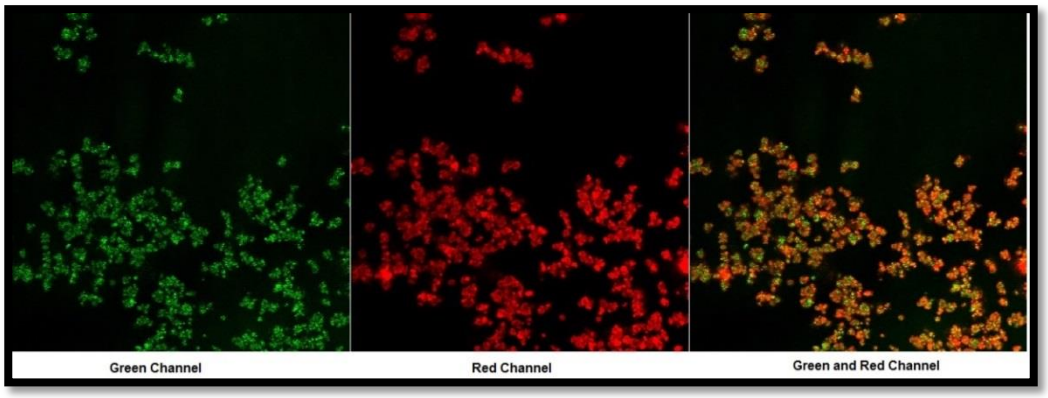

Figure 4-5 Confocal microscopic image, split view, of spray-dried microparticles containing the fluorescent nanoparticles (red) adsorbed with FITC-BSA (green)

4.3.5 In vitro Release Studies

In vitro release studies were performed on BSA adsorbed cationic NPs/NCMPs and reported as cumulative percentage BSA released over time (Figure 4-6). An initial burst release of 22.45±2.39% (BSA) was observed followed by continuous release up to 5 h, with a BSA release of 73.74±6.60%. After this time period, a slow continuous release was observed with release of 88.85±4.38% over 48 h.

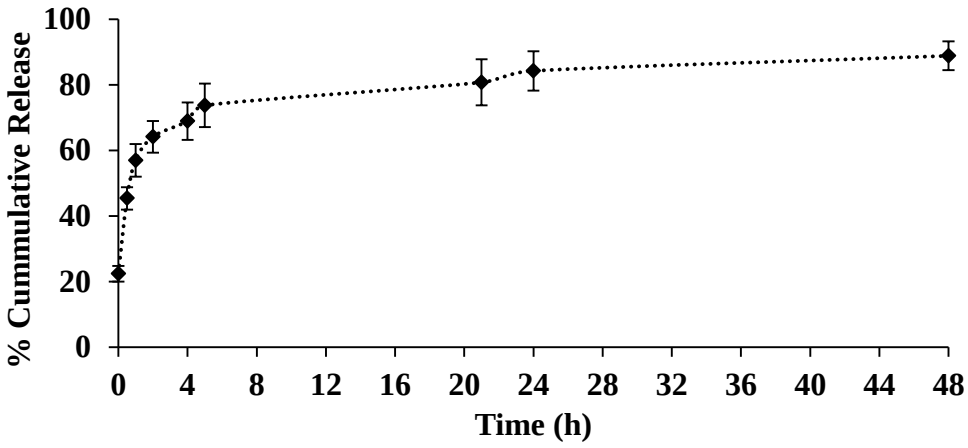

Figure 4-6 In vitro release profile for bovine serum albumin (BSA) from BSA adsorbed cationic nanocomposite microparticles in phosphate buffer saline, pH 7.4 ***(Mean±SD, n=3)***

4.3.6 Investigation of BSA Structure and Activity

The primary structure of BSA released from BSA adsorbed cationic NPs/NCMPs after 48 h was analysed using SDS-PAGE. As shown in Figure 4-7 below, standard BSA displays a white band (lane 2) adjacent to the MW standards (lane 1). In addition, the bands for released BSA from BSA adsorbed cationic NPs/NCMPs (lane 3-5) are identical to that of the standard BSA indicating its stability during and after the SD process.

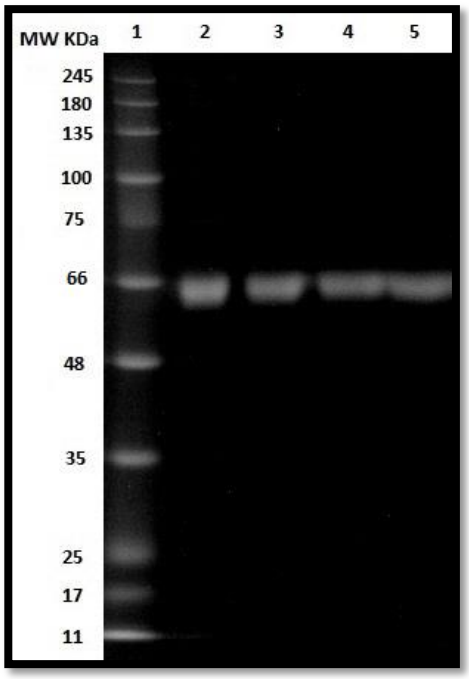

Figure 4-7 SDS-PAGE of Lane 1: MW standards, broad range (Bio-Rad Laboratories, Hercules CA, USA), Lane 2: bovine serum albumin (BSA) standard, Lane 3, 4 and 5: Released BSA from BSA adsorbed cationic nanocomposite microparticles after 48 h

Conformational changes of BSA in the supernatant after adsorption and BSA released from the delivery system were determined by CD spectroscopy. The CD spectra of standard BSA, BSA supernatant and BSA released are shown in Figure

4-8a and 4-8b. As expected, the CD spectra show two valleys at 208 and 222 nm characteristic of α-helical structure. The data for the spectra are presented in Table 4-3, where standard BSA, BSA released and BSA supernatant showed that the predominant structure of the peptide was helical displaying 51, 43 and 50.5% helicity, respectively. In addition, the spectral data obtained for standard BSA are in good agreement with previous reports [230,258]. Comparing the CD results of BSA released with that of standard BSA, the α-helix content decreased by 8% and the β-sheet content increased by 8.4%.

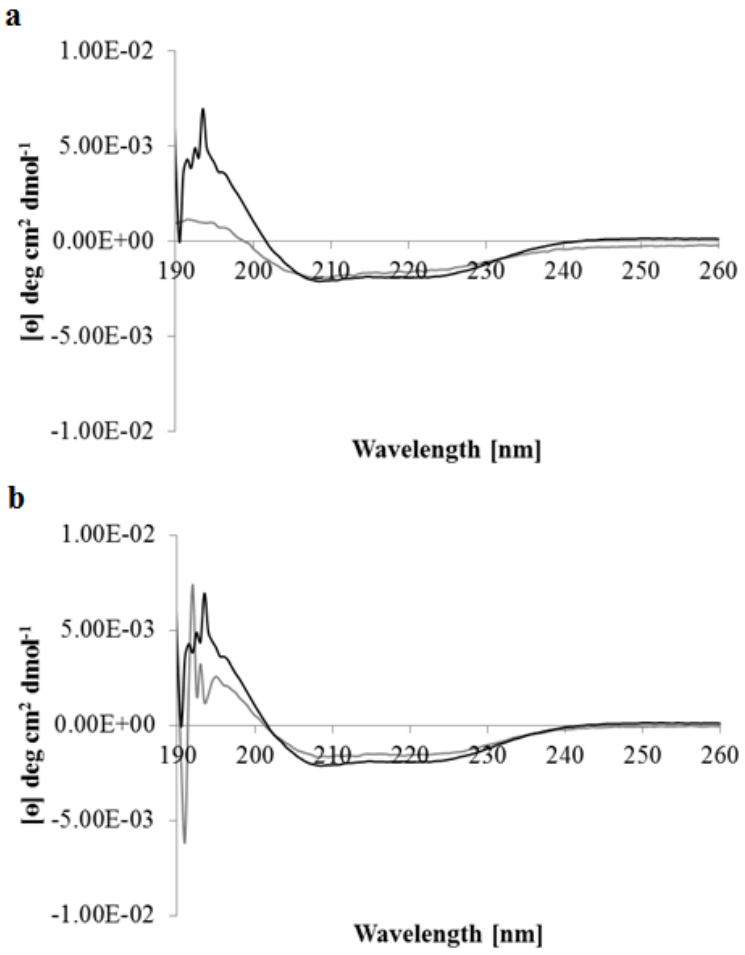

Figure 4-8 Circular dichroism spectra of standard bovine serum albumin (BSA) (black) (a) supernatant BSA (grey) and (b) BSA released (grey)

Table 4-3 The percentages of the secondary structures of standard, supernatant and released bovine serum albumin (BSA) samples

Sample	Helix	Strand	Turns	Unordered
Standard BSA	51.0±0.007	21.1±0.070	06.0±0.010	18.0±0.007
BSA Supernatant	50.5±0.049	24.5±0.021	11.0±0.042	14.0±0.280
BSA Released	43.0±0.021	29.5±0.007	07.0±0.000	21.0±0.000

The esterolytic activity of the released BSA sample was investigated using 4-nitrophenyl acetate esterase and was calculated to be 78.76±1.54% relative to standard BSA.

4.3.7 In vitro Aerosolisation Studies

The percentage mass of BSA recovered from the NGI was approximately 83%, well within the pharmacopeial limit of 75-125% of the average delivered dose [259]. The deposition data obtained from spray-dried formulations displayed a FPM of 16.57±0.74 µg (per capsule of 12.5 mg of cationic NPs/NCMPs), FPF of 70.67±4.07% and MMAD of 2.80±0.21 µm suggesting that the formulation was capable of delivering efficient BSA to the lungs. Figure 4-9 shows the percentage stage-wise deposition of BSA in NGI.

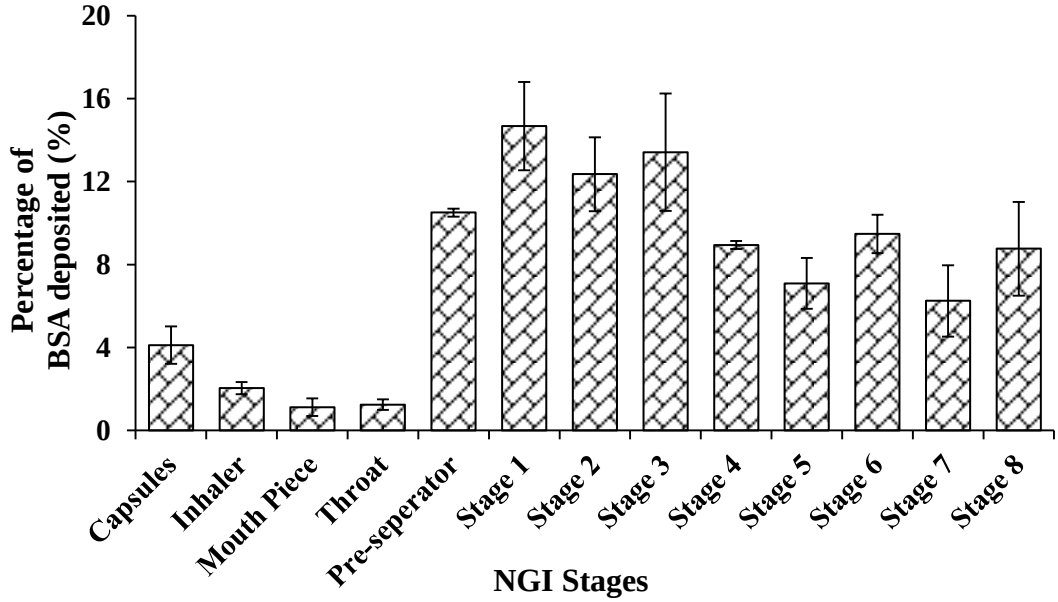

Figure 4-9 The percentage deposition of bovine serum albumin (BSA) stage-wise in Next Generation Impactor (NGI) ***(Mean±SD, n=3)***

4.3.8 Cell Viability Study

The cytotoxicity of cationic NPs and NCMPs was assessed by the MTT assay [206] using A549 cells. The cationic NPs and NCMPs (Figure 4-10) indicated a decrease in cell viability with an increase in concentration. The particles showed a cell viability of 74.55±12.29% (NPs), 95.07±14.50% (NCMPs) at 78.12 µg/ml concentration that reduced to 50.50±9.41% (NPs), 75.76±03.55% (NCMPs) at 156.25 µg/ml concentration after 24 h exposure. Above 156.25 µg/ml concentration, the NPs and NCMPs showed cell survival less than 50%.

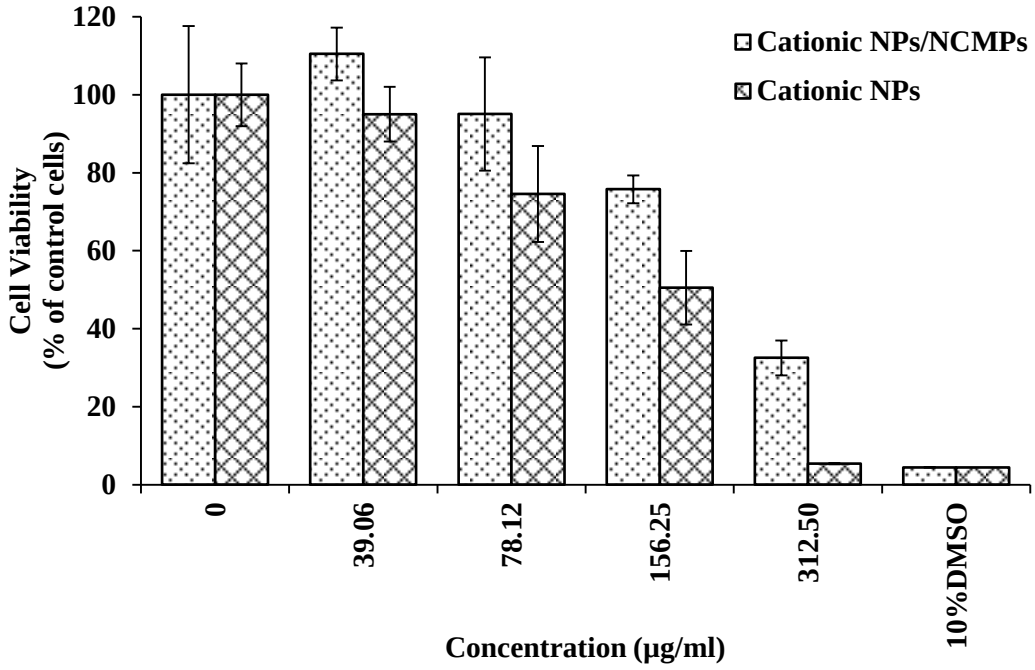

Figure 4-10 A549 cell viability measured by MTT assay after 24 h exposure to cationic nanoparticles (NPs) and nanocomposite microparticles (NPs/NCMPs) ***(Mean±SD, n=3)***

4.4 Discussion

4.4.1 Preparation and Characterisation of Nanoparticles

Surfactants are often employed in the NP preparation process to increase the physical stability and decrease agglomeration. Herein, the cationic surfactant, DMAB, was employed to prepare positively charged NPs. Its use as a surfactant in preparing cationic NPs has been previously reported in the literature [248,250,256,257,260]. In this study, the effect of DMAB concentration on the particle size and surface charge of NPs was investigated. It was observed that with an increase in the concentration of DMAB surfactant, the particle size of NPs decreased accompanied with an increase in the surface charge. The smaller size

achieved at the higher concentration of surfactant could be attributed to the presence of the surfactant at the interface as previously reported by Bhardwaj *et al.* [248]. Similar results with respect to particle size and surface charge were previously obtained with DMAB and have been reported by others [248,250,256,257].

The DMAB concentration of 2% w/w was chosen as the optimum for producing NPs with positive charge as the particle size achieved, 128.64±06.01 nm, was comparable to that of the anionic NPs produced using PVA alone as surfactant, 128.50±06.57 nm. However, the particle size of both types of NPs increased to 200-225 nm after removal of the surfactant by washing (centrifugation). This similarity in particle size of NPs, after centrifugation, of the anionic and cationic NPs enabled the investigation of effect of surface charge on protein adsorption and furthermore the effect on their uptake by DCs.

As mentioned in chapter 3, the adsorption of proteins onto polymeric NPs is believed to be dominated by hydrophobic, electrostatic interactions and hydrogen bonding [228]. Here, the effect of BSA adsorption onto the polymeric DMAB-modified cationic NPs wherein the BSA is negatively charged was investigated [237]. The adsorption of BSA onto the cationic NPs increased significantly with an increase in the loading concentration of BSA. This was because more BSA was available for binding and further supports the dominance of electrostatic interactions between the BSA and cationic NPs. In addition, the adsorption of BSA onto the surface of cationic NPs was confirmed by an increase in the particle size of NPs after adsorption accompanied with a change in surface charge from

positive to almost neutral. This change in surface charge could be due to the orientation the BSA molecules have assumed on the surface of cationic NPs for their stability thus exposing only certain charges. In addition, the adsorption of BSA was also characterised by confocal microscopy which depicts the association of BSA molecules with the cationic NPs.

The adsorption data (section 3.3.4 and 4.3.2) suggest that under similar conditions the anionic NPs achieved similar adsorption of BSA of 10.23±1.87 µg per mg of NPs for 100:20 (NP:BSA) compared to 10.01±1.19 µg per mg of NPs for 100:4 (NP:BSA) for cationic NPs. The adsorption data also indicated that cationic NPs attracted more BSA protein molecules onto their surface compared to the anionic NPs, resulting in higher BSA adsorption at similar NP:BSA ratios. This further confirmed that the main interactions in the adsorption process for cationic NPs under the given conditions are electrostatic in nature rather than hydrophobic or hydrogen bonding. Similarly, Li *et al.* have recently shown that adsorption of negatively charged ovalbumin onto positively charged aluminium hydroxide NPs was mainly driven by electrostatic interactions [261]. Singh *et al.* have shown that anionic and cationic PLGA particles surface adsorbed with a variety of antigens, including plasmid DNA, recombinant proteins, immunostimulatory oligonucleotides resulted in the induction of significantly enhanced immune responses in comparison with alum [262,263]. Besides, achieving higher adsorption at lower concentrations of added protein, this reduces the amount of NPs required to be delivered and for expensive recombinant proteins reduces the amount of initial protein required thereby reducing the cost of the final product.

4.4.2 Characterisation of Nanocomposite Microparticles

The NCMPs were produced by SD using L-leu as a microcarrier. The NCMPs produced containing the cationic NPs had a rough surface and were irregularly shaped of a similar nature to that observed with NCMPs containing the anionic NPs. Rough and wrinkled surface characteristics are typical for NCMPs produced using L-leu as an excipient (see section 3.4.2 for more detailed explanation) and has been widely reported in the literature [218,219,238,239,245,264].

The residual moisture content in the SD formulations induces aggregation and leads to variation in size distribution [56]. In addition, a higher percentage of moisture affects the stability of the formulation and the aerosolisation properties resulting in poor deposition with a subsequent reduction in NPs for DC uptake. The moisture content obtained was low and was comparable to anionic NPs/NCMPs. Moreover, low percentages of moisture content (~1-1.5%) in MPs prepared using this polymer have previously been measured and reported [160,240].

The in vitro release data showed that 88% of the BSA was released over 48 h; lower than the release obtained from anionic NPs/NCMPs (95%). In addition, the burst release observed from cationic NPs/NCMPs was 22% compared to 30% for anionic NPs/NCMPs signifying the stronger interactions between cationic NPs and BSA.

The stability of released BSA was investigated using SDS-PAGE (primary structure) and CD (secondary structure). The identical bands obtained for standard BSA and released BSA confirmed that the protein had not degraded into smaller

components and that it remained intact during the adsorption and SD process. This was further confirmed by CD spectra data wherein the released BSA sample displayed the presence of α-helix (43%) though slightly less than the standard BSA (51%). The BSA released from cationic NPs/NCMPs retained more secondary structure (43%) compared to anionic NPs/NCMPs (36%) suggesting that the type of adsorption process had an impact on desorption of BSA from NPs. Furthermore, the released BSA sample retained approximately 78% of relative residual esterolytic activity compared to standard BSA. The reduction in activity was expected as a reduction in the helical content was observed in the CD spectra.

The FPF and MMAD values suggest an excellent aerosolisation performance and deep lung deposition profile in the bronchial-alveolar region of the lungs [65]. The FPF values obtained with the cationic NPs/NCMPs (70.67±4.07%) was not significantly different from that of the anionic NPs/NCMPs (76.95±5.61%) ($p > 0.05$, ANOVA/Tukey's comparison). However, the MMAD values indicate significantly smaller sized particles for the anionic NPs/NCMPs (1.21±0.67) compared to cationic NPs/NCMPs (2.80±0.21) ($p < 0.05$, ANOVA/Tukey's comparison). Although the MMAD values differ the deposition would still be in the respirable airways as the values are in the range of 1-5 µm.

The aerosol properties of the spray-dried formulation predict an effective delivery to the lungs via inhalation. The NCMPs containing the DMAB-modified cationic NPs were relatively toxic compared to the anionic NPs/NCMPs; however, the probability of achieving such high local concentrations can be excluded as after inhalation the dose would be deposited and spread in different parts of the lungs and not be deposited in a focused area [248]. The difference in cell viability

between the NPs and NPs/NCMPs, at similar concentrations, could be attributed to the lower amount of NPs present in NCMPs due to dilution with L-leu for SD. One drawback that is often associated with cationic molecules is their cytotoxicity that limits the dosage to be administered to a minimum thereby resulting in low efficiency [265]. Fischer *et al.* reported that the use of cationic particles, made of different polymers, upon interaction with the negatively charged cell surface is known to cause toxicity. Besides, it was also noted that the magnitude of the cytotoxicity of different polymers were highly dependent on time and concentration [266]. In addition, Harush-Frenkel *et al.* reported that cationic NPs were shown to cause more toxicity concerns compared to anionic NPs [267,268]. However, in the case of DMAB-modified cationic PGA-co-PDL NPs, high adsorption of BSA onto NPs can be achieved thus requiring a low dosage of NPs and NPs/NCMPs to generate an effective immune response addressing toxicity concerns. Moreover, the amount of protein to be adsorbed could be varied depending on the antigen.

Cationic particles have the advantage of interacting efficiently with the negatively charged proteoglycans on the cell surface of phagocytes such as macrophages and DCs that play an important role in generating an immune response [269]. Kim *et al.* have recently reported the use of cationic NPs for delivery of protein drugs to non-small cell lung tumours [270]. In addition, Kwon *et al.* have reported successful and more efficient delivery of cationic NPs carrying model antigen, ovalbumin, to bone marrow DCs compared to neutral NPs while the toxicity of both cationic and neutral NPs remained similar at concentrations of 125-250

μg/ml [265]. Furthermore, it has been reported that cationic particles ranging from nano up to 1 micron diameter could be effectively taken up by DCs [252,271].

4.5 Conclusions

The DMAB-modified cationic PGA-co-PDL NPs of a similar size to that of the anionic PGA-co-PDL NPs and of appropriate size to target DCs were successfully produced. The adsorption of BSA onto the cationic NPs in the ratio of 100:4 (NP:BSA) for 1 h at room temperature produced similar adsorption (10.01±1.19 μg of protein per mg of NPs) compared to anionic NPs at 100:20 ratio. The BSA adsorbed cationic NPs were successfully spray-dried using L-leu into NCMPs producing a yield of 48.00±5.66%, with irregular and wrinkled surface morphology. The BSA released from the NCMPs was shown to maintain its structure under SDS-PAGE and CD analysis with 78% relative residual esterolytic activity. Moreover, the FPF of 70.67±4.07% and MMAD of 2.80±0.21 μm values indicate deep lung deposition in the bronchial-alveolar region.

5. Pulmonary vaccine delivery of nanocomposite microparticles containing pneumococcal surface protein A

5.1 Introduction

Streptococcus pneumoniae is the leading cause of bacterial pneumonia worldwide, especially amongst the immunocompromised, elderly over the age of 50 and children under the age of 5 [272]. It is also known to cause other invasive diseases such as septicaemia and meningitis [54]. Currently, two pneumococcal vaccine types are available, polysaccharide vaccine (23-valent) and conjugate vaccine (7, 10 or 13-valent) [9,39]. The conjugate vaccines have shown higher preventive efficacy for invasive infections compared to polysaccharide vaccines; however, there is an emergence of diseases caused by non-vaccine serotypes [273]. Moreover, conjugate vaccines are expensive, complicated and time consuming to manufacture thus limiting their usage especially in the LMICs where a significant burden of the disease is reported [55,273]. Additionally, with 94 serotypes identified and a steady rise in diseases by non-vaccine serotypes being reported, further emphasis on identifying and developing alternate vaccine candidates to be employed in an effective vaccine delivery system has gained importance [49].

Institutes such as the US NIH and PATH have elaborated on the usage of pneumococcal proteins as alternate vaccine candidates for their ubiquitous presence across serotypes [46]. These proteins have the ability to protect against all serotypes thus preventing prevalence of specific serotypes [39,46]. Among the different types of pneumococcal proteins such as PspA, PspC and pneumolysin; PspA is one of the most promising candidates and has been widely investigated by several groups [46,49,54–56,273]. The main function of PspA is to prevent the deposition of complement on the surface of the bacterium thereby inhibiting opsonisation and death by apolactoferrin at mucosal sites [55,273].

Vaccination with PspA has been shown to induce protective antibodies in humans [274–276]. However, recombinant protein based vaccines are poorly immunogenic generating low antibody responses and thus require the addition of an adjuvant to boost their efficacy [273]. Despite decades of research on adjuvants, only a few of them (e.g. alum salts, MF59, AS03) have been licensed [277]. The main hurdle in their development has always been safety [177]. However, research is now focused on delivering antigens via particulate carriers where the antigen can be associated with the particles acting as delivery systems with the added benefit of augmenting the generated immune response upon uptake by APCs [173,177]. In addition, particulate antigens are known to generate a stronger immune response compared to soluble antigens [278]. As such, recent research has increasingly focused on using polymeric NPs as delivery systems for antigen delivery [55–57,235,278,279]. It has also been shown by different groups that polymeric particles have enhanced the immunogenicity of PspA [55–57].

Pneumococcal infections are mostly preceded by colonisation of the upper airways and nasal carriage, and this is a primary source of infection in humans [57,280]. Therefore, an optimal vaccine strategy would be to deliver the antigen via a mucosal route providing protection against both the colonising bacteria and invasive disease [29,57]. In addition, the activation of the immune system requires the effective delivery of antigen to APCs such as DCs which process the internalised antigen thereby generating an immune response [265].

In this chapter, a dry powder vaccine containing PspA adsorbed polymeric NPs for delivery via inhalation was developed. In addition, the effect of surface charge of NPs on their uptake by DCs has been visualised. Furthermore, the effect of

preparation process on the stability, integrity and antigenicity of PspA was investigated and reported.

5.2 Materials and Methods

5.2.1 Preparation of Nanoparticles

The anionic and cationic PGA-co-PDL NPs were prepared as described in sections 2.2.3.1 and 2.2.3.2, respectively. The optimum conditions used to produce anionic NPs were; 200 mg of PGA-co-PDL in 2 ml DCM, 5 ml of 10% w/v PVA (1st aq. phase), 2 min sonication, 20 ml of 0.75% w/v PVA (2nd aq. phase) and cationic NPs were; 200 mg of PGA-co-PDL and 2% w/w DMAB in 2 ml DCM, 5 ml of 5% w/v PVA (1st aq. phase), 2 min sonication, and 20 ml of 0.75% w/v PVA (2nd aq. phase).

5.2.2 Production and Purification of PspA4Pro

Recombinant PspA4Pro was produced, purified and supplied by Dr Eliane Miyaji and Dr Viviane Gonçalves from the Insituto Butantan, Brazil.

The protein was produced and purified using previously published methods with slight modifications [281–283]. The production of recombinant PspA4Pro was performed in 5 L bioreactors using; fed-batch cultivation with defined medium containing glycerol as carbon source and lactose as inducer [281] or batch cultivation with complex medium containing glucose, glycerol and lactose for auto-induction [282]. The purification method consisted of cell disruption in a continuous high pressure homogenizer at 500 bar for 8 min, precipitation of the

homogenate with 0.1% cationic detergent cetyltrimethylammonium bromide, pellet removal by centrifugation, anion exchange chromatography in Q-Sepharose, cryoprecipitation at pH 4.0 and cation exchange chromatography in SP-Sepharose [283]. The desired PspA4Pro purity (>95%) was reached with recovery ranging from 14% to 33%. The developed process also removed LPS, yielding acceptable levels of endotoxin (0.3-0.6 EU/ml) in the final product [284]. The purified PspA4Pro was recognised by antibodies, was able to bind lactoferrin and presented the characteristic α-helical secondary structure.

5.2.3 PspA4Pro Adsorption and Quantification

The NP suspensions were collected by centrifugation (78,000 g, 40 min, 4 °C) and surface adsorbed with PspA4Pro. The adsorption onto anionic and cationic NPs was performed at ratios of 100:20 (NP:PspA4Pro) and 100:4 (NP:PspA4Pro) respectively, as described in section 2.2.5.

The particle size, PDI and zeta-potential of anionic and cationic NPs with and without PspA4Pro adsorption were characterised as described in section 2.2.5.1.

5.2.4 Preparation and Characterisation of Nanocomposite Microparticles

The NCMPs were prepared by SD as described in section 2.2.7. The resultant NCMPs were characterised for yield, particle size and morphology as described in section 2.2.8.

5.2.5 In vitro Release Studies

The in vitro release studies were performed as described in section 2.2.10.

5.2.6 Investigation of PspA4Pro Structure

The released PspA4Pro was evaluated for stability using SDS-PAGE for primary structure and CD for secondary structure as described in section 2.2.11.

5.2.7 Antigenicity of Released PspA4Pro

The ability of anti-PspA antibody to bind to the released PspA4Pro, defined as antigenicity, was determined using an enzyme-linked immunosorbent assay (ELISA) as previously described by Haughney *et al.* with slight modifications [55]. Briefly, the concentration of released PspA4Pro was adjusted to 0.5 µg/ml and 50 µl coated on a high binding chemistry 96-well plate (Costar 96-Well Microplates, Cole-Parmer, UK) followed by incubation overnight at 4 ºC. Next, the PspA4Pro solution was removed from the wells and blocking buffer, PBS with 1% fish gelatin (Sigma Aldrich, UK), was added and incubated for 2 h at room temperature. After the incubation, the buffer was gently removed and the wells were washed three times with PBS containing 0.5% Tween 20 (PBS-T). The anti-PspA monoclonal antibody 22003 (QED Bioscience, San Diego, CA) (100 µl) at 1 µg/ml concentration was then added to each well and incubated overnight at 4 ºC. The plates were then washed three times with PBS-T followed by addition of 100 µl of alkaline phosphatase-conjugated goat anti-mouse IgG (heavy and light chain) (Jackson ImmunoResearch Europe Ltd, UK) at a 0.1 µg/ml concentration. The plates were incubated for 2 h at room temperature. To this, 200 µl of alkaline

phosphatase yellow (pNPP) liquid substrate buffer (Sigma Aldrich, UK) was added and incubated for 15 min at room temperature to develop the ELISA. The colorimetric changes observed were measured at an absorbance of 405 nm using a microplate reader (Epoch, BioTek Instruments Ltd, UK). The ratio of absorbance between the released PspA4Pro and the native protein was measured and represented as relative antigenicity.

5.2.8 In vitro Aerosolisation Studies

The aerosol properties of the PspA4Pro adsorbed anionic NPs/NCMPs were determined as described in section 2.2.12.

5.2.9 Cell Viability Study

The cytotoxicity of both anionic and cationic NPs after 4 h exposure to DCs was determined using MTT assay as described in section 2.2.13.

5.2.10 Cellular Uptake of NPs by DCs

The uptake of anionic and cationic NPs by DCs in cell culture medium and PBS were visualised using the CLSM (Carl Zeiss LSM 710, UK). The DCs ($2x10^5$ cells per well) were seeded onto an 8-well chamber slides (Nunc Lab-Tek, Thermo Scientific, UK) and incubated at 37 ºC for 48 h allowing the cells to adhere to the wells. Anionic NPs at a concentration of 10 µg/ml and cationic NPs at a concentration of 2.5 µg/ml were incubated for 1 h at 37 ºC with DCs. Following this, the supernatant was removed, washed three times with PBS and the DCs were fixed with 4% paraformaldehyde (Fisher Scientific, UK) for 10 min

at room temperature. The DCs were then washed three times with PBS and 100 µl of 5 µg/ml wheat germ agglutinin antibody (WGA, Alexa Fluor® 488 Conjugate, Life Technologies, UK) was added and incubated at 37 ºC for 15 min. The excess antibody was removed by washing three times with PBS followed by staining the nucleus of DCs with 100 µl of 20 µg/ml 4',6-diamidino-2-phenylindole, dilactate (DAPI, Sigma Aldrich, UK), and then incubated for 10 min at room temperature. Excess DAPI was removed by washing three times with PBS. The wells were then visualised under a confocal microscope.

5.3 Results

5.3.1 PspA4Pro Adsorption and Quantification

The adsorption of PspA4Pro onto anionic and cationic NPs was performed under optimised conditions (using the results obtained in chapters 3 and 4): at a ratio of 100:20 (NP:PspA4Pro) corresponding to 500 µg/ml PspA4Pro for anionic NPs and 100:4 corresponding to 100 µg/ml PspA4Pro for cationic NPs, and 1 h adsorption time at room temperature. The average adsorption of PspA4Pro onto NPs (µg per mg of NPs) was 19.68±2.74 for anionic NPs and 18.77±0.44 for cationic NPs.

Table 5-1 lists the particle size, PDI and zeta-potential of PGA-co-PDL anionic and cationic NPs with and without PspA4Pro adsorption. The significant increase in particle size ($p < 0.05$, ANOVA/Tukey's comparison) of both anionic and cationic NPs accompanied with a change in the surface charge is ascribed to the adsorption of PspA4Pro onto NPs.

Table 5-1 Particle size, PDI and zeta-potential of PGA-co-PDL nanoparticles (NPs) with and without pneumococcal surface protein A (PspA4Pro) adsorption *(Mean±SD, n=3)*

	Without PspA4Pro adsorption	With PspA4Pro adsorption
Anionic NPs		
Particle Size (nm)	203.90±02.55[a*]	322.83±04.25 [b*]
PDI	0.205±0.007	0.402±0.018
Zeta-potential (mV)	-24.56±0.50	-13.23±0.11
Cationic NPs		
Particle Size (nm)	234.65±10.25 [a*]	373.56±06.27 [b*]
PDI	0.200±0.010	0.397±0.008
Zeta-potential (mV)	+20.50±0.17	+23.43±0.55

[a] NPs characterised after centrifugation but without adsorption of PspA4Pro, [b] NPs characterised after centrifugation and PspA4Pro adsorption, * $p < 0.05$, ANOVA/Tukey's comparison

5.3.2 Characterization of Nanocomposite Microparticles

5.3.2.1 Yield, Particle Size and Morphology

A reasonable yield of spray-dried NCMPs was obtained; with 55.55±6.64% for the PspA4Pro adsorbed anionic NPs/NCMPs and 53.98±2.23% for the PspA4Pro adsorbed cationic NPs/NCMPs.

The SEM pictures (Figure 5-1) of anionic and cationic NCMPs revealed the shape to be irregular and surface texture corrugated. The size of NCMPs calculated from the SEM pictures was found to be approximately 1.99±0.25 µm.

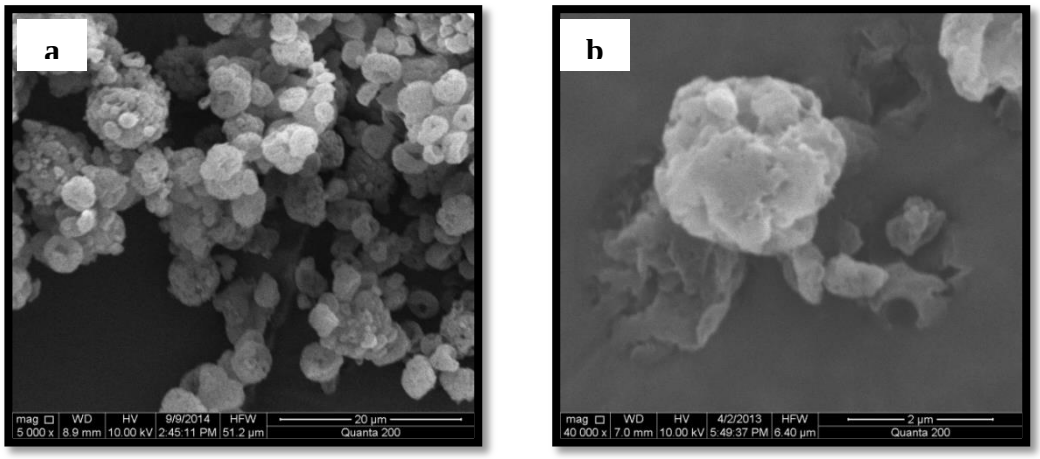

Figure 5-1 Scanning electron microscope pictures of nanocomposite microparticles (a) 20 µm and (b) 2 µm

5.3.3 In vitro Release Studies

In vitro release studies were performed on NCMPs containing either anionic or cationic NPs and reported as the cumulative percentage of PspA4Pro released over time (Figure 5-2). An initial release of 40.59±4.94% (anionic NPs/NCMPs) and 3.00±0.28% (cationic NPs/NCMPs) was observed followed by continuous release of PspA4Pro with 94.30±2.90% (anionic NPs/NCMPs) and 43.80±3.75% (cationic NPs/NCMPs) over 48 h. Moreover, complete recovery of PspA4Pro from cationic NPs/NCMPs was observed upon addition of 2% SDS to the release media.

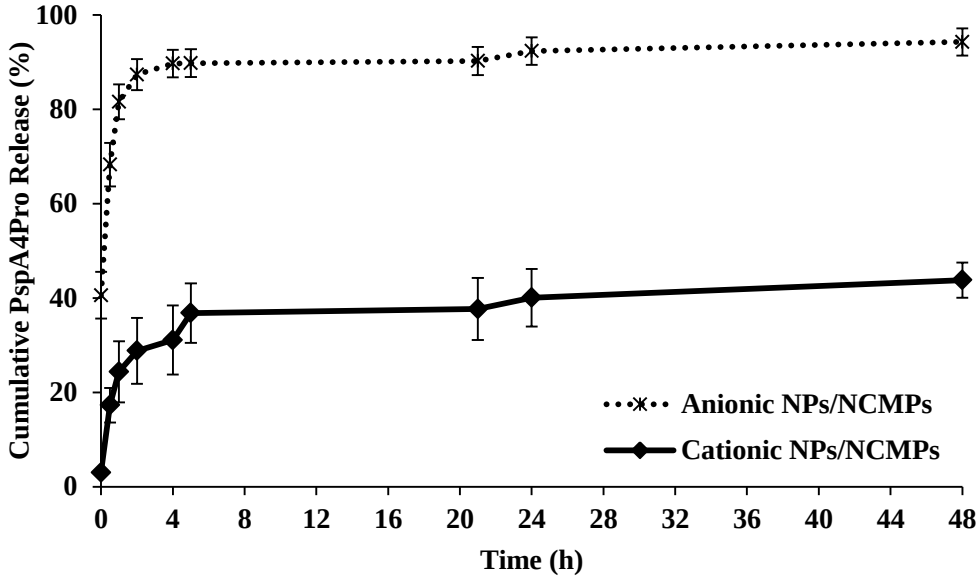

Figure 5-2 In vitro release profiles for pneumococcal surface protein A (PspA4Pro) from PspA4Pro adsorbed anionic and cationic nanocomposite microparticles in phosphate buffer saline, pH 7.4 ***(Mean±SD, n=3)***

5.3.4 Investigation of PspA4Pro Structure

The PspA4Pro released from the adsorbed anionic or cationic NPs/NCMPs was analysed for primary and secondary structure using SDS-PAGE and CD, respectively. Figure 5-3 indicates that the PspA4Pro released from NCMPs remained intact, based on the presence of a single band between 43 and 68 kDa, and no other bands of either small or large MW were visible indicating no degradation or aggregation, respectively.

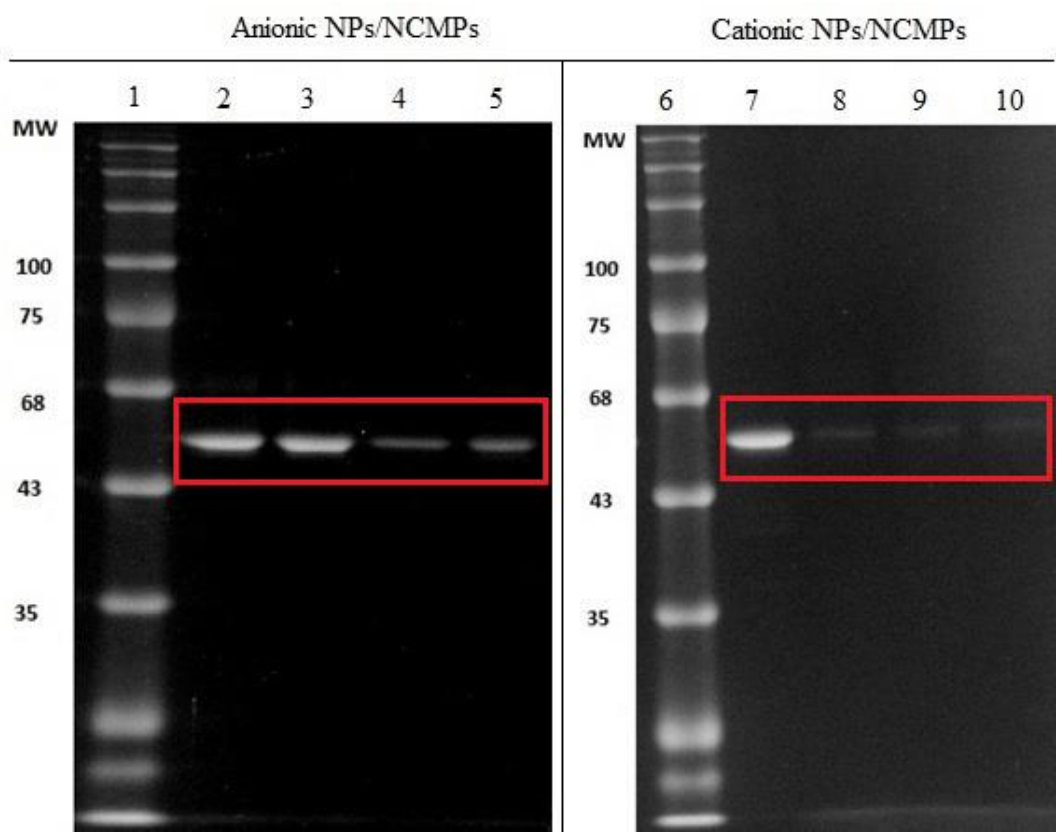

Figure 5-3 SDS-PAGE of Lane 1, 6: MW standards, broad range (Bio-Rad Laboratories, Hercules CA, USA), Lane 2, 3, 7: pneumococcal surface protein A (PspA4Pro) standard, Lane 4, 5, 8-10: Released PspA4Pro from anionic or cationic nanocomposite microparticles after 48 h

The conformational changes of PspA4Pro released from the adsorbed anionic or cationic NPs/NCMPs and PspA4Pro supernatant after adsorption were investigated by CD spectroscopy. Figure 5-4a to d represent the CD spectra of standard PspA4Pro, PspA4Pro supernatant, and PspA4Pro released from the NPs/NCMPs. The spectra indicate two characteristic minima at 208 and 222 nm, known to be associated with a α-helical structure. The data for the spectra presented in Table 5-2, for standard PspA4Pro, PspA4Pro supernatant and PspA4Pro released, indicated that the predominant structure of the protein was helical displaying 64.5, 64 and 51% helicity for anionic NPs/NCMPs, and 64.5,

50 and 44% for cationic NPs/NCMPs. Comparing the CD results of anionic and cationic formulations, the α-helical content of PspA4Pro released when compared to the standard, decreased by 13.5% for anionic NPs/NCMPs while that of cationic NPs/NCMPs decreased by 20.5%.

Table 5-2 The percentages of secondary structures of standard, supernatant and released pneumococcal surface protein A (PspA4Pro) samples

Sample	Helix	Strand	Turns	Unordered
Anionic NPs/NCMPs				
Standard PspA4Pro	64.50±0.02	06.00±0.00	07.50±0.00	22.00±0.01
PspA4Pro Supernatant	64.00±0.02	07.00±0.01	08.00±0.01	20.50±0.01
PspA4Pro Released	51.00±0.03	21.00±0.01	07.50±0.01	20.00±0.03
Cationic NPs/NCMPs				
Standard PspA4Pro	64.50±0.02	06.00±0.00	07.50±0.00	22.00±0.01
PspA4Pro Supernatant	50.00±0.02	14.50±0.02	15.00±0.02	20.00±0.01
PspA4Pro Released	44.00±0.03	28.00±0.01	07.00±0.00	20.00±0.00

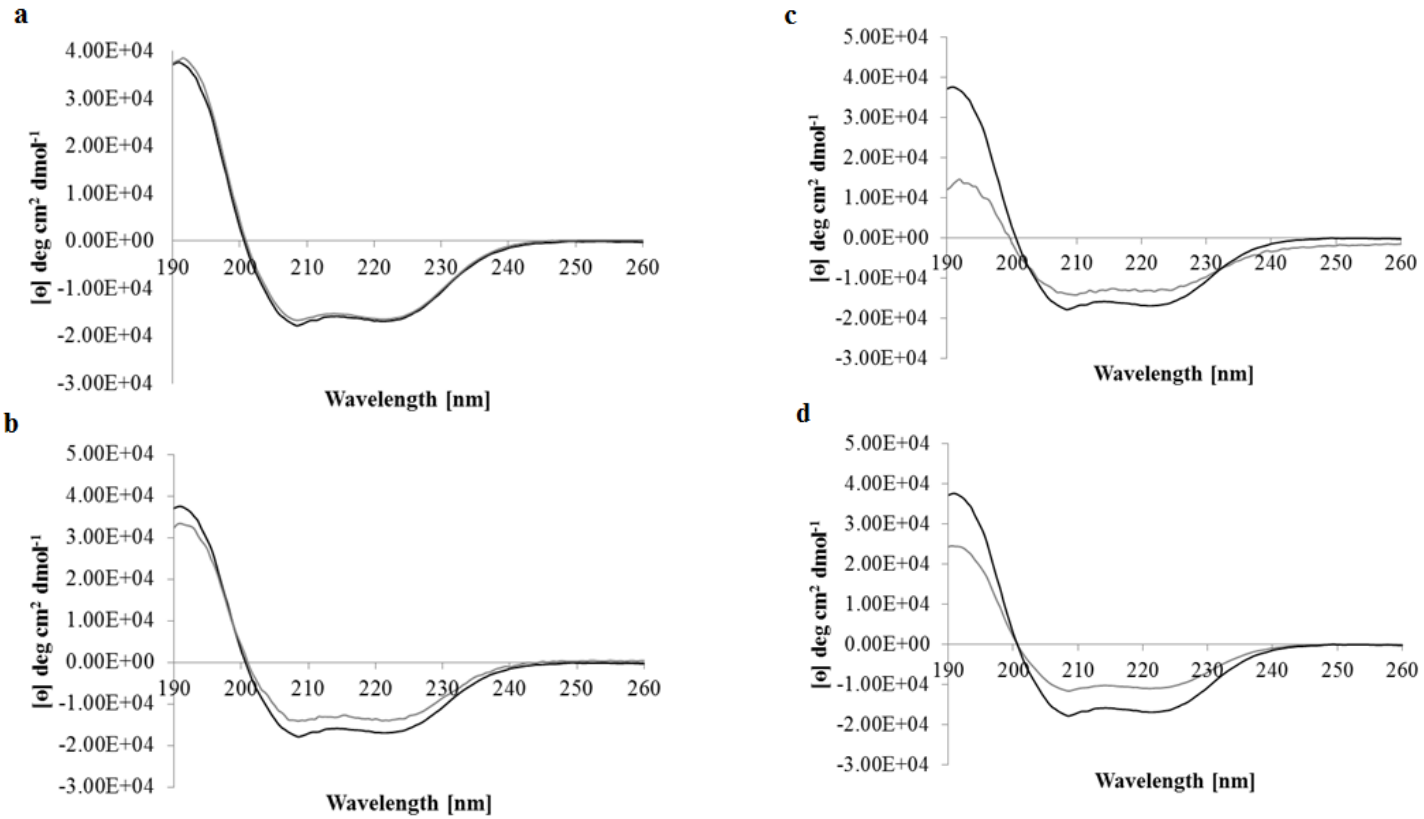

Figure 5-4 Circular dichroism spectra of pneumococcal surface protein A (PspA4Pro) released from: anionic nanocomposite microparticles, standard (black) (a) supernatant (grey) and (b) released (grey); cationic nanocomposite microparticles, standard (black) (c) supernatant (grey) and (d) released (grey)

5.3.5 Antigenicity of Released PspA4Pro

The antigenicity of released PspA4Pro was determined using ELISA with a specific PspA monoclonal antibody and represented as relative antigenicity. The assay measures the ability of released PspA4Pro to bind and be recognised by an anti-PspA antibody. Figure 5-5 shows that the PspA4Pro released from the formulations maintained its antigenicity with relative antigenicity of 0.97±0.20 for anionic and 0.85±0.05 for cationic formulations.

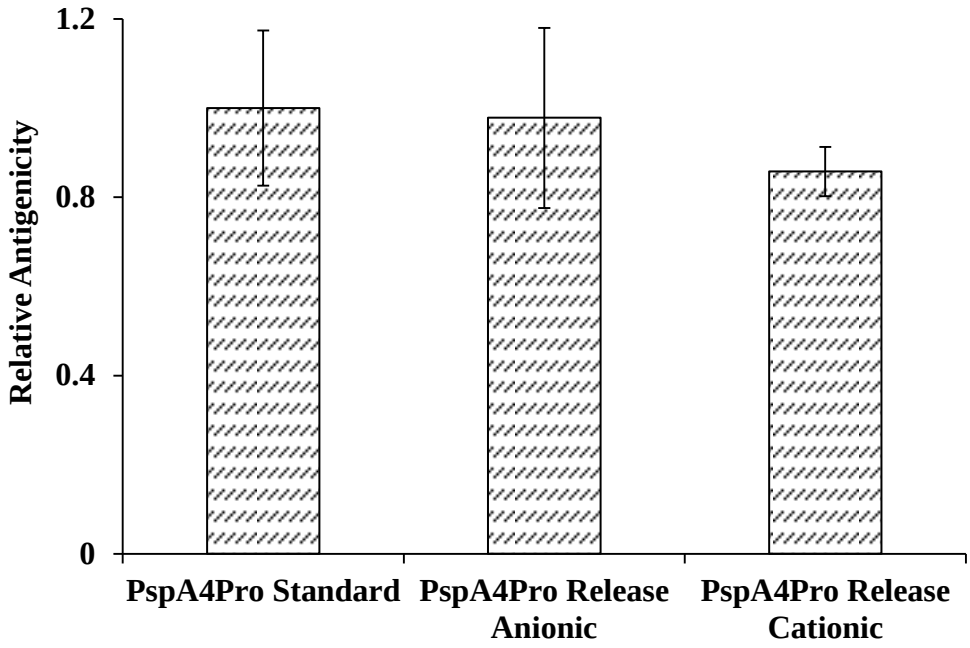

Figure 5-5 Antigenicity of pneumococcal surface protein A (PspA4Pro) upon release from anionic and cationic formulations

5.3.6 In vitro Aerosolisation Studies

The aerosol behaviour of PspA4Pro adsorbed anionic NPs/NCMPs was determined using NGI. The percent mass of PspA4Pro recovered from the NGI was approximately 85%, which is within the pharmacopeia limit (75-125%) of the

average delivered dose [259]. The deposition data obtained displayed a FPM of 90.04±12.84 µg (per capsule of 12.5 mg), FPF of 74.31±1.32% and MMAD of 1.70±0.03 µm suggesting that the formulation was capable of delivering efficient PspA4Pro to the bronchial-alveolar region of the lungs. Figure 5-6 shows the percentage stage-wise deposition of PspA4Pro in NGI.

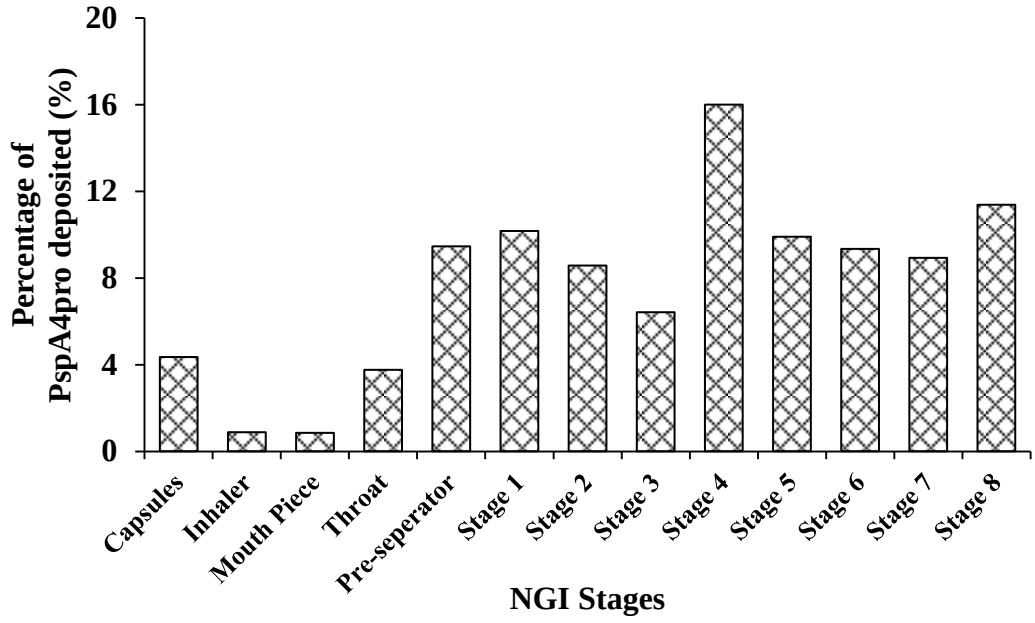

Figure 5-6 The percentage deposition of pneumococcal surface protein A (PspA4Pro) stage-wise in Next Generation Impactor *(Mean±SD, n=2)*

5.3.7 Cell Viability Study

The toxicity of empty anionic and cationic NPs following 4 h incubation using a DC cell line, were assessed by the MTT assay [206]. The NPs (Figure 5-7) showed increased cell death with an increase in concentration. The anionic NPs showed up to 90% cell viability at 19.53 µg/ml concentration that reduced to ~55% at 1.25 mg/ml concentration, whereas cationic NPs showed a steady

decrease in viability with concentration demonstrating ~50% viability at 19.53 µg/ml concentration.

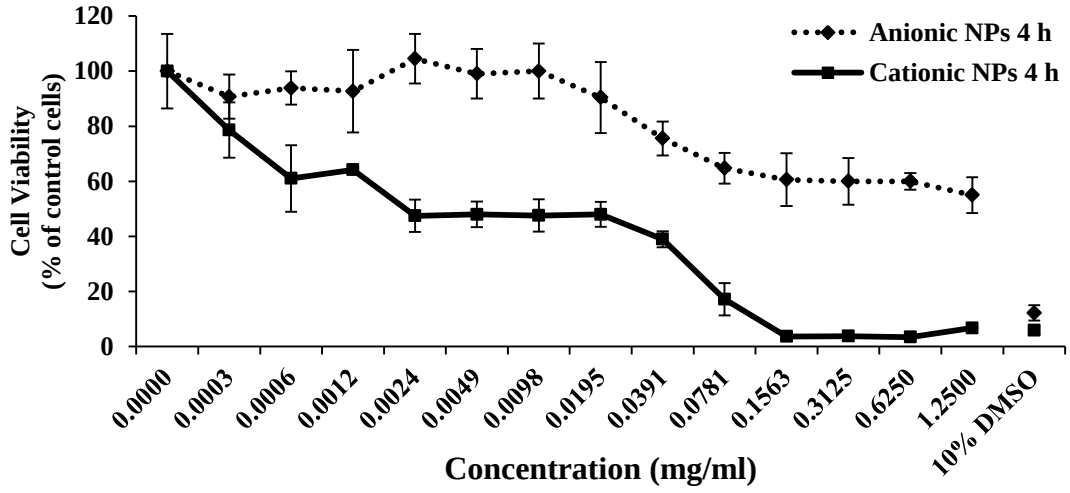

Figure 5-7 Dendritic cells viability measured by MTT assay after 4 h exposure to anionic and cationic PGA-co-PDL nanoparticles (NPs) ***(Mean±SD, n=3)***

5.3.8 Cellular Uptake of NPs by DCs

The uptake of anionic and cationic NR/NPs by DCs was observed using confocal microscopy. The cell wall of the DCs (stained with WGA Alexa Fluor® 488), the nucleus (stained with DAPI) and the NPs (containing Nile Red) were observed under the green, blue and red channel, respectively. Irrespective of the surface charge, the red fluorescence was seen inside the cells indicating the presence of NPs. Figures 5-8 and 5-9 depict the split view of DCs incubated with anionic and cationic NR/NPs for 1 h in cell culture medium and PBS buffer, respectively. In addition, Figure 5-10 shows the orthogonal view of anionic and cationic NR/NPs uptake in cell culture medium and PBS buffer.

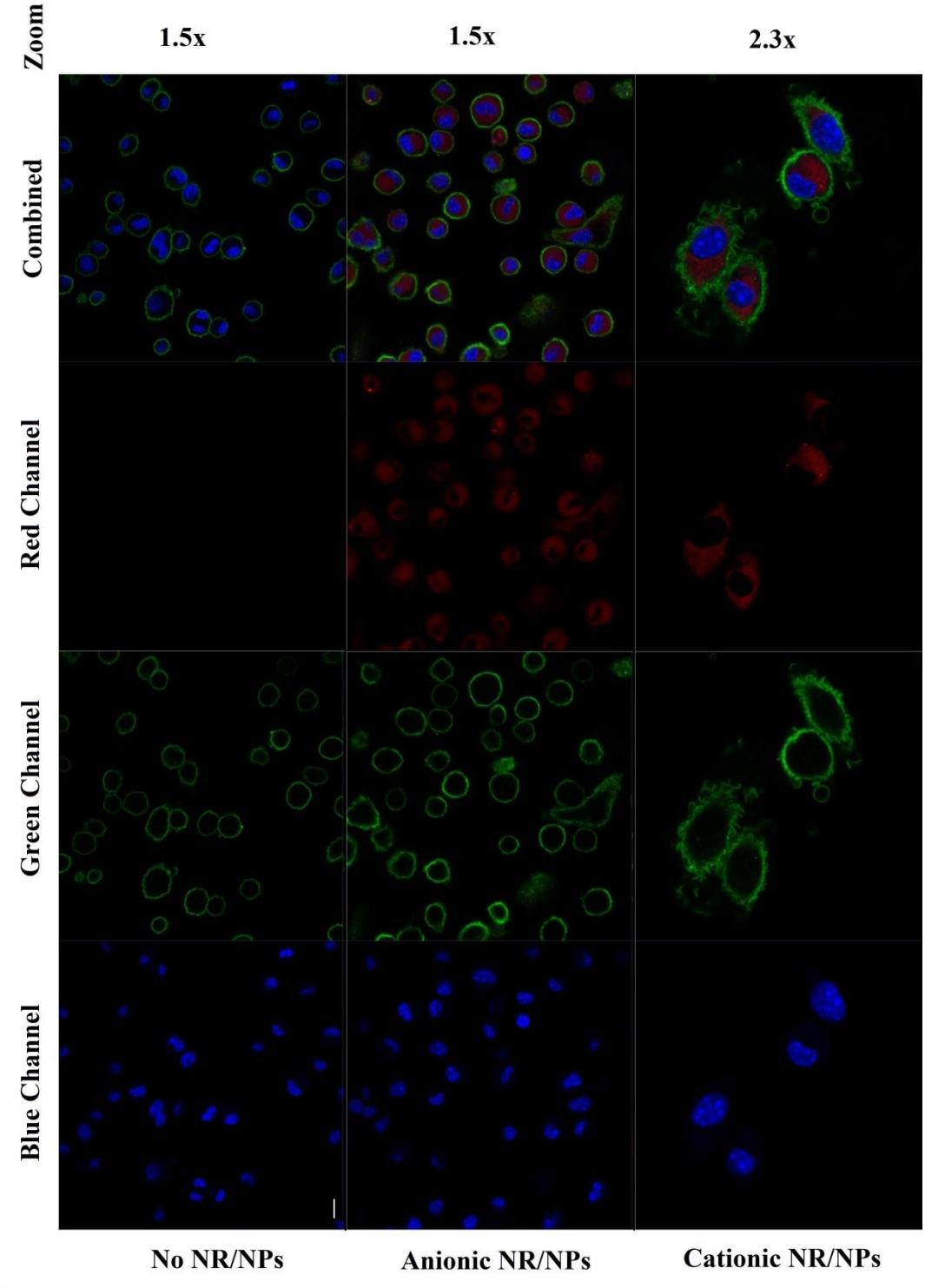

Figure 5-8 Confocal microscopic images depicting a split view of dendritic cells (40X lens) incubated in the absence and presence of anionic and cationic nile red (NR)/nanoparticles (NPs) in cell culture medium for 1 h (Scale bar – 20 µm)

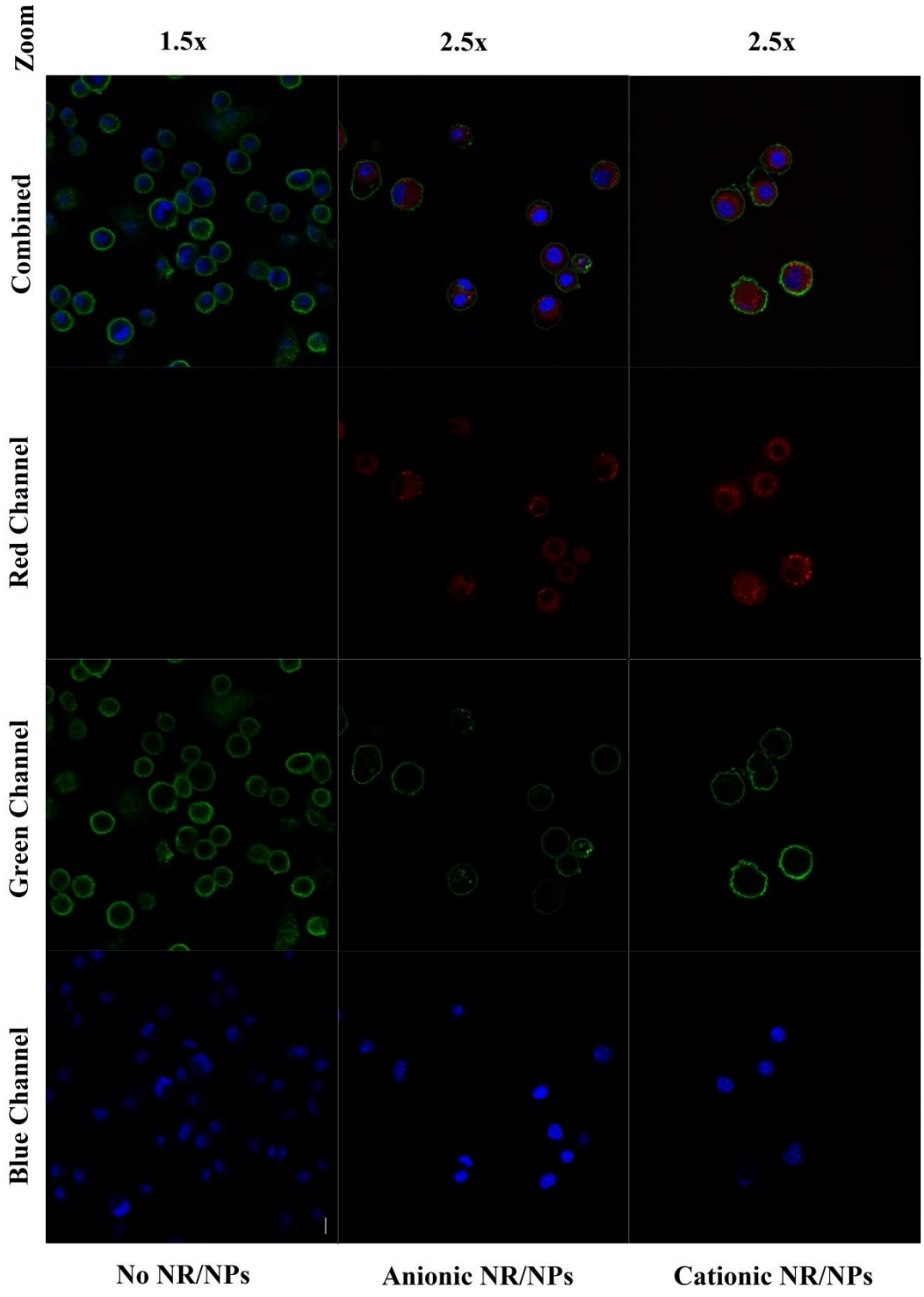

Figure 5-9 Confocal microscopic images depicting a split view of dendritic cells (40X lens) incubated in the absence and presence of anionic and cationic nile red (NR)/nanoparticles (NPs) in phosphate buffer saline for 1 h (Scale bar – 20 µm)

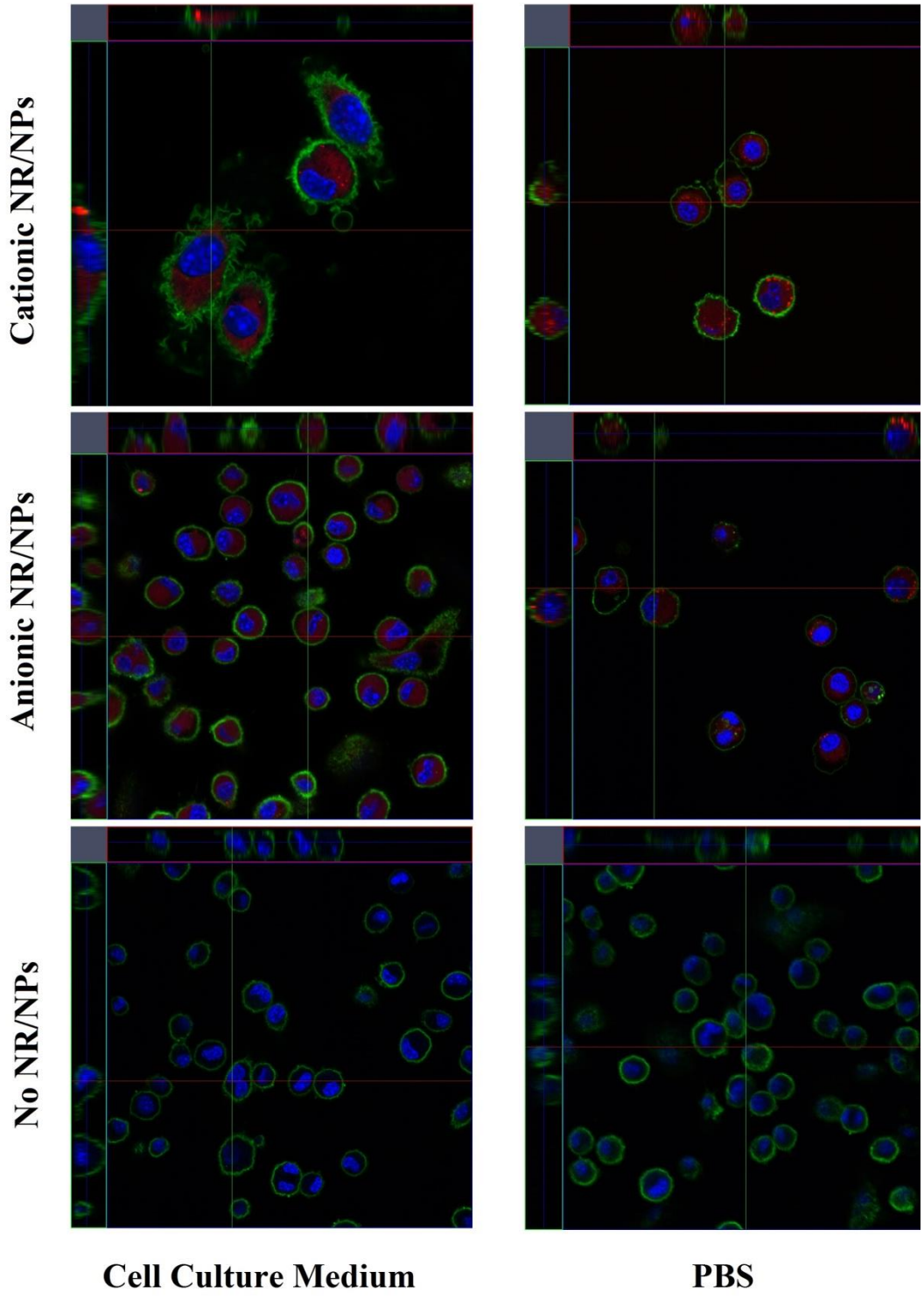

Figure 5-10 Confocal microscopic images depicting an orthogonal view of dendritic cells (40X lens) incubated in the absence and presence of anionic and cationic nile red (NR)/nanoparticles (NPs) in cell culture medium and phosphate buffer saline (PBS) for 1 h

5.4 Discussion

The results obtained with BSA as a model protein were promising for carrying out further work using PspA4Pro. However, it must be noted that each protein has a different size, structure and mechanism of degradation. Here, the optimum conditions inferred from BSA have been utilised for PspA4Pro adsorption onto the surface of anionic and cationic NPs, investigated protein stability and spray-dried to produce NCMPs to develop a pneumococcal protein vaccine against *S. pneumoniae* to be delivered via dry powder inhalation.

The PspA4Pro was adsorbed onto anionic and cationic NPs at the optimum conditions previously determined using BSA, and an adsorption of ~20 µg of PspA4Pro per mg of NPs was achieved for both NP types. The adsorption achieved with PspA4Pro is almost twice that of BSA (~10 µg per mg of NPs). This could be related to the MW of PspA4Pro (~43-50 kDa) being smaller than BSA (~66 kDa) thus providing more space on the NPs for PspA4Pro to adsorb. In addition, the elongated structure of PspA4Pro could have accommodated more proteins on the surface of NPs [285].

PspA has both negative and positive charges; however, in distilled water (pH ~7) the protein carries a net negative charge as the pH is greater than the pI of PspA (4.82). The adsorption process for both anionic and cationic NPs was carried out in distilled water and thus the forces involved in the adsorption process were different for anionic and cationic NPs. At the pH used, the protein is negative and hydrophobic interactions and hydrogen bonding would be the dominant forces of adsorption onto anionic NPs whereas it is electrostatic interactions that will

dominate for the cationic NPs. Adsorption of PspA4Pro onto the surface of anionic and cationic NPs led to an increase in the hydrodynamic diameter of the resultant mixture evident from the increase in particle size observed. In addition, a decrease in surface charge was observed which could be due to the orientation the protein molecules adopt on the surface of the NPs exposing only a small part of the protein. Similar results have been reported by Gordon *et al.* and Koppolu *et al.* [278,286]. The fact that the cationic NPs retained their positive charge after adsorption would facilitate uptake by APCs upon interaction with the proteoglycans on their surface as previously observed for cationic particles [268,278,287].

The PspA4Pro adsorbed anionic and cationic NPs were spray-dried into NCMPs using L-leu as a microcarrier. The produced NCMPs displayed a rough and wrinkled surface texture, typical of particles spray-dried with L-leu and this has been widely reported in the literature [218,219,238,239,245,264].

The in vitro release data indicated that PspA4Pro adsorbed onto anionic NPs showed a burst release of 40% with nearly complete release (~94%) within 48 h whereas cationic NPs showed a 3% burst release and only ~43% release over 48 h. This suggests that, contrary to anionic NPs, the interaction between the protein and cationic NPs was too strong for easy desorption to occur. Though high release was observed for anionic NPs/NCMPs, this would not be a limiting factor for vaccination because any protein released can still be taken up by DCs for processing and presentation, and that which is adsorbed can also be taken up potentially giving an adjuvant effect as reported by Ghotbi *et al.*, Cruz *et al*. and others [115,288,289]. Further, it has been established that for NPs to act as

immune potentiator or adjuvant, the attachment of NPs and antigen is not necessary; hence, the particles can still be taken up by DCs enhancing the immune response [290,291]. Moreover, studies in the literature have reported the uptake of particles by DCs within 1-2 h of incubation [115,213,292,293].

The structure of PspA4Pro released from anionic and cationic NPs/NCMPs was investigated using SDS-PAGE (primary structure) and CD (secondary structure). The SDS-PAGE of PspA4Pro released from the formulations confirmed that the protein had not degraded based on the presence of a single band. This shows that the protein remained intact during the adsorption, SD process and desorption [55]. In addition, the CD spectral data obtained for the released PspA4Pro confirmed the presence of α-helix and β-sheets. However, there is a decrease in the helical content observed for both the formulations, more so for the cationic (~20%) than the anionic NPs/NCMPs (~13%). This effect could be due to the adsorption and desorption process or SD. Besides, the antigenicity of released PspA4Pro for both the formulations showed the ability of the released sample to effectively recognise and bind to the anti-PspA monoclonal antibody. The results obtained with SDS-PAGE and CD provides an indication that PspA delivered via NPs is stable and retains antigenicity for immune response.

The FPF (~74%) and MMAD (~1.7 μm) obtained for the PspA4Pro adsorbed anionic NPs/NCMPs suggest an excellent aerosolisation performance similar to that observed for BSA adsorbed anionic or cationic NPs/NCMPs. The short supply of PspA4Pro meant that not all samples could be assessed for aerosolisation. Due to the better toxicity profile, CD data and antigenicity compared to cationic NPs/NCMPs, only the aerosolisation properties of anionic

NPs/NCMPs were investigated. Moreover, it can be assumed that the aerosol behaviour would be similar for the cationic NPs/NCMPs (based on similar data observed for BSA).

A dose of 1-5 µg of PspA was enough to generate an immune response in mice when administered subcutaneously or intramuscularly [55,56,294]. However, when PspA was administered nasally (through a mucosal site) with an adjuvant, a dose of only 100 ng was required to generate an immune response equivalent to that elicited by oral administration of 7.5 µg [295]. Considering that the PGA-co-PDL NPs/NCMPs produced here are to be administered via inhalation, i.e. through a mucosal site, the dose required would be about 100 ng of PspA for mice requiring NCMPs concentrations lower than 20 µg/ml. It must also be remembered that the dosage of PspA4Pro would be different for human immunisation (yet to be determined based on the results in animals).

It has now become evident that particulate antigens provide a Th1 and/or Th2 type immune responses [235,296,297]. In addition, the size, charge, shape and site of delivery all affect the extent of uptake and thus the immune response generated [235]. Over the years, it has become more established and convincing that NPs compared to MPs show higher activated DCs and as a result induce stronger immune responses [113,235,278]. A study conducted by Joshi *et al.* has also shown that nano sized PLA particles (300 nm) were more readily taken up by DCs and generated effective CTL responses than micro sized particles (1, 7 and 17 µm) [235]. Similar results of particles made of different polymers with size < 500 nm being effectively taken up by DCs have been reported in the literature [113,235,278].

Here, to substantiate claims of effective uptake by DCs upon producing NPs of size ~ 300 nm, their uptake in JAWS II DC cell type was visualised using confocal microscopy. The uptake of empty anionic and cationic NPs upon incubation with DCs for 1 h in cell culture medium and PBS was investigated. In cell culture media, NR fluorescence was detected when anionic and cationic NR/NPs were co-incubated with DCs for 1 h indicating the presence of NR/NPs within the DCs. This confirms the uptake of NR/NPs by DCs thereby effectively endorsing the size of NPs produced for vaccine delivery. However, Xu *et al.* have recently observed that NR, a lipophilic dye often used to stain intercellular lipid bodies, was released in the presence of cell culture medium and/or transferred directly to the cell membrane of contacting cells [298].

To investigate if the red fluorescence signals seen within the DCs is indeed the NR/NPs or the released NR, the uptake studies were repeated by co-incubating the NR/NPs with DCs in PBS medium. The presence of red fluorescence colour was evident for both anionic and cationic NR/NPs confirming the internalisation of NR/NPs by DCs rather than NR alone. However, the obtained fluorescence signal was not quantified due to non-specific staining visible in some regions of the well in the chamber slide and to avoid false positive results. However, based on observations from Xu *et al.* [298], the actual cellular uptake of NR/NPs (using PBS) would be less compared to suggested uptake (using cell culture media), if quantified using FACS.

5.5 Conclusions

The results obtained above show that PspA4pro can effectively be adsorbed onto anionic and cationic NPs (~20 µg of PspA4Pro per mg of NPs). The stability (primary and secondary structure) of the released PspA4Pro was maintained to a large extent and relative antigenicity has been retained for anionic and cationic NPs/NCMPs. In addition, the aerosol properties (FPF of 74.31±1.32% and MMAD of 1.70±0.03 µm) indicate deposition in the respirable airways i.e. the bronchial-alveolar region of the lungs, ideal for antigen uptake by DCs. Moreover, the anionic and cationic NR/NPs when co-incubated with DCs showed internalisation within 1 h. Further investigations should focus on determining the activity and immunogenicity of the released PspA4Pro.

6. Overview

6.1 Overview

Pneumonia, caused by *S. pneumoniae*, is the leading bacterial cause of death especially among the immunocompromised, elderly above the age of 50 and children under the age of 5 [3,4]. The polysaccharide capsule covering the pneumococcus bacteria, with 94 different identified serotypes, is one of the most important virulent factors responsible for causing the disease [11,15]. Although different vaccines such as PPV23, PCV7, 10 and 13 are available, they are expensive to produce and distribute [39,40]. However, the variation in serotype distribution across geographical locations and rise in dominance of disease due to non-vaccine serotype coverage has led to significant attention in the need for the development of alternate vaccine candidates [39,40]. Pneumococcal proteins, such as PspA, have gained much attention as potential candidates in vaccine delivery for their ubiquitous presence across different families of pneumococcus [49,50]. Moreover, the ideal route of delivery to target a pneumonia vaccine would be the pulmonary route as it is the natural entry portal for pathogens and delivery to the lungs also produces mucosal immunisation. So far, very little research has been published in the literature using PspA as a candidate to develop drug delivery systems for vaccination purposes [55–57]. In this project, a potential dry powder vaccine formulation was developed containing polymeric PGA-co-PDL NPs with different surface charges, adsorbed with PspA4Pro and formulated into NCMPs using L-leu as a microcarrier to be delivered via inhalation.

The important goals achieved in this project are described below:

6.2 Optimisation of Size and Charge of NPs

The true APCs, DCs, have a remarkable ability to internalise, process, and present antigens and thus an effective vaccine delivery system would target the DCs [73]. Several studies have shown that NPs (anionic and cationic) smaller than 500 nm are optimum for effective uptake by DCs and for generating a stronger immune response compared to antigen alone [113,212,213]. However, these studies cannot be directly compared to pulmonary delivery as the DCs in the lung differ from that of other tissues such as skin.

The first goal was to produce NPs of an optimum size that could be taken up by DCs. The size of anionic NPs was optimised using a Taguchi orthogonal array DoE, for efficient uptake by DCs. It was found that parameters such as MW of the polymer, the surfactant concentration and volume of organic solvent were the most significant factors in determining the particle size of the produced NPs. An optimum amount of surfactant was required to effectively cover all the NP surfaces thereby preventing aggregation and impacting the particle size obtained. Such effects were also observed and reported by Douglas *et al.* [231], and Mitra and Lin [232]. In addition, the MW of polymer and volume of organic solvent were known to have an effect on particle size through changes in viscosity. High viscosity solutions make it difficult for the emulsion to be broken down into smaller particles because of the lower stirring efficiency at the same stirrer speed. Similar phenomena was also reported by Jalil *et al.* [233] and Mittal *et al.* [234] who found that the size of particles tend to increase with an increase in polymer MW.

To study the effect of NPs surface charge on protein adsorption and uptake by DCs, a cationic surfactant, DMAB, was used to modify the surface charge of NPs from negative to positive. DMAB (2% w/v) was found to be the optimum concentration to obtain cationic NPs of a similar size to that obtained for anionic NPs. Further, the use of DMAB as a stabiliser to produce cationic polymeric NPs has been explored and reported by others [248,250,256,257,299]. However, in the case of both anionic and cationic NPs, after two washing steps to remove the unbound and extra surfactant the particle size increased to ~250 nm which is still suitable for an effective uptake by DCs.

6.2.1 DC Uptake of Anionic and Cationic NPs

Compared to MPs, NPs have been shown to induce a higher activation of DCs resulting in the induction of a stronger immune response [113,235,278]. Additionally, the size, charge, shape of particles and delivery site all have an impact on the uptake by DCs influencing the immune response generation [235]. The empty anionic and cationic polymeric NR/NPs produced (~250 nm) co-incubated with JAWS II DC cell line for 1 h showed an effective uptake when visualised under confocal microscopy.

6.3 Protein Adsorption onto the Surface of NPs

The antigen can either be encapsulated within or adsorbed onto the surface of NPs. Adsorption has the benefit of preventing contact with the organic solvent employed in the NP preparation process where the antigen is encapsulated in the double emulsion solvent evaporation method [226]. Additionally, the presentation of antigen to the immune system would be very similar to the presentation by the

pathogen itself and could thus aid in uptake and provoke a similar immune response [182]. Herein, it was successfully demonstrated that adsorption could be used as an alternative to encapsulation and that the antigen could still largely maintain its structure and retain its activity. Also, the subtle changes that occur in the structure of protein after adsorption could also increase the chances of proteolytic processing by the immune system leading to enhanced antigen presentation [210,300].

The adsorption of a model protein, BSA, onto the surface of NPs was found to be concentration and time dependent with adsorption of approximately 10 µg per mg of NPs achieved using 100:20 (NP:BSA) ratio for anionic NPs and 100:4 ratio for cationic NPs. The high level of adsorption achieved at a lower concentration of BSA for cationic NPs suggests that the adsorption was mainly dominated by electrostatic and ionic interactions, whereas for negatively charged BSA (at pH 7) onto anionic NPs it was mainly by hydrogen bonding. Additionally, the adsorption of BSA onto NPs was characterised and confirmed by an increase in particle size and visually by observation under the confocal microscope. Moreover, it was found that nanosized protein aggregates could not be collected with the centrifugation conditions employed here thereby further verifying the adsorption of protein onto NPs.

PspA4Pro has a net negative charge in distilled water at pH 7, though it has both negative and positive ends. Further, the adsorption increased to 20 µg per mg of NPs compared to 10 µg per mg for BSA thus requiring lower dosage of NPs to deliver a greater amount of PspA4Pro. This would help design cost effective programmes for LMICs and healthcare providers. Studies published by Florindo

et al. [226,301], Li *et al.* [302] amongst others have shown that proteins can be adsorbed onto NPs and delivered for a strong immune response [209,229,300].

6.4 Spray-drying of Protein Adsorbed NPs into NCMPs

Dry powder formulation has major advantages for pulmonary administration compared to pMDIs and nebulisers [303]. It provides reduced administration time, no storage requirement at low temperatures and potentially higher lung deposition [89,303]. Spray or freeze-drying of proteins alone often results in degradation or inactivation of proteins thus requiring stabilising excipients [304,305]. Several technologies have been explored and reported for producing protein dry powder formulations for delivery via inhalation with the most commonly used excipients such as lactose, trehalose, L-leu, mannitol alone or in combination as microcarriers in SD [217–219,306]. In addition, the produced dry powder particles must be in the size range of 1-5 µm for effective deposition in the respirable airways [220,221].

Here, the protein adsorbed NPs were successfully spray-dried with L-leu solution under optimised SD conditions to produce NCMPs. The NCMPs displayed a rough and corrugated surface, typical when spray-dried with L-leu. It has been established in the literature that L-leu spray-dried particles have a low density and are capable of forming a shell thereby encapsulating the particles within [245,306,307]. The obtained dry powders were characterised for aerosol properties using a NGI. The NCMP formulations containing either protein adsorbed anionic or cationic NPs showed FPF values ~70-75% and MMAD values between ~1-3 µm suggesting that the particles would deposit in the

bronchial-alveolar region of the lungs. Such results were also reported by others when they used L-leu as an excipient in SD [218,219,239,244,245,306]. Moreover, the low moisture content (<1%) determined in the formulations confirms the efficient drying conditions employed in the SD process and also helps in storage, stability of powders.

The A549 cell line showed good tolerance to anionic NPs/NCMPs up to 1.25 mg/ml concentration and for cationic NPs/NCMPs up to 156.25 µg/ml concentration (corresponding to ~1.25 µg of PspA4Pro). As expected and reported by others, the cationic particles were more toxic compared to anionic [248,265,266]. However, due to the high loading capacity that was achieved with cationic NPs, lower amounts would be sufficient to deliver the required amount of antigen and generate an immune response.

6.5 Investigation of Structure and Activity of Released Protein

The challenge often faced with the formulation of proteins is retaining their structure and activity as they are often denatured in the process of developing a formulation. Herein, it was shown that the protein released from the formulation largely maintained its structure and retained activity. The BSA and PspA4Pro released have an intact primary structure that was not affected by adsorption or SD process. However, the secondary structure (α-helix) for both BSA and PspA4Pro was slightly reduced across all formulations and this could be due to the adsorption and desorption process. This slight decrease in α-helical content has been observed and reported by others [230,308,309]. The activity of BSA

(after release from NCMPs) was ~75% and for PspA4Pro, the ELISA indicated the relative antigenicity, the ability to bind to anti-PspA antibody, to be close to 1 confirming the tertiary structure. The SDS-PAGE and CD results indicated that PspA4Pro delivered via NPs would be stable with antigenicity retained for immune response.

7. Future Work

7.1 Future Work

Further studies for the project could be divided into two parts; protein activity, and formulation optimisation and stability. The final formulations containing the PsA4Pro have been supplied to Instituto Butantan, Brazil for evaluation of activity, immunogenicity and pneumococcal challenge in animal models. The activity of released protein can be measured using the lactoferrin assay [55]. In addition, the immunogenicity of PspA4Pro formulation can be evaluated by measuring the upregulation of MHC II, CD 40, CD 80, CD 83 and CD 86 surface markers expressed on DCs using flow cytometry.

Inulin, an oligosaccharide with MW of 4 kDa, has been previously reported by others as an additive in dry powder vaccine formulations [89,303,305,310–312]. The addition of inulin to L-leu solution for SD has produced dry powders with a greater yield and smooth morphology (appendix-2). In addition, the collected dry powders had low residual moisture content (<2%). However, further investigations will focus on the aerosolisation properties of individual formulations compared to L-leu alone. Moreover, the long term stability of the dry powder formulation at different temperatures and humidity conditions has to be evaluated. Stability at ambient conditions is highly desirable for convenience of use in terms of avoiding any cold-chain requirements, preventing moisture adsorption which can result in aggregation leading to poor powder flow and lung deposition, as well as affecting PspA4Pro stability and integrity. The stability of NCMPs will be determined using X-ray powder diffraction and DSC to evaluate changes in the crystallinity of the particles. The PspA4Pro stability at the

conditions mentioned above will be evaluated using SDS-PAGE, the integrity using CD and the activity using lactoferrin assay.

References

1. Ryan KJ. Streptococci and Enterococci. In: Ryan KJ, Ray CG, editors. Sherris Med. Microbiol. An Introd. to Infect. Dis. Fourth Edi. McGraw-Hill, USA. 2004;273–96.

2. Ferreira DM, Jambo KC, Gordon SB. Experimental human pneumococcal carriage models for vaccine research. Trends Microbiol. 2011;19:464–70.

3. Wardlaw TM, Johansson EW, Hodge M. Pneumonia: the forgotten killer of children. World Health Organization. 2006;1–40.

4. Wardlaw T, Salama P, Johansson EW, Mason E. Pneumonia: the leading killer of children. Lancet. 2006;368:1048–50.

5. Nair H, Simões EAF, Rudan I, Gessner BD, Azziz-Baumgartner E, Zhang JSF, et al. Global and regional burden of hospital admissions for severe acute lower respiratory infections in young children in 2010: a systematic analysis. Lancet. 2013;381:1380–90.

6. Drijkoningen JJC, Rohde GGU. Pneumococcal infection in adults: burden of disease. Clin. Microbiol. Infect. 2014;20:45–51.

7. World Health Organization. Pneumonia [Internet]. World Heal. Organ. Media Cent. 2013 [cited 2014 Jul 12]. Available from: http://www.who.int/mediacentre/factsheets/fs331/. Date Accessed: 09/12/2014.

8. O'Brien KL, Wolfson LJ, Watt JP, Henkle E, Deloria-Knoll M, McCall N, et al. Burden of disease caused by Streptococcus pneumoniae in children younger than 5 years: global estimates. Lancet. 2009;374:893–902.

9. Bogaert D, Hermans PWM, Adrian P V, Rümke HC, de Groot R. Pneumococcal vaccines: an update on current strategies. Vaccine. 2004;22:2209–20.

10. Obaro S, Adegbola R. The pneumococcus: carriage, disease and conjugate vaccines. J. Med. Microbiol. 2002;51:98–104.

11. Van der Poll T, Opal SM. Pathogenesis, treatment, and prevention of pneumococcal pneumonia. Lancet. 2009;374:1543–56.

12. Patterson CM, Loebinger MR. Community acquired pneumonia: assessment and treatment. Clin. Med. 2012;12 283–6.

13. Trotter C, Stuart J, George R, Miller E. Increasing hospital admissions for pneumonia, England. Emerg Infect Dis. 2008;14:727–33.

14. Isturiz RE, Luna CM, Ramirez J. Clinical and economic burden of pneumonia among adults in Latin America. Int. J. Infect. Dis. 2010;852–856.

15. Bogaert D, De Groot R, Hermans PWM. Streptococcus pneumoniae colonisation: the key to pneumococcal disease. Lancet Infect. Dis. 2004;4:144–54.

16. Henriques-Normark B, Tuomanen EI. The pneumococcus: Epidemiology, microbiology, and pathogenesis. Cold Spring Harb. Perspect. Med. 2013;3(7):1-15.

17. Organization WH. World Health Statistics 2011 in WHO Statistical Information System (WHOSIS). World Heatlh Organization. 2011;1–171.

18. UNICEF. Committing to child survival: A promise renewed, progress report 2013. New York. 2013;1–56.

19. Liu L, Johnson HL, Cousens S, Perin J, Scott S, Lawn JE, et al. Global, regional, and national causes of child mortality: an updated systematic analysis for 2010 with time trends since 2000. Lancet. 2012;379:2151–61.

20. Walker CLF, Rudan I, Liu L, Nair H, Theodoratou E, Bhutta ZA, et al. Global burden of childhood pneumonia and diarrhoea. Lancet. 2013;381:1405–16.

21. UNICEF. Pneumonia and diarrhoea: Tackling deadliest diseases for world's poorest children can yield huge gains. New York. 2012;1–86.

22. Welte T, Torres A, Nathwani D. Clinical and economic burden of community-acquired pneumonia among adults in Europe. Thorax. 2012;67 71–9.

23. Bertsias A, Tsiligianni IG, Duijker G, Siafakas N, Lionis C. Studying the burden of community-acquired pneumonia in adults aged >=50 years in primary health care: an observational study in rural Crete, Greece. Npj Prim. Care Respir. Med. 2014;24:1-8.

24. Almirall J, Bolibar I, Vidal J, Sauca G, Coll P, Niklasson B, et al. Epidemiology of community-acquired pneumonia in adults: a population-based study. Eur. Respir. J. 2000;15 757–63.

25. Marrie TJ, Huang JQ. Epidemiology of community-acquired pneumonia in Edmonton, Alberta: An emergency department-based study. Can. Respir. J. 2005;12:139–42.

26. Broulette J, Yu H, Pyenson B, Iwasaki K, Sato R. The incidence rate and economic burden of community-acquired pneumonia in a working-age population. Am. Heal. Drug Benefits. 2013;6:494–503.

27. Kadioglu A, Weiser JN, Paton JC, Andrew PW. The role of Streptococcus pneumoniae virulence factors in host respiratory colonization and disease. Nat Rev Micro. 2008;6:288–301.

28. Mook-Kanamori BB, Geldhoff M, van der Poll T, van de Beek D. Pathogenesis and pathophysiology of pneumococcal meningitis. Clin. Microbiol. Rev. 2011;24 557–91.

29. Jedrzejas MJ. Pneumococcal virulence factors: Structure and function. Microbiol. Mol. Biol. Rev. 001;65 187–207.

30. Pérez-Dorado I, Galan-Bartual S, Hermoso JA. Pneumococcal surface proteins: when the whole is greater than the sum of its parts. Mol. Oral Microbiol. 2012;27:221–45.

31. Mitchell AM, Mitchell TJ. Streptococcus pneumoniae: virulence factors and variation. Clin. Microbiol. Infect. 2010;16:411–8.

32. Rubins JB, Janoff EN. Pneumolysin: A multifunctional pneumococcal virulence factor. J. Lab. Clin. Med. 1998;131:21–7.

33. Davis KM, Akinbi HT, Standish AJ, Weiser JN. Resistance to Mucosal Lysozyme Compensates for the Fitness Deficit of Peptidoglycan Modifications by Streptococcus pneumoniae. PLoS Pathog. 2008;4(12):1-11.

34. Weiser JN, Bae D, Fasching C, Scamurra RW, Ratner AJ, Janoff EN. Antibody-enhanced pneumococcal adherence requires IgA1 protease. Proc. Natl. Acad. Sci. 2003;100 4215–20.

35. Shaper M, Hollingshead SK, Benjamin WH, Briles DE. PspA Protects Streptococcus pneumoniae from killing by apolactoferrin, and antibody to PspA enhances killing of pneumococci by apolactoferrin. Infect. Immun. 2004;72(9):5031–40.

36. Lim WS, Baudouin S V, George RC, Hill AT, Jamieson C, Le Jeune I, et al. BTS guidelines for the management of community acquired pneumonia in adults: update 2009. Thorax. 2009;64(iii)1–55.

37. Woodhead M, Blasi F, Ewig S, Garau J, Huchon G, Ieven M, et al. Guidelines for the management of adult lower respiratory tract infections - Full version. Clin. Microbiol. Infect. 2011;17:1–59.

38. Mandell LA, Wunderink RG, Anzueto A, Bartlett JG, Campbell GD, Dean NC, et al. Infectious diseases society of america/american thoracic society consensus guidelines on the management of community-acquired pneumonia in adults. Clin. Infect. Dis. 2007;44:27–72.

39. Wang S, Curtiss III R. Development of Streptococcus pneumoniae vaccines using live vectors. Vaccines. 2014;2:49–88.

40. Moffitt KL, Malley R. Next generation pneumococcal vaccines. Curr. Opin. Immunol. 2011;23:407–13.

41. Pittet LF, Posfay-Barbe KM. Pneumococcal vaccines for children: a global public health priority. Clin. Microbiol. Infect. 2012;18:25–36.

42. Mahoney RT, Krattiger A, Clemens JD, Curtiss R. The introduction of new vaccines into developing countries. IV: Global Access Strategies. Vaccine. 2007;25:4003–11.

43. Chiu C, McIntyre P. Pneumococcal vaccines: past, present and future. Aust. Prescr. 2013;36:88–93.

44. Aspa J. The future is now in community-acquired pneumonia, cardiovascular complications and conjugate vaccines. Arch. Bronconeumol. (English Version). 48:347–8.

45. Singleton R, Hennessy T, Bulkow L, Al E. Invasive pneumococcal disease caused by nonvaccine serotypes among alaska native children with high levels of 7-valent pneumococcal conjugate vaccine coverage. JAMA. 2007;297:1784–92.

46. Ginsburg AS, Nahm MH, Khambaty FM, Alderson MR. Issues and challenges in the development of pneumococcal protein vaccines. Expert Rev. Vaccines. 2012;11:279–85.

47. Miyaji EN, Oliveira MS, Carvalho E, Ho PL. Serotype-independent pneumococcal vaccines. Cell. Mol. Life Sci. 2013;70:3303–26.

48. Darrieux M, Goulart C, Briles D, Leite LC de C. Current status and perspectives on protein-based pneumococcal vaccines. Crit. Rev. Microbiol. 2013;1–11.

49. Moreno AT, Oliveira MLS, Ferreira DM, Ho PL, Darrieux M, Leite LCC, et al. Immunization of mice with single PspA fragments induces antibodies capable of mediating complement deposition on different pneumococcal strains and cross-protection. Clin. Vaccine Immunol. 2010;17(3):439–46.

50. Jedrzejas MJ, Lamani E, Becker RS. Characterization of selected strains of pneumococcal surface protein A. J. Biol. Chem. 2001;276:33121–8.

51. Hollingshead SK, Becker R, Briles DE. Diversity of PspA: Mosaic genes and evidence for past recombination in Streptococcus pneumoniae. Infect. Immun. 2000;68:5889–900.

52. Rolo D, Ardanuy C, Fleites A, Martín R, Liñares J. Diversity of pneumococcal surface protein A (PspA) among prevalent clones in Spain. BMC Microbiol. 2009;9:80.

53. McDaniel LS. Use of insertional inactivation to facilitate studies of biological properties of pneumococcal surface protein A (PspA). J. Exp. Med. 1987;165:381–94.

54. Ferreira DM, Miyaji EN, Oliveira MLS, Darrieux M, Arêas APM, Ho PL, et al. DNA vaccines expressing pneumococcal surface protein A (PspA) elicit protection levels comparable to recombinant protein. J. Med. Microbiol. 2006;55 375–8.

55. Haughney SL, Petersen LK, Schoofs AD, Ramer-Tait AE, King JD, Briles DE, et al. Retention of structure, antigenicity, and biological function of pneumococcal surface protein A (PspA) released from polyanhydride nanoparticles. Acta Biomater. 2013;9:8262–71.

56. Anish C, Upadhyay AK, Sehgal D, Panda AK. Influences of process and formulation parameters on powder flow properties and immunogenicity of spray dried polymer particles entrapping recombinant pneumococcal surface protein A. Int. J. Pharm. 2014;466:198–210.

57. Kong IG, Sato A, Yuki Y, Nochi T, Takahashi H, Sawada S, et al. Nanogel-based PspA intranasal vaccine prevents invasive disease and nasal colonization by Streptococcus pneumoniae. Infect. Immun. 2013;81(5):1625–34.

58. Moore QC, Johnson L, Repka M, McDaniel LS. Immunization with PspA incorporated into a poly(ethylene oxide) matrix elicits protective immunity against Streptococcus pneumoniae. Clin. Vaccine Immunol. 2007;14(6):789–91.

59. Moore QC, Bosarge JR, Quin LR, McDaniel LS. Enhanced protective immunity against pneumococcal infection with PspA DNA and protein. Vaccine. 2006;24:5755–61.

60. Olafsdottir TA, Lingnau K, Nagy E, Jonsdottir I. Novel protein-based pneumococcal vaccines administered with the th1-promoting adjuvant IC31 induce protective immunity against pneumococcal disease in neonatal mice. Infect. Immun. 2012;80(1):461–8.

61. Effros RM. Anatomy, development, and physiology of the lungs. GI Motil. online. 16 May 200. 2006;1.

62. Kleinstreuer C, Zhang Z, Li Z. Modeling airflow and particle transport/deposition in pulmonary airways. Respir. Physiol. & Neurobiol. 2008;163:128–38.

63. Kleinstreuer C, Zhang Z, Donohue JF. Targeted drug-aerosol delivery in the human respiratory system. Annu. Rev. Biomed. Eng. 2008;10:195–220.

64. Gehr P. Annexe A. Anatomy and morphology of the respiratory tract. Ann. ICRP. 1994;24:121–66.

65. Kunda NK, Somavarapu S, Gordon SB, Hutcheon GA, Saleem IY. Nanocarriers targeting dendritic cells for pulmonary vaccine delivery. Pharm. Res. 2013;30:325–41.

66. Barbas-Filho J V, Ferreira MA, Sesso A, Kairalla RA, Carvalho CRR, Capelozzi VL. Evidence of type II pneumocyte apoptosis in the pathogenesis of idiopathic pulmonary fibrosis (IFP)/usual interstitial pneumonia (UIP). J. Clin. Pathol. 2001;54(2):132–8.

67. Scheuch G, Kohlhaeufl MJ, Brand P, Siekmeier R. Clinical perspectives on pulmonary systemic and macromolecular delivery. Adv. Drug Deliv. Rev. 2006;58:996–1008.

68. Blank F, Stumbles P, von Garnier C. Opportunities and challenges of the pulmonary route for vaccination. Expert Opin. Drug Deliv. 2011;8:547–63.

69. McGhee JR, Fujihashi K. Inside the mucosal immune system. PLoS Biol. 2012;10:1-5.

70. Seipp R. Mucosal immunity and vaccines [Internet]. Sci. Creat. Q. 2006 [cited 2014 Aug 16]. Available from: http://www.scq.ubc.ca/mucosal-immunity-and-vaccines/. Date Accessed: 09/12/2014

71. Holmgren J, Czerkinsky C. Mucosal immunity and vaccines. Nat Med. 2005;11:45-53.

72. Shen X, Lagergård T, Yang Y, Lindblad M, Fredriksson M, Holmgren J. Systemic and mucosal immune responses in mice after mucosal immunization with group b streptococcus type iii capsular polysaccharide-cholera toxin b subunit conjugate Vaccine. Infect. Immun. 2000;68:5749–55.

73. Sou T, Meeusen EN, de Veer M, Morton DA V, Kaminskas LM, McIntosh MP. New developments in dry powder pulmonary vaccine delivery. Trends Biotechnol. 2011;29:191–8.

74. Li A V, Moon JJ, Abraham W, Suh H, Elkhader J, Seidman MA, et al. Generation of effector memory t cell–based mucosal and systemic immunity with pulmonary nanoparticle vaccination. Sci. Transl. Med. 2013;5(204):130.

75. Agu RU, Ugwoke MI, Armand M, Kinget R, Verbeke N. The lung as a route for systemic delivery of therapeutic proteins and peptides. Respir. Res. 2001;2(4):198–209.

76. Leak L, Jamuar M. Ultrastructure of pulmonary lymphatic vessels. Am Rev Respir Dis. 1983;128(2):59–65.

77. Patton JS. Mechanisms of macromolecule absorption by the lungs. Adv. Drug Deliv. Rev. 1996;19:3–36.

78. Onoue S, Hashimoto N, Yamada S. Dry powder inhalation systems for pulmonary delivery of therapeutic peptides and proteins. Expert Opin. Ther. Pat. 2008;18:429–42.

79. Patton JS, Fishburn CS, Weers JG. The Lungs as a portal of entry for systemic drug delivery. Proc. Am. Thorac. Soc. 2004;1:338–44.

80. Smola M, Vandamme T, Sokolowski A. Nanocarriers as pulmonary drug delivery systems to treat and to diagnose respiratory and non respiratory diseases. Int. J. Nanomedicine. 2008;3(1):1–19.

81. Leleux J, Roy K. Micro and nanoparticle-based delivery systems for vaccine immunotherapy: an immunological and materials perspective. Adv. Healthc. Mater. 2013;2:72–94.

82. Akagi T, Baba M, Akashi M. Biodegradable nanoparticles as vaccine adjuvants and delivery systems : regulation of immune responses by nanoparticle-based vaccine. 2012;31–64.

83. Labiris NR, Dolovich MB. Pulmonary drug delivery. Part II: The role of inhalant delivery devices and drug formulations in therapeutic effectiveness of aerosolized medications. Br. J. Clin. Pharmacol. 2003;56:600–12.

84. Sanders M. Inhalation therapy: An historical review. Prim. Care Respir. J. 2007;16:71–81.

85. Mack GS. Pfizer dumps Exubera. Nat Biotech. 2007;25:1331–2.

86. De Swart RL, LiCalsi C, Quirk A V, van Amerongen G, Nodelman V, Alcock R, et al. Measles vaccination of macaques by dry powder inhalation. Vaccine. 2007;25:1183–90.

87. Fourie PB, Germishuizen WA, Wong Y-L, Edwards DA. Spray drying TB vaccines for pulmonary administration. Expert Opin. Biol. Ther. 2008;8:857–63.

88. LiCalsi C, Maniaci MJ, Christensen T, Phillips E, Ward GH, Witham C. A powder formulation of measles vaccine for aerosol delivery. Vaccine. 2001;19:2629–36.

89. Amorij JP, Saluja V, Petersen AH, Hinrichs WLJ, Huckriede A, Frijlink HW. Pulmonary delivery of an inulin-stabilized influenza subunit vaccine prepared by spray-freeze drying induces systemic, mucosal humoral as well as cell-mediated immune responses in BALB/c mice. Vaccine. 2007;25:8707–17.

90. Thomas C, Rawat A, Hope-Weeks L, Ahsan F. Aerosolized PLA and PLGA nanoparticles enhance humoral, mucosal and cytokine responses to hepatitis b vaccine. Mol. Pharm. 2010;8:405–15.

91. Ballester M, Nembrini C, Dhar N, de Titta A, de Piano C, Pasquier M, et al. Nanoparticle conjugation and pulmonary delivery enhance the protective efficacy of Ag85B and CpG against tuberculosis. Vaccine. 2011;29:6959–66.

92. Muttil P, Pulliam B, Garcia-Contreras L, Fallon J, Wang C, Hickey A, et al. Pulmonary immunization of guinea pigs with diphtheria CRM-197 antigen as nanoparticle aggregate dry powders enhance local and systemic immune responses. AAPS J. 2010;12:699–707.

93. Alpar HO, Somavarapu S, Atuah KN, Bramwell VW. Biodegradable mucoadhesive particulates for nasal and pulmonary antigen and DNA delivery. Adv. Drug Deliv. Rev. 2005;57:411–30.

94. Vermaelen K, Pauwels R. Pulmonary dendritic cells. Am. J. Respir. Crit. Care Med. 2005;172:530–51.

95. Banchereau J, Steinman RM. Dendritic cells and the control of immunity. Nature. 1998;392:245–52.

96. Nobelprize.org. The Nobel prize in physiology or medicine 2011 [Internet]. 2011. Available from: http://www.nobelprize.org/nobel_prizes/medicine/laureates/2011/. Date Accessed: 09/12/2014

97. Banchereau J, Briere F, Caux C, Davoust J, Lebecque S, Liu Y-J, et al. Immunobiology of dendritic cells. Annu. Rev. Immunol. 2000;18:767–811.

98. Lassila O, Vainio O, Matzinger P. Can B cells turn on virgin T cells? Nature. 1988;334:253–5.

99. Guermonprez P, Valladeau J, Zitvogel L, Théry C, Amigorena S. Antigen presentation and t cell stimulation by dendritic cells. Annu. Rev. Immunol. 2002;20:621–67.

100. Foged C, Sundblad A, Hovgaard L. Targeting vaccines to dendritic cells. Pharm. Res. 2002;19:229–38.

101. Lambrecht BN, Hammad H. Biology of lung dendritic cells at the origin of asthma. Immunity. 2009;31:412–24.

102. Geurts van Kessel CH, Lambrecht BN. Division of labor between dendritic cell subsets of the lung. Mucosal Immunol. 2008;1:442–50.

103. Lommatzsch M, Bratke K, Bier A, Julius P, Kuepper M, Luttmann W, et al. Airway dendritic cell phenotypes in inflammatory diseases of the human lung. Eur. Respir. J. 2007;30:878–86.

104. Ba-Omar TA, Al-Riyami B. Microscopic study of human alveolar macrophages. Microsc. Microanal. 2008;14:1518–9.

105. Kiama SG, Cochand L, Karlsson L, Nicod LP, Gehr P. Evaluation of phagocytic activity in human monocyte-derived dendritic cells. J Aerosol Med. 2001;14:289–99.

106. Von Garnier C, Nicod LP. Immunology taught by lung dendritic cells. Swiss Med Wkly. 2009;139:186–92.

107. Demedts IK, Brusselle GG, Vermaelen KY, Pauwels RA. Identification and characterization of human pulmonary dendritic cells. Am. J. Respir. Cell Mol. Biol. 2005;32:177–84.

108. Gallucci S, Matzinger P. Danger signals: SOS to the immune system. Curr. Opin. Immunol. 2001;13:114–9.

109. Copland MJ, Baird MA, Rades T, McKenzie JL, Becker B, Reck F, et al. Liposomal delivery of antigen to human dendritic cells. Vaccine. 2003;21:883–90.

110. Burgdorf S, Lukacs-Kornek V, Kurts C. The mannose receptor mediates uptake of soluble but not of cell-associated antigen for cross-presentation. J. Immunol. 2006;176:6770–6.

111. Platt CD, Ma JK, Chalouni C, Ebersold M, Bou-Reslan H, Carano RAD, et al. Mature dendritic cells use endocytic receptors to capture and present antigens. Proc. Natl. Acad. Sci. 2010;107:4287–92.

112. Thornton EE, Looney MR, Bose O, Sen D, Sheppard D, Locksley R, et al. Spatiotemporally separated antigen uptake by alveolar dendritic cells and airway presentation to T cells in the lung. J. Exp. Med. 2012;209(6):1183-99.

113. Foged C, Brodin B, Frokjaer S, Sundblad A. Particle size and surface charge affect particle uptake by human dendritic cells in an in vitro model. Int. J. Pharm. 2005;298:315–22.

114. Reddy ST, Swartz MA, Hubbell JA. Targeting dendritic cells with biomaterials: developing the next generation of vaccines. Trends Immunol. 2006;27:573–9.

115. Cruz LJ, Tacken PJ, Pots JM, Torensma R, Buschow SI, Figdor CG. Comparison of antibodies and carbohydrates to target vaccines to human dendritic cells via DC-SIGN. Biomaterials. 2012;33:4229–39.

116. Caminschi I, Maraskovsky E, Heath WR. Targeting dendritic cells in vivo for cancer therapy. Front. Immunol. 2012;3.

117. Jain S, Vyas SP. Mannosylated niosomes as adjuvant-carrier system for oral mucosal immunization. J. Liposome Res. 2006;16:331–45.

118. Sung JC, Pulliam BL, Edwards DA. Nanoparticles for drug delivery to the lungs. Trends Biotechnol. 2007;25:563–70.

119. Nemmar A, Hoet PHM, Vanquickenborne B, Dinsdale D, Thomeer M, Hoylaerts MF, et al. Passage of Inhaled Particles Into the Blood Circulation in Humans. Circ. 2002;105 411–4.

120. Bailey MM, Berkland CJ. Nanoparticle formulations in pulmonary drug delivery. Med. Res. Rev. 2009;29:196–212.

121. O'Donnell KP, Smyth HDC. Macro- and microstructure of the airways for drug delivery. In: Smyth HDC, Hickey AJ, editors. Control. Pulm. Drug Deliv. SE - 1. Springer New York. 2011;1–19.

122. Des Rieux A, Fievez V, Garinot M, Schneider Y-J, Préat V. Nanoparticles as potential oral delivery systems of proteins and vaccines: A mechanistic approach. J. Control. Release. 2006;116:1–27.

123. Shi Y, Porter W, Merdan T, Li LC. Recent advances in intravenous delivery of poorly water-soluble compounds. Expert Opin. Drug Deliv. 2009;6:1261–82.

124. Cevc G, Vierl U. Nanotechnology and the transdermal route: A state of the art review and critical appraisal. J. Control. Release. 2010;141:277–99.

125. Wadhwa S, Paliwal R, Paliwal SR, Vyas SP. Nanocarriers in ocular drug delivery: An update review. Curr. Pharm. Des. 2009;15:2724–50.

126. Ragab DM, Rohani S. Particle engineering strategies via crystallization for pulmonary drug delivery. Org. Process Res. Dev. 2009;13:1215–23.

127. Rogueda PGA, Traini D. The nanoscale in pulmonary delivery. Part 2: formulation platforms. Expert Opin. Drug Deliv. 2007;4:607–20.

128. Heffernan MJ, Kasturi SP, Yang SC, Pulendran B, Murthy N. The stimulation of CD8+ T cells by dendritic cells pulsed with polyketal microparticles containing ion-paired protein antigen and poly(inosinic acid)–poly(cytidylic acid). Biomaterials. 2009;30:910–8.

129. Hao J, Kwissa M, Pulendran B, Murthy N. Peptide crosslinked micelles: A new strategy for the design and synthesis of peptide vaccines. Int. J. Nanomedicine. 2006;1:97–103.

130. Lu D, Hickey AJ. Liposomal dry powders as aerosols for pulmonary delivery of proteins. AAPS PharmSciTech. 2005;6(4):E641–8.

131. Barnier Quer C, Robson Marsden H, Romeijn S, Zope H, Kros A, Jiskoot W. Polymersomes enhance the immunogenicity of influenza subunit vaccine. Polym. Chem. 2011;2:1482–5.

132. Jain KK. Drug delivery systems. Totowa, NJ: Humana; 2008.

133. Mansour HM, Rhee Y, Wu X. Nanomedicine in pulmonary delivery. Int. J. Nanomedicine. 2009;4:299–319.

134. Amidi M, Pellikaan HC, Hirschberg H, de Boer AH, Crommelin DJA, Hennink WE, et al. Diphtheria toxoid-containing microparticulate powder formulations for pulmonary vaccination: Preparation, characterization and evaluation in guinea pigs. Vaccine. 2007;25:6818–29.

135. Morimoto K, Katsumata H, Yabuta T, Iwanaga K, Kakemi M, Tabata Y, et al. Gelatin microspheres as a pulmonary delivery system: Evaluation of salmon calcitonin absorption. J. Pharm. Pharmacol. 2000;52:611–7.

136. Surendrakumar K, Martyn GP, Hodgers ECM, Jansen M, Blair JA. Sustained release of insulin from sodium hyaluronate based dry powder formulations after pulmonary delivery to beagle dogs. J. Control. Release. 2003;91:385–94.

137. Zhang Q, Shen Z, Nagai T. Prolonged hypoglycemic effect of insulin-loaded polybutylcyanoacrylate nanoparticles after pulmonary administration to normal rats. Int. J. Pharm. 2001;218:75–80.

138. Rytting E, Nguyen J, Wang X, Kissel T. Biodegradable polymeric nanocarriers for pulmonary drug delivery. Expert Opin. Drug Deliv. 2008;5:629–39.

139. Panyam J, Labhasetwar V. Biodegradable nanoparticles for drug and gene delivery to cells and tissue. Adv. Drug Deliv. Rev. 2003;55:329–47.

140. Kumari A, Yadav SK, Yadav SC. Biodegradable polymeric nanoparticles based drug delivery systems. Colloids Surfaces B Biointerfaces. 2010;75:1–18.

141. Nicolas J, Mura S, Brambilla D, Mackiewicz N, Couvreur P. Design, functionalization strategies and biomedical applications of targeted biodegradable/biocompatible polymer-based nanocarriers for drug delivery. Chem. Soc. Rev. 2013;42:1147–235.

142. Kumar M, Kong X, Behera AK, Hellermann GR, Lockey RF, Mohapatra SS. Chitosan IFN-gamma-pDNA Nanoparticle (CIN) therapy for allergic asthma. Genet. Vaccines Ther. 2003;1(1):3.

143. Garcia-Contreras L, Morçöl T, Bell SD, Hickey A. Evaluation of novel particles as pulmonary delivery systems for insulin in rats. AAPS PharmSci. 2003;5:10–20.

144. Ungaro F, d'Emmanuele di Villa Bianca R, Giovino C, Miro A, Sorrentino R, Quaglia F, et al. Insulin-loaded PLGA/cyclodextrin large porous particles with

improved aerosolization properties: In vivo deposition and hypoglycaemic activity after delivery to rat lungs. J. Control. Release. 2009;135:25–34.

145. Hamishehkar H, Emami J, Najafabadi AR, Gilani K, Minaiyan M, Hassanzadeh K, et al. Pharmacokinetics and pharmacodynamics of controlled release insulin loaded PLGA microcapsules using dry powder inhaler in diabetic rats. Biopharm. Drug Dispos. 2010;31:189–201.

146. Blair J, Coghlan D, Langner E, Jansen M, Askey-Sarvar A. Sustained delivery of insulin via the lung using SoliDose technology. Respir. Drug Deliv. VIII. 2002;411–4.

147. Yamamoto H, Kuno Y, Sugimoto S, Takeuchi H, Kawashima Y. Surface-modified PLGA nanosphere with chitosan improved pulmonary delivery of calcitonin by mucoadhesion and opening of the intercellular tight junctions. J. Control. Release. 2005;102:373–81.

148. Kawashima Y, Yamamoto H, Takeuchi H, Fujioka S, Hino T. Pulmonary delivery of insulin with nebulized dl-lactide/glycolide copolymer (PLGA) nanospheres to prolong hypoglycemic effect. J. Control. Release. 1999;62:279–87.

149. Muttil P, Prego C, Garcia-Contreras L, Pulliam B, Fallon J, Wang C, et al. Immunization of guinea pigs with novel hepatitis b antigen as nanoparticle aggregate powders administered by the pulmonary route. AAPS J. 2010;12:330–7.

150. Chronopoulou L, Massimi M, Giardi MF, Cametti C, Devirgiliis LC, Dentini M, et al. Chitosan-coated PLGA nanoparticles: A sustained drug release strategy for cell cultures. Colloids Surfaces B Biointerfaces. 2013;103:310–7.

151. Gupta A, Gupta RK, Gupta GS. Targeting cells for drug and gene delivery: Emerging applications of mannans and mannan binding lectins. J Sci Ind Res. 2009;68:465–83.

152. Yang Y-Y, Wan J-P, Chung T-S, Pallathadka PK, Ng S, Heller J. POE–PEG–POE triblock copolymeric microspheres containing protein: I. Preparation and characterization. J. Control. Release. 2001;75:115–28.

153. Bolhassani A, Safaiyan S, Rafati S. Improvement of different vaccine delivery systems for cancer therapy. Mol. Cancer. 2011;10:3.

154. Doria-Rose NA, Haigwood NL. DNA vaccine strategies: candidates for immune modulation and immunization regimens. Methods. 2003;31:207–16.

155. Bivas-Benita M, van Meijgaarden KE, Franken KLMC, Junginger HE, Borchard G, Ottenhoff THM, et al. Pulmonary delivery of chitosan-DNA nanoparticles enhances the immunogenicity of a DNA vaccine encoding HLA-

A*0201-restricted T-cell epitopes of Mycobacterium tuberculosis. Vaccine. 2004;22:1609–15.

156. Rajeev A J. The manufacturing techniques of various drug loaded biodegradable poly(lactide-co-glycolide) (PLGA) devices. Biomaterials. 2000;21:2475–90.

157. Anderson JM, Shive MS. Biodegradation and biocompatibility of PLA and PLGA microspheres. Adv. Drug Deliv. Rev. 1997;28:5–24.

158. Fiore VF, Lofton MC, Roser-Page S, Yang SC, Roman J, Murthy N, et al. Polyketal microparticles for therapeutic delivery to the lung. Biomaterials. 2010;31:810–7.

159. Kallinteri P, Higgins S, Hutcheon GA, St. Pourçain CB, Garnett MC. Novel functionalized biodegradable polymers for nanoparticle drug delivery systems. Biomacromolecules. 2005;6:1885–94.

160. Tawfeek H, Khidr S, Samy E, Ahmed S, Murphy M, Mohammed A, et al. Poly(Glycerol Adipate-co-ω-Pentadecalactone) spray-dried microparticles as sustained release carriers for pulmonary delivery. Pharm. Res. 2011;28:2086–97.

161. Tawfeek HM, Evans AR, Iftikhar A, Mohammed AR, Shabir A, Somavarapu S, et al. Dry powder inhalation of macromolecules using novel PEG-co-polyester microparticle carriers. Int. J. Pharm. 2013;441:611–9.

162. Gaskell EE, Hobbs G, Rostron C, Hutcheon GA. Encapsulation and release of α-chymotrypsin from poly(glycerol adipate-co-ω-pentadecalactone) microparticles. J. Microencapsul. 2008;25:187–95.

163. Thompson CJ, Hansford D, Higgins S, Rostron C, Hutcheon GA, Munday DL. Evaluation of ibuprofen-loaded microspheres prepared from novel copolyesters. Int. J. Pharm. 2007;329:53–61.

164. Yadav SC, Kumari A, Yadav R. Development of peptide and protein nanotherapeutics by nanoencapsulation and nanobioconjugation. Peptides. 2011;32:173–87.

165. Pinto Reis C, Neufeld RJ, Ribeiro AJ, Veiga F. Nanoencapsulation I. Methods for preparation of drug-loaded polymeric nanoparticles. Nanomedicine; 2006;2:8–21.

166. Dinarvand R, Sepehri N, Manoochehri S, Rouhani H, Atyabi F. Polylactide-co-glycolide nanoparticles for controlled delivery of anticancer agents . Int. J. Nanomedicine. 2011;6:877–95.

167. Soppimath KS, Aminabhavi TM, Kulkarni AR, Rudzinski WE. Biodegradable polymeric nanoparticles as drug delivery devices. J. Control. Release. 2001;70:1–20.

168. Bivas-Benita M, Romeijn S, Junginger HE, Borchard G. PLGA–PEI nanoparticles for gene delivery to pulmonary epithelium. Eur. J. Pharm. Biopharm. 2004;58:1–6.

169. Bivas-Benita M, Lin MY, Bal SM, van Meijgaarden KE, Franken KLMC, Friggen AH, et al. Pulmonary delivery of DNA encoding Mycobacterium tuberculosis latency antigen Rv1733c associated to PLGA–PEI nanoparticles enhances T cell responses in a DNA prime/protein boost vaccination regimen in mice. Vaccine. 2009;27:4010–7.

170. Pulliam B, Sung JC, Edwards DA. Design of nanoparticle-based dry powder pulmonary vaccines. Expert Opin. Drug Deliv. 2007;4:651–63.

171. Allen TM, Cullis PR. Drug delivery systems: Entering the mainstream. Science. 2004;303(5565):1818–22.

172. Petrovsky N, Aguilar JC. Vaccine adjuvants: Current state and future trends. Immunol Cell Biol. 2004;82:488–96.

173. O'Hagan DT, MacKichan ML, Singh M. Recent developments in adjuvants for vaccines against infectious diseases. Biomol. Eng. 2001;18:69–85.

174. Wilson-Welder JH, Torres MP, Kipper MJ, Mallapragada SK, Wannemuehler MJ, Narasimhan B. Vaccine adjuvants: Current challenges and future approaches. J. Pharm. Sci. 2009;98:1278–316.

175. Amorij J-P, Kersten GFA, Saluja V, Tonnis WF, Hinrichs WLJ, Slütter B, et al. Towards tailored vaccine delivery: Needs, challenges and perspectives. J. Control. Release.

176. Nottenburg C. Types of adjuvants: In introduction to adjuvant patent landscape [Internet]. Available from: http://www.patentlens.net/daisy/adjuvants/Background/Adjuvant_types.html. Date Accessed: 09/12/2014

177. O'Hagan DT. New generation vaccine adjuvants. eLS. John Wiley & Sons, Ltd. 2007.

178. Akagi T, Wang X, Uto T, Baba M, Akashi M. Protein direct delivery to dendritic cells using nanoparticles based on amphiphilic poly(amino acid) derivatives. Biomaterials. 2007;28:3427–36.

179. Jilek S, Merkle HP, Walter E. DNA-loaded biodegradable microparticles as vaccine delivery systems and their interaction with dendritic cells. Adv. Drug Deliv. Rev. 2005;57:377–90.

180. Uto T, Wang X, Sato K, Haraguchi M, Akagi T, Akashi M, et al. Targeting of antigen to dendritic cells with poly(γ-glutamic acid) nanoparticles induces antigen-specific humoral and cellular immunity. J. Immunol. 2007;178 2979–86.

181. Uto T, Akagi T, Hamasaki T, Akashi M, Baba M. Modulation of innate and adaptive immunity by biodegradable nanoparticles. Immunol. Lett. 2009;125:46–52.

182. Gregory AE, Williamson D, Titball R. Vaccine delivery using nanoparticles. Front. Cell. Infect. Microbiol. 2013;3:13.

183. Mohan T, Verma P, Nageswara RD. Novel adjuvants & delivery vehicles for vaccines development: A road ahead. Indian J. Med. Res. 2013;138:779–95.

184. Vauthier C, Bouchemal K. Methods for the preparation and manufacture of polymeric nanoparticles. Pharm. Res. 2009;26:1025–58.

185. LiCalsi C, Christensen T, Bennett J V, Phillips E, Witham C. Dry powder inhalation as a potential delivery method for vaccines. Vaccine. 1999;17:1796–803.

186. Pilcer G, Amighi K. Formulation strategy and use of excipients in pulmonary drug delivery. Int. J. Pharm. 2010;392:1–19.

187. Malcolmson RJ, Embleton JK. Dry powder formulations for pulmonary delivery. Pharm. Sci. & Technol. Today. 1998;1:394–8.

188. Peltonen L, Valo H, Kolakovic R, Laaksonen T, Hirvonen J. Electrospraying, spray drying and related techniques for production and formulation of drug nanoparticles. Expert Opin. Drug Deliv. 2010;7:705–19.

189. Heng D, Lee SH, Ng WK, Tan RBH. The nano spray dryer B-90. Expert Opin. Drug Deliv. 2011;8:965–72.

190. Matinkhoo S, Lynch KH, Dennis JJ, Finlay WH, Vehring R. Spray-dried respirable powders containing bacteriophages for the treatment of pulmonary infections. J. Pharm. Sci. 2011;100:5197–205.

191. Saluja V, Amorij JP, Kapteyn JC, de Boer AH, Frijlink HW, Hinrichs WLJ. A comparison between spray drying and spray freeze drying to produce an influenza subunit vaccine powder for inhalation. J. Control. Release. 2010;144:127–33.

192. Jin TH, Tsao E, Goudsmit J, Dheenadhayalan V, Sadoff J. Stabilizing formulations for inhalable powders of an adenovirus 35-vectored tuberculosis (TB) vaccine (AERAS-402). Vaccine. 2010;28:4369–75.

193. Garcia-Contreras L, Wong Y-L, Muttil P, Padilla D, Sadoff J, DeRousse J, et al. Immunization by a bacterial aerosol. Proc. Natl. Acad. Sci. 2008;105:4656–60.

194. Lu D, Garcia-Contreras L, Muttil P, Padilla D, Xu D, Liu J, et al. Pulmonary immunization using antigen 85-B polymeric microparticles to boost tuberculosis immunity. AAPS J. 2010;12:338–47.

195. Folkesson HG, Weström BR, Dahlbäck M, Lundin S, Karlsson BW. Passage of aerosolized BSA and the nona-peptide dDAVP via the respiratory tract in young and adult rats. Exp. Lung Res. 1992;18:595–614.

196. Brain JD, Knudson DE, Sorokin SP, Davis MA. Pulmonary distribution of particles given by intratracheal instillation or by aerosol inhalation. Environ. Res. 1976;11:13–33.

197. Thompson CJ, Hansford D, Higgins S, Hutcheon GA, Rostron C, Munday DL. Enzymatic synthesis and evaluation of new novel ω-pentadecalactone polymers for the production of biodegradable microspheres. J. Microencapsul. 2006;23:213–26.

198. Namekawa S, Uyama H, Kobayashi S. Enzymatic synthesis of polyesters from lactones, dicarboxylic acid divinyl esters, and glycols through combination of ring-opening polymerization and polycondensation. Biomacromolecules. 2000;1:335–8.

199. Umrethia M, Kett VL, Andrews GP, Malcolm RK, Woolfson AD. Selection of an analytical method for evaluating bovine serum albumin concentrations in pharmaceutical polymeric formulations. J. Pharm. Biomed. Anal. 2010;51:1175–9.

200. Hamidi M, Zarei N. A reversed-phase high-performance liquid chromatography method for bovine serum albumin assay in pharmaceutical dosage forms and protein/antigen delivery systems. Drug Test. Anal. 2009;1:214–8.

201. Greenfield NJ. Using circular dichroism spectra to estimate protein secondary structure. Nat. Protoc. 2007;1:2876–90.

202. Henzler Wildman KA, Lee D-K, Ramamoorthy A. Mechanism of lipid bilayer disruption by the human antimicrobial peptide, LL-37†. Biochemistry. 2003;42:6545–58.

203. Whitmore L, Woollett B, Miles AJ, Janes RW, Wallace BA. The protein circular dichroism data bank, a Web-based site for access to circular dichroism spectroscopic data. Structure. 2010;18:1267–9.

204. Whitmore L, Wallace BA. Protein secondary structure analyses from circular dichroism spectroscopy: Methods and reference databases . Biopolymers. 2008;89:392–400.

205. Whitmore L, Wallace BA. DICHROWEB, an online server for protein secondary structure analyses from circular dichroism spectroscopic data. Nucleic Acids Res. 2004;32 W668–W673.

206. Mosmann T. Rapid colorimetric assay for cellular growth and survival: Application to proliferation and cytotoxicity assays. J. Immunol. Methods. 1983;65:55–63.

207. Sullivan VJ, Mikszta JA, Laurent P, Huang J, Ford B. Noninvasive delivery technologies: Respiratory delivery of vaccines. Expert Opin. Drug Deliv. 2006;3:87–95.

208. Chung SW, Hil-lal TA, Byun Y. Strategies for non-invasive delivery of biologics. J. Drug Target. 2012;20:481–501.

209. Duncan G, Jess TJ, Mohamed F, Price NC, Kelly SM, van der Walle CF. The influence of protein solubilisation, conformation and size on the burst release from poly(lactide-co-glycolide) microspheres. J. Control. Release. 2005;110:34–48.

210. Peek LJ, Middaugh CR, Berkland C. Nanotechnology in vaccine delivery. Adv. Drug Deliv. Rev. 2008;60:915–28.

211. Saleem IY, Vordermeier M, Barralet JE, Coombes AGA. Improving peptide-based assays to differentiate between vaccination and Mycobacterium bovis infection in cattle using nanoparticle carriers for adsorbed antigens. J. Control. Release. 2005;102:551–61.

212. Manolova V, Flace A, Bauer M, Schwarz K, Saudan P, Bachmann MF. Nanoparticles target distinct dendritic cell populations according to their size. Eur. J. Immunol. 2008;38:1404–13.

213. Kim H, Uto T, Akagi T, Baba M, Akashi M. Amphiphilic poly(amino acid) nanoparticles induce size-dependent dendritic cell maturation. Adv. Funct. Mater. 2010;20:3925–31.

214. Bilati U, Allémann E, Doelker E. Poly(D,L-lactide-co-glycolide) protein-loaded nanoparticles prepared by the double emulsion method—processing and formulation issues for enhanced entrapment efficiency. J. Microencapsul. 2005;22:205–14.

215. Li X, Deng X, Yuan M, Xiong C, Huang Z, Zhang Y, et al. Investigation on process parameters involved in preparation of poly-dl-lactide-poly(ethylene glycol) microspheres containing Leptospira interrogans antigens. Int. J. Pharm. 1999;178:245–55.

216. Sanad R, Abdel Malak N, El-Bayoomy T, AA B. Preparation and characterization of oxybenzone-loaded solid lipid nanoparticles (SLNs) with enhanced safety and sunscreening efficacy: SPF and UVA-PF. Drug Discov. Ther. 2010;4:472–83.

217. Stevanovic M, Uskokovic D. Poly(lactide-co-glycolide)-based micro and nanoparticles for the controlled drug delivery of vitamins. Curr. Nanosci. 2009;1–14.

218. Li H-Y, Seville PC, Williamson IJ, Birchall JC. The use of amino acids to enhance the aerosolisation of spray-dried powders for pulmonary gene therapy. J. Gene Med. 2005;7:343–53.

219. Seville PC, Learoyd TP, Li H-Y, Williamson IJ, Birchall JC. Amino acid-modified spray-dried powders with enhanced aerosolisation properties for pulmonary drug delivery. Powder Technol. 2007;178:40–50.

220. Bosquillon C, Lombry C, Préat V, Vanbever R. Influence of formulation excipients and physical characteristics of inhalation dry powders on their aerosolization performance. J. Control. Release. 2001;70:329–39.

221. Al-fagih IM, Alanazi FK, Hutcheon GA, Saleem I. Recent advances using supercritical fluid techniques for pulmonary administration of macromolecules via dry powder formulations. Drug Deliv. Lett. 2011;1:128–34.

222. Kim K Do, Kim SH, Kim HT. Applying the Taguchi method to the optimization for the synthesis of TiO2 nanoparticles by hydrolysis of TEOT in micelles. Colloids Surfaces A Physicochem. Eng. Asp. 2005;254:99–105.

223. Abbate V, Kong X, Bansal SS. Photocrosslinked bovine serum albumin hydrogels with partial retention of esterase activity. Enzyme Microb. Technol. 2012;50:130–6.

224. Anhorn MG, Mahler H-C, Langer K. Freeze drying of human serum albumin (HSA) nanoparticles with different excipients. Int. J. Pharm. 2008;363:162–9.

225. Hirsjärvi S, Peltonen L, Hirvonen J. Effect of sugars, surfactant, and tangential flow filtration on the freeze-drying of poly(lactic acid) nanoparticles. AAPS PharmSciTech. 2009;10:488–94.

226. Florindo HF, Pandit S, Gonçalves LMD, Alpar HO, Almeida AJ. Surface modified polymeric nanoparticles for immunisation against equine strangles. Int. J. Pharm. 2010;390:25–31.

227. Yoon J-Y, Kim J-H, Kim W-S. Interpretation of protein adsorption phenomena onto functional microspheres. Colloids Surfaces B Biointerfaces. 1998;12:15–22.

228. Yoon J-Y, Kim J-H, Kim W-S. The relationship of interaction forces in the protein adsorption onto polymeric microspheres. Colloids Surfaces A Physicochem. Eng. Asp. 1999;153:413–9.

229. Calis S, Jeyanthi R, Tsai T, Mehta R, DeLuca P. Adsorption of salmon calcitonin to plga microspheres. Pharm. Res. 1995;12:1072–6.

230. Zhang J, Ma X, Guo Y, Yang L, Shen Q, Wang H, et al. Size-controllable preparation of bovine serum albumin-conjugated PbS nanoparticles. Mater. Chem. Phys. 2010;119:112–7.

231. Pinto Reis C, Neufeld RJ, Ribeiro AJ, Veiga F. Nanoencapsulation I. Methods for preparation of drug-loaded polymeric nanoparticles. Nanomedicine. 2006;2:8–21.

232. Mitra A, Lin S. Effect of surfactant on fabrication and characterization of paclitaxel-loaded polybutylcyanoacrylate nanoparticulate delivery systems. J. Pharm. Pharmacol. 2003;55:895–902.

233. Jalil R, Nixon JR. Microencapsulation using poly (L-lactic Acid) III: Effect of polymer molecular weight on the microcapsule properties. J. Microencapsul. 1990;7:41–52.

234. Mittal G, Sahana DK, Bhardwaj V, Ravi Kumar MN V. Estradiol loaded PLGA nanoparticles for oral administration: Effect of polymer molecular weight and copolymer composition on release behavior in vitro and in vivo. J. Control. Release. 2007;119:77–85.

235. Joshi V, Geary S, Salem A. Biodegradable particles as vaccine delivery systems: Size matters. AAPS J. 2013;15:85–94.

236. Sloat BR, Sandoval MA, Hau AM, He Y, Cui Z. Strong antibody responses induced by protein antigens conjugated onto the surface of lecithin-based nanoparticles. J. Control. Release. 2010;141:93–100.

237. Regev O, Khalfin R, Zussman E, Cohen Y. About the albumin structure in solution and related electro-spinnability issues. Int. J. Biol. Macromol. 2010;47:261–5.

238. Li H-Y, Neill H, Innocent R, Seville P, Williamson I, Birchall JC. Enhanced dispersibility and deposition of spray-dried powders for pulmonary gene therapy. J. Drug Target. 2003;11:425–32.

239. Sou T, Kaminskas LM, Nguyen T-H, Carlberg R, McIntosh MP, Morton DA V. The effect of amino acid excipients on morphology and solid-state properties of multi-component spray-dried formulations for pulmonary delivery of biomacromolecules. Eur. J. Pharm. Biopharm. 2013;83:234–43.

240. Jensen DK, Jensen LB, Koocheki S, Bengtson L, Cun D, Nielsen HM, et al. Design of an inhalable dry powder formulation of DOTAP-modified PLGA nanoparticles loaded with siRNA. J. Control. Release. 2012;157:141–8.

241. Yang L, Guo Y, Ma X, Hu Z, Zhu S, Zhang X, et al. Cooperativity between pepsin and crystallization of calcium carbonate in distilled water. J. Inorg. Biochem. 2003;93:197–203.

242. Tildon JT, Ogilvie JW. The esterase activity of bovine mercaptalbumin. The reaction of the protein with p-nitrophenyl acetate. J. Biol. Chem. 1972;247:1265–71.

243. Córdova J, Ryan JD, Boonyaratanakornkit BB, Clark DS. Esterase activity of bovine serum albumin up to 160°C: A new benchmark for biocatalysis. Enzyme Microb. Technol. 2008;42:278–83.

244. Feng AL, Boraey MA, Gwin MA, Finlay PR, Kuehl PJ, Vehring R. Mechanistic models facilitate efficient development of leucine containing microparticles for pulmonary drug delivery. Int. J. Pharm. 2011;409:156–63.

245. Najafabadi AR, Gilani K, Barghi M, Rafiee-Tehrani M. The effect of vehicle on physical properties and aerosolisation behaviour of disodium cromoglycate microparticles spray dried alone or with l-leucine. Int. J. Pharm. 2004;285:97–108.

246. Todoroff J, Ucakar B, Inglese M, Vandermarliere S, Fillee C, Renauld J-C, et al. Targeting the deep lungs, Poloxamer 407 and a CpG oligonucleotide optimize immune responses to Mycobacterium tuberculosis antigen 85A following pulmonary delivery. Eur. J. Pharm. Biopharm. 2013;84(1):40-8.

247. Menzel M, Muellinger B, Weber N, Haeussinger K, Ziegler-Heitbrock L. Inhalative vaccination with pneumococcal polysaccharide in healthy volunteers. Vaccine. 2005;23:5113–9.

248. Bhardwaj V, Ankola DD, Gupta SC, Schneider M, Lehr C-M, Kumar MNVR. PLGA nanoparticles stabilized with cationic surfactant: Safety studies and application in oral delivery of paclitaxel to treat chemical-induced breast cancer in rat. Pharm. Res. 2009;26:2495–503.

249. Peetla C, Labhasetwar V. Effect of molecular structure of cationic surfactants on biophysical interactions of surfactant-modified nanoparticles with a model membrane and cellular uptake. Langmuir. 2009;25:2369–77.

250. Chen H, Zheng Y, Tian G, Tian Y, Zeng X, Liu G, et al. Oral delivery of DMAB-modified docetaxel-loaded plga-tpgs nanoparticles for cancer chemotherapy. Nanoscale Res. Lett. 2010;6:4.

251. Soenen SJ, Demeester J, De Smedt SC, Braeckmans K. Turning a frown upside down: Exploiting nanoparticle toxicity for anticancer therapy. Nano Today. 2013;8:121–5.

252. Thiele L, Merkle H, Walter E. Phagocytosis and phagosomal fate of surface-modified microparticles in dendritic cells and macrophages. Pharm. Res. 2003;20:221–8.

253. Gupta NK, Tomar P, Sharma V, Dixit VK. Development and characterization of chitosan coated poly-(ε-caprolactone) nanoparticulate system for effective immunization against influenza. Vaccine. 2011;29:9026–37.

254. Wang G, Pan L, Zhang Y, Wang Y, Zhang Z, Lü J, et al. Intranasal delivery of cationic plga nano/microparticles- loaded FMDV DNA vaccine encoding IL-6 elicited protective immunity against FMDV challenge. PLoS One. 2011;6:e27605.

255. Saljoughian N, Zahedifard F, Doroud D, Doustdari F, Vasei M, Papadopoulou B, et al. Cationic solid–lipid nanoparticles are as efficient as electroporation in DNA vaccination against visceral leishmaniasis in mice. Parasite Immunol. 2013;35:397–408.

256. Hariharan S, Bhardwaj V, Bala I, Sitterberg J, Bakowsky U, Ravi Kumar MN V. Design of estradiol loaded PLGA nanoparticulate formulations: A potential oral delivery system for hormone therapy. Pharm. Res. 2006;23:184–95.

257. Kwon H-Y, Lee J-Y, Choi S-W, Jang Y, Kim J-H. Preparation of PLGA nanoparticles containing estrogen by emulsification–diffusion method. Colloids Surfaces A Physicochem. Eng. Asp. 2001;182:123–30.

258. Norde W, Giacomelli CE. BSA structural changes during homomolecular exchange between the adsorbed and the dissolved states. J. Biotechnol. 2000;79:259–68.

259. 2.9.18. Preparations for inhalation: Aerodynamic assessment of fine particles. Eur. pharmacopoeia 7.0. Strasbourg: Council of Europe, European Directorate for the Quality of Medicines & HealthCare. 2010;274–5.

260. Mei L, Sun H, Song C. Local delivery of modified paclitaxel-loaded poly(ε-caprolactone)/pluronic F68 nanoparticles for long-term inhibition of hyperplasia. J. Pharm. Sci. 2009;98:2040–50.

261. Li X, Aldayel AM, Cui Z. Aluminum hydroxide nanoparticles show a stronger vaccine adjuvant activity than traditional aluminum hydroxide microparticles. J. Control. Release. 2014;173:148–57.

262. Singh M, Kazzaz J, Ugozzoli M, Malyala P, Chesko J, O'Hagan DT. Polylactide-Co-glycolide microparticles with surface adsorbed antigens as vaccine delivery systems. Curr. Drug Deliv. 2006;3:115–20.

263. Singh M, Kazzaz J, Ugozzoli M, Chesko J, O'Hagan DT. Charged polylactide co-glycolide microparticles as antigen delivery systems. Expert Opin. Biol. Ther. 2004;4:483–91.

264. Rabbani NR, Seville PC. The influence of formulation components on the aerosolisation properties of spray-dried powders. J. Control. Release. 2005;110:130–40.

265. Kwon YJ, Standley SM, Goh SL, Fréchet JMJ. Enhanced antigen presentation and immunostimulation of dendritic cells using acid-degradable cationic nanoparticles. J. Control. Release. 2005;105:199–212.

266. Fischer D, Li Y, Ahlemeyer B, Krieglstein J, Kissel T. In vitro cytotoxicity testing of polycations: influence of polymer structure on cell viability and hemolysis. Biomaterials. 2003;24:1121–31.

267. Harush-Frenkel O, Bivas-Benita M, Nassar T, Springer C, Sherman Y, Avital A, et al. A safety and tolerability study of differently-charged nanoparticles for local pulmonary drug delivery. Toxicol. Appl. Pharmacol. 2010;246:83–90.

268. Harush-Frenkel O, Rozentur E, Benita S, Altschuler Y. Surface charge of nanoparticles determines their endocytic and transcytotic pathway in polarized MDCK cells. Biomacromolecules. 2008;9:435–43.

269. Malmsten M, Siegel G. Electrostatic and ion-binding effects on the adsorption of proteoglycans. J. Colloid Interface Sci. 1995;170:120–7.

270. Kim SK, Foote MB, Huang L. The targeted intracellular delivery of cytochrome C protein to tumors using lipid-apolipoprotein nanoparticles. Biomaterials. 2012;33:3959–66.

271. Thiele L, Rothen-Rutishauser B, Jilek S, Wunderli-Allenspach H, Merkle HP, Walter E. Evaluation of particle uptake in human blood monocyte-derived cells in vitro. Does phagocytosis activity of dendritic cells measure up with macrophages? J. Control. Release. 2001;76:59–71.

272. Barazzone GC, Carvalho R, Kraschowetz S, Horta AL, Sargo CR, Silva AJ, et al. Production and purification of recombinant fragment of pneumococcal surface protein A (PspA) in Escherichia coli. Procedia Vaccinol. 2011;4:27–35.

273. Vadesilho CFM, Ferreira DM, Moreno AT, Chavez-Olortegui C, Machado de Avila RA, Oliveira MLS, et al. Characterization of the antibody response elicited by immunization with pneumococcal surface protein A (PspA) as recombinant protein or DNA vaccine and analysis of protection against an

intranasal lethal challenge with Streptococcus pneumoniae. Microb. Pathog. 2012;53:243–9.

274. Ochs MM, Bartlett W, Briles DE, Hicks B, Jurkuvenas A, Lau P, et al. Vaccine-induced human antibodies to PspA augment complement C3 deposition on Streptococcus pneumoniae. Microb. Pathog. 2008;44:204–14.

275. Kolberg J, Aase A, Næss LM, Aaberge IS, Caugant DA. Human antibody responses to pneumococcal surface protein A and capsular polysaccharides during acute and convalescent stages of invasive disease in adult patients. Pathog. Dis. 2014;70:40–50.

276. Briles DE, Hollingshead SK, King J, Swift A, Braun PA, Park MK, et al. Immunization of humans with recombinant pneumococcal surface protein a (rPspA) Elicits antibodies that passively protect mice from fatal infection with Streptococcus pneumoniae bearing heterologous PspA. J. Infect. Dis. 2000;182 1694–701.

277. Rappuoli R, Mandl CW, Black S, De Gregorio E. Vaccines for the twenty-first century society. Nat Rev Immunol. 2011;11:865–72.

278. Koppolu B, Zaharoff DA. The effect of antigen encapsulation in chitosan particles on uptake, activation and presentation by antigen presenting cells. Biomaterials. 2013;34:2359–69.

279. Amy D. Schoofs. Development of a protein antigen based pneumococcal vaccine utilizing a polyanhydride nanoparticle delivery platform. Graduate Theses and Dissertations, University of Iowa. 2013;1–72.

280. Faden H, Duffy L, Wasielewski R, Wolf J, Krystofik D, Tung Y. Relationship between Nasopharyngeal Colonization and the Development of Otitis Media in Children. J. Infect. Dis. . 1997;175 1440–5.

281. Horta ACL, Sargo CR, da Silva AJ, de Carvalho Gonzaga M, dos Santos MP, Gonçalves VM, et al. Intensification of high cell-density cultivations of rE. coli for production of S. pneumoniae antigenic surface protein, PspA3, using model-based adaptive control. Bioprocess Biosyst. Eng. 2012;35:1269–80.

282. Horta ACL, Silva AJ, Sargo CR, Velez AM, Gonzaga MC, Giordano RC, et al. A supervision and control tool based on artificial intelligence for high cell density cultivations. Brazilian J. Chem. Eng. 2014;31:457–68.

283. Carvalho RJ, Cabrera-Crespo J, Tanizaki MM, Gonçalves VM. Development of production and purification processes of recombinant fragment of pneumococcal surface protein A in Escherichia coli using different carbon sources and chromatography sequences. Appl. Microbiol. Biotechnol. 2012;94:683–94.

284. Brito LA, Singh M. Acceptable levels of endotoxin in vaccine formulations during preclinical research. J. Pharm. Sci. 2011;100:34–7.

285. Stolnik S, Daudali B, Arien A, Whetstone J, Heald C., Garnett M., et al. The effect of surface coverage and conformation of poly(ethylene oxide) (PEO) chains of poloxamer 407 on the biological fate of model colloidal drug carriers. Biochim. Biophys. Acta - Biomembr. 2001;1514:261–79.

286. Gordon S, Saupe A, McBurney W, Rades T, Hook S. Comparison of chitosan nanoparticles and chitosan hydrogels for vaccine delivery. J. Pharm. Pharmacol. 2008;60:1591–600.

287. He C, Hu Y, Yin L, Tang C, Yin C. Effects of particle size and surface charge on cellular uptake and biodistribution of polymeric nanoparticles. Biomaterials. 2010;31:3657–66.

288. Carrillo-Conde B, Song E-H, Chavez-Santoscoy A, Phanse Y, Ramer-Tait AE, Pohl NLB, et al. Mannose-functionalized "pathogen-like" polyanhydride nanoparticles target C-type lectin receptors on dendritic cells. Mol. Pharm. 2011;8:1877–86.

289. Ghotbi Z, Haddadi A, Hamdy S, Hung RW, Samuel J, Lavasanifar A. Active targeting of dendritic cells with mannan-decorated PLGA nanoparticles. J. Drug Target. 2011;19:281–92.

290. Zhao L, Seth A, Wibowo N, Zhao C-X, Mitter N, Yu C, et al. Nanoparticle vaccines. Vaccine. 2014;32:327–37.

291. Wibowo N. Engineering viral capsomeres as a vaccine platform. The University of Queensland. 2012;85–107.

292. Torres MP, Wilson-Welder JH, Lopac SK, Phanse Y, Carrillo-Conde B, Ramer-Tait AE, et al. Polyanhydride microparticles enhance dendritic cell antigen presentation and activation. Acta Biomater. 2011;7:2857–64.

293. Karagouni E, Kammona O, Margaroni M, Kotti K, Karageorgiou V, Gaitanaki C, et al. Uptake of BSA-FITC loaded PLGA nanoparticles by bone marrow-derived dendritic cells induces maturation but not IL-12 or IL-10 production. Nanosci. Nanotechnol. Lett. 2013;5:498–504.

294. Lima FA, Miyaji EN, Quintilio W, Raw I, Ho PL, Oliveira MLS. Pneumococcal surface protein A does not affect the immune responses to a combined diphtheria tetanus and pertussis vaccine in mice. Vaccine. 2013;31:2465–70.

295. Yamamoto M, Briles DE, Yamamoto S, Ohmura M, Kiyono H, McGhee JR. A nontoxic adjuvant for mucosal immunity to pneumococcal surface protein A. J. Immunol. . 1998;161 4115–21.

296. Gamvrellis A, Leong D, Hanley JC, Xiang SD, Mottram P, Plebanski M. Vaccines that facilitate antigen entry into dendritic cells. Immunol Cell Biol. 2004;82:506–16.

297. Couvreur P, Vauthier C. Nanotechnology: Intelligent design to treat complex disease. Pharm. Res. 2006;23:1417–50.

298. Xu P, Gullotti E, Tong L, Highley CB, Errabelli DR, Hasan T, et al. Intracellular drug delivery by poly(lactic-co-glycolic acid) nanoparticles, Revisited. Mol. Pharm. 2008;6:190–201.

299. Labhasetwar V, Song C, Humphrey W, Shebuski R, Levy RJ. Arterial uptake of biodegradable nanoparticles: Effect of surface modifications. J. Pharm. Sci. 1998;87:1229–34.

300. Jones LS, Peek LJ, Power J, Markham A, Yazzie B, Middaugh CR. Effects of adsorption to aluminum salt adjuvants on the structure and stability of model protein antigens. J. Biol. Chem. 2005;280 13406–14.

301. Florindo HF, Pandit S, Lacerda L, Gonçalves LMD, Alpar HO, Almeida a J. The enhancement of the immune response against S. equi antigens through the intranasal administration of poly-ε-caprolactone-based nanoparticles. Biomaterials. 2009;30(5): 879–91.

302. Li X, Aldayel AM, Cui Z. Aluminum hydroxide nanoparticles show a stronger vaccine adjuvant activity than traditional aluminum hydroxide microparticles. J. Control. Release. 2014;173:148–57.

303. Zijlstra GS, J. Ponsioen B, A. Hummel S, Sanders N, Hinrichs WLJ, de Boer AH, et al. Formulation and process development of (recombinant human) deoxyribonuclease I as a powder for inhalation. Pharm. Dev. Technol. 2009;14:358–68.

304. Andya J, Maa Y-F, Costantino H, Nguyen P-A, Dasovich N, Sweeney T, et al. The effect of formulation excipients on protein stability and aerosol performance of spray-dried powders of a recombinant humanized anti-IgE monoclonal antibody1. Pharm. Res. 1999;16:350–8.

305. Hinrichs WL., Prinsen M., Frijlink H. Inulin glasses for the stabilization of therapeutic proteins. Int. J. Pharm. 2001;215:163–74.

306. Lucas P, Anderson K, Potter U, Staniforth J. Enhancement of small particle size dry powder aerosol formulations using an ultra low density additive. Pharm. Res. 1999;16:1643–7.

307. Vehring R. Pharmaceutical particle engineering via spray drying. Pharm. Res. 2008;25:999–1022.

308. Jiang M, Wu Y, He Y, Nie J. Synthesis and characterization of an amphiphilic hyperbranched poly(amine-ester)-co-D,L-lactide (HPAE-co-PLA) copolymers and their nanoparticles for protein drug delivery. J. Appl. Polym. Sci. 2010;117:1156–67.

309. Determan AS, Trewyn BG, Lin VS-Y, Nilsen-Hamilton M, Narasimhan B. Encapsulation, stabilization, and release of BSA-FITC from polyanhydride microspheres. J. Control. Release. 2004;100:97–109.

310. De Jonge J, Amorij J-P, Hinrichs WLJ, Wilschut J, Huckriede A, Frijlink HW. Inulin sugar glasses preserve the structural integrity and biological activity of influenza virosomes during freeze-drying and storage. Eur. J. Pharm. Sci. 2007;32:33–44.

311. Audouy SAL, van der Schaaf G, Hinrichs WLJ, Frijlink HW, Wilschut J, Huckriede A. Development of a dried influenza whole inactivated virus vaccine for pulmonary immunization. Vaccine. 2011;29:4345–52.

312. Amorij J-P, Meulenaar J, Hinrichs WLJ, Stegmann T, Huckriede A, Coenen F, et al. Rational design of an influenza subunit vaccine powder with sugar glass technology: preventing conformational changes of haemagglutinin during freezing and freeze-drying. Vaccine. 2007;25:6447–57.

Appendices

Appendix-1

Validation results of HPLC analytical method for bovine serum albumin (BSA)

True Value (µg/ml)	Measured Value (µg/ml) (Mean±SD)		% Relative standard deviation (RSD)		% Accuracy		LOD (µg/ml)	LOQ (µg/ml)
	Intra-day	Inter-day	Intra-day	Inter-day	Intra-day	Inter-day		
10	09.71±0.08	09.57±0.14	0.83	1.45	102.90	104.30	1.98	3.24
20	20.29±0.05	20.35±0.22	0.24	1.09	98.53	98.23		
40	42.47±0.30	43.48±1.12	0.71	2.59	93.81	91.29		

Note: LOD – Limit of Detection, LOQ – Limit of Quantification

Appendix-2

Scanning electron microscope pictures of nanocomposite microparticles produced using L-leu and inulin

Formulation	X5000	X20000	X30000
Form. 1 Inulin – 0 % L-Leu – 60 % NPs – 40%	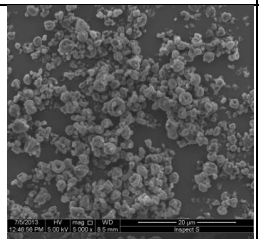	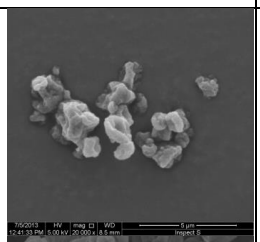	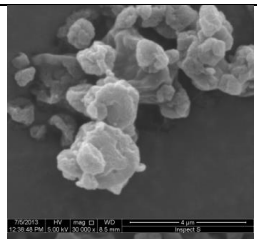
Form. 2 Inulin – 15 % L-Leu – 45 % NPs – 40%	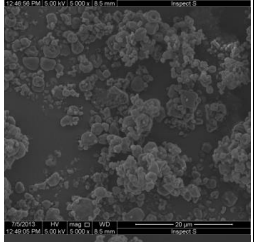	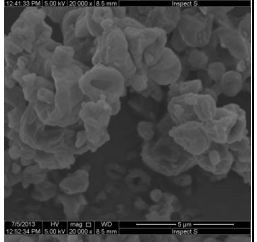	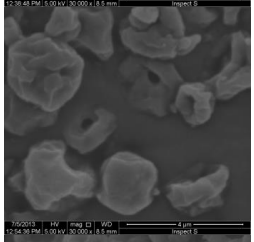
Form. 3 Inulin – 30 % L-Leu – 30 % NPs – 40%	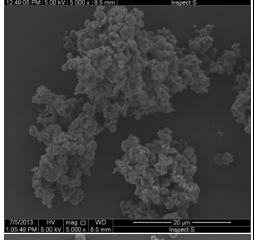	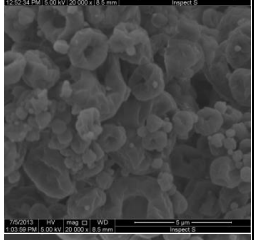	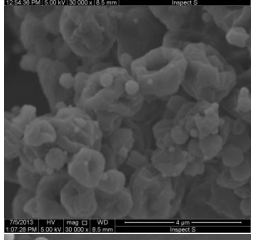
Form. 4 Inulin – 45 % L-Leu – 15 % NPs – 40%	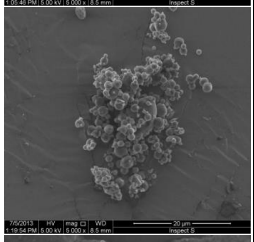	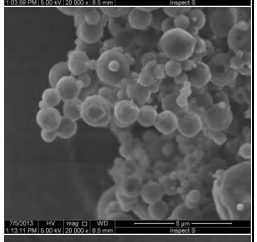	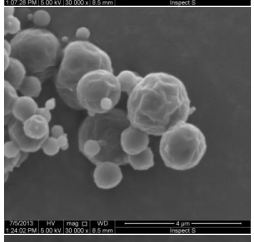
Form. 5 Inulin – 60 % L-Leu – 0 % NPs – 40%	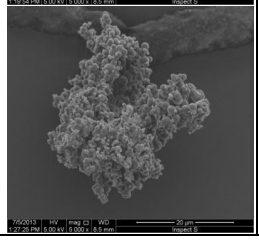	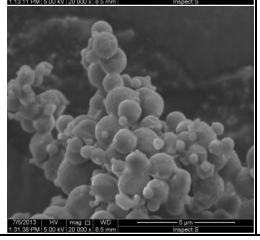	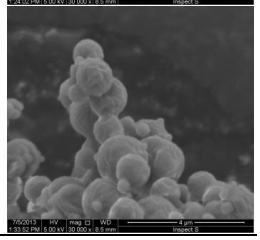

Characterisation of nanocomposite microparticles produced using L-leu and inulin

Formulation	Yield (%)	Tap density	Particle size (µm, SEM)
Form. 1 Inulin – 0 % L-Leu – 60 % NPs – 40%	51.42±00.50	0.18±0.0096	1.97±0.29
Form. 2 Inulin – 15 % L-Leu – 45 % NPs – 40%	53.82±01.25	0.19±0.0105	1.88±0.65
Form. 3 Inulin – 30 % L-Leu – 30 % NPs – 40%	68.50±12.87	0.22±0.0005	1.81±0.39
Form. 4 Inulin – 45 % L-Leu – 15 % NPs – 40%	73.85±00.21	0.16±0.0003	1.57±0.31
Form. 5 Inulin – 60 % L-Leu – 0 % NPs – 40%	69.25±04.60	0.14±0.0002	1.55±0.32

List of Publications and Awards

Publications

Chapter 1 sections 1.2-1.5 are taken from publications 1 and 2; Chapter 3 and corresponding methods from chapter 2 are published in publication 3; Chapter 4 and corresponding methods from chapter 2 are to be published in publication 5

1 **Kunda NK**, Somavarapu S, Gordon SB, Hutcheon GA, Saleem IY. "**Nanocarriers targeting dendritic cells for pulmonary vaccine delivery**" Pharmaceutical Research (2012):1-17.

2 **Kunda NK**, Alfagih IM, Saleem IY, Hutcheon GA. "**Polymer-based delivery systems for the pulmonary delivery of macromolecules" in Pulmonary Drug Delivery: Advances and Challenges** by Professors Ali Nokhodchi & Gary Martin (Book Chapter). John Wiley & Sons (Accepted, launch Feb 2015)

3 **Kunda NK**, Alfagih IM, Somavarapu S, Tawfeek HM, Hutcheon GA, Saleem IY. "**Bovine serum albumin adsorbed PGA-co-PDL nanocarriers for vaccine delivery via dry powder inhalation**" Pharmaceutical Research (2014): In Press; DOI: 10.1007/s11095-014-1538-5

4 Merchant Z, Taylor KM, Staphleton P, Razak SA, **Kunda NK**, Alfagih IM, Saleem IY, Somavarapu S. **"Engineering hydrophobically modified chitosan for enhancing the dispersion of respirable microparticles of Levofloxacin"** European Journal of Pharmaceutics and Biopharmaceutics (2014): In Press; DOI: 10.1016/j.ejpb.2014.09.005

5 **Kunda NK**, Alfagih IM, Merchant Z, Somavarapu S, Hutcheon GA, Saleem IY. "**Cationic surfactant, DMAB, stabilised PGA-co-PDL nanoparticles adsorbed with a model protein for pulmonary delivery"** *(Submitted: European Journal of Pharmaceutics and Biopharmaceutics)*

6 Alfagih IM, **Kunda NK**, Alanazi F, Somavarapu S, Hutcheon GA, Saleem IY. "**Pulmonary delivery of protein using nanocomposite microparticle carriers**" *(Submitted: International Journal of Pharmaceutics)*

Oral Presentations

- INTERREG IV A2Seas: UoG - AAPS Chapter Conference 2014 – 16 – 18th July 2014
  - **Nanocarriers for Vaccine Delivery**
- University of Greenwich AAPS Student Chapter Conference 2013 –25th March 2013
- Faculty Research Seminar Day (Faculty of Science), LJMU – 12th June 2013
  - **Dry Powder Inhalation of Proteins (as vaccines) using Polymeric Nanocarriers**

Conference Proceedings (4-page abstracts)

- **Kunda NK**, Alfagih IM, Somavarapu S, Hutcheon GA, Saleem IY. **Pulmonary Vaccine Delivery of Protein Adsorbed PGA-co-PDL Nanocomposite Microparticles.** Drug Delivery to the Lungs - DDL23 – December 2012, Edinburgh, Scotland, UK (Published in Journal of Aerosol Medicine and Pulmonary Drug Delivery. October 2013:A9)
- Alfagih IM, **Kunda NK**, Alanazi FK, Hutcheon GA, Saleem IY. **Protein loaded PGA-co-PDL Nanocomposite Microparticles for Inhalation.** Drug Delivery to the Lungs - DDL23 – December 2012, Edinburgh, Scotland, UK (Published in Journal of Aerosol Medicine and Pulmonary Drug Delivery. October 2013:A13-A14)

Selected Abstracts

- **Kunda NK**, Somavarapu S, Hutcheon GA, Saleem IY. **PGA-co-PDL Nanocarriers adsorbed with PspA for Pulmonary Vaccine Delivery.** 2014 AAPS Annual Meeting & Exposition – San Diego, CA, USA
- **Kunda NK**, Hutcheon GA, Saleem IY. **Protein Adsorption onto Polymer-based Nanocarriers for Vaccine Delivery.** 2014 European Society of Biomaterials - Liverpool, UK
- **Kunda NK**, Somavarapu S, Hutcheon GA, Saleem IY. **Comparison of Adsorption Efficiency between Negatively and Positively Charged PGA-**

co-PDL Nanoparticles. 2014 AAPS National Biotechnology Conference – San Diego, CA, USA

- **Kunda NK**, Somavarapu S, Hutcheon GA, Saleem IY. **Protein Adsorbed PGA-co-PDL Nanocarriers for Vaccine Delivery.** 2013 AAPS Annual Meeting & Exposition – San Antonio, TX, USA
- **Kunda NK**, Chavan T, Somavarapu S, Hutcheon GA, Saleem IY. **PGA-co-PDL Nanoparticles Coated with Protein Formulated as Dry Powder Nanocomposite Microparticles for Pulmonary Vaccine Delivery.** 2012 AAPS National Biotechnology Conference – San Diego, CA, USA

Awards and Honours

Moderator – **The ABCs of Fusion Peptides and Proteins** – American Association of Pharmaceutical Scientists (AAPS) National Biotechnology Conference, San Diego, CA (May 19-21, 2014)

Co-chair – The Faculty Research Seminar Day, 2013 and 2014 (LJMU)

Associate Fellow of the Higher Education Academy (UK)

Member of Royal Society of Chemistry (MRSC)

Funding

2014	The Aerosol Society Travelship	£ 500
2014	AAPS Formulation Design and Development Section Travelship	$ 750
2013/ 2014	CN Davies Award, The Aerosol Society	£ 600
2013	Faculty of Science Research Seminar Day, LJMU (Oral Prize)	£ 500
2013	AAPS Pharmaceuticals Global Health Focus Group Travelship	$ 500
2012	AAPS Formulation Design and Development Section Travelship	$ 500
2012	The Aerosol Society Travelship	£ 250
2012	Faculty of Science Research Seminar Day, LJMU (Poster Prize)	£ 1000

Pharm Res (2013) 30:325–341
DOI 10.1007/s11095-012-0891-5

EXPERT REVIEW

Nanocarriers Targeting Dendritic Cells for Pulmonary Vaccine Delivery

Nitesh K. Kunda • Satyanarayana Somavarapu • Stephen B. Gordon • Gillian A. Hutcheon • Imran Y. Saleem

Received: 11 June 2012 / Accepted: 18 September 2012 / Published online: 9 October 2012

ABSTRACT Pulmonary vaccine delivery has gained significant attention as an alternate route for vaccination without the use of needles. Immunization through the pulmonary route induces both mucosal and systemic immunity, and the delivery of antigens in a dry powder state can overcome some challenges such as cold-chain and availability of medical personnel compared to traditional liquid-based vaccines. Antigens formulated as nanoparticles (NPs) reach the respiratory airways of the lungs providing greater chance of uptake by relevant immune cells. In addition, effective targeting of antigens to the most 'professional' antigen presenting cells (APCs), the dendritic cells (DCs) yields an enhanced immune response and the use of an adjuvant further augments the generated immune response thus requiring less antigen/dosage to achieve vaccination. This review discusses the pulmonary delivery of vaccines, methods of preparing NPs for antigen delivery and targeting, the importance of targeting DCs and different techniques involved in formulating dry powders suitable for inhalation.

KEY WORDS antigen presenting cells · dendritic cells · dry powder · polymeric nanoparticles · pulmonary delivery of vaccines

N. K. Kunda · G. A. Hutcheon · I. Y. Saleem (✉)
Formulation and Drug Delivery Research
School of Pharmacy and Biomolecular Science
Liverpool John Moores University
James Parsons Building, Byrom Street
Liverpool L3 3AF, UK
e-mail: I.Saleem@ljmu.ac.uk

S. Somavarapu
Department of Pharmaceutics, School of Pharmacy
University College London
London, UK

S. B. Gordon
Respiratory Infection Group, Liverpool School of Tropical Medicine
Liverpool, UK

ABBREVIATIONS

AMs	alveolar macrophages
APCs	antigen presenting cells
BAL	bronchoalveolar lavage
CLRs	C-type lectin receptors
DCs	dendritic cells
DPI	dry powder inhalations
FD	freeze-drying
HLA	human leukocyte antigen
ILs	interleukins
LN	lymph node
MHC	major histocompatibility complex
MN	mannan
NPs	nanoparticles
PCL	poly-ε-caprolactone
PEG	polyethylene glycol
PEI	polyethyleneimine
PLA	polylactide or poly-L-lactic acid
PLGA	poly lactic-co-glycolic-acid
PRRs	pattern recognition receptors
PVA	polyvinyl alcohol
SCF	supercritical fluid
SD	spray-drying
SFD	spray-freeze drying
TLRs	toll-like receptors
TMC	N-trimethyl chitosan
VLPs	virus-like particles

INTRODUCTION

New therapeutic biopharmaceuticals have made it possible to treat and/or prevent many diseases which were untreatable a decade ago (1). The majority of these biopharmaceuticals are administered via parenteral routes because they are degraded by acid and proteases in the stomach or

have high first-pass metabolism and as such are not suitable for oral delivery. The formulation of biopharmaceuticals in non-invasive delivery systems in order to make them more acceptable to patients has gained significant attention but the pharmaceutical challenges are stability, integrity and effectiveness within the therapeutic dose (1,2). The leading non-invasive systems are buccal, nasal, pulmonary, sublingual and transdermal routes—this review will focus on the pulmonary route and on vaccine delivery in particular.

Pulmonary delivery of vaccines has gained major attention for achieving both mucosal and systemic immunity (3). An optimum formulation containing antigens in the dry state as nanoparticles (NPs) can result in greater stability and a better immune response compared to traditional liquid-based vaccines (3). NPs as colloidal carriers offer protection of biopharmaceuticals against degradation, and targeted delivery to specific sites of action. NPs can be developed with variable physico-chemical characteristics such as size, structure, morphology, surface texture and composition, and thus can be delivered either orally, parenterally or locally (4).

This review discusses the pulmonary delivery of vaccines, methods of preparing NPs, the importance of targeting dendritic cells (DCs) (antigen presenting cells-APCs) and different techniques involved in making dry powders suitable for inhalation. Progress in the delivery of biopharmaceuticals via buccal (5–7), nasal (8), sublingual (9) and transdermal (10) routes has previously been reported elsewhere and is beyond the scope of this review.

Since the term 'vaccination' was coined by Edward Jenner in 1796, it has been arguably the most important scientific advance in the battle against infectious diseases (11). According to the World Health Organization (WHO), around 2.5 million children's lives are saved each year due to the availability of vaccines against a variety of antigens (12). However, in low and middle income countries (LMIC) a lack of infrastructure such as cold-chain and trained medical personnel essential for the administration of traditional liquid-based vaccine formulations, means that many eligible children and adults are not vaccinated (12). Table I below provides a list of reported cases by disease according to World Health Statistics (WHS) 2011 (13). Hence, there is a global need to develop effective and reliable vaccine strategies that are non-invasive, easily accessible and affordable (14). To address the issues with liquid-based vaccine formulations in LMIC, non-invasive routes of delivery, which do not have the requirements of cold-chain or trained personnel are being investigated (3).

Of all the non-invasive routes of delivery, pulmonary delivery can overcome some of the current challenges of vaccination such as invasiveness, accessibility, and vaccine stability and integrity by delivering vaccines as dry powder inhalations (DPI) (14). In addition, the pulmonary route has gained much attention as it is the main entry portal for pathogens (2,15).

Table I List of Reported Cases by Disease According to World Health Statistics (WHS) 2011

Disease	Reported Cases (WHS 2011)[a]
Diptheria	857
Malaria	81,735,305 (1990–2009)
Measles	222,318
Mumps	546,684
Tetanus	9,836
Tuberculosis	5,797,317
Pneumonia (Children <5 years)	~1,400,000 (18% of all child deaths in 2008) (120)

[a] Data provided not necessarily for the year 2011, more details at http://www.who.int/whosis/whostat/2011/en/index.html

PULMONARY VACCINE DELIVERY

Pulmonary delivery as a route of drug administration can be traced back 4000 years to India where people suffering from cough suppressed it by inhaling the leaves of *Atropa Belladonna* (16). Later in the 19th and 20th centuries, people suffering from asthma smoked cigarettes containing tobacco and stramonium powder to alleviate their symptoms (16). The first inhaling apparatus for dry powder delivery was patented in London in 1864 (17). Since then much progress has been made in developing devices such as nebulizers, metered dose inhalers and DPIs for delivery of therapeutics. With recent advancements in pulmonary delivery devices and recombinant protein technology the first peptide DPI formulation, Exubera (Nektar/Pfizer), was approved and released into the market in January 2006. This was soon withdrawn for several reasons including bulkiness of the device, complicated administration, contraindication in smokers and insufficient evidence with regulatory bodies regarding the patients preference of Exubera (inhaled dosage form) compared to other dosage forms (18). This led, however, to further research and development of DPI of biopharmaceuticals, and currently many investigations are being pursued by the pharmaceutical industry such as the AIR system (Alkermes/Eli Lilly), the Technosphere system (Mannkind) and Kos inhaled insulin (Kos Pharm/Abbott) for Type I/II diabetes, and Granulocyte-colony-stimulating factor (G-CSF) for Neutropenia (Amgen) (19). This has been followed by investigations into DPI of vaccines (20–24).

Anatomy of the Human Lung

The human lung, weighing about 1 kg, is divided by the pleural membranes into three lobes on the right and two

lobes on the left (25). Once inhaled, the air passes through the nose and mouth, from the larynx to trachea and to the series of around 16 generations of conductive bronchi and bronchioles (25,26). From the 17th generation of bronchioles, alveoli begin to appear in the walls (respiratory airways) and by the 20th generation of airways, the entire walls are composed of alveoli, commonly referred to as alveolar ducts. At the 23rd generation, the alveolar ducts end in blind sacs, lined with alveoli, and are referred to as alveolar sacs (Fig. 1) (25–27). It is estimated that on an average a human lung consists of about 300 million alveoli providing a surface area of exchange of 80–90 sq. m (25,28).

The submucosal glands and the 'goblet cells' (present on the bronchial surface) secrete mucus onto the bronchial surfaces. The submucosal glands also help in producing an electrolyte solution on which the mucus rests. The mucus covering the airways is transported towards the mouth with the coordinated movement of cilia present on top of the ciliated columnar cells. This mucus transported to the mouth is then swallowed. This process of mucus movement from the bronchial surfaces to the mouth for swallowing is mainly responsible for removing any foreign material that lands on the bronchial surfaces (25).

The alveoli and the pulmonary capillaries are separated by a barrier composing of endothelial cells, interstitial space, and pneumocytes (pulmonary epithelial cells). The pneumocytes are divided into two types, type I and type II cells. Type I are very flat and cover the alveolar surface whereas type II are irregularly shaped containing lamellar bodies that are secreted as surfactant, and they can further divide and produce type I and type II cells (25).

Lung as a Delivery Site for Drugs

The lung is an excellent choice for the delivery of biopharmaceuticals for the treatment of both local and systemic disorders as it offers several advantages such as; large surface area (80 sq. m), dense vasculature, rapid absorption leading to an immediate onset of action, thin alveolar epithelium, less enzymatic activity than gut and a high capacity for solute exchange (29). With regards to the delivery of vaccines, a high density of APCs including alveolar macrophages (AMs), DCs and B cells represent an ideal target to induce a strong immune response resulting in both mucosal and systemic immunity (14). Recent research has confirmed that the induction of an immune response at one mucosal site elicits an immune response at distant mucosal sites by mucosal lymphocyte trafficking leading to both mucosal and systemic immunization (15,30). There is some evidence that mucosal immunization may also reduce the dosage required to achieve the desired immunity compared to liquid formulations administered via the parenteral route (3).

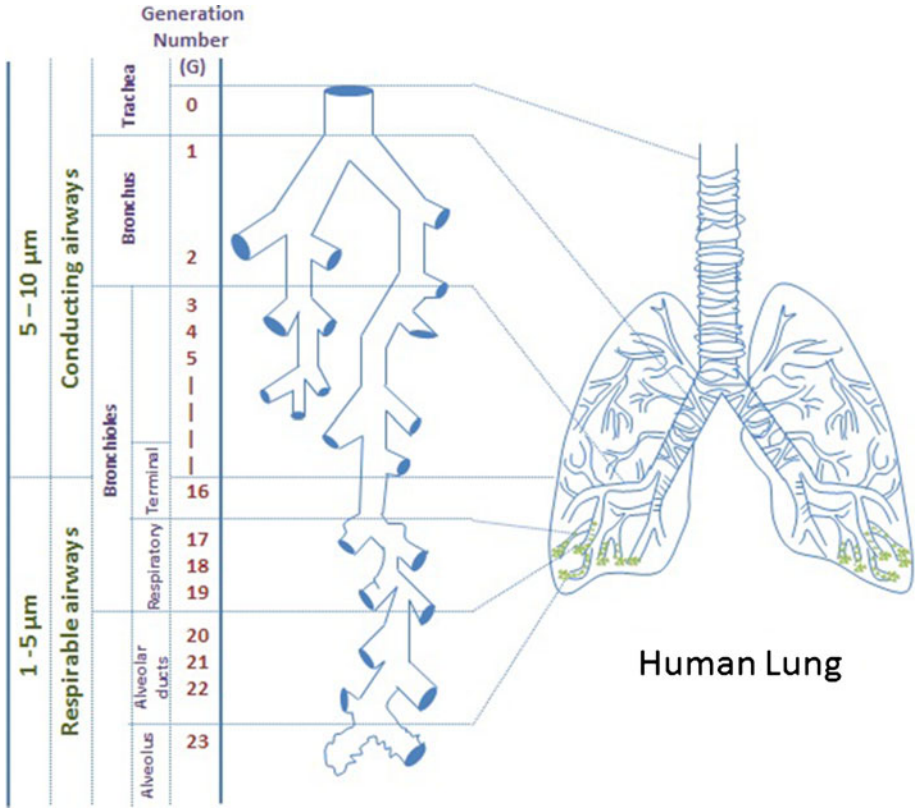

Fig. 1 Diagram of the human lung and particle deposition based on size.

Pulmonary *vs.* Parenteral Vaccine Delivery

In the development of novel anti-tuberculosis vaccines, Ballester M *et al.* demonstrated, that inhaled vaccine compared favorably to the conventional intradermal delivery route. In particular, vaccination with NP-Ag85B and immune-stimulatory oligonucleotide CpG as a Th1-promoting adjuvant via the pulmonary route modified the pulmonary immune response and provided significant protection following a *Mycobacterium tuberculosis (Mtb)* aerosol challenge (31).

Muttil P *et al.* successfully prepared poly lactic-co-glycolic-acid (PLGA) NPs entrapping diphtheria CRM-197 antigen (CrmAg) with a size of 200±50 nm by the emulsification solvent diffusion and double-emulsion methods. The NPs were then spray-dried with L-leucine and the resulting spray-dried powders of formalin-treated/untreated CrmAg nanoaggregates were delivered to the lungs of guinea pigs. This study evaluated the immune response elicited in guinea pigs following pulmonary and parenteral immunizations with the dry powders and the highest titer of serum IgG antibody was observed in guinea pigs immunized by the intramuscular route whereas high IgA titers were observed for dry powder formulations administered by the pulmonary route. This demonstrates that pulmonary immunization with dry powder vaccines leads to a high mucosal immune response in the respiratory tract and sufficient neutralizing antibodies in the systemic circulation to provide protection against diphtheria (32).

An ideal vaccine formulation for mass vaccination would induce the desired immunity upon administration of a single dose. Moreover, it is important to target APCs like DCs to illicit a strong and durable immune response with a single dose aimed at both systemic and mucosal immunity (33).

Dendritic Cells

Dendritic cells (DCs) were first identified in 1868 by Paul Langerhans in the basal layer of the epidermis (34). However, it took more than a century to properly identify them as white blood cells related to macrophages and monocytes, and to understand their importance in the control of immunity (34,35). In 2011, the Nobel Prize in Physiology or Medicine was awarded to Ralph M. Steinman for his discovery of DCs and their role in adaptive immunity paving the way for more research in the field of immunity and vaccines (36). It has become evident over the years that DCs are APCs, true 'professionals' (37) with exceptional capability to internalize, process and present antigens through major histocompatibility complex (MHC) class I and II pathways. DCs induce a strong immune response by activating naïve T-cells which are produced in the bone marrow and have the capability to respond to novel pathogens that have not been processed before (38,39). The role of DCs in initiating a primary immune response has now been shown to be greater than the role played by macrophages and the B-cells (40).

The lung is armed with an intricate network of DCs that can be found throughout the conducting airways, lung interstitium, lung vasculature, pleura, and bronchial lymph nodes (41,42). It is now apparent that there are at least five different subsets of DCs in the murine lung; resident DCs, plasmacytoid DCs, alveolar DCs, inflammatory DCs and interferon-producing killer DCs (41,42). The data for the subsets of DCs in the human lung is rare (43) owing to the need to obtain lung tissue, as they are not found in the bronchoalveolar lavage (BAL) fluid. However, studies on the human AMs are common as they are readily obtained from BAL (44). The AMs are primarily phagocytes with poor APC function and live in the air space, whereas immature DCs have high APC function but lower phagocytic function and live mainly in the interstitium (45). In the human lung, the mucosal surface in the conducting airways consists of ciliated epithelial cells, interspersed goblet cells, macrophages and DCs (46). The DC population in this region is mainly composed of myeloid DCs (mDCs), however, a fraction of plasmacytoid DCs (pDCs) can be found (46). These mDCs have a high capability for antigen uptake but less ability to stimulate the T cells (46). Moreover, the human DCs are generated from haematopoietic stem cells, mDCs from bone marrow–derived monocytic precursors and pDCs from lymphoid progenitors (34). The mDCs and pDCs are activated by a different set of pathogenic stimuli making them functionally distinct reflected by the different expression of cell surface receptors such as Toll-like receptors (TLRs) (34,46). The lung parenchyma consisting of lung interstitium, respiratory and terminal bronchioles, and alveoli is mainly composed of 80% macrophages with rest being DCs and T cells. The 'immature' resident DCs are highly capable of detecting, capturing and processing the encountered antigen (34,46).

The human DCs are identified by over expression of human leukocyte antigen (HLA) DR (major histocompatibility complex class II) with the absence of monocyte, lymphocyte, natural killer cell and granulocyte lineage markers (43). In addition, the specific markers for identifying the mDCs include $CD11c^+$, $CD1a^+$, BDCA-1^+, BDCA-3^+, HLA-DR^+ whereas for the pDCs they are $CD11c^-$, HLA-DR^+, BDCA-2^+ and $CD123^+$ (43,46,47).

Inhaled antigens or antigen particulates are believed to encounter the wide spread DC network that lines the alveolar epithelium and are subsequently taken up by cellular processes extending into the alveolar lining fluid (33). Antigens are then processed and fragments of antigenic peptides are presented on the surface through MHC class I and II pathways for recognition by the T-cell receptors present on T-cells (40). This process is often referred to as antigen

presentation and typically takes place in the regional lymph node after chemokine dependent migration of the antigen loaded DC. Also, APCs perceive danger signals from cells and offer co-stimulatory signals (48) through co-stimulatory molecules present on their surface for recognition by receptors on recirculating T-cells to initiate an immune response in the lymph node (40). Upon encountering the danger signals, immature DCs change to a mature stage where they present the antigen on their surface. This step is usually concurrent with the migration of DCs from peripheral tissue to the lymph node for T-cell activation (Fig. 2). It is believed that soon after antigen presentation, the DCs undergo apoptosis in the lymph nodes (40).

Antigen uptake by DCs occurs by macro-pinocytosis, receptor-mediated endocytosis (macrophage mannose receptor) and/or phagocytosis (49–52). Recent research by Foged *et al.* has shown that both particle size and surface charge of the material to be delivered plays an important role in determining the uptake by human DCs derived from blood. Furthermore, it was recognised that for optimal uptake by DCs the preferred particle size was 0.5 μm (diameter). Uptake of large particles (~ 1 μm) was greatly enhanced when they displayed a positive surface charge (53). In addition, a study conducted by Manolova *et al.* revealed that upon intracutaneous injection of polystyrene beads of varying sizes the large particles (500–2000 nm) associated with DCs from the site of injection and depended

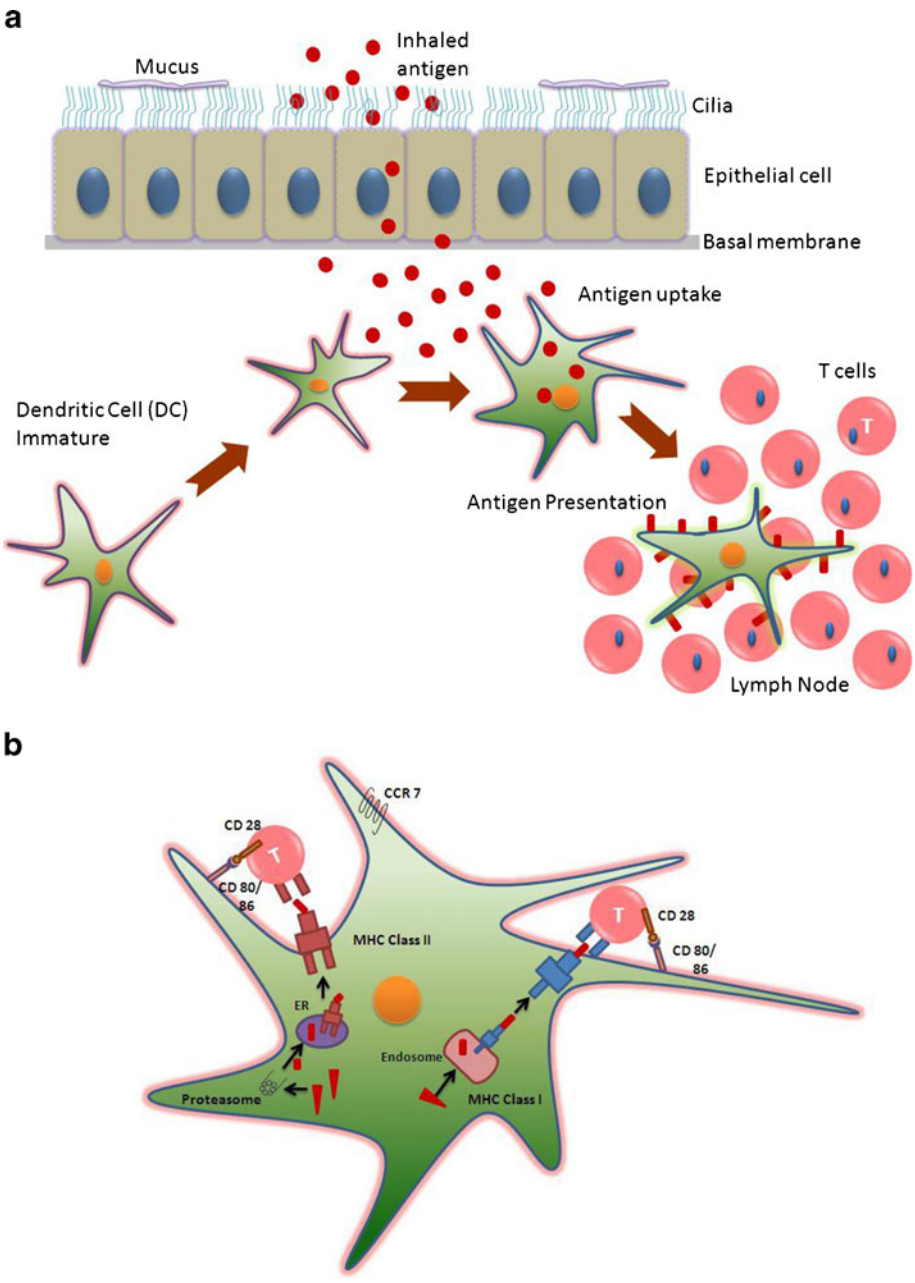

Fig. 2 Antigen uptake and presentation by dendritic cells (DCs) in the airways. (**a**) Upon exposure of an inhaled antigen the immature DCs migrate towards the site of attack. DCs at this stage express a wide variety of receptors (Fc, C-type lectin receptors etc.) and uptake the antigen. Simultaneously, some DCs upregulate the CC-chemokine receptor 7 (CCR7) and migrate towards the lymphatic vessels expressing CC-chemokine ligand 21 (CCL-21) where they are carried to the draining lymph node. After antigen uptake and activation, high amounts of peptide-loaded major histocompatibility complex (MHC) molecules and T-cell co-stimulatory receptors appear on the surface of DCs. The DCs then migrate to the lymph nodes and activate the antigen specific T-cells. (**b**) After antigen uptake, the antigen is either processed through MHC class I (either through endogenous or exogenous pathway) or MHC class II (the antigen is degraded in endosomes and the obtained polypeptide is transported and loaded onto MHC II molecules) and DCs present it on their surface for specific T-cell activation. *ER – Endoplasmic reticulum.

largely on them for cellular transport, whereas small particles (20–200 nm) and virus-like particles (VLPs) (30 nm) drained freely to the lymph nodes (LNs) and were present in LN-resident DCs and macrophages (54). However, this cannot be directly compared to pulmonary delivery as the DCs in the lung differ from those of the skin.

Targeting Antigen to the DC

Antigen can be targeted to DCs, for enhanced immune response, by making particles that bind to the specific receptors expressed on the DC surface (49–51). Effective targeting of vaccines to the DCs results in the possibility of a reduced vaccine dose, less side effects, improved efficacy and enhanced immune response (40).

Vaccines can be targeted to DCs in different ways (40,55–57). DCs contain pattern recognition receptors (PRRs) that aid in detecting the presence of a pathogen through interaction with pathogen-associated molecular patterns. More specifically, C-type lectin receptors (CLRs), a type of PRR, bind to sugar moieties (e.g., mannose, glucan) in a calcium-dependent manner present on the pathogen's surface. This leads to antigen internalization through receptor mediated endocytosis resulting in antigen presentation to T-cells (58,59). Vaccines can also be targeted to DCs with antibodies having an affinity towards specific receptors present on their surface (e.g. anti-DEC205, anti-CD11c), internalization through phagocytosis and conjugation of danger signals that effectively bind to Toll-like receptors (TLRs) or cytokine receptors thereby inducing DC maturation (40,55). Table II lists some formulations that have been effectively targeted to DCs for an enhanced immune response. There are currently no publications that establish targeting of pulmonary DCs through pulmonary delivery of dry powder vaccines.

Nanoparticles for Inhalation

Generally nanoparticles (NPs) are referred to as particles in the size range of 1—100 nm, however for drug delivery NPs larger than 100 nm are required for efficient drug loading, and have been in use for the last 40 years (60). NPs are used as drug carriers either by encapsulating, dissolving, surface adsorbing or chemically attaching the active substance (60). NPs have a large surface area-to-volume ratio and also an increased saturation solubility thus favoring application in the field of drug delivery. In delivery of NPs to the lung by inhalation, deposition takes place through impaction, sedimentation, interception or diffusion (Table III) depending on particle size, density, airflow, breathing rate, respiratory volume and the health of the individual (61,62). These are discussed in greater detail by Smyth HDC *et al.* (63) and definitions are summarized in Table III.

The deposition of particles in the lungs is evaluated using the aerodynamic particle size, which is defined as the diameter of a sphere (density-1 g/cm^3) in air that has the same velocity as the particle in consideration (60). This is defined by the equation

$$d_a = d_g\sqrt{\rho/\rho_a}$$

where ρ is the mass density of the particle, ρ_a is the unit density (1 g/cm^3) and d_g is the geometric diameter.

Particles greater than 10 μm (d_a) in size are commonly impacted in the throat or sedimented in the bronchial region whereas particles less than 1 μm (d_a) in size are exhaled and not likely to be deposited in the alveolar region. It is expected that particles in the size range of 1 to 5 μm (d_a)

Table II Examples of Formulations Targeting Dendritic Cells (DCs)

Formulation	Target	Model drug	Model	Ref
Polyanhydride NPs with dimannose	Mannose receptor CD206	NA	*In vitro*	(58)
MN-decorated PLGA NPs	Mannose receptor CD206	NA	*In vitro*	(121)
PLGA NPs	DEC-205 receptor	Ovalbumin	Mice	(122)
PLGA NPs	Humanized targeting antibody hD1 (DC-SIGN)	FITC-TT/DQ Green BSA	*In vitro*	(123)
PLGA NPs coated with streptavidin	gp120, ManLAM, Lex, aDC-SIGN 1, aDC-SIGN 2, aDC-SIGN 3	DQ-BSA, gp100$_{272\text{-}300}$ and FITC-TT	*In vitro*	(56)
Carbon magnetic NPs (CMNPs)	Endocytosis	Hen egg lysozyme (HEL)	Mice	(124)
Polystyrene and PLGA microparticles	CD40, Fcg, α(v)β3 and α(v)β5	NA	*In vitro*	(125)
Acid degradable particles	DEC-205 receptor	Ovalbumin	Mice	(124)
PAMAM dendrimer	Mannose receptor CD206	Ovalbumin	Mice	(126)
Liposome (with tri-mannose) (L-Phosphatidylcholine + M3-DPPE)	Mannose receptor CD206	FITC-Ovalbumin	*In vitro*	(127)
Niosomes (coated with polysaccharide o-palmitoyl MN)	Mannose receptor CD206	TT	Albino Rats	(128)

M3- DPPE trimannose-dipalmitoylphosphatidylethanolamine, *ManLAM* Mannosylated lipoarabinomannan, *MN* Mannan, *Niosomes* Sorbiton Span 60, cholesterol, stearylamine, *PAMAM* Polyamidoamine, *PLGA* poly lactic-co-glycolic-acid, *TT* Tetanus Toxoid, *NA* Not Applicable

Table III Broad Descriptions of Impaction, Sedimentation, Interception and Diffusion

Impaction	The delivered particles, due to inertia, do not change their path and as the airflow changes with bifurcations they tend to get impacted on the airway surface. This is mostly experienced by large particles and is highly dependent on the aerodynamic properties of the particles.
Sedimentation	The settling down of the delivered particles. This is generally observed in the bronchioles and alveoli.
Interception	This occurs when particles, due to their shape and size, interact with the airway surface and is experienced when the particles are close to the airway wall.
Diffusion	Is the transport of particles from a region of higher concentration to lower concentration, is observed for particles that are less than 0.5 μm in diameter and occurs in the regions where the airflow is low. This is highly dependent on the geometric diameter of the particles.

avoid deposition in the throat and reach the respirable airways (Fig. 1) and the periphery of the lung (61). Particles less than 1 μm (referred to as NPs) are driven by diffusion and are most likely to be exhaled, hence they are therefore often delivered within microparticles. In addition, upon long term storage NPs tend to aggregate due to high particle-particle interactions (60). Microparticles prepared from NPs are typically about 1–5 μm in size and usually also encompass inert pharmaceutical excipients (sugars, amino acids etc.) that act as carriers. The excipients dissolve upon encountering the respiratory environment thereby releasing the NPs.

Different types of NPs have been explored for vaccine delivery and antigenic peptides or proteins are either surface adsorbed or encapsulated within the NPs. Table IV outlines some types of NPs evaluated for vaccine delivery.

This review focuses on polymer-based NPs because they have been extensively investigated as vaccine delivery systems due to their enhanced uptake by phagocytic cells, thereby facilitating antigen internalization and presentation in DCs. In addition, both antigen and materials that augment the immune response (adjuvants) can be encompassed together in nanocomposite microparticles, resulting in their simultaneous delivery (64).

Polymer-Based Nanoparticles

Wide varieties of polymers, both natural and synthetic, have been exploited to form biodegradable NPs. In addition, some of the polymers can act as adjuvants themselves (65). Natural polymers that have been widely investigated for formulating NPs include albumin, alginate, chitosan, collagen, cyclodextrin and gelatin; synthetic polymers include polyesters, polylactides, polyacrylates, polylactones and polyanhydrides (66,67). While natural polymers have a relatively short duration of drug release, synthetic polymers can be tailored to release the drug over days to several weeks allowing the usage of a single dose rather than multiple doses (65).

Biodegradable polymers have gained significant attention for the preparation of NPs for drug delivery and are often favored as they offer several advantages such as controlled or sustained drug release, biocompatibility with the surrounding tissues and cells, low toxicity, are nonthrombogenic and are more stable in the blood (66,68). Biodegradable polymer-based NPs also offer an additional advantage for vaccine delivery systems by acting as adjuvants and aiding in activating both cellular and humoral immune responses (69). It has been

Table IV Examples Of Nanoparticles Currently Being Evaluated For Vaccine Delivery

Nanoparticles	Description	Size	Vaccine	Ref
Micelles (Peptide Cross-linked micelles-PCMs)	PCMs are composed of block copolymers and encapsulate immuno stimulatory DNA in the core and bind peptide antigens through disulphide linkages. In the presence of a high concentration of glutathione they deliver antigenic peptides and immuno stimulatory DNA to APCs	50 nm	HIV peptide vaccine	(129)
Liposomes	Dimyristoyl phosphatyl-choline (DMPC):cholesterol(CH)-(7:3) liposomes were prepared by dehydration-rehydration followed by freezing-thawing method. The enzyme, GUS, was successfully encapsulated and showed encouraging activity following aerosolization	~ 6.4 μm (with 1:4 liposome:mannitol)	β-Gluc-uronidase – enzyme (GUS)	(130)
Polymersomes	poly(g-benzyl-L-glutamate)-K (PBLG50-K) polymersomes were prepared by the solvent removal method and influenza hemagglutinin (HA) was surface adsorbed. When tested *in vivo*, polymersomes acted as an immune adjuvant and showed an improved immunogenicity.	250 nm	influenza hemagglutinin (HA) – subunit vaccine	(131)
Polymer-based	Porous poly-L-lactic acid (PLA) and poly lactic-co-glycolic-acid (PLGA) NPs were prepared by a double-emulsion-solvent evaporation method encapsulating HBsAg and were tested for pulmonary delivery in rat spleen homogenates. The study demonstrated enhanced immune responses.	474–900 nm	hepatitis B surface antigen (HBsAg)	(24)

reported that upon phagocytosis by APCs, such as DCs, these NPs release the antigen intercellularly and elicit CD8+ and CD4+ T cell responses (70).

In a study performed by Bivas-Benita M *et al.*, the potential of enhanced immunogenicity upon pulmonary delivery of DNA encapsulated in chitosan NPs was evaluated. Chitosan-DNA NPs were prepared by the complexation-coacervation method and the resultant DNA-loaded NPs had an average size of 376± 59 nm (n=5), zeta-potential of 21±4 mV (n=5) and a loading efficiency of 99%. Pulmonary administration of the chitosan-DNA NPs was shown to induce increased levels of IFN-γ secretion compared to pulmonary delivery of the plasmid in solution via the intramuscular immunization route. This indicates the plausibility of achieving pulmonary delivery of DNA vaccines with increased immunogenicity against tuberculosis compared to immunization through intramuscular route (71).

The polylactides PLA and PLGA are the most broadly investigated synthetic polymers in the field of drug delivery (66,67,72). These are rapidly hydrolyzed upon implantation into the body and are eventually removed by the citric acid cycle. The hydrolyzed products form at very slow rate and include lactic acid and glycolic acid which are biologically compatible and easily metabolized making them safe and non-toxic (66,73). However, the acidic degradation products can cause problems by eliciting inflammation and also a reduction in pH within the microparticles resulting in the hydrolysis of the biopharmaceuticals (74).

Muttil *et al.* prepared novel NP-aggregate formulations using poly(lactic-co-glycolic acid) (PLGA) and recombinant hepatitis B surface antigen (rHBsAg) and showed that the dry powder formulations elicited a high mucosal immune response after pulmonary immunization of guinea pigs without the need for adjuvants. They prepared three different formulations of dry powders by spray-drying with leucine, (1) rHBsAg encapsulated within PLGA/polyethylene glycol (PEG) NPs (antigen NPs, AgNSD), (2) a physical mixture of rHBsAg and blank PLGA/PEG NPs (antigen NP admixture (AgNASD), and (3) rHBsAg encapsulated in PLGA/PEG NPs with free rHBsAg (antigen NPs plus free antigen). All the particles had mass median aerodynamic diameters (MMAD) of around 4.8 μm and a fine particle fraction (FPF) of 50%. After immunization the highest titre of serum IgG antibodies was observed in the control group immunized with alum adsorbed with rHBsAg (Alum Ag) (IM route) whereas the highest IgA titres were observed for animal groups immunized with powder formulations via the pulmonary route. It was also noteworthy, guinea pigs immunized with AgNASD dry powder exhibited IgG titers above 1,000 mIU/ml in the serum (required 10 mIU/ml) suggesting the potential of administering novel dry powder formulations via the pulmonary route (75).

Recently a new class of biodegradable polymers, polyketals, have been developed and are largely being investigated for drug delivery purposes (76,77). This class of polymers have non-acidic degradation products and pH-sensitive ketal linkages in their backbone. These polyketals offer several advantages for vaccine delivery such as exhibiting pH-dependent hydrolysis but yet are degradable in acidic phagolysosomes. Polyketal copolymers degrade into biocompatible small molecules minimizing inflammation compared to PLGA. An aliphatic polyketal, poly(cyclohexane-1,4-diyl acetone dimethylene ketal) (PCADK) degrades into acetone and 1,4-cyclohexanedimethanol which are both biocompatible, and has a hydrolysis half-life of 24 days at pH 4.5 (77). This was later modified to a co-polyketal termed PK3 synthesized from 1,4-cyclohexanedimethanol and 1,5-pentanediol with a hydrolysis half-life of 1.8 days at pH 4.5 (64) making it much suitable for vaccine delivery.

Heffernan MJ and Murthy N successfully prepared acid-sensitive polyketal NPs that released the loaded therapeutics in the acidic environments of tumors, inflammatory tissues and phagosomes. Polyketal NPs, 280–520 nm in diameter, were prepared by an oil-in-water (O/W) emulsion method using poly(1,4-phenyleneacetone dimethylene ketal) (PPADK), a new hydrophobic polymer that undergoes acid-catalysed hydrolysis into low molecular weight hydrophilic compounds. (76). Heffernan *et al.* used polyketal PK3 to formulate a model vaccine that elicits CD8+ T cell responses. PK3 microparticles encapsulating ovalbumin (OVA), poly(inosinic acid)–poly(cytidylic acid) (poly(I:C)) - a TLR3 (Toll like receptor) agonist and a double-stranded RNA analog were prepared using single emulsion method. PK3-OVA-poly(I:C) microparticles (1–3 μm) at a dosage of 0.01 μg/mL were then supplied to murine splenic DCs and a higher percentage of IFNγ-producing CD8+ T cells, TNF-α and IL-2 production in CD8+ T cells were observed than with DCs treated with PK3-OVA particles or soluble OVA/poly(I:C) implying polyketal PK3 microparticles have potential for vaccine delivery (64).

Preparation of Polymer-Based Nanoparticles

Different methods have been employed to synthesize polymer-based NPs depending on the subsequent application and type of drug. Polymer-based NPs can either encapsulate or surface adsorb the drug (68,78). Here we review some of the most widely used methods to prepare polymer-based NPs. However, a more detailed review and analysis of these methods can be found at Reis P *et al.* (78) and Avnesh K *et al.* (68).

Emulsification/Solvent Evaporation and Nanoprecipitation. Emulsification/solvent evaporation, also referred to as solvent emulsion–evaporation, involves the emulsification of an organic polymer solution into an aqueous phase followed by the evaporation of the organic solvent (78). The polymer with or without the drug is dissolved in a volatile organic solvent like acetone, ethyl acetate, chloroform or dichloromethane etc. and is then transferred into stirring aqueous

phase with or without the presence of an emulsifier or stabilizer. This emulsion is then sonicated to evaporate the organic solvent and form NPs (68) (Fig. 3a). The size of the resultant particles can be controlled by varying the type, viscosity and amount of organic and aqueous phases, stir rate and temperature (78).

Singh J *et al.* prepared diphtheria toxoid (DT) loaded poly-(ε-caprolactone) (PCL) NPs via a double emulsification solvent evaporation method (w/o/w) for investigating their potential as a mucosal vaccine delivery system. Briefly, DT was added to the internal aqueous phase containing 0.25 ml 10%w/v polyvinyl alcohol (PVA). The solution was emulsified with the organic phase comprising 100 mg of PCL in 5 mL of dichloromethane (DCM), using a homogenizer at 12,000 rpm for 2 min. The formulations were then stirred magnetically at ambient temperatures and pressure for 15–18 h to allow solvent evaporation and NP formation. The resultant NPs were approximately 267 ± 3 nm in size with a zeta-potential of −2.6 ± 1.2 mV. Also, the PCL NPs induced DT serum specific IgG antibody responses significantly higher than PLGA (79).

The nanoprecipitation method is a single step method which is usually employed for entrapping hydrophobic drug moieties. In this method, the drug and the polymer are dissolved in a water-miscible solvent, such as acetone, acetonitrile or methanol (80). This organic phase is then added drop-wise to an aqueous phase with or without an emulsifier/stabilizer under magnetic stirring (68). NPs are formed due to rapid solvent diffusion and the solvent is finally removed from the emulsion under reduced pressure (81) (Fig. 3b).

Lee JS *et al.* prepared poly(ethylene glycol)-poly(ε-caprolactone) (MPEG-PCL) NPs via a nanoprecipitation method. Firstly, a predetermined concentration of MPEG-PCL block copolymer was dissolved in 10 mL of organic solvent (acetone, acetonitrile or THF). This polymer solution was then added drop wise into deionized water (100 mL) under magnetic stirring. The organic solvent was then evaporated under reduced pressure using a rotary evaporator, and the resultant NPs were isolated from the aqueous solution. Using different organic solvents and concentrations of polymer yielded NPs particles between ~50 to 150 nm (82).

Emulsification and Solvent Displacement. The emulsification and solvent displacement method is also known as emulsification solvent diffusion. This method involves the precipitation of the polymer from an organic solution and subsequent diffusion of the organic solvent into an aqueous phase (78). The solvent that aids in the formation of emulsion must be miscible with water. For example, the organic polymer solution can be added to an aqueous phase, which often contains a stabilizer, under strong stirring. Upon the formation of the emulsion (O/W), a large quantity of water is added so as to dilute it favoring the diffusion of additional organic solvent from the dispersed droplets. This process leads to the precipitation of the polymer (81). An interfacial turbulence is created between the two phases as the solvent diffuses resulting in the formation of smaller particles and is believed that as the water-miscible solvent concentration increases the NPs tend to acquire a smaller size (80) (Fig. 3c).

Ranjan AP *et al.* have recently prepared biodegradable NPs containing indocynanine green (ICG) using chitosan modified poly(L-lactide-co-epsilon-caprolactone) (PLCL): poloxamer (Pluronic F68) blended polymer by an emulsification solvent diffusion technique. PVA and chitosan were used as stabilizers in the process of making the NPs. The average particle size of the resultant NPs was between 146 ±

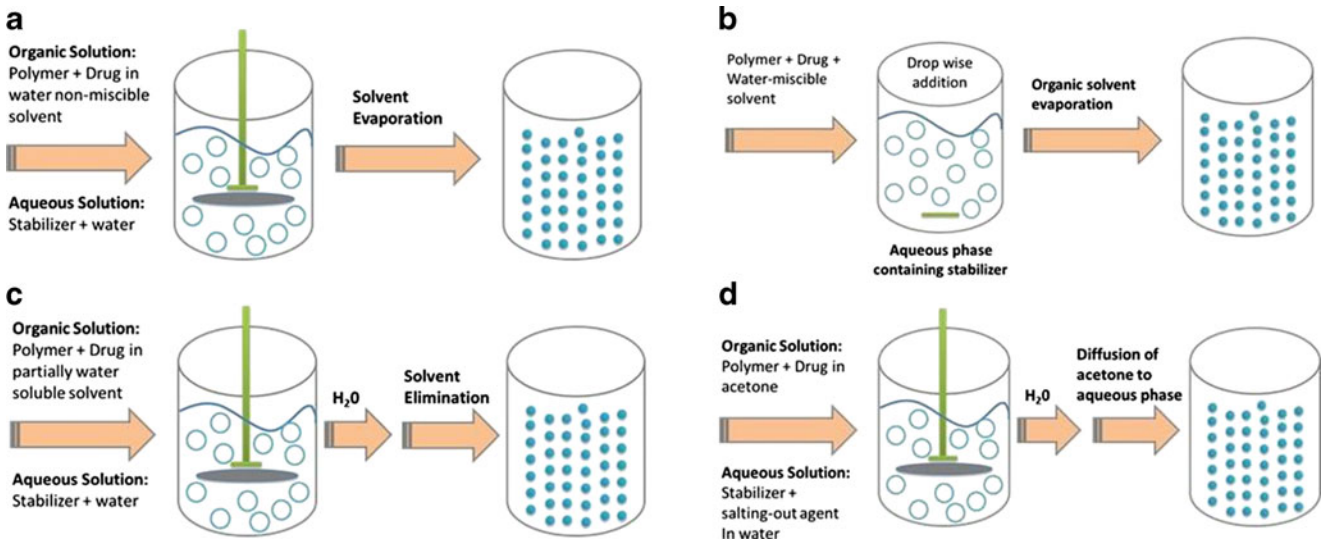

Fig. 3 Schematic representation of (**a**) emulsification/solvent evaporation technique, (**b**) emulsification and solvent displacement technique, (**c**) salting-out technique and (**d**) nanoprecipitation technique.

3.7 to 260±4.5 nm and the zeta potential progressively increased from −41.6 to +25.3 mV with increasing amounts of chitosan (83).

Salting Out. The salting out method is based on the separation of a water-miscible organic phase from an aqueous solution by adding salting out agents (78,80,84). Briefly, the polymer is dissolved in a water-miscible organic solvent such as acetone or tetrahydrofuran (THF) which is then added under strong stirring to an aqueous solution containing salting out agents (for example magnesium chloride, calcium chloride) and an emulsifier or stabilizer to form an O/W emulsion (80,81,85). This O/W emulsion is diluted by adding a large volume of water under mild stirring thus reducing the salt concentration/ionic strength and favouring the movement of the water-miscible organic solvent into the aqueous phase. This process leads to the formation of nanospheres and as a final step the NPs formed are freed from the salting out agents either by centrifugation or cross-flow filtration (80) (Fig.3d).

Konnan YN *et al.* prepared sub-200 nm NPs using a salting out method. Typically, a solution of PLGA and PLA in THF was added under mechanical stirring to an aqueous phase containing PVA and magnesium chloride hexahydrate ($MgCl_2.6H_2O$) as a salting out agent forming an O/W emulsion. To this, a large volume of water was added favoring migration of the water-miscible organic solvent into the aqueous phase forming NPs which were later purified by cross flow filtration (86).

Table V lists some of the advantages and disadvantages of nanoparticle preparation methods (77).

Encapsulation or Adsorption

A high loading capacity is one of the most desired qualities of NP-based vaccines. The main advantage of having a high loading capacity is that the amount of polymer required to carry the drug/vaccine is reduced (81) hence minimizing any toxic effects from the polymer. Drugs/vaccines can be loaded into or onto NPs using two approaches (Fig. 4) (87). The first is encapsulation where the drug/vaccine is incorporated into the NP at the time of preparation; the second is adsorption where the drug/vaccine is either chemically or physically adsorbed onto the NP after preparation.

It is important to note that the chemical structure of the drug/vaccine, the polymer and the conditions of drug loading influence the amount of drug/vaccine bound to the NPs and the type of interactions that occur between them (81). In addition, the encapsulation or adsorption of a drug/vaccine depends on the disease to be treated or prevented, route of administration, manufacturing feasibility and economic challenges.

Bivas-Benita M *et al.* prepared PLGA–polyethyleneimine (PEI) NPs by an interfacial deposition (88) method. The resultant NPs were loaded with Mycobacterium tuberculosis (Mtb) Antigen 85B (Ag85B) by adding the NP suspension to 25 μg/mL DNA plasmid solution. The characterization studies revealed that the particle size increased from 235 to 275 nm when resuspended in water and 271 nm in saline with the mean zeta potential increase from +38.8 mV to +40.6 mV respectively. The NPs greatly stimulated human DCs resulting in the secretion of IL-12 and TNF-α at comparable levels to that observed after stimulation using lipopolysaccharide (LPS) (89).

Biodegradable polymer-based NPs have been widely explored and appear to be well tolerated when administered into the body. These NPs have gained significant attention and are being accepted as effective delivery systems with the development of NP based vaccines (90,91). In addition, the NP based vaccines need to be formulated appropriately, as dry powders and at low cost to help achieve effective mass vaccination.

Adjuvants

Modern day vaccines contain pure recombinant or synthetic antigens that are less immunogenic than live or killed whole organism vaccines. Thus, in order to obtain a strong immune response upon administration of antigen and provide long term protection against the infection, adjuvants are included within the formulation (92). Adjuvants are substances used in combination with an antigen to produce a stronger and more robust immune response than the antigen alone (93). Adjuvants also provide a depot for the

Table V Advantages and Disadvantages of Nanoparticle Preparation Methods

Method	Advantages	Disadvantages
Emulsification/Solvent Evaporation	Hydrophilic and hydrophobic drugs can be encapsulated	Agglomeration of nanodroplets during evaporation
Emulsification and Solvent Displacement	Control over the size of nanoparticles	Possibility of water-soluble drug leaking into the external aqueous phase, Large amounts of water to be removed
Salting Out	High loading efficiency, Easy scale-up	Removal of electrolytes, Incompatibility of salting-out agents with drugs
Nanoprecipitation	Simple, fast and reproducible, Easy scale-up, Low surfactant concentrations required	Less polymer in the organic phase

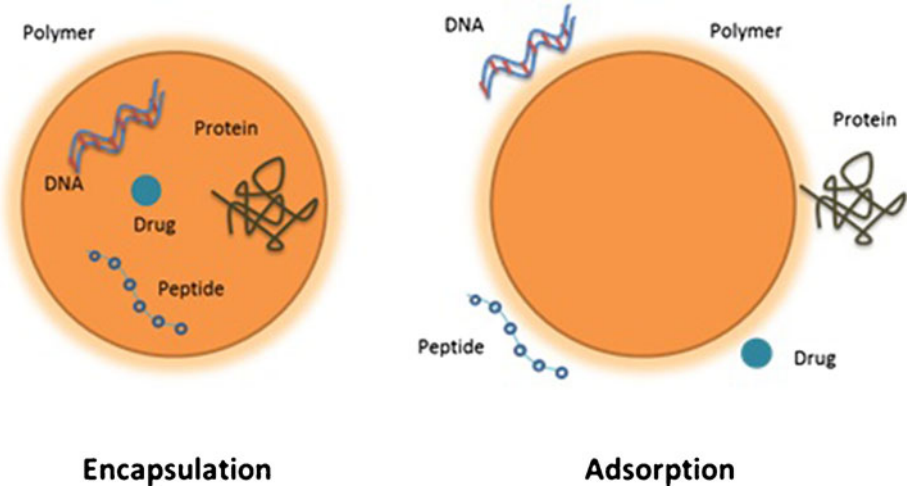

Fig. 4 The molecule of interest (DNA/Drug/Peptide/Protein) is either encapsulated *(Left)* within or surface adsorbed *(Right)* onto the polymer-based nanoparticle.

antigen favoring a slow release, reduce the dose of antigen required to generate a strong immune response, modulate the immune response, aid in targeting the APCs, and provide danger signals helping the immune system respond to the antigen (92–94). The selection of an adjuvant depends on the antigen, delivery system, route of administration and possible side-effects. However, an ideal adjuvant should have a long shelf life and be safe, stable, biodegradable, economical and should not induce an immune response against themselves (92).

Despite massive efforts over nearly 90 years into the research and development of adjuvants, the list of adjuvants that are clinically approved is short. The prime reason being their safety coupled with limited data on the predictability of safety using available animal models (95). The serious adverse events in the recent clinical trials of Merck's (96) and Novartis's (NCT00369031) (97) HIV vaccines using adenovirus- and toxin-based adjuvanted delivery systems has moved the research into further investigations in developing nutritive adjuvanted delivery systems (Vitamins A, C, D, E, flavonoids and plant oils). These may prove safer in clinical trials (98,99). Table VI lists adjuvants in development or licensed for human use.

Alum salts have a well-established safety record, are the most widely used human adjuvants and are used as standards to assess other adjuvants (92,93,95,100). Despite their wide use their mechanism is poorly understood and thus rarely induce human responses (92).

Wee JLK *et al.* used a sheep animal model to evaluate the delivery of ISCOMATRIX adjuvanted influenza vaccine via its mucosal site of infection for improved vaccine effectiveness. Upon pulmonary immunization with low antigen doses (0.04 μg) of adjuvanted influenza equivalent serum antibody levels were induced when compared to an almost 375-fold higher dose (15 μg) unadjuvanted influenza delivered subcutaneously suggesting the successful use of this combination for improved protection (101).

DRY POWDER PREPARATION TECHNIQUES

The use of liquid suspensions of NPs are often accompanied by several disadvantages such as particle aggregation and sedimentation leading to physico-chemical instability, reduced or loss of biological activity of the drug, contamination, and hydrolysis leading to degradation of the polymer (102). To overcome these problems, preparations can be stored and transported in a dry form (102). In addition, for vaccines, the delivery of a dry powder by inhalation has the potential benefits of a) increased stability during transport and administration, b) increased safety by eliminating contamination risks and c) improved cost-effectiveness (103). The most commonly used methods for transforming liquid preparations into dry powders are freeze-drying, spray-drying, spray-freeze-drying and the use of super critical fluid technologies. Each of these methods has advantages and disadvantages and are selected depending on the desired attributes such as narrow particle size

Table VI List of Adjuvants in Either Development, Testing or for Human Use

Category	Examples
Mineral Salts	Aluminium hydroxide (Alum)
	Potassium aluminium sulphate
	Aluminium phosphate
Oil emulsions	MF59
Particulate adjuvants	Virosomes
	ISCOMS (Immuno stimulating complexes)
Microbial derivatives	Monophosphoryl lipid A-MPL$^{(TM)}$
Plant derivatives	QS-21 (Saponin)
	ADVAX
Miscellaneous	AS04 (liposome formulation containing MPLA & QS-21), polymeric adjuvants, CpG oligodeoxynucleotides, vitamins

distribution, improved bioavailability, enhanced stability, improved dispersibility and controlled release (104,105).

Freeze-Drying

Freeze-drying, also known as lyophilisation, is commonly used in industry to ensure long term stability and preservation of the original properties of various biological products such as viruses, vaccines, proteins, peptides and their carriers; NPs and liposomes (102,106). This process comprises of removing water from a frozen sample by sublimation and desorption under vacuum (106) and can be divided into three steps: freezing (solidification), primary drying (ice sublimation) and secondary drying (desorption of unfrozen water) (102). However, this process is relatively slow, very expensive and generates various stresses on the biological product during both the freezing and drying steps (106). Protectants in the form of excipients are usually added to stabilize the products, avoid aggregation and to ensure acceptable tonicity and reconstitution (106,107). Sugars such as glucose, sucrose, trehalose, mannitol, lactose, dextran or maltose with or without surfactants such as poly(vinyl) alcohol or poloxamer 188 are often employed as protectants to stabilize the product and prevent coalescence (107,108). The concentration and the NP/sugar mass ratio also play an important role in determining the stability and long term storage of the final product (102). Anhorn MG *et al.* evaluated the effect of different concentrations of sucrose, mannitol and trehalose as cryoprotectants on the physico-chemical characteristics of resulting NPs by analyzing the appearance, particle-size and polydispersity index (107). Long term stability studies indicated that the absence of cryoprotectants led to particle growth whereas their presence reduced aggregation. Particles freeze-dried with sucrose and trehalose at 2% and 3%w/v had more controlled particle size and these sugars appeared to be superior to mannitol at similar concentrations (107).

Spray-Drying

Spray-drying is a one-step preparation of dry powders. It is a process that converts liquid feed (solution, suspension or colloidal dispersion) into dry particles (109). The process can be divided into four parts (110): atomization (1), spray-air contact (2), drying (3) and separation (4). The liquid feed is atomized *(1)* to break the liquid into droplets and this spray form comes into contact with a hot gas *(2)*, causing rapid evaporation of the droplets to form dry particles *(3)*. The dry particles are then separated from the hot gas with the help of a cyclone *(4)* (105). Compared to particles obtained from micronization using milling, spray-dried particles are more spherical and have a homogenous size-distribution resulting in a higher respirable fraction which is advantageous for pulmonary delivery (105). In addition, spray-drying has the advantage of being; simple, easily scalable, cost-effective, suitable for heat-sensitive products and enables high drug loading (110). An economically acceptable yield can now be achieved with the fourth and newest generation of laboratory-scale spray dryer developed by Büchi, the Nano Spray Dryer B-90. This nano spray dryer can generate particles of size ranging from 300 nm to 5 μm for milligram sample quantities at high yields (up to 90%) (111). However, there is a chance of degradation of macromolecules during the process due to high shear stress in the nozzle and thermal stress while drying (105). Fourie PB *et al.* (21) describes the challenges such as thermal stress, osmotic stress, and scalability involved with spray-drying of vaccines. Fourie PB *et al.* formulated a dry powder TB vaccine for delivery to the lung by preparing *Mycobacterium bovis* Bacillus Calmette–Guérin (BCG) spray-dried particles which, when administered into *M. tuberculosis* infected guinea-pigs, resulted in enhanced immunogenicity levels compared to an equal dose injected subcutaneously into control animals (21).

Spray-Freeze-Drying

Spray-freeze-drying (SFD) is a drying process that usually involves atomization, rapid freezing and lyophilisation (112). A solution containing the drug is sprayed into a vessel that contains a cryogenic liquid such as nitrogen, oxygen or argon. As the boiling temperatures of these cryogenic liquids are very low they cause the droplets to freeze instantly. The resulting droplets are then collected and lyophilized to obtain porous dry powder particles suitable for respiration (105). The advantage of SFD is the ability to produce particles with adjustable sizes (112) and as it is conducted at sub-ambient temperature, thermolabile polymers and highly potent biopharmaceuticals can be formulated into dry powder products (105). However, the major disadvantage of this technique is the stresses associated with freezing and drying, which may cause irreversible damage to proteins (113). This is displayed as structural denaturation, aggregation and loss of biological activity upon rehydration (105). In addition, loss of stability due to unfolding and aggregation remains a major challenge (113) and also the method has low process efficacy, is time consuming, and expensive (114).

Amorij J-P *et al.* showed that an influenza subunit vaccine powder prepared by SFD using oligosaccharide inulin as a stabilizer and delivered via the pulmonary route to BALB/c mice induced systemic humoral (IgG), cell-mediated (Il-4, IFN-γ) and mucosal immune responses (IgA, IgG). Whereas vaccination with a liquid subunit vaccine via either pulmonary or intramuscular route induced only systemic humoral (IgG) immune responses suggesting that powder vaccine formulations could be beneficial for immunization (23).

Supercritical Fluid Technology

Supercritical fluids (SCF) are compressed gases or liquids above their critical temperatures (Tc) and pressures (Pc), and possess

several advantages of both gases and liquids (105). The density and thus solvating power can be controlled by varying the temperature and pressure. SCF can be prepared using carbon dioxide (CO_2), water, propane, acetone, nitrous oxide (N_2O), trifluoromethane, chlorodifluoromethane, diethyl ether, water, or CO_2 with ethanol (114). However, because of its accessible critical point at 31°C and 74 bar, its low cost and non-toxicity, CO_2 is the most widely used solvent in SCF. In addition, its low critical temperature makes supercritical (SC) CO_2 suitable for handling heat-labile solutes at conditions close to room temperature. Therefore, SC CO_2 has potential as an alternative to conventional organic solvents for use in solvent-based processes for forming solid dosage forms (105).

There are two major principles for particle precipitation with supercritical fluids. One employs SCF as a solvent and the other as an antisolvent (115). In the first, the drug is dissolved in the SCF followed by sudden decompression, after which the solution is passed through an orifice and rapidly expanded at low pressure. Rapid Expansion of a Supercritical Solution (RESS) employs this principle (114). In the second process, the solute is insoluble in SCF and hence utilizes SCF as an antisolvent. A solute is dissolved in an organic solvent and then precipitated by the SCF (antisolvent). Precipitation occurs when the SCF is absorbed by the organic solvent followed by expansion of the liquid phase and a decrease in the solvation power leading to particle formation. The Gas Anti-Solvent (GAS), Aerosol Solvent Extraction System (ASES), Supercritical Fluid Antisolvent (SAS), Precipitation with Compressed Antisolvent (PCA), Solution Enhanced Dispersion by Supercritical Fluids (SEDS), and supercritical fluid extraction of emulsion (SFEE) are the processes that employ this second principle (114). Using these techniques, particles can be formed in a well-ordered fashion to achieve the desired morphology and any negative effects on the macromolecules can be minimized (105,113). Thorough discussions of these techniques including their advantages and disadvantages have been recently published by Al-fagih I *et al.* (114) and elsewhere (105,113,115–118).

The fine powders produced via SCF precipitation are often less charged than those produced mechanically allowing them to flow more freely and thus to be more easily dispersed from a DPI. In addition, SCF processes allow the production of inhalable particles that are more uniform in terms of crystallinity, morphology, particle-size distribution and shape than those produced via jet milling. In spite of its potential, SCF is still classified as an emerging technology that is still to be exploited in DPI products; with concerns being raised over the potential denaturing effects of the solvents/antisolvents used in this process (105). Amidi M *et al.* prepared diphtheria toxoid (DT) containing microparticles using a supercritical fluid (SCF) spraying process and obtained dry powder microparticles with a median volume diameter between 2 and 3 μm. Pulmonary immunization of guinea pigs with DT-TMC (N-Trimethyl chitosan) microparticles resulted in a strong immunological response as reflected by the induction of IgM, IgG, IgG1 and IgG2 antibodies comparable to or significantly higher than those achieved after subcutaneous (SC) administration of alum-adsorbed DT demonstrating an effective new delivery system for pulmonary administered DT antigen (119).

Table VII highlights some recent studies that have employed various dry powder preparation techniques and the subsequent evaluation for vaccine delivery.

CONCLUSION

Pulmonary administration has gained significant attention in the recent years as a potential non-invasive route for vaccines, and has also shown great promise as an effective means of vaccination. Much of the success is due to the lung's large surface area (80 sq. m), and rich blood supply leading to rapid absorption coupled with an abundance of

Table VII Recent Studies on Dry Powder Particle-Based Vaccine Delivery

Disease	Antigen	Carrier/Stabilizer	Dry Powder Preparation	Size (μm)	Model	Ref
Bacterial Infections	Bacteriophages	Trehalose, Leucine	SD	2.5–2.8	NA	(132)
Diptheria	Diptheria Toxoid	Chitosan	SCF	3–4	GP	(119)
Diptheria	Diphtheria CRM-197 antigen	L-leucine	SD	~ 5	GP	(32)
Hepatitis B	Recombinant hepatitis B surface antigen (rHBsAg)	Leucine	SD	4.8	GP	(75)
Influenza	Influenza monovalent	Inulin	SD, SFD	2.6 (SD), 10.5 (SFD)	M	(133)
Influenza	Influenza subunit	Inulin	SFD	~ 10	M	(23)
Tuberculosis	Ad35-vectored tuberculosis (TB) AERAS-402	Mannitol-cyclodextrin-trehalose-dextran, MCTD	SD	3.2–3.5	NA	(134)
Tuberculosis	Bacille Calmette-Guerin (BCG)	Leucine	SD	2–3	GP	(135)
Tuberculosis	Recombinant antigen 85B (rAg85B)	NA	SD	2.8	GP	(136)

SD Spray drying, *SFD* Spray-freeze drying, *SCF* Supercritical Fluid; *M* Mice, *GP* Guinea Pigs; *NA* Not Applicable

local APCs that present antigen in a way to induce both mucosal and systemic immune response. Recent progress in targeting vaccines specifically to DCs for an enhanced immune response with low doses has paved way for developing new vaccine technology. Polymer-based NPs offer the advantage of biodegradabiltiy, avoiding antigen degradation if encapsulated and through chemical attachments can target DCs. However, more research is needed to understand the fate of NPs after inhalation, their interaction with the biological cells and their toxicity (nanotoxicity). The method of formulation of NP based vaccines into dry powders is of equal importance as it provides the opportunity to maintain the stability and integrity of the antigen, ease of transport and administration. The right combination of polymer chemistry, polymer-based NPs, immunology, dry powder technology, delivery device and animal models will lead to the discovery of next generation of vaccine delivery systems.

REFERENCES

1. Brown LR. Commercial challenges of protein drug delivery. Expet Opin Drug Deliv. 2005;2:29–42.
2. Sullivan VJ, Mikszta JA, Laurent P, Huang J, Ford B. Noninvasive delivery technologies: respiratory delivery of vaccines. Expet Opin Drug Deliv. 2006;3:87–95.
3. Sou T, Meeusen EN, de Veer M, Morton DAV, Kaminskas LM, McIntosh MP. New developments in dry powder pulmonary vaccine delivery. Trends Biotechnol. 2011;29:191–8.
4. Galindo-Rodriguez S, Allémann E, Fessi H, Doelker E. Physicochemical parameters associated with nanoparticle formation in the salting-out, emulsification-diffusion, and nanoprecipitation methods. Pharm Res. 2004;21:1428–39.
5. Rossi S, Sandri G, Caramella C. Buccal delivery systems for peptides: recent advances. Am J Drug Deliv. 2005;3:215–25.
6. Shojaei AH, Chang RK, Guo X, Burnside BA, Couch RA. Systemic drug delivery *via* the buccal mucosal route. Pharm Tech:70–81 (2001).
7. Kumria Rand GG. Emerging trends in insulin delivery: Buccal route. J Diabetol. 2011;2:1–9.
8. Ozsoy Y, Gungor S, Cevher E. Nasal delivery of high molecular weight drugs. Molecules. 2009;14:3754–79.
9. Patel VF, Liu F, Brown MB. Advances in oral transmucosal drug delivery. J Control Release. 2011;153:106–16.
10. Kalluriand H, Banga A. Transdermal delivery of proteins. AAPS PharmSciTech. 2011;12:431–41.
11. Carstens MG. Opportunities and challenges in vaccine delivery. Eur J Pharm Sci. 2009;36:605–8.
12. Maurice J, Davey S. State of the world's vaccines and immunization. http://www.unicef.org/media/files/SOWVI_full_report_english_LR1.pdf (accessed 17/02/2012 2012).
13. W.H. Organization. World Health Statistics 2011 in WHO Statistical Information System (WHOSIS). http://www.who.int/whosis/whostat/2011/en/index.html (accessed 17/04 2012).
14. Blank F, Stumbles P, von Garnier C. Opportunities and challenges of the pulmonary route for vaccination. Expet Opin Drug Deliv. 2011;8:547–63.
15. Holmgren J, Czerkinsky C. Mucosal immunity and vaccines. Nat Med (2005).
16. Labiris NR, Dolovich MB. Pulmonary drug delivery. Part II: The role of inhalant delivery devices and drug formulations in therapeutic effectiveness of aerosolized medications. Br J Clin Pharmacol. 2003;56:600–12.
17. Sanders M. Inhalation therapy: an historical review. Prim Care Respir J. 2007;16:71–81.
18. Mack GS. Pfizer dumps Exubera. Nat Biotech. 2007;25:1331–2.
19. Onoue S, Hashimoto N, Yamada S. Dry powder inhalation systems for pulmonary delivery of therapeutic peptides and proteins. Expert Opin Ther Pat. 2008;18:429–42.
20. de Swart RL, LiCalsi C, Quirk AV, van Amerongen G, Nodelman V, Alcock R, *et al.* Measles vaccination of macaques by dry powder inhalation. Vaccine. 2007;25:1183–90.
21. Fourie P, Germishuizen W, Wong Y-L, Edwards D. Spray drying TB vaccines for pulmonary administration. Expert Opin Biol Ther. 2008;8:857–63.
22. LiCalsi C, Maniaci MJ, Christensen T, Phillips E, Ward GH, Witham C. A powder formulation of measles vaccine for aerosol delivery. Vaccine. 2001;19:2629–36.
23. Amorij JP, Saluja V, Petersen AH, Hinrichs WLJ, Huckriede A, Frijlink HW. Pulmonary delivery of an inulin-stabilized influenza subunit vaccine prepared by spray-freeze drying induces systemic, mucosal humoral as well as cell-mediated immune responses in BALB/c mice. Vaccine. 2007;25:8707–17.
24. Thomas C, Rawat A, Hope-Weeks L, Ahsan F. Aerosolized PLA and PLGA Nanoparticles Enhance Humoral. Mucosal and Cytokine Responses to Hepatitis B Vaccine. Mol Pharm. 2010;8:405–15.
25. Effros RM. Anatomy, development, and physiology of the lungs. GI Motility online. 1: (2006).
26. Kleinstreuer C, Zhang Z, Li Z. Modeling airflow and particle transport/deposition in pulmonary airways. Respir Physiol Neurobiol. 2008;163:128–38.
27. Kleinstreuer C, Zhang Z, Donohue JF. Targeted drug-aerosol delivery in the human respiratory system. Annu Rev Biomed Eng. 2008;10:195–220.
28. Gehr P. Annexe A. Anatomy and morphology of the respiratory tract. Ann ICRP. 1994;24:121–66.
29. Scheuch G, Kohlhaeufl MJ, Brand P, Siekmeier R. Clinical perspectives on pulmonary systemic and macromolecular delivery. Adv Drug Deliv Rev. 2006;58:996–1008.
30. Shen X, Lagergård T, Yang Y, Lindblad M, Fredriksson M, Holmgren J. Systemic and Mucosal Immune Responses in Mice after Mucosal Immunization with Group B Streptococcus Type III Capsular Polysaccharide-Cholera Toxin B Subunit Conjugate Vaccine. Infect Immun. 2000;68:5749–55.
31. Ballester M, Nembrini C, Dhar N, de Titta A, de Piano C, Pasquier M, *et al.* Nanoparticle conjugation and pulmonary delivery enhance the protective efficacy of Ag85B and CpG against tuberculosis. Vaccine. 2011;29:6959–66.
32. Muttil P, Pulliam B, Garcia-Contreras L, Fallon J, Wang C, Hickey A, *et al.* Pulmonary immunization of Guinea Pigs with diphtheria CRM-197 antigen as nanoparticle aggregate dry powders enhance local and systemic immune responses. AAPS J. 2010;12:699–707.
33. Alpar HO, Somavarapu S, Atuah KN, Bramwell VW. Biodegradable mucoadhesive particulates for nasal and pulmonary antigen and DNA delivery. Adv Drug Deliv Rev. 2005;57:411–30.
34. Vermaelen K, Pauwels R. Pulmonary Dendritic Cells. Am J Respir Crit Care Med. 2005;172:530–51.
35. Banchereau J, Steinman RM. Dendritic cells and the control of immunity. Nature. 1998;392:245–52.
36. Nobelprize.org. The Nobel Prize in Physiology or Medicine 2011. http://www.nobelprize.org/nobel_prizes/medicine/laureates/2011/ (accessed 19 Apr 2012).

37. Lassila O, Vainio O, Matzinger P. Can B cells turn on virgin T cells? Nature. 1988;334:253–5.
38. Banchereau J, Briere F, Caux C, Davoust J, Lebecque S, Liu Y-J, *et al.* Immunobiology of Dendritic Cells. Annu Rev Immunol. 2000;18:767–811.
39. Guermonprez P, Valladeau J, Zitvogel L, Théry C, Amigorena S. Antigen Presentation and T Cell Stimulation by Dendritic Cells. Annu Rev Immunol. 2002;20:621–67.
40. Foged C, Sundblad A, Hovgaard L. Targeting Vaccines to Dendritic Cells. Pharm Res. 2002;19:229–38.
41. Lambrecht BN, Hammad H. Biology of Lung dendritic cells at the origin of asthma. Immunity. 2009;31:412–24.
42. GeurtsvanKessel CH, Lambrecht BN. Division of labor between dendritic cell subsets of the lung. Mucosal Immunol. 2008;1:442–50.
43. Lommatzsch M, Bratke K, Bier A, Julius P, Kuepper M, Luttmann W, *et al.* Airway dendritic cell phenotypes in inflammatory diseases of the human lung. Eur Respir J. 2007;30:878–86.
44. Ba-Omar T, Al-Riyami B. Microscopic study of human alveolar macrophages. Microsc Microanal. 2008;14:1518–9.
45. Kiama SG, Cochand L, Karlsson L, Nicod LP, Gehr P. Evaluation of phagocytic activity in human monocyte-derived dendritic cells. J Aerosol Med. 2001;14:289–99.
46. von Garnier C, Nicod LP. Immunology taught by lung dendritic cells. Swiss Med Wkly. 2009;139:186–92.
47. Demedts IK, Brusselle GG, Vermaelen KY, Pauwels RA. Identification and characterization of human pulmonary dendritic cells. Am J Respir Cell Mol Biol. 2005;32:177–84.
48. Gallucci S, Matzinger P. Danger signals: SOS to the immune system. Curr Opin Immunol. 2001;13:114–9.
49. Copland MJ, Baird MA, Rades T, McKenzie JL, Becker B, Reck F, *et al.* Liposomal delivery of antigen to human dendritic cells. Vaccine. 2003;21:883–90.
50. Burgdorf S, Lukacs-Kornek V, Kurts C. The mannose receptor mediates uptake of soluble but not of cell-associated antigen for cross-presentation. J Immunol. 2006;176:6770–6.
51. Platt CD, Ma JK, Chalouni C, Ebersold M, Bou-Reslan H, Carano RAD, *et al.* Mature dendritic cells use endocytic receptors to capture and present antigens. Proc Natl Acad Sci. 2010;107:4287–92.
52. Thornton EE, Looney MR, Bose O, Sen D, Sheppard D, Locksley R, Huang X, Krummel MF. Spatiotemporally separated antigen uptake by alveolar dendritic cells and airway presentation to T cells in the lung. The Journal of Experimental Medicine (2012).
53. Foged C, Brodin B, Frokjaer S, Sundblad A. Particle size and surface charge affect particle uptake by human dendritic cells in an *in vitro* model. Int J Pharm. 2005;298:315–22.
54. Manolova V, Flace A, Bauer M, Schwarz K, Saudan P, Bachmann MF. Nanoparticles target distinct dendritic cell populations according to their size. Eur J Immunol. 2008;38:1404–13.
55. Reddy ST, Swartz MA, Hubbell JA. Targeting dendritic cells with biomaterials: developing the next generation of vaccines. Trends Immunol. 2006;27:573–9.
56. Cruz LJ, Tacken PJ, Pots JM, Torensma R, Buschow SI, Figdor CG. Comparison of antibodies and carbohydrates to target vaccines to human dendritic cells via DC-SIGN. Biomaterials. 2012;33:4229–39.
57. Caminschi I, Maraskovsky E, Heath WR. Targeting dendritic cells *in vivo* for cancer therapy. Frontiers in Immunology. 3: (2012).
58. Carrillo-Conde B, Song E-H, Chavez-Santoscoy A, Phanse Y, Ramer-Tait AE, Pohl NLB, *et al.* Mannose-functionalized "Pathogen-like" polyanhydride nanoparticles target c-type lectin receptors on dendritic cells. Mol Pharm. 2011;8:1877–86.
59. Geijtenbeek TBH, Gringhuis SI. Signalling through C-type lectin receptors: shaping immune responses. Nat Rev Immunol. 2009;9:465–79.
60. Sung JC, Pulliam BL, Edwards DA. Nanoparticles for drug delivery to the lungs. Trends Biotechnol. 2007;25:563–70.
61. Bailey MM, Berkland CJ. Nanoparticle formulations in pulmonary drug delivery. Med Res Rev. 2009;29:196–212.
62. Smola M, Vandamme T, Sokolowski A. Nanocarriers as pulmonary drug delivery systems to treat and to diagnose respiratory and non respiratory diseases. Int J Nanomedicine. 2008;3:1–19.
63. Smyth HDC, Smyth HH, Hickey AJ. *Macro and Microstructure of the Airways for Drug Delivery* in Controlled Pulmonary Drug Delivery, Springer, 2011.
64. Heffernan MJ, Kasturi SP, Yang SC, Pulendran B, Murthy N. The stimulation of CD8+ T cells by dendritic cells pulsed with polyketal microparticles containing ion-paired protein antigen and poly(inosinic acid)–poly(cytidylic acid). Biomaterials. 2009;30:910–8.
65. Rice-Ficht AC, Arenas-Gamboa AM, Kahl-McDonagh MM, Ficht TA. Polymeric particles in vaccine delivery. Curr Opin Microbiol. 2010;13:106–12.
66. Panyam J, Labhasetwar V. Biodegradable nanoparticles for drug and gene delivery to cells and tissue. Adv Drug Deliv Rev. 2003;55:329–47.
67. Rytting E, Nguyen J, Wang X, Kissel T. Biodegradable polymeric nanocarriers for pulmonary drug delivery. Expet Opin Drug Deliv. 2008;5:629–39.
68. Kumari A, Yadav SK, Yadav SC. Biodegradable polymeric nanoparticles based drug delivery systems. Colloids Surf B Biointerfaces. 2010;75:1–18.
69. Bolhassani A, Safaiyan S, Rafati S. Improvement of different vaccine delivery systems for cancer therapy. Mol Cancer. 2011;10:3.
70. Doria-Rose NA, Haigwood NL. DNA vaccine strategies: candidates for immune modulation and immunization regimens. Methods. 2003;31:207–16.
71. Bivas-Benita M, van Meijgaarden KE, Franken KLMC, Junginger HE, Borchard G, Ottenhoff THM, *et al.* Pulmonary delivery of chitosan-DNA nanoparticles enhances the immunogenicity of a DNA vaccine encoding HLA-A*0201-restricted T-cell epitopes of Mycobacterium tuberculosis. Vaccine. 2004;22:1609–15.
72. Jain JRA. The manufacturing techniques of various drug loaded biodegradable poly(lactide-co-glycolide) (PLGA) devices. Biomaterials. 2000;21:2475–90.
73. Anderson JM, Shive MS. Biodegradation and biocompatibility of PLA and PLGA microspheres. Adv Drug Deliv Rev. 1997;28:5–24.
74. Fiore VF, Lofton MC, Roser-Page S, Yang SC, Roman J, Murthy N, *et al.* Polyketal microparticles for therapeutic delivery to the lung. Biomaterials. 2010;31:810–7.
75. Muttil P, Prego C, Garcia-Contreras L, Pulliam B, Fallon J, Wang C, *et al.* Immunization of Guinea Pigs with Novel Hepatitis B Antigen as Nanoparticle Aggregate Powders Administered by the Pulmonary Route. AAPS J. 2010;12:330–7.
76. Heffernan MJ, Murthy N. Polyketal nanoparticles: a new pH-sensitive biodegradable drug delivery vehicle. Bioconjug Chem. 2005;16:1340–2.
77. Yang SC, Bhide M, Crispe IN, Pierce RH, Murthy N. Polyketal copolymers: a new acid-sensitive delivery vehicle for treating acute inflammatory diseases. Bioconjug Chem. 2008;19:1164–9.
78. Pinto Reis C, Neufeld RJ, Ribeiro AJ, Veiga F. Nanoencapsulation I. Methods for preparation of drug-loaded polymeric nanoparticles. Nanomedicine Nanotechnol Biol Med. 2006;2:8–21.
79. Singh J, Pandit S, Bramwell VW, Alpar HO. Diphtheria toxoid loaded poly-(ε-caprolactone) nanoparticles as mucosal vaccine delivery systems. Methods. 2006;38:96–105.

80. Mahapatro A, Singh D. Biodegradable nanoparticles are excellent vehicle for site directed *in-vivo* delivery of drugs and vaccines. J Nanobiotechnology. 2011;9:55.
81. Dinarvand R, Sepehri N, Manoochehri S, Rouhani H, Atyabi F. Polylactide-co-glycolide nanoparticles for controlled delivery of anticancer agents. Int J Nanomedicine. 2011;6:877–95.
82. Lee JS, Hwang SJ, Lee DS, Kim SC, Kim DJ. Formation of Poly (ethylene glycol)-Poly(ε-caprolactone) Nanoparticles via Nanoprecipitation. Macromol Res. 2009;17:72–8.
83. Ranjan AP, Zeglam K, Mukerjee A, Thamake S, Vishwanatha JK. A sustained release formulation of chitosan modified PLCL: poloxamer blend nanoparticles loaded with optical agent for animal imaging. Nanotechnology. 2011;22:1–10.
84. Allémann E, Gurny R, Doelker E. Preparation of aqueous polymeric nanodispersions by a reversible salting-out process: influence of process parameters on particle size. Int J Pharm. 1992;87:247–53.
85. Muthu M. Nanoparticles based on PLGA and its co-polymer: An overview, 2009.
86. Konan YN, Gurny R, Allémann E. Preparation and characterization of sterile and freeze-dried sub-200 nm nanoparticles. Int J Pharm. 2002;233:239–52.
87. Soppimath KS, Aminabhavi TM, Kulkarni AR, Rudzinski WE. Biodegradable polymeric nanoparticles as drug delivery devices. J Control Release. 2001;70:1–20.
88. Bivas-Benita M, Romeijn S, Junginger HE, Borchard G. PLGA–PEI nanoparticles for gene delivery to pulmonary epithelium. Eur J Pharm Biopharm. 2004;58:1–6.
89. Bivas-Benita M, Lin MY, Bal SM, van Meijgaarden KE, Franken KLMC, Friggen AH, *et al.* Pulmonary delivery of DNA encoding Mycobacterium tuberculosis latency antigen Rv1733c associated to PLGA–PEI nanoparticles enhances T cell responses in a DNA prime/protein boost vaccination regimen in mice. Vaccine. 2009;27:4010–7.
90. Pulliam B, Sung JC, Edwards DA. Design of nanoparticle-based dry powder pulmonary vaccines. Expet Opin Drug Deliv. 2007;4:651–63.
91. Allen TM, Cullis PR. Drug delivery systems: entering the mainstream. Science. 2004;303:1818–22.
92. Petrovsky N, Aguilar JC. Vaccine adjuvants: current state and future trends. Immunol Cell Biol. 2004;82:488–96.
93. O'Hagan DT, MacKichan ML, Singh M. Recent developments in adjuvants for vaccines against infectious diseases. Biomol Eng. 2001;18:69–85.
94. Wilson-Welder JH, Torres MP, Kipper MJ, Mallapragada SK, Wannemuehler MJ, Narasimhan B. Vaccine adjuvants: current challenges and future approaches. J Pharm Sci. 2009;98:1278–316.
95. Amorij J-P, Kersten GFA, Saluja V, Tonnis WF, Hinrichs WLJ, Slütter B, Bal SM, Bouwstra JA, Huckriede A, Jiskoot W. Towards tailored vaccine delivery: Needs, challenges and perspectives. Journal of Controlled Release.
96. Sekaly R-P. The failed HIV Merck vaccine study: a step back or a launching point for future vaccine development? J Exp Med. 2008;205:7–12.
97. Lewis DJM, Huo Z, Barnett S, Kromann I, Giemza R, Galiza E, *et al.* Transient facial nerve paralysis (Bell's Palsy) following intranasal delivery of a genetically detoxified mutant of *Escherichia coli* heat labile toxin. PLoS One. 2009;4:e6999.
98. Vajdy M. Immunomodulatory properties of vitamins, flavonoids and plant oils and their potential as vaccine adjuvants and delivery systems. Expert Opin Biol Ther. 2011;11:1501–13.
99. Skountzou I, Quan F-S, Jacob J, Compans RW, Kang S-M. Transcutaneous immunization with inactivated influenza virus induces protective immune responses. Vaccine. 2006;24:6110–9.
100. Nottenburg C. Types of adjuvants: In Introduction to Adjuvant Patent Landscape. http://www.patentlens.net/daisy/adjuvants/Background/Adjuvant_types.html (accessed 14th April 2012).
101. Wee JLK, Scheerlinck JPY, Snibson KJ, Edwards S, Pearse M, Quinn C, *et al.* Pulmonary delivery of ISCOMATRIX influenza vaccine induces both systemic and mucosal immunity with antigen dose sparing. Mucosal Immunol. 2008;1:489–96.
102. Vauthier C, Bouchemal K. Methods for the preparation and manufacture of polymeric nanoparticles. Pharm Res. 2009; 26:1025–58.
103. LiCalsi C, Christensen T, Bennett JV, Phillips E, Witham C. Dry powder inhalation as a potential delivery method for vaccines. Vaccine. 1999;17:1796–803.
104. Mansour HM, Rhee Y, Wu X. Nanomedicine in pulmonary delivery. Int J Nanomedicine. 2009;4:299–319.
105. Pilcer G, Amighi K. Formulation strategy and use of excipients in pulmonary drug delivery. Int J Pharm. 2010;392:1–19.
106. Abdelwahed W, Degobert G, Stainmesse S, Fessi H. Freeze-drying of nanoparticles: formulation, process and storage considerations. Adv Drug Deliv Rev. 2006;58:1688–713.
107. Anhorn MG, Mahler H-C, Langer K. Freeze drying of human serum albumin (HSA) nanoparticles with different excipients. Int J Pharm. 2008;363:162–9.
108. Hirsjärvi S, Peltonen L, Hirvonen J. Effect of sugars, surfactant, and tangential flow filtration on the freeze-drying of Poly(lactic acid) nanoparticles. AAPS PharmSciTech. 2009;10:488–94.
109. Malcolmson RJ, Embleton JK. Dry powder formulations for pulmonary delivery. Pharmaceut Sci Tech Today. 1998;1:394–8.
110. Peltonen L, Valo H, Kolakovic R, Laaksonen T, Hirvonen J. Electrospraying, spray drying and related techniques for production and formulation of drug nanoparticles. Expet Opin Drug Deliv. 2010;7:705–19.
111. Heng D, Lee SH, Ng WK, Tan RB. The nano spray dryer B-90. Expet Opin Drug Deliv. 2011;8:965–72.
112. Amorij JP, Huckriede A, Wilschut J, Frijlink H, Hinrichs W. Development of stable influenza vaccine powder formulations: challenges and possibilities. Pharm Res. 2008;25:1256–73.
113. Shoyele SA, Cawthorne S. Particle engineering techniques for inhaled biopharmaceuticals. Adv Drug Deliv Rev. 2006;58:1009–29.
114. Al-fagih IM, Alanazi FK, Hutcheon GA, Saleem IY. Recent advances using supercritical fluid techniques for pulmonary administration of macromolecules via dry powder formulations. Drug Deliv Lett. 2011;1:128–34.
115. Okamoto H, Danjo K. Application of supercritical fluid to preparation of powders of high-molecular weight drugs for inhalation. Adv Drug Deliv Rev. 2008;60:433–46.
116. Byrappa K, Ohara S, Adschiri T. Nanoparticles synthesis using supercritical fluid technology – towards biomedical applications. Adv Drug Deliv Rev. 2008;60:299–327.
117. Kenji M. Biodegradable particle formation for drug and gene delivery using supercritical fluid and dense gas. Adv Drug Deliv Rev. 2008;60:411–32.
118. Pasquali I, Bettini R, Giordano F. Supercritical fluid technologies: an innovative approach for manipulating the solid-state of pharmaceuticals. Adv Drug Deliv Rev. 2008;60:399–410.
119. Amidi M, Pellikaan HC, Hirschberg H, de Boer AH, Crommelin DJA, Hennink WE, *et al.* Diphtheria toxoid-containing microparticulate powder formulations for pulmonary vaccination: preparation, characterization and evaluation in guinea pigs. Vaccine. 2007;25:6818–29.
120. W.H. Organization. Pneumonia. http://www.who.int/mediacentre/factsheets/fs331/en/index.html (accessed 17/04 2012).
121. Ghotbi Z, Haddadi A, Hamdy S, Hung RW, Samuel J, Lavasanifar A. Active targeting of dendritic cells with mannan-decorated PLGA nanoparticles. J Drug Target. 2011;19:281–92.

122. Bandyopadhyay A, Fine RL, Demento S, Bockenstedt LK, Fahmy TM. The impact of nanoparticle ligand density on dendritic-cell targeted vaccines. Biomaterials. 2011;32:3094–105.
123. Cruz LJ, Tacken PJ, Fokkink R, Joosten B, Stuart MC, Albericio F, *et al.* Targeted PLGA nano- but not microparticles specifically deliver antigen to human dendritic cells via DC-SIGN *in vitro*. J Control Release. 2010;144:118–26.
124. Kwon YJ, James E, Shastri N, Fréchet JMJ. *In vivo* targeting of dendritic cells for activation of cellular immunity using vaccine carriers based on pH-responsive microparticles. Proc Natl Acad Sci U S A. 2005;102:18264–8.
125. Kempf M, Mandal B, Jilek S, Thiele L, Vörös J, Textor M, *et al.* Improved stimulation of human dendritic cells by receptor engagement with surface-modified microparticles. J Drug Target. 2003;11:11–8.
126. Sheng K-C, Kalkanidis M, Pouniotis DS, Esparon S, Tang CK, Apostolopoulos V, *et al.* Delivery of antigen using a novel mannosylated dendrimer potentiates immunogenicity *in vitro* and *in vivo*. Eur J Immunol. 2008;38:424–36.
127. White KL, Rades T, Furneaux RH, Tyler PC, Hook S. Mannosylated liposomes as antigen delivery vehicles for targeting to dendritic cells. J Pharm Pharmacol. 2006;58:729–37.
128. Jain S, Vyas SP. Mannosylated niosomes as adjuvant-carrier system for oral mucosal immunization. J Liposome Res. 2006;16:331–45.
129. Hao J, Kwissa M, Pulendran B, Murthy N. Peptide crosslinked micelles: a new strategy for the design and synthesis of peptide vaccines. Int J Nanomedicine. 2006;1:97–103.
130. Lu D, Hickey AJ. Liposomal dry powders as aerosols for pulmonary delivery of proteins. AAPS PharmSciTech. 2005;6:E641–8.
131. Barnier Quer C, Robson Marsden H, Romeijn S, Zope H, Kros A, Jiskoot W. Polymersomes enhance the immunogenicity of influenza subunit vaccine. Polym Chem. 2011;2:1482–5.
132. Matinkhoo S, Lynch KH, Dennis JJ, Finlay WH, Vehring R. Spray-dried respirable powders containing bacteriophages for the treatment of pulmonary infections. J Pharm Sci. 2011;100:5197–205.
133. Saluja V, Amorij JP, Kapteyn JC, de Boer AH, Frijlink HW, Hinrichs WLJ. A comparison between spray drying and spray freeze drying to produce an influenza subunit vaccine powder for inhalation. J Control Release. 2010;144:127–33.
134. Jin TH, Tsao E, Goudsmit J, Dheenadhayalan V, Sadoff J. Stabilizing formulations for inhalable powders of an adenovirus 35-vectored tuberculosis (TB) vaccine (AERAS-402). Vaccine. 2010;28:4369–75.
135. Garcia-Contreras L, Wong Y-L, Muttil P, Padilla D, Sadoff J, DeRousse J, *et al.* Immunization by a bacterial aerosol. Proc Natl Acad Sci. 2008;105:4656–60.
136. Lu D, Garcia-Contreras L, Muttil P, Padilla D, Xu D, Liu J, *et al.* Pulmonary Immunization Using Antigen 85-B Polymeric Microparticles to Boost Tuberculosis Immunity. AAPS J. 2010;12:338–47.

Pulmonary Vaccine Delivery of Protein Adsorbed PGA-co-PDL Nanocomposite Microparticles

N K Kunda[1], I M Alfagih[1,2], S Somavarapu[3], G A Hutcheon[1], I Y Saleem[1]

1. School of Pharmacy and Biomolecular Sciences, Liverpool John Moores University, Liverpool, UK
2. Department of Pharmaceutics, King Saud University, Riyadh, Saudi Arabia
3. The School of Pharmacy, University College London, London, UK

Summary: Purpose: To formulate bovine serum albumin (BSA) adsorbed poly(glycerol adipate-co-ω-pentadecalactone) [PGA-co-PDL] nanoparticles (NPs) within lactose and L-leucine microparticle carriers for dry powder inhalation. **Methods:** NPs were prepared by oil-in-water (O/W) single emulsion solvent evaporation method and freeze-dried with different Sucrose:NP ratios. Particle size and polydispersity index (PDI) were characterised before and after freeze-drying. BSA (0.5 and 1mg/ml) were adsorbed onto 20mg of NPs equivalent freeze-dried powder at room temperature over 1h using HulaMixer™. Protein loading was determined using bicinchoninic acid (BCA) assay. The NPs were spray-dried in aqueous suspension of lactose (1:5) or L-leucine (1:1.5) using a Büchi 290 mini-spray dryer. The resultant nanocomposite microparticles (NCMPs) were characterised for toxicity (MTT assay), aerosolization (Next Generation Impactor) and *in-vitro* release study.
Results: NPs (148.90±5.00nm, PDI 0.07±0.03) suitable for targeting lung dendritic cells were produced. Sucrose:NP (5:1) ratio was shown to be the optimum for maintaining the particle size (206.42±10.36nm, PDI 0.35±0.10) after freeze-drying. BSA adsorption resulted in 26.02±0.09µg of protein per mg of NPs. Spray-drying resulted in NCMPs with 51.3% (lactose) and 50.01% (L-leucine) yield. *In-vitro* release study at 37°C for 24h showed an initial burst release of 3.91±0.05% (lactose) and 16.70±0.24% with 88.03±2.85% over 24h (L-leucine). Aerosolization studies indicated fine particle fraction (FPF) 57.88±11.51% and mass median aerodynamic diameter (MMAD) 1.83±0.07µm (lactose), and FPF 77.85±1.25% and MMAD 1.77±0.09 (L-leucine). The cell viability was 87.01±14.11% with L-leucine based NCMPs (1.25mg/ml). **Conclusion:** PGA-co-PDL/L-leu NCMPs may be a promising carrier for pulmonary vaccine delivery due to high adsorption and excellent aerosolisation behaviour.

Introduction:
The majority of the vaccines available are administered via the parenteral route. However, in low and middle income countries (LMICs), due to a lack of infrastructure such as cold-chain and trained medical personnel which are essential for parenteral administration, the majority of the population is unable to get vaccinated. Recent advances in the non-invasive delivery systems, such as pulmonary delivery, has helped in formulating these and making them more patient compliant and readily acceptable [1,2]. Moreover, the pulmonary route has gained significant attention as it is the main portal of entry for pathogens coupled with the lung being an excellent choice for delivery. The pulmonary route offers several advantages such as, large surface area (80 m^2), high vasculature, rapid absorption leading to an immediate onset of action, thin alveolar epithelium, less enzymatic activity compared to the gut, and an abundance of antigen presenting cells (such as macrophages, dendritic cells (DCs)) for targeting vaccines [3]. Furthermore, nanoparticles (NPs) due to their size can target DCs enhancing the immune response. In addition, the biodegradable polymeric NPs offer numerous advantages such as controlled or sustained drug release, biocompatibility with the surrounding tissues and cells, lower toxicity compared to non-biodegradable polymers, non-thrombogenic, act as adjuvants and are more stable in blood [4].

Objective:
The aim of this study was to adsorb a model protein, bovine serum albumin (BSA), onto poly(glycerol adipate-co-ω-pentadecalactone), PGA-co-PDL, NPs, and formulate into nanocomposite microparticles (NCMPs) for pulmonary vaccine delivery via dry powder inhalation. The NCMPs were prepared via spray drying using lactose or L-Leucine as microparticle carriers. The formulations were characterised for their adsorption, particle size, surface charge, *in vitro* release and aerosolisation performance.

Methods:

Nanocomposite microparticles preparation

Preparation of NPs: The BSA adsorbed PGA-co-PDL NPs were fabricated using a modified oil-in-water (o/w) single emulsion solvent evaporation method [5]. The taguchi L_{18} orthogonal array design of experiment (DoE) was used to optimize the formulation parameters to achieve NPs (~150nm) for targeting the lung DCs (n=2). Briefly, PGA-co-PDL (synthesised in our laboratory, MW 14.7 KDa) was dissolved in 2 ml dichloromethane and probe sonicated upon addition to 5 ml of 1st aqueous solution of 10% w/v polyvinyl alcohol (PVA) in dry ice for 2 min to obtain an emulsion. This was immediately added drop wise to 20 ml of 2nd aqueous solution (0.75% w/v PVA) under magnetic stirring at a speed of 500 RPM. The whole mixture was left magnetically stirring at room temperature for 3 h. The NPs were collected by centrifugation (36,000 RPM for 40 min), washed twice with distilled water and were frozen (24h, -80°C) followed by freeze-drying (FD) (-50 ± 5°C, 0.054 ± 0.002 Mbar, 48h) with different cryoprotectant Sucrose:NPs ratios of 1.25:1, 2.5:1 and 5:1.
Surface adsorption: 4 ml of BSA (0.5 and 1 mg/ml) were surface adsorbed onto 20 mg of NPs equivalent sucrose:NP (5:1) FD powder at room temperature over 1h using HulaMixer™. The BSA adsorbed NPs were collected by centrifugation (36,000 RPM for 40 min).

Preparation of nanocomposite microparticles (NCMPs): The BSA adsorbed NPs were resuspended in 20ml aqueous solution containing lactose (PGA-co-PDL:lactose, 1: 5) or L-leucine (PGA-co-PDL:L-leucine, 1: 1.5), and spray dried using a mini-spray dryer (Büchi, B-290 Flawil, Switzerland) as previously reported [6] to form NCMPs.

Nanocomposite microparticles characterization

Surface adsorption and spray dried yield: 150 µl of the supernatant was analysed using the Thermo Scientific Pierce BCA protein assay kit for determining the protein concentration. The amount of BSA adsorbed was calculated by subtracting the amount of protein remaining in the supernatant from the amount of protein initially added. The yield of spray dried NCMPs was quantified as a percentage mass of expected total powder yield (n=3).

Particle size and polydispersity index (PDI): The NPs size and PDI was measured on a Malvern Zetasizer, U.K. Briefly, 100 µl of suspension and 10 mg of freeze-dried powder was diluted to 5 ml using distilled water and the measurements recorded at 25 ºC (n=3).

Aerosolisation study (Next Generation Impactor): The aerodynamic particle size distribution was determined using the Next Generation Impactor (NGI). The BSA adsorbed NCMPs were weighed (10 capsules each with 8 mg SD powder for the PGA-co-PDL/Lac NCMPs and 4 capsules each with 6 mg SD powder for the PGA-co-PDL/L-leu NCMPs) and manually loaded into the hydroxypropyl methylcellulose, HPMC, capsule (size 3), and placed in a cyclohaler. The samples were drawn through the induction port into the NGI operated at a flow rate of 60 L/min for 4 s (corresponding to a pressure drop of 4 kPa across the inhaler) and collected using a known volume of distilled water, and left on a roller-shaker for 48h. The samples were then analysed and the amount of BSA deposited was determined using the BCA assay. The fine particle fraction (%FPF) (defined as the mass of drug deposited (d_{ae}<4.6 µm), expressed as a percentage of the emitted dose), and the mass median aerodynamic diameter (MMAD), were determined (n=3).

In-vitro release study: 10mg samples of the BSA adsorbed NCMPs were placed in vials and dispersed in 4 ml of phosphate-buffered saline (PBS). The samples were incubated at 37°C in the HulaMixer™ set at 10 rpm. At predetermined time intervals up to 24h, the samples were centrifuged (36,000 RPM for 40 min) and 1ml of the supernatant removed and replaced with fresh medium. The supernatant was analysed by Bradford assay for the PGA-co-PDL/Lac NCMPs and BCA assay for the PGA-co-PDL/L-leu NCMPs (n=3).

Cell viability study: The *in vitro* cytotoxicity of the non-adsorbed PGA-co-PDL, 1.5% Leu NCMPs was evaluated using the 3-[4,5-dimethylthiazol-2-yl]-3,5 diphenyl tetrazolium bromide (MTT) assay, that depends on the cellular reductive capacity to metabolize the MTT to a highly colored formazan product. The adenocarcinomic human alveolar basal epithelial cell line, A549 cells were seeded in 100 µl (2.5×10^5 cells/ml) of RPMI-1640 medium supplemented with 10% fetal calf serum/1% Antibiotic/Antimycotic solution (complete medium) in 96-well plates and pre-incubated for 24h in a incubator at 37°C supplied with 5% CO_2. Then, 100 µl of freshly prepared NCMP dispersions in complete medium were added to the wells to an appropriate concentration (0 – 2.5 mg/ml) (n=3), and 10% dimethyl sulfoxide (DMSO) as positive control. The formulations were assayed for toxicity over 24h of incubation. After the incubation period, 20 µl of a 5 mg/ml MTT solution in PBS was added to each well. After 2h, the culture medium was gently removed and replaced by 100 µl of dimethyl sulfoxide in order to dissolve the formazan crystals. The absorbance of the solubilised dye, which correlates with the number of living cells, was measured at 570 nm. The percentage of viable cells in each well was calculated as the absorbance ratio between nanoparticle-treated and untreated control cells.

Results and Discussion:

Preparation of NPs

The taguchi DoE (L_{18}) was designed using 7 factors (1 factor–2 levels, 6 factors–3 levels) to determine the optimum levels for each factor/parameter in achieving the desired PGA-co-PDL NP size (~150 nm) for targeting DCs.

Table 1 Taguchi's Experimental Design L_{18} (7 factors) for producing PGA-co-PDL nanoparticles

Parameters / Levels	Units	1	2	3
MW of Polymer	KDa	14	23	-
Org Sol (DCM)	ml	1	1.5	2
Aq. Vol (PVA)	ml	3	4	5
1st Aq. conc (PVA)	% w/v	2.5	5	10
Sonication time	min	1	2	5
Stirrer - Speed	RPM	400	500	600
2nd Aq. conc (PVA)	% w/v	0.5	0.75	1

Eighteen runs obtained using the taguchi DoE were performed and the resulting optimum parameters are listed in table 2. The PGA-co-PDL NPs prepared using these parameters showed a size of 148.9 ± 5.00 nm, PDI 0.07 ± 0.03 indicating its suitability for targeting the lung DCs (Fig 1a & 1b) (n=3).

Table 2 Optimum levels for each parameter and relative importance (rank) determined using Taguchi DoE (L_{18})

Parameters	MW of Polymer (KDa)	Org Sol (DCM) (ml)	Aq. Vol (PVA) (ml)	1st Aq. conc (PVA) (% w/v)	Sonication time (min)	Stirrer – Speed (RPM)	2nd Aq. conc (PVA) (% w/v)
Levels	14	2	5	10	2	500	0.5
Rank by importance	3	2	5	1	4	6	7

The freeze-dried nanoparticulate suspensions without any cryoprotectants resulted in a significant increase in particle size compared to those with cryoprotectants. The Sucrose:NP (5:1) ratio was the optimum for maintaining the particle size 206.42 ± 10.36 nm and PDI 0.35 ± 0.10 after freeze-drying (Fig 1a & 1b) (n=3).

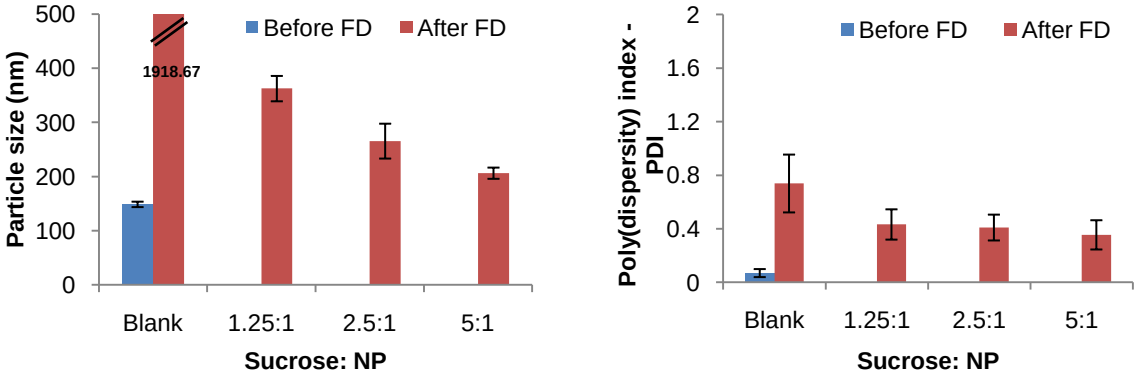

Fig 1 (a) Effect of freeze-drying on particle size, **(b)** Effect of freeze-drying on PDI for different sucrose:NP (1.25:1, 2.5:1, 5:1) ratios *(Mean ± SD, n=3)*

Characterisation

Surface adsorption: No difference in adsorption was observed at 0.5 and 1 mg/ml concentrations of BSA over 1h (Table 3).

Table 3 Surface adsorption of BSA (0.5 and 1 mg/ml) onto 20 mg of NPs over 1 h *(Mean ± SD, n=3)*

BSA concentration	1 mg/ml	0.5 mg/ml
BSA adsorbed (µg/mg of NPs)	26.85 ± 0.32	26.52 ± 0.26

Spray drying yield: A reasonable yield of spray drying, 51.32 ± 3.2% for the BSA adsorbed PGA-co-PDL/Lac NCMPs and 50.01 ± 0.3% for the BSA adsorbed PGA-co-PDL/L-leu NCMPs was obtained.

Aerosolisation study: The aerodynamic particle characteristics of the BSA adsorbed PGA-co-PDL/Lac NCMPs (FPF of 57.88 ± 11.51%, MMAD of 1.83 ± 0.07 µm) and PGA-co-PDL/L-leu NCMPs (FPF of 77.85 ± 1.25%, MMAD of 1.77 ± 0.09 µm) indicated both formulations were capable of delivering efficient BSA to the lungs, and were likely to deposit the NPs in the bronchial-alveolar region of the lungs due to the MMAD results obtained. Furthermore, the NPs due to their size should be effectively taken up by the immune cells triggering an immune response. In addition, it is expected that the PGA-co-PDL NPs will eventually degrade into its individual components (glycerol, divinyl adipate and pentadecalactone).

In vitro release study: *In vitro* release studies comparing the PGA-co-PDL/Lac NCMPs and the PGA-co-PDL/L-leu NCMPs were performed and reported as cumulative percentage BSA released over time (Fig 2). An initial burst release was observed for both the formulations; however, the release of BSA from the PGA-co-PDL/Lac NCMPs (3.91±0.05%) was less than that of the PGA-co-PDL/L-leu NCMPs (16.70±0.24%). The rapid release continued for both the formulations up to 4h, where the PGA-co-PDL/Lac NCMPs (23.47±0.07%) released less BSA than that of the PGA-co-PDL/L-leu NCMPs (71.00±2.35%). After this time period, the release of BSA reached a plateau, providing a slow continuous release phase up to 24h which later reached 27.40±0.07% for the PGA-co-PDL/Lac NCMPs and 88.03±2.85% for the PGA-co-PDL/L-leu NCMPs indicating an excellent release profile for the PGA-co-PDL/L-leu NCMPs.

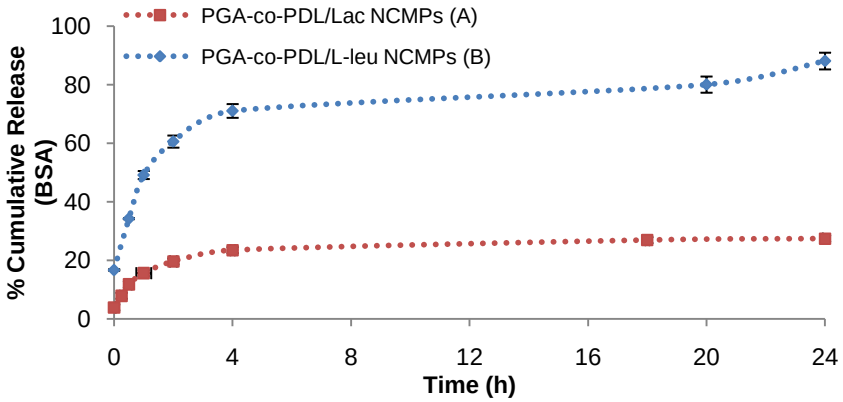

Figure 2 *In vitro* release profiles for BSA adsorbed PGA-co-PDL/Lac (A) and PGA-co-PDL/L-leu (B) NCMPs in phosphate buffer saline, pH 7.4 *(Mean ± SD, n=3)*

Cell viability study: The non-adsorbed PGA-co-PDL NCMPs appear to be well tolerated by the A549 cells, with a cell viability of 87.01±14.11% at 1.25 mg/ml concentration after 24 h exposure indicating a good toxicity profile.

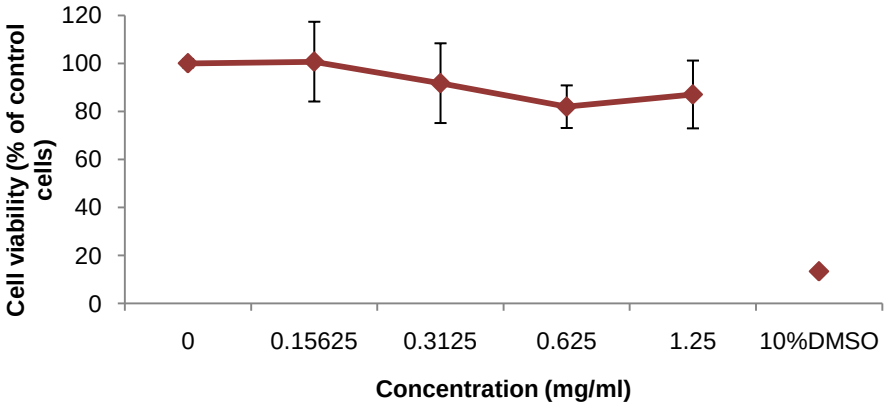

Figure 3 A549 cell viability measured by MTT assay after 24 h exposure to PGA-co-PDL NCMPs *(Mean ± SD, n=3)*

Conclusion:

The results indicate effective BSA adsorption onto the surface of PGA-co-PDL NPs and the aerosolisation data shows suitability of both the PGA-co-PDL/Lac and the PGA-co-PDL/L-leu NCMPs for pulmonary vaccine delivery. However, the superior FPF %, MMAD and *in vitro* release profile of the PGA-co-PDL/L-leu NCMPs compared to that of the PGA-co-PDL/Lac NCMPs suggests efficient delivery of BSA to the lungs thus an enhanced immune response. Moreover, the PGA-co-PDL NCMPs displayed a good toxicity profile. Further investigations will be aimed at optimizing the adsorption time, concentration of the protein followed by evaluation of protein integrity, uptake and immune response using the lung DC models.

Acknowledgements:

Nitesh Kunda would like to thank Liverpool John Moores University for their financial support in conducting this study.

References:

1. Brown LR. Commercial challenges of protein drug delivery. Exp. Opin. Drug Deliv. 2005:2:29–42.
2. Sullivan VJ, Mikszta JA, Laurent P, Huang J and Ford B. Noninvasive delivery technologies: respiratory delivery of vaccines. Exp. Opin. Drug Deliv. 2006: 387-95.
3. Scheuch G, Kohlhaeufl MJ, Brand P, Siekmeier R, Clinical perspectives on pulmonary systemic and macromolecular delivery, Adv. Drug Deliv. Rev. 2006;58:996–1008.
4. Panyam J, Labhasetwar V: Biodegradable nanoparticles for drug and gene delivery to cells and tissue. Adv. Drug Deliv. Rev. 2003: 55:329-347.
5. Pinto Reis C, Neufeld RJ António RJ, Veiga F. Nanomedicine: nanotechnology, biology, and medicine. 2006: 2:8-21.
6. Tawfeek H, Khidr S, Samy E, Ahmed S, Murphy M, Mohammed A, Shabir A, Hutcheon G, Saleem I. Poly(Glycerol Adipate-co-ω-Pentadecalactone) Spray-Dried Microparticles as Sustained Release Carriers for Pulmonary Delivery**.** Pharm. Res., 2011: 28(9): 2086-2097.

Pharm Res
DOI 10.1007/s11095-014-1538-5

RESEARCH PAPER

Bovine Serum Albumin Adsorbed PGA-co-PDL Nanocarriers for Vaccine Delivery *via* Dry Powder Inhalation

Nitesh K. Kunda • Iman M. Alfagih • Sarah Rachel Dennison • Hesham M. Tawfeek • Satyanarayana Somavarapu • Gillian A. Hutcheon • Imran Y. Saleem

Received: 24 March 2014 / Accepted: 29 September 2014

ABSTRACT

Purpose Dry powder vaccine delivery *via* the pulmonary route has gained significant attention as an alternate route to parenteral delivery. In this study, we investigated bovine serum albumin (BSA) adsorbed poly(glycerol adipate-co-ω-pentadecalactone), PGA-co-PDL polymeric nanoparticles (NPs) within L-leucine (L-leu) microcarriers for dry powder inhalation.

Methods NPs were prepared by oil-in-water single emulsion-solvent evaporation and particle size optimised using Taguchi's design of experiment. BSA was adsorbed onto NPs at different ratios at room temperature. The NPs were spray-dried in aqueous suspension of L-leu (1:1.5) using a Büchi-290 mini-spray dryer. The resultant nanocomposite microparticles (NCMPs) were characterised for toxicity (MTT assay), aerosolization (Next Generation Impactor), *in vitro* release study and BSA was characterized using SDS-PAGE and CD respectively.

Results NPs of size 128.50 ± 6.57 nm, PDI 0.07 ± 0.03 suitable for targeting lung dendritic cells were produced. BSA adsorption for 1 h resulted in 10.23 ± 1.87 μg of protein per mg of NPs. Spray-drying with L-leu resulted in NCMPs with 42.35 ± 3.17% yield. *In vitro* release study at 37°C showed an initial burst release of 30.15 ± 2.33% with 95.15 ± 1.08% over 48 h. Aerosolization studies indicated fine particle fraction (FPF%) $d_{ae} < 4.46$ μm as 76.95 ± 5.61% and mass median aerodynamic diameter (MMAD) of 1.21 ± 0.67 μm. The cell viability was 87.01 ± 14.11% (A549 cell line) and 106.04 ± 21.14% (16HBE14o- cell line) with L-leu based NCMPs at 1.25 mg/ml concentration after 24 h treatment. The SDS-PAGE and CD confirmed the primary and secondary structure of the released BSA.

Conclusions The results suggest that PGA-co-PDL/L-leu NCMPs may be a promising carrier for pulmonary vaccine delivery due to excellent BSA adsorption and aerosolization behaviour.

KEY WORDS dry powder inhalation · nanoparticles · pulmonary delivery · spray drying · vaccines

ABBREVIATIONS

APCs	Antigen presenting cells
BSA	Bovine serum albumin
DCs	Dendritic cells
DoE	Design of experiment
LN	Lymph node
NPs	Nanoparticles
NCMPs	Nanocomposite microparticles
PGA-co-PDL	Poly(glycerol adipate-co-ω-pentadecalactone)
PLA	Polylactide or poly-L-lactic acid
PLGA	Poly lactic-co-glycolic-acid
PVA	Polyvinyl alcohol
SD	Spray-drying

INTRODUCTION

Vaccination refers to induction of an immune response using antigens coupled with adjuvants for generating a protective immunity against plausible future infections (1,2). Traditional

N. K. Kunda · I. M. Alfagih · G. A. Hutcheon · I. Y. Saleem (✉)
Formulation and Drug Delivery Research, School of Pharmacy and Biomolecular Sciences, Liverpool John Moores University, James Parson Building, Byrom Street, Liverpool L3 3AF, UK
e-mail: I.Saleem@ljmu.ac.uk

I. M. Alfagih
Department of Pharmaceutics, College of Pharmacy, King Saud University, Riyadh, Saudi Arabia

S. R. Dennison
Research and Innovation, University of Central Lancashire, Preston, UK

H. M. Tawfeek
Department of Industrial Pharmacy, Faculty of Pharmacy, Assiut University, Assiut, Egypt

S. Somavarapu
Department of Pharmaceutics, School of Pharmacy, University College London, London, UK

Published online: 09 October 2014

vaccines are often administered *via* the parenteral route requiring infrastructure such as cold-chain, sterilized water for reconstitution of dry powder vaccines and trained medical personnel. Lack of these facilities in low and middle income countries (LMICs) is leading to many eligible children and adults not getting vaccinated (3). Moreover, the majority of the potential vaccines in development employ purified subunits or recombinant proteins that are often poorly immunogenic thus needing adjuvants and effective delivery systems to generate an optimal immune response (1,2). To address these issues, particulate delivery systems and non-invasive routes of delivery are being investigated. The pulmonary route has gained significant attention for delivery of vaccines as it is one of the main entry portals for pathogens, and can address some of the challenges such as invasiveness, cold-chain requirement, and stability of the antigen by delivering the antigen as a dry powder (3).

Biodegradable polymeric nanoparticles (NPs) have gained significant attention and are largely being explored as delivery vehicles for delivery of peptides, proteins, antigens, DNA *etc.* (3–5). These polymers offer controlled or sustained drug release, biocompatibility with surrounding cells and tissues, degrade into low molecular weight non-toxic products and act as adjuvants helping in generating cellular and humoral immune responses (1,3,6). In this current investigation we aim to use poly(glycerol adipate-co-ω-pentadecalactone), PGA-co-PDL, a biodegradable polyester polymer, that has extensively been studied by our group for delivery of both small molecule and model drugs (dexamethasone phosphate, ibuprofen, sodium fluorescein), and large molecule drugs (α-chymotrypsin, DNase I) (7–10).

In these biodegradable polymeric nanoparticulate formulations, the vaccine antigens (*i.e.* proteins, peptides *etc.*) are either adsorbed onto the surface or encapsulated within the particles (3). Encapsulated antigens are protected by polymeric NPs and their release can be modified by tailoring the properties of the polymers. Adsorbed antigen, however, offers enhanced stability and activity over the encapsulated antigen by avoiding contact with organic solvents employed during particle preparation steps (11–13).

Recent strategies for effective vaccine delivery have been to target the dendritic cells (DCs), the true professional antigen presenting cells (APCs) (14). DCs have the exceptional ability to internalize, and in lymph nodes (LNs) they process and present antigens through major histocompatibility complex (MHC) class I and II pathways thereby activating naïve T-cells resulting in induction of a strong immune response (3,14,15). A study conducted by Manolova *et al.* indicates the importance of particle size in determining the uptake by DCs, where it was shown that upon intracutaneous injection of polystyrene beads of varying sizes, large particles (500–2,000 nm) associated with DCs from the site of injection whereas small particles (20–200 nm) drained freely to the LNs and were present in LN resident DCs (15). In addition, Kim *et al.* have shown that uptake of 200 nm sized NPs by bone marrow DCs to be more than that of 30 nm sized NPs (16). Furthermore, Foged *et al.* has shown that particle size of 500 nm or below were preferred and have shown fast and efficient up take by human DCs derived from blood (17). The above literature suggests that smaller particles of 200 to 500 nm could effectively be up taken by DCs and thus generates a stronger immune response compared to vaccine alone. However, these studies cannot be directly compared to lung DCs but owing to the lack of information on the effect of NP size on uptake by lung DCs the same can be assumed.

In this study, the Taguchi L_{18} orthogonal array design of experiment (DoE) was used to optimize the formulation parameters to achieve NPs (~150 nm) for targeting the lung DCs. The literature suggests that factors such as molecular weight (MW) of the polymer, organic solvent, aqueous phase, sonication time and stirrer speed have an influence on the size of the resultant NPs (18–20) and these were evaluated using the experimental design.

As a dry powder, the nanosized particles cannot be directly used for inhalation as their size is too small and it is expected that majority of the inhaled dose will be exhaled depositing very minimal doses in the lung (21). Thus, these NPs are formulated into nanocomposite microparticles (NCMPs) using additives such as lactose (22), L-leucine (L-leu) (22,23), trehalose (24), mannitol (24) by various manufacturing techniques such as freeze drying, spray drying (SD), spray-freeze drying or supercritical fluid technologies (3,25). The NCMPs in the size range of 1 to 5 μm in diameter are reported to be deposited in the respirable airways and periphery of the lung (26). The additives used to form NCMPs dissolve upon encountering the respiratory environment thereby releasing the NPs (27).

In this project, we aim to produce PGA-co-PDL NPs of optimum size to be effectively taken up by the DCs, surface adsorb a model protein, bovine serum albumin (BSA) and formulate into nanocomposite microparticles (NCMPs) using L-leu as a carrier for delivery *via* dry powder inhalation.

MATERIALS AND METHODS

Materials

Dichloromethane (DCM) was purchased from BDH, laboratory supplies, UK. Novozyme 435 (a lipase from *Candida antartica* immobilized on a microporous acrylic resin) was purchased from Biocatalytics, USA. Acetonitrile (HPLC grade), albumin tagged with fluorescein isothiocyanate (FITC-BSA), bovine serum albumin (BSA, MW 67 KDa), phosphate buffered saline (PBS, pH 7.4) tablets, poly(vinyl alcohol) (PVA, MW 9–10 KDa, 80%), trifluoroacetic acid (TFA, HPLC grade), RPMI-1640 medium with L-glutamine and $NaHCO_3$, thiazoly blue tetrazolium bromide (MTT), tween 80® and ω-pentadecalactone were obtained from Sigma-Aldrich, UK. L-leucine (L-leu) was purchased from BioUltra, Sigma, UK. Seventy-five cm^2/tissue

culture flasks with vented cap, 96-well flat bottom plates, acetone, antibiotic/ antimycotic solution (100X), dimethyl sulfoxide (DMSO) were purchased from Fisher Scientific, UK. Divinyladipate was obtained from Fluorochem, UK. Fetal calf serum (FCS) heat inactivated was purchased from Biosera UK. poly(glycerol adipate-co-ω-pentadecalactone) (PGA-co-PDL), MW of 14.7, 24.0 KDa was synthesized in our laboratory at LJMU and micro BCA™ protein assay kit was purchased from Thermo Scientific, UK. A549 cell line was purchased from ATCC. 16HBE14o- cells were obtained from Dr Dieter Gruenert from the California Pacific Medical Center, University of California San Francisco, USA.

Polymer Synthesis

The PGA-co-PDL polymer of MW of 14.7, 24.0 KDa was synthesized in our laboratory *via* enzyme catalyzed co-polymerization of three monomers as described by Thompson *et al.* (28). The synthesized linear polyester was characterized by gel permeation chromatography, GPC (Viscotek TDA Model 300 using OmniSEC3 operating software), pre-calibrated with polystyrene standards (polystyrene standards kit, Supelco, USA), and ^{1}H-NMR spectroscopy (Bruker AVANCE 300 MHz, Inverse probe with B-ACS 60, Auto sampler with gradient chemming) as described by Thompson *et al.* (28).

Preparation of Nanoparticles

PGA-co-PDL NPs were fabricated using a modified oil-in-water (o/w) single emulsion solvent evaporation method (29). Briefly, 200 mg PGA-co-PDL polymer (MW 14.7 KDa) (and Nile Red, NR 0.5 mg for characterization of protein adsorption onto the surface of PGA-co-PDL *via* confocal microscopy) was dissolved in 2 ml DCM and probe sonicated (20 μm amplitude) upon addition to 5 ml of 10%*w/v* poly(vinyl alcohol) (PVA) (1st aqueous solution) for 2 min to obtain an emulsion. This whole process was performed using ice. This was immediately added drop wise to 20 ml of 2nd aqueous solution (0.75%*w/v* PVA) under magnetic stirring at a speed of 500 RPM. The whole mixture was left stirring at room temperature for 3 h to facilitate the evaporation of DCM. The particle size, PDI and zeta-potential were then characterised as mentioned in "Nanoparticle Characterization" Section. The NP suspensions were collected by centrifugation (78,000 g, 40 min, 4°C) and surface adsorbed with protein as indicated in "Protein Adsorption" Section.

Taguchi Design of Experiment (DoE)

In order to evaluate the influence of formulation parameters and minimize the number of experiments, Taguchi DoE being appropriate to study large number of factors, was employed through Minitab® 16 Statistical Software. Seven factors, namely, polymer MW, organic solvent, internal aqueous phase concentration and volume, sonication time, stirrer speed and external aqueous phase concentration were evaluated by constructing and using L_{18} orthogonal array design with 1 factor, MW, at 2 levels and remaining 6 factors at 3 levels (Table I).

The design was applied to identify the significant factors that would affect the size of PGA-co-PDL NPs. Optimum conditions were indicated by high signal-to-noise (S/N) ratios, where signal factor (S) is the outcome, the particle size, and noise factors (N) are parameters such as humidity, temperature, experience of the experimenter *etc.* A greater S/N ratio corresponds to minimum variance of the outcome, the particle size *i.e.* a better performance. In other words, the experimental parameter having the least variability is the optimum condition (30). The optimization of size was carried out using the Taguchi's 'smaller-is-better' criterion *i.e.* to get the outcome, the particle size, to an ideal target of zero or as small as possible.

Protein Adsorption

NP suspension (equivalent to 10 mg *i.e.* 1.25 ml of suspension) was centrifuged (78,000 g, 40 min, 4°C) and the resultant pellet was resuspended in vials containing 4 ml of BSA (or FITC-BSA for characterization of protein adsorption onto the surface of PGA-co-PDL *via* confocal microscopy), for 1 h, at different ratios of 100: 4, 100: 10 and 100: 20 (NP: BSA) corresponding to 100, 250 and 500 μg/ml BSA concentrations, respectively. The resulting suspension (for 100: 20) was left rotating for 30 min, 1, 2 and 24 h at 20 RPM on a HulaMixer™ Sample Mixer (Life Technologies, Invitrogen, UK). After respective time points, the protein adsorbed NP suspensions were centrifuged and the supernatant analysed for protein content using micro BCA protein assay kit. The amount of BSA adsorbed per milligram of NPs ($n=3$) was calculated using Eq. 1:

Table I Taguchi's Experimental Design L_{18} for Producing PGA-co-PDL Nanoparticles

Levels	Units	1	2	3
A—MW of Polymer	KDa	14.7	24.0	–
B—Org Sol (DCM)	ml	1	1.5	2
C—Aq. Vol (PVA)	ml	3	4	5
D—1st Aq. Conc (PVA)	%*w/v*	2.5	5	10
E—Sonication Time	min	1	2	5
F—Stirrer Speed	RPM	400	500	600
G—2nd Aq. Conc (PVA)	%*w/v*	0.5	0.75	1

$$\text{Adsorption}(\mu g \text{ per mg of NPs}) = \frac{(\text{Initial protein conc-Supernatant protein conc})}{\text{Amount of NPs}} \quad (1)$$

The particle size and PDI were then characterised as mentioned in "Nanoparticle Characterization" Section.

Nanoparticle Characterization

Particle size, poly dispersity index (PDI, a number between 0 and 1 describing the homogeneity of the sample) and zeta-potential were measured by laser diffraction using a laser particle size analyser (Zetasizer Nano ZS, Malvern Instruments Ltd, UK). For NPs suspension, an aliquot of 100 µl was diluted with 5 ml of deionized water and for NP suspensions with and without BSA adsorption, 2 mg of NPs were resuspended in 5 mL of deionized water, loaded into a cuvette and the measurements were recorded at 25°C ($n=3$).

Nanocomposite Microparticles

Spray-drying was employed to incorporate the NPs into nanocomposite microparticles (NCMPs) using L-leu as a carrier, and at nanoparticles-to-carrier ratio of 1:1.5 *w/w*. Blank NPs, BSA-loaded NPs or FITC-BSA-loaded NR NPs were dispersed in 20 ml water with L-leu dissolved and spray-dried using a Büchi B-290 mini spray-dryer (Büchi Labortechnik, Flawil, Switzerland) with a nozzle atomizer, and nozzle orifice diameter of 0.7 mm. The SD was performed at a feed rate 10%, an atomizing air flow of 400 L/h, aspirator capacity of 100% and an inlet temperature of 100°C (outlet temperature approximately 45–47°C). The dry particles (PGA-co-PDL/L-leu NCMPs) were separated from the air stream using a high-performance cyclone (Büchi Labortechnik), and the dry particles were collected and stored in desiccator until further use.

Nanocomposite Microparticles Characterization

Yield

The dry powder yield was determined as the difference in the weight of the sample vial before and after product collection. The weight difference was compared to the initial total dry mass and the yield in % (*w/w*) was calculated ($n=3$).

Particle Size and Morphology

To confirm the recovery of NPs from NCMPs with an appropriate size range for cellular uptake, particle size and PDI of NPs following re-dispersion of blank and loaded NCMPs in water were measured. The measurements were recorded as mentioned in "Nanoparticle Characterization" Section, where 5 mg of NCMPs were dispersed in 2 ml of deionized water then loaded into a cuvette and the measurements were recorded at 25°C ($n=3$).

Spray dried PGA-co-PDL/L-Leu NCMPs samples were mounted on aluminium stubs (pin stubs, 13 mm) layered with a sticky conductive carbon tab and coated with palladium (10–15 nm) using a sputter coater (EmiTech K 550X Gold Sputter Coater, 25 mA for 3 min). The particles were then visualized using scanning electron microscopy (FEI Quanta™ 200 ESEM, Holland).

Confocal Laser Scanning Microscopy

FITC-BSA-loaded NR NPs spray-dried into NCMPs were observed under confocal microscope to visualise the adsorption of BSA onto the NPs. Briefly, a Zeiss 510 Meta laser scanning microscope mounted on a Axiovert 200 M BP computer-controlled inverted microscope was used to obtain the confocal images. A few milligrams of spray-dried NCMPs were placed in a single well of 8-well chambered (Fisher Scientific, UK) and imaged by excitation at a wavelength of 488 nm (green channel for FITC-BSA), 543 nm (red channel for Nile Red NPs) and a Plan Neofluar 63×/0.30 numerical aperture (NA) objective lens. Image analysis was carried out using the Zeiss LSM software.

Protein Quantification by HPLC

An HPLC method was developed to quantify the amount of BSA present in NCMPs. The chromatographic conditions were as follows: HPLC system Agilent 1100 series (Santa Clara, CA, USA) equipped with a column (Aeris 3.6 µm C4 200A Wide Pore 4.6 mm i.d. × 150 mm length), security cartridge of the same material (Phenomenex, UK) and software for data processing; mobile phase was composed of (A) 0.1% TFA in water and (B) 0.1% TFA in acetonitrile with a gradient flow of A/B from 80:20 to 35:65 in 25 min, post-time 6 min; flow rate of 0.8 ml/min; injection volume of 100 µl; run temperature 40°C; UV detection at 214 nm and BSA retention time of 14.4 min. BSA calibration curve was prepared by accurate dilution of a previously prepared stock solution (1 mg/ml) in HPLC water and PBS (pH 7.4) to obtain the following concentrations: 0.5, 1, 2.5, 5, 10, 25, 50, 100 and 200 µg/ml of BSA ($n=9$, $R^2=0.999$). All solutions used in the process were filtered using 0.45 µm filters prior to use. Limit of Detection (LOD) in water—1.98 µg/ml, PBS—1.48 µg/ml and Limit of Quantification (LOQ) in water—3.24 µg/ml, PBS—3.20 µg/ml.

In Vitro Release Studies

BSA adsorbed PGA-co-PDL/L-leu NCMPs (20 mg) were transferred into eppendorfs and dispersed in 2 ml of PBS, pH 7.4. The samples were incubated at 37°C and left rotating for 48 h at 20 RPM on a HulaMixer™ Sample Mixer (Life Technologies, Invitrogen, UK). At pre-determined time intervals up to 48 h, the samples were centrifuged (accuSpin Micro 17, Fisher Scientific, UK) at 17,000 g for 30 min and 1 ml of the supernatant removed and replaced with fresh medium. The supernatant was analysed using the HPLC method as mentioned above. Each experiment was repeated in triplicate and the result was the mean value of three different samples ($n=3$). The percentage cumulative BSA released was calculated using Eq. 2:

$$\%\ \text{Cumulative BSA released} = \frac{\text{Cumulative BSA released}}{\text{BSA loaded}} \times 100 \qquad (2)$$

Sodium Dodecyl Sulfate-Polyacrylamide Gel Electrophoresis (SDS-PAGE)

The primary structure of BSA released from the NCMPs after SD was determined by SDS-PAGE. SDS-PAGE was performed on CVS10D omniPAGE vertical gel electrophoresis system (Geneflow Limited, UK) with 9% stacking gel prepared using ProtoGel stacking buffer (Geneflow Limited, UK) containing 0.4% of SDS. Protein molecular weight markers in the range 10–220 KDa (Geneflow Limited, UK) and BSA were used as control. The protein loading buffer blue (2X) (0.5 M Tris–HCl (pH 6.8), 4.4% (*w/v*) SDS, 20% (*v/v*) Glycerol, 2% (*v/v*) 2- mercaptoethanol and bromphenol blue in distilled/deionised water) was added to the samples in 1:1 (*v/v*) buffer-to-sample ratio. After loading the samples (25 µl sample per well), the gel was run for approximately 2.5 h at a voltage of 100 V with Tris-Glycine-SDS PAGE buffer (10X) (Geneflow Limited, UK) containing 0.25 M Tris base, 1.92 M glycine and 1% (*w/v*) SDS. The gel was stained with colloidal coomassie blue and then destained in distilled water overnight. An image of the gel was scanned on a gel scanner (GS-700 Imaging Densitometer, Bio-Rad) equipped with Quantity One software.

Circular Dichroism (CD)

The secondary structure of standard BSA (control), BSA supernatant (after 1 h adsorption followed by centrifugation) and BSA released from NPs after 48 h was determined by measuring circular dichroism spectra. All CD experiments were performed using a J-815 spectropolarimeter (Jasco, UK) at 20°C as previously described (31). Five scans per sample using a 10 mm path-length cell were performed over a wavelength range 260 to 180 nm at a data pitch of 0.5 nm, band width of 1 nm and a scan speed 50 nm min^{-1}. Far-UV CD spectra were collated for standard BSA, supernatant BSA in HPLC grade water, BSA released in PBS for 48 h. For all spectra, the baseline acquired in the absence of sample was subtracted (32). The secondary structure of the samples was estimated using the CDSSTR method (33) from the DichroWeb server (33–35).

Activity

The activity of BSA was investigated using 4-nitrophenyl acetate esterase substrate (NPA, Sigma Aldrich, UK) as described by Abbate *et al.* (36). Briefly, 1.2 ml of released BSA sample (50 µg/ml) in PBS was added to freshly prepared NPA solution (15 µl of a 5 mM solution in ACN) and incubated for 1 h using HulaMixer™ Sample Mixer. Thereafter, the solution was transferred to a plastic cuvette and absorbance measured at 405 nm. For positive control, standard BSA (50 µg/ml) was treated exactly the same as released sample whereas for negative control, PBS buffer alone was treated as sample. The relative residual esterolytic activity of the samples was calculated as the ratio of absorbance between the released BSA/standard BSA, with the esterolytic activity obtained for standard BSA considered to be 100%.

In Vitro Aerosolization Studies

The Next Generation Impactor (NGI) was employed to assess the aerosol performance of spray-dried NCMPs. The BSA adsorbed NCMPs were weighed (4 capsules each corresponding to 12.5 mg spray-dried, powder equivalent to 5 mg of NPs) and manually loaded into the hydroxypropyl methylcellulose, HPMC, capsule (size 3), and placed in a Cyclohaler® (Teva pharma). The samples were drawn through the induction port into the NGI using a pump (Copley Scientific, Nottingham, UK) operated at a flow rate of 60 L/min for 4 s. The plates were coated with 1% tween 80: acetone solution and samples collected using a known volume of distilled water, and left on a roller-shaker for 48 h for the BSA to be released from NCMPs. The samples were centrifuged using an ultracentrifuge (as mentioned in "Preparation of Nanoparticles" Section) and the supernatants analysed using HPLC method as mentioned above to determine the amount of BSA deposited. The Fine Particle Fraction (FPF, %) was determined as the fraction of emitted dose deposited in the NGI with $d_{ae} < 4.46$ µm, the mass median aerodynamic diameter (MMAD) was calculated from log-probability analysis, and the fine particle dose (FPD) was expressed as the mass of drug deposited in the NGI with $d_{ae} < 4.46$ µm ($n=3$).

Cell Viability Study

The *in vitro* cytotoxicity of the empty PGA-co-PDL/L-leu NCMPs was evaluated using the MTT assay. The adenocarcinomic human alveolar basal epithelial cell line, A549 (passage no. 32) or 16HBE14o- cells (passage no. 32) were seeded in 100 µl (2.5×10^5 cells/ml) of RPMI-1640 medium supplemented with 10% fetal calf serum/1% Antibiotic/Antimycotic solution (complete medium) in 96-well plates and placed in an incubator at 37°C for 24 h supplemented with 5% CO_2. Then, 100 µl of freshly prepared NCMP dispersions in complete medium were added to the wells to an appropriate concentration (0–2.5 mg/ml) ($n=3$), and 10% dimethyl sulfoxide (DMSO) as a positive control. The formulations were assayed for toxicity over 24 h of incubation, followed by the addition of 40 µl of a 5 mg/ml MTT solution in PBS to each well. After 2 h of incubation at 37°C, the culture medium was gently removed and replaced by 100 µl of dimethyl sulfoxide in order to dissolve the formazan crystals. The absorbance of the solubilised dye, which correlates with the number of living cells, was measured at 570 nm using a plate reader (Molecular Devices, SpectraMAX 190). The percentage of viable cells in each well was calculated as the absorbance ratio between nanoparticle-treated and untreated control cells.

Statistical Analysis

All statistical analysis was performed using Minitab® 16 Statistical Software. One-way analysis of variance (ANOVA) using Minitab® 16 Statistical Software with the Tukey's comparison was employed for comparing the formulations with each other. Statistically significant differences were assumed when $p<0.05$. All values are expressed as their mean±standard deviation.

RESULTS

Polymer Synthesis

The synthesized PGA-co-PDL co-polymer (monomer ratio, 1:1:1) was a white powder with a molecular weight of 14.7, 24.0 KDa for 6 h, 24 h as determined by the GPC. The integration pattern of the co-polymer was confirmed by ^{1}H-NMR spectra, (δH $CDCl_3$, 300 MHz): 1.34 (s, 22 H, H-g), 1.65 (m, 8 H, H-e, e′, h), 2.32 (m, 6 H, H-d, d′, i), 4.05 (q)-4.18 (m) (6 H, H-a, b, c, f), 5.2 (s, H, H-j).

Taguchi Design of Experiment (DoE)

The Taguchi design was applied in this study to identify the significant factors that would influence the size of PGA-co-PDL NPs. Considering seven factors (1 factor at 2 levels and 6 factors at 3 levels) to be investigated, non-usage of an experimental design would have resulted in $2*3^6=1{,}458$ individual experiments which would be an arduous task and inefficient. The Taguchi L_{18} orthogonal array design resulted in 18 runs to be performed to yield the optimum conditions for each factor in achieving the smallest PGA-co-PDL NP size. Table II illustrates the structure of the L_{18} orthogonal array, the corresponding results and S/N ratios.

The results obtained from 18 runs indicated particle sizes ranging from 138.7±6.4 nm (run 3) to 459.4±69.5 nm (run 11). Figure 1 shows the mean S/N graph of the particle size for each parameter level. The parameter with the largest range and corresponding rank (indicates the relative importance compared to other parameters) was considered as the critical factor affecting that particle size.

Analysis of the particle sizes of 18 runs using the Taguchi's 'smaller-is-better' criterion in Minitab® 16 Statistical Software, the optimum conditions inferred from the range, rank and the S/N response graph were A1B3C3D3E2F2G2. The optimum formulation made using these conditions yielded NPs with a size of 128.50±6.57 nm lower than the minimum size of 138.7±6.4 nm obtained using run 3, PDI of 0.07±0.03 and zeta-potential of −10.2±3.75 mV.

Protein Adsorption

Figure 2a shows the amount of BSA adsorbed per mg of NPs for different concentrations of BSA loaded. The average adsorption of BSA, µg per mg of NPs, increased significantly from 100: 4 (NP: BSA) loading concentration (4.75±0.39), 100: 10 (6.59±1.28) to 100: 20 (10.23±1.87) ($p<0.05$, ANOVA/Tukey's comparison).

Figure 2b shows the amount of BSA adsorbed in µg per mg of NPs at different time points for 100: 20 (NP: BSA) loading concentration. The average adsorption increased significantly from 30 min (1.84±0.82) to 1 h (10.23±1.87) ($p<0.05$, ANOVA/Tukey's comparison) with no significant difference beyond 1 h compared to that of 2 h (8.76±0.34) and 24 h (8.95±0.39) ($p>0.05$, ANOVA/Tukey's comparison) indicating maximum adsorption at 1 h.

Table III lists the particle size and PDI of PGA-co-PDL NPs with and without BSA adsorption. As seen, there is a significant increase ($p<0.05$, ANOVA/Tukey's comparison) in size which is attributed to the adsorption of BSA onto NPs as confirmed using confocal microscopy ("Confocal Laser Scanning Microscopy" Section).

Table II Structure of Taguchi's L_{18} Orthogonal Array, Corresponding Particle Size and S/N Ratios *(Mean ± SD, n = 6)*

Runs	Parameters							Particle Size (nm)	PDI	S/N Ratio (dB)
	A	B	C	D	E	F	G			
Run 1	1	1	1	1	1	1	1	315.5 ± 6.90	0.151 ± 0.05	−49.979
Run 2	1	1	2	2	2	2	2	186.5 ± 4.30	0.097 ± 0.03	−45.412
Run 3	1	1	3	3	3	3	3	138.7 ± 6.40	0.093 ± 0.01	−42.843
Run 4	1	2	1	1	2	2	3	210.1 ± 18.7	0.116 ± 0.04	−46.449
Run 5	1	2	2	2	3	3	1	208.7 ± 49.9	0.123 ± 0.06	−46.389
Run 6	1	2	3	3	1	1	2	182.0 ± 3.20	0.075 ± 0.04	−45.199
Run 7	1	3	1	2	1	3	2	192.9 ± 9.30	0.077 ± 0.04	−45.705
Run 8	1	3	2	3	2	1	3	149.3 ± 2.50	0.075 ± 0.01	−43.481
Run 9	1	3	3	1	3	2	1	192.9 ± 23.0	0.050 ± 0.03	−45.704
Run 10	2	1	1	3	3	2	2	269.1 ± 68.9	0.205 ± 0.04	−48.598
Run 11	2	1	2	1	1	3	3	459.4 ± 69.5	0.233 ± 0.02	−53.243
Run 12	2	1	3	2	2	1	1	242.5 ± 19.1	0.188 ± 0.06	−47.694
Run 13	2	2	1	2	3	1	3	253.2 ± 47.3	0.155 ± 0.10	−48.069
Run 14	2	2	2	3	1	2	1	217.3 ± 18.9	0.116 ± 0.01	−46.742
Run 15	2	2	3	1	2	3	2	240.5 ± 35.1	0.133 ± 0.05	−47.622
Run 16	2	3	1	3	2	3	1	169.3 ± 7.60	0.144 ± 0.04	−44.573
Run 17	2	3	2	1	3	1	2	235.9 ± 29.6	0.119 ± 0.08	−47.453
Run 18	2	3	3	2	1	2	3	221.7 ± 11.0	0.150 ± 0.04	−46.915

A—MW of Polymer, B—Org Sol (DCM), C—Aq. Vol (PVA), D—1st Aq. conc (PVA), E—Sonication time, F—Stirrer Speed and G—2nd Aq. conc (PVA)

Nanocomposite Microparticles Characterization

Yield

A reasonable yield of SD, 40.36 ± 1.80% for the empty PGA-co-PDL NCMPs and 42.35 ± 3.17% for the BSA adsorbed PGA-co-PDL/L-leu NCMPs was obtained.

Particle Size and Morphology

The size of NPs after recovery from spray-dried blank NCMPs in water was 210.03 ± 15.57 nm and PDI 0.355 ± 0.067 and for that of BSA loaded NCMPs was 282.46 ± 2.17 nm and PDI 0.36 ± 0.008, which is in the range of 200 to 500 nm for uptake by dendritic cells (DCs) (16–18).

The shape and surface texture of NCMPs were investigated using scanning electron microscopy (Fig. 3). Photomicrographs of NCMPs showed irregular and corrugated microparticles.

Confocal Laser Scanning Microscopy

CLSM was used to observe the interaction of BSA with NPs. The microscopic images in Fig. 4a (split view) and 4b

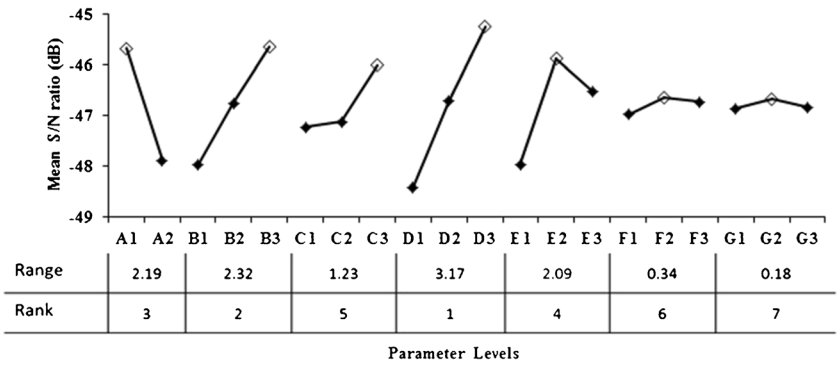

Fig. 1 Mean S/N graph for particle size response. Letters (*A–E*) denote the experimental parameters and numeric values denote the parameter levels (*white diamond* indicates maximum S/N value) *(Mean ± SD, n = 6)*; Note: *A*—MW of Polymer, *B*—Org Sol (DCM), *C*—Aq. Vol (PVA), *D*—1st Aq. conc (PVA), *E*—Sonication time, *F*—Stirrer Speed and *G*—2nd Aq. conc (PVA).

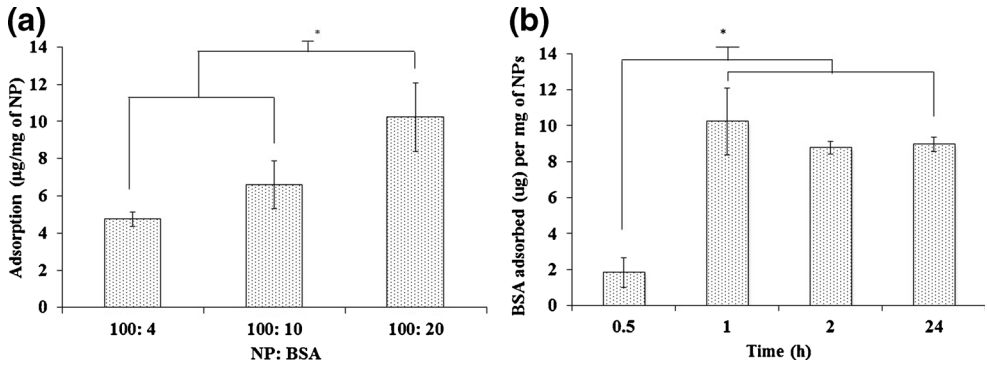

Fig. 2 Amount of BSA adsorbed per mg of NPs at different (**a**) BSA loading concentrations (NP: BSA) and (**b**) time points for 100: 20 (NP: BSA) BSA loading concentration, * is $p < 0.05$, ANOVA/Tukey's comparison *(Mean ± SD, n = 3)*.

(orthogonal view) shows the spray-dried NCMPs containing the fluorescent NPs (red, labelled using NR dye) adsorbed with FITC-BSA (green). The image shows that FITC-BSA was evidently only present where the NPs were present, indicating their association. Moreover, the increase in size observed after adsorption also confirms the adsorption of BSA onto PGA-co-PDL NPs (Table III).

In Vitro Release Studies

In vitro release studies were performed on NCMPs and reported as cumulative percentage BSA released over time (Fig. 5). An initial burst release of 30.15 ± 2.33% (BSA) was observed followed by continuous release up to 5 h, with BSA release of 86.07 ± 0.95%. After this time period, a slow continuous release of BSA was observed with release of 95.15 ± 1.08% over 48 h, indicating an excellent release profile for the PGA-co-PDL/L-leu NCMPs.

Protein Stability (SDS-PAGE and CD) and Activity

The primary structure of BSA released from the NCMPs was investigated using SDS-PAGE analysis. Figure 6 reveals identical bands for the standard BSA and desorbed BSA from NCMPs without any newly noticeable bands of high and low molecular BSA.

The secondary structure analysis was performed using CD spectral data. Figure 7a and b shows the structure of standard BSA, BSA supernatant and BSA released. In Fig 7a, the CD spectra show minima at 221–222 and 209–210 nm and maximum at about 195 nm for both samples, which is characteristic of α-helical structure. Further structural analysis showed that the predominant structure of the protein was helical displaying 51 and 62.5% helicity respectively (Table IV). Moreover, the experimental data obtained for the standard BSA are in good agreement with previous reports (37). Figure 7b shows that BSA released displayed double minima at 208 and 222 nm and further spectra analysis indicated this sample adopted a reduced level helical conformation (*circa* 36% helical) (Table IV). Comparing the CD results of BSA released with that of standard BSA, the content of α-helix decreases by 15%, the β-sheet content increases by 8.9%, the turns content increases by 1%, and the random coils' content increases by 3%, respectively.

The residual esterolytic activity of the released BSA sample was calculated to be 77.73 ± 3.19% relative to standard BSA.

In Vitro Aerosolization Studies

The deposition data obtained from spray-dried formulations displayed a FPD of 112.87 ± 33.64 µg, FPF of 76.95 ± 5.61% and MMAD of 1.21 ± 0.67 µm. This suggest that the BSA adsorbed PGA-co-PDL/L-leu NCMPs were capable of delivering efficient BSA to the lungs, and are expected to deposit the majority of the emitted dose to the bronchial-alveolar region of the lungs (3).

Table III Particle Size and PDI of PGA-co-PDL Nanoparticles Without and with BSA Adsorption

	NP suspension	Without BSA adsorption	With BSA adsorption
Particle Size (nm)	128.50 ± 6.57[a]	203.9 ± 2.55[b*]	299.03 ± 32.02[c*]
PDI	0.070 ± 0.030	0.205 ± 0.007	0.322 ± 0.060

[*] $p < 0.05$, ANOVA/Tukey's comparison

[a] NPs characterised immediately after preparation without centrifugation, [b] NPs characterised after centrifugation but without adsorption of BSA, [c] NPs characterised after centrifugation and BSA adsorption

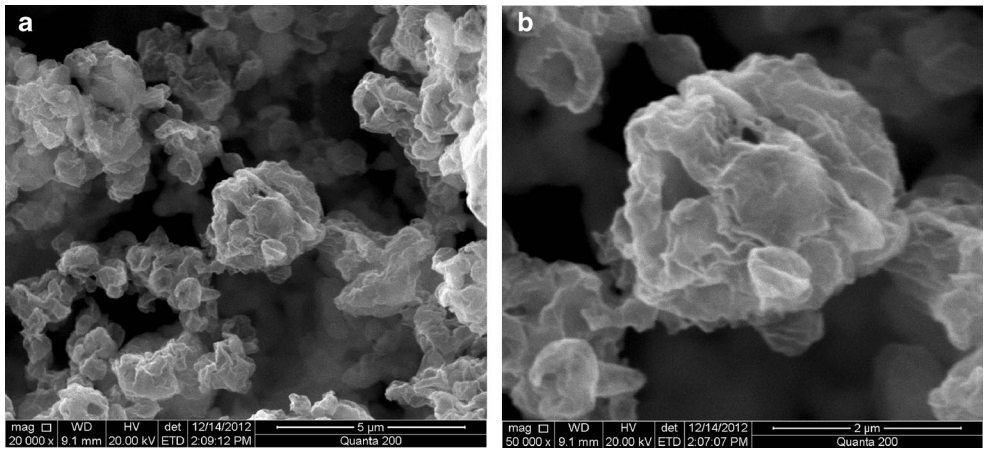

Fig. 3 SEM pictures of PGA-co-PDL/L-Leu Nanocomposite Microparticles (**a**) 5 μm and (**b**) 2 μm.

Cell Viability Study

The non-adsorbed PGA-co-PDL NCMPs appear to be well tolerated by both the cell lines, with a cell viability of 87.01 ± 14.11% (A549 cell line) and 106.04 ± 21.14% (16HBE14o- cell line) (Fig. 8) at 1.25 mg/ml concentration after 24 h exposure indicating a good toxicity profile without any significant difference in cell viability between particle loadings. This provides an indication about the feasibility of using PGA-co-PDL polymers as safe carriers for pulmonary drug delivery.

DISCUSSION

Nanoparticle Preparation and Characterization

The PGA-co-PDL NPs were prepared using a modified oil-in-water (o/w) single emulsion solvent evaporation method (29). The results of 18 runs, suggested by Taguchi's L_{18} orthogonal array, resulted in NPs of size < 150 nm. However, this increases to about 200–300 nm after centrifugation and BSA adsorption. This according to the literature suggests an effective uptake by DCs (15–17). The effects of each factor are discussed in detail below:

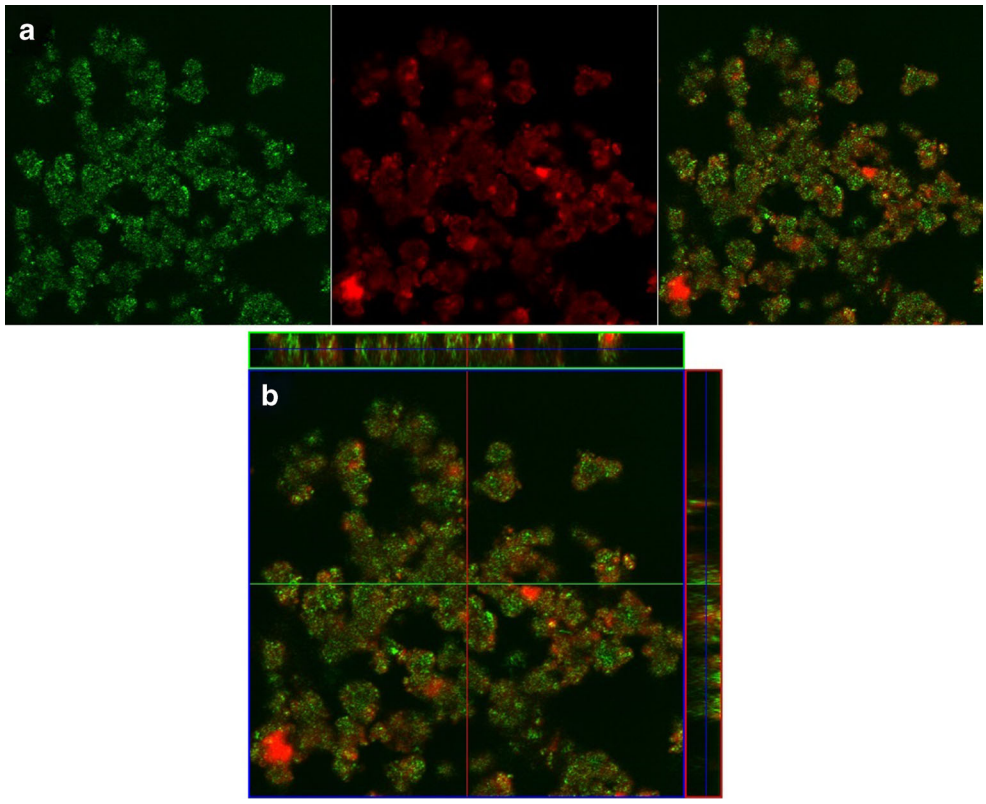

Fig. 4 Confocal microscopic image of spray-dried microparticles containing the fluorescent nanoparticles (*red*, labelled using nile red dye) adsorbed with FITC-BSA (*green*) (**a**) Split view and (**b**) Orthogonal view.

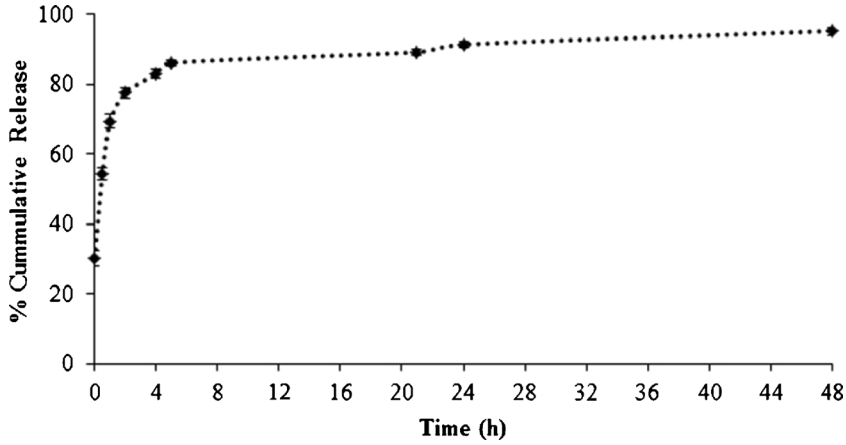

Fig. 5 *In vitro* release profiles for BSA adsorbed PGA-co-PDL/L-leu NCMPs in phosphate buffer saline, pH 7.4 *(Mean ± SD, n = 3)*.

Factor D, PVA concentration (range = 3.17, rank = 1), is the most important factor affecting the particle size. The S/N ratios at three levels indicated that particle size almost linearly decreased with increase in surfactant concentration from 2.5 to 10%*w*/*v* (S/N ratio, $r^2 = 0.997$). The particle size decreases because at lower concentrations there is inadequate amount of surfactant to cover all the surfaces of PGA-co-PDL NPs (38). The uncovered NPs then tend to aggregate until a point where there is adequate amount of surfactant to cover the total surface area of the aggregated NPs, and form a stable system leading to larger particles. However, with an increase in surfactant concentration it was possible to efficiently cover all the surfaces of NPs thereby stabilizing the system avoiding aggregation and resulting in smaller PGA-co-PDL NPs (38). This effect of decrease in particle size with an increase in surfactant concentration, PVA, was also observed by Mitra and Lin (39).

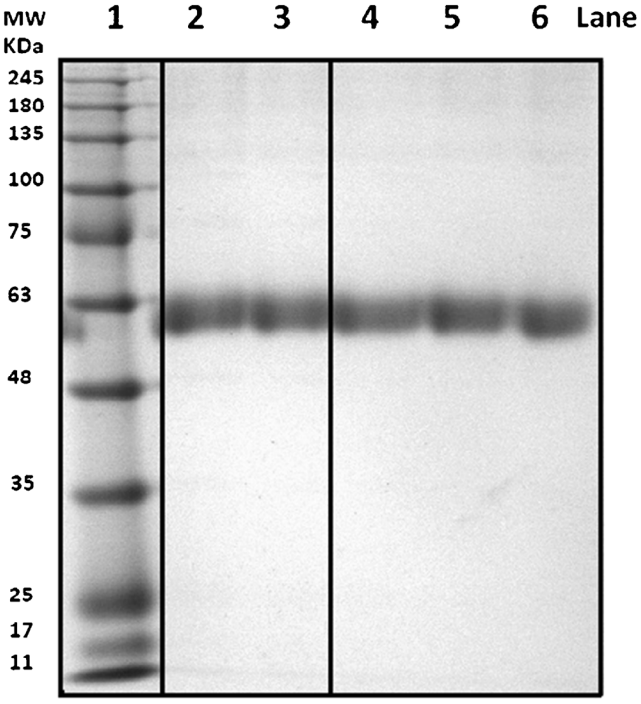

Fig. 6 SDS-PAGE of *Lane 1*: molecular weight standards, broad range (Bio-Rad Laboratories, Hercules CA, USA), *Lane 2*, *3*: BSA standards, *Lane 4*, *5*, *6*: Desorbed BSA from PGA-co-PDL/L-leu NCMPs after 24 h.

The S/N ratios of factor A, molecular weight of the polymer (range = 2.19, rank = 3), at two levels, suggested a directly proportional relationship with MW of polymer, *i.e.* the particle size decreases with a decrease in the MW of the polymer. This can also be evident from the lower particle size measurements observed using 14.7 KDa MW polymer (runs 1–9) relative to 24 KDa MW polymer (runs 10–18). As the MW of polymer increases, the viscosity of the polymeric solution also increases, thereby imposing difficulty in breaking them into smaller emulsion droplets when compared to lower MW polymer requiring lower efficiency to breakdown under similar conditions. This increase in size of the particles has also been observed by others and is reported to be associated with high MW polymers (5,40,41).

The S/N ratios of factor B, volume of organic solvent (DCM, range = 2.32, rank = 2), at three levels indicated that particle size almost linearly decreased with increase in volume from 1 to 2 ml (S/N ratio, $r^2 = 0.999$). This decrease in particle size is attributed to the decrease in viscosities of the polymer solution (keeping the amount and MW of polymer constant). This makes it easier to break into smaller emulsion droplets resulting in a decreased particle size as explained above. This effect could also be observed with factor C, volume of 1st aqueous phase (range = 1.23, rank = 5), where a decrease in volume increased the viscosity thereby resulting in an increase in particle size.

The S/N ratios for factor E, sonication time (range = 2.09, rank = 4), did not follow any particular trend; however, the 2nd level was found to be the optimum for achieving smaller particle size. The S/N ratios for parameters F, stirrer speed (the speed at which the magnetic bar was rotating for evaporation of DCM in the external phase) and G, 2nd PVA concentration have a low range of 0.34 and 0.18 respectively indicating that they have a minimal influence over the size of

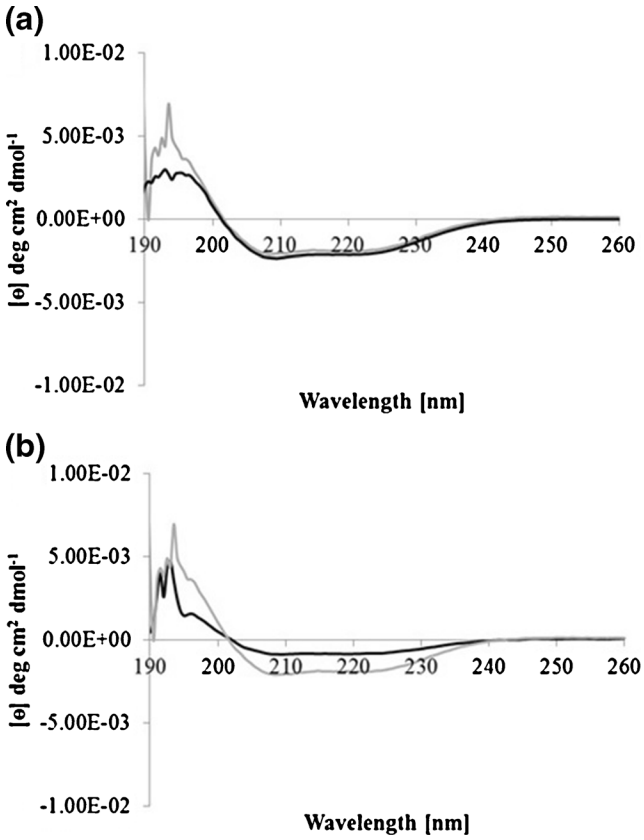

Fig. 7 CD spectra of (**a**) standard BSA (*grey*) and supernatant BSA (*black*) and (**b**) standard BSA (*grey*) and BSA released (*black*).

NPs produced. Therefore, the optimum conditions inferred result in NPs of size suitable for cellular uptake into DC as established in the literature (15–17,42,43).

The adsorption of BSA onto NPs is expected to be mainly driven by hydrophobic, electrostatic (ionic) interactions and hydrogen bonding (44). However, in this study as the NPs, evident from zeta-potential values, are negatively charged and BSA in water is also highly negatively charged (45) suggesting that the electrostatic interactions are minimal and that the adsorption process is dominated by the hydrophobic interactions and hydrogen bonding. The BSA adsorption onto NPs increased with an increase in NP: BSA ratio from 100: 4 to 100: 20, which was expected as the amount of BSA available for adsorption increased. Figure 2b suggests that the surface of NPs was saturated with BSA after 1 h suggesting maximum adsorption with 100: 20 (NP: BSA) BSA loading concentration.

Table IV The Percentages of the Secondary Structures of Standard, Supernatant and Released BSA Samples

Sample	Helix	Strand	Turns	Unordered
Standard BSA	51 ± 0.007	21.1 ± 0.07	6.0 ± 0.01	18 ± 0.007
Supernatant BSA	62.5 ± 0.035	22.0 ± 0.021	5.5 ± 0.05	9.5 ± 0.06
Released BSA	36.0 ± 0	30.0 ± 0	7.0 ± 0	21 ± 0.007

The content and level of secondary structure elements in the peptide was calculated from spectral data using the DichroWeb server software as described in "Materials and Methods" Section

Nanocomposite Microparticles Characterization

NCMPs were produced by SD using L-leu as a carrier and a dispersibility enhancer. The SEM pictures (Fig. 3) show irregular or wrinkled surface which is due to an excessive build-up of vapour pressure during water evaporation in the SD process and occurs with hydrophobic amino acids, such as L-Leu (8,46,47).

The release profile shows more than 90% of the BSA released within 48 h this is because of weaker hydrophobic interactions between BSA and NPs compared to the strong ionic interactions. Moreover, the identical bands observed for BSA standard and desorbed BSA from NCMPs suggests that protein has maintained its primary structure and was neither degraded nor affected by the adsorption and SD procedure.

The secondary structure of BSA in the formulation was analysed using CD spectroscopy, a valuable technique in analysing the protein structure (31). The BSA released samples confirms the presence of α-helix and β-sheets though decreased compared to standard BSA. However, in protein secondary structure, it is believed that the β-sheet structure is sometimes observed as a special α-helix only with two amino acid residues through stretching resulting from the breakage of hydrogen bond (37,48).

It is established that BSA possesses an enzyme-like activity with the ability to hydrolyse substrates such as p-nitophenyl esters (36,49,50). In this study, the released BSA sample retained approximately 77% of relative residual esterolytic activity compared to standard BSA. A reduction in BSA activity to 60% was also observed by Abbate *et al.* when released from biohybrid hydrogels (36). The adsorption and desorption process of BSA could have influenced the structure (evident from a decreased helicity determined by CD) and thus the activity. However, the

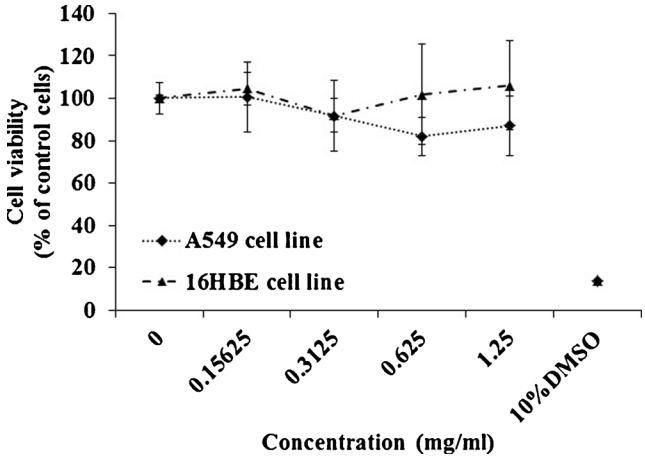

Fig. 8 A549 & 16HBE14o- cell viability measured by MTT assay after 24 h exposure to PGA-co-PDL NCMPs *(Mean ± SD, n = 3)*.

retention of 77% ester hydrolysis activity would encourage the exploration of the delivery system for further usage.

The FPF value suggests an excellent aerosolization performance and deep lung deposition profile. The surface activity of the relatively strong hydrophobic alkyl side chain of L-leu accumulating at the particle surface during SD reduces the surface free energy of the dry powder and cohesive inter-particulate interactions and this might be a plausible explanation for the enhanced dispersibility (8,23). In addition, the dispersibility enhancing property of L-leu resulting from its corrugated surface that reduces the contact points between particles leads to an improved aerosolization characteristic of powders (22,47,51). Similar reports have also demonstrated the enhanced aerosol performance with L-leu containing formulations (22,47,51,52). Moreover, the MMAD values show an efficient delivery of NCMPs containing BSA to the deep lungs mainly to the bronchial-alveolar region (3). A study by Todoroff *et al.* have shown that more intense specific immune responses could be achieved by targeting the antigen to the deep lungs than to the upper airways (53). Also, Menzel *et al.* have shown that upon inhalation of Pneumovax®, a pneumococcal polysaccharide vaccine, by healthy volunteers the vaccine deposited in the alveolar region displayed increased serum antibody levels compared to that deposited in the larger airways (54). Thus, this deposition to the deep lungs may generate stronger immune responses.

The NGI data suggests a deposition mainly in the bronchial-alveolar region of the lungs (3), thus the cell viability studies were performed on A549 cell line (adenocarcinomic human alveolar basal epithelial cells) and 16HBE14o- cell line (human bronchial epithelial cells). The results show that both the cell lines were tolerant to the NCMPs up to 1.25 mg/ml concentration encouraging further investigation in animals.

CONCLUSIONS

PGA-co-PDL NPs of appropriate size to target DCs were successfully produced using Taguchi L_{18} orthogonal array DoE. BSA adsorption onto NPs in the ratio of 100: 20 (NP: BSA) for 1 h at room temperature produced the maximum adsorption of BSA (10.23 ± 1.87 μg of protein per mg of NPs). The BSA adsorbed NPs were successfully spray-dried using L-leu into NCMPs producing a yield of $42.35 \pm 3.17\%$ and the NCMPs had irregular and corrugated morphology. The BSA released from the NCMPs was shown to be maintaining its structure under SDS-PAGE and CD analysis with 77% of relative residual esterolytic activity. Moreover, FPF of $76.49 \pm 6.26\%$ and MMAD of 1.21 ± 0.67 μm values indicate deep lung deposition with NCMPs showing a low toxicity profile. This study suggests that PGA-co-PDL NCMPs could be used as a novel carrier for pulmonary vaccine delivery.

ACKNOWLEDGMENTS AND DISCLOSURES

We would like to thank Dr Mark Murphy (Liverpool John Moores University, Liverpool, UK) for his help with confocal microscopy studies

REFERENCES

1. Leleux J, Roy K. Micro and nanoparticle-based delivery systems for vaccine immunotherapy: an immunological and materials perspective. Adv Healthc Mater. 2013;2:72–94.
2. Akagi T, Baba M, Akashi M. Biodegradable nanoparticles as vaccine adjuvants and delivery systems: regulation of immune responses by nanoparticle-based vaccine. Adv Polym Sci. 2012;247:31–64.
3. Kunda N, Somavarapu S, Gordon S, Hutcheon G, Saleem I. Nanocarriers targeting dendritic cells for pulmonary vaccine delivery. Pharm Res. 2013;30:325–41.
4. Amorij JP, Saluja V, Petersen AH, Hinrichs WLJ, Huckriede A, Frijlink HW. Pulmonary delivery of an inulin-stabilized influenza subunit vaccine prepared by spray-freeze drying induces systemic, mucosal humoral as well as cell-mediated immune responses in BALB/c mice. Vaccine. 2007;25:8707–17.
5. Thomas C, Rawat A, Hope-Weeks L, Ahsan F. Aerosolized PLA and PLGA nanoparticles enhance humoral, mucosal and cytokine responses to hepatitis B vaccine. Mol Pharm. 2010;8:405–15.
6. Panyam J, Labhasetwar V. Biodegradable nanoparticles for drug and gene delivery to cells and tissue. Adv Drug Deliv Rev. 2003;55:329–47.
7. Kallinteri P, Higgins S, Hutcheon GA, St. Pourçain CB, Garnett MC. Novel functionalized biodegradable polymers for nanoparticle drug delivery systems. Biomacromolecules. 2005;6:1885–94.
8. Tawfeek H, Khidr S, Samy E, Ahmed S, Murphy M, Mohammed A, *et al.* Poly(glycerol adipate-co-ω-pentadecalactone) spray-dried microparticles as sustained release carriers for pulmonary delivery. Pharm Res. 2011;28:2086–97.
9. Tawfeek HM, Evans AR, Iftikhar A, Mohammed AR, Shabir A, Somavarapu S, *et al.* Dry powder inhalation of macromolecules using novel PEG-co-polyester microparticle carriers. Int J Pharm. 2013;441:611–9.
10. Thompson CJ, Hansford D, Higgins S, Rostron C, Hutcheon GA, Munday DL. Evaluation of ibuprofen-loaded microspheres prepared from novel copolyesters. Int J Pharm. 2007;329:53–61.
11. Duncan G, Jess TJ, Mohamed F, Price NC, Kelly SM, Van der Walle CF. The influence of protein solubilisation, conformation and size on the burst release from poly(lactide-co-glycolide) microspheres. J Control Release. 2005;110:34–48.
12. Peek LJ, Middaugh CR, Berkland C. Nanotechnology in vaccine delivery. Adv Drug Deliv Rev. 2008;60:915–28.
13. Saleem IY, Vordermeier M, Barralet JE, Coombes AGA. Improving peptide-based assays to differentiate between vaccination and mycobacterium bovis infection in cattle using nanoparticle carriers for adsorbed antigens. J Control Release. 2005;102:551–61.
14. Sou T, Meeusen EN, De Veer M, Morton DA V, Kaminskas LM, McIntosh MP. New developments in dry powder pulmonary vaccine delivery. Trends Biotechnol. 2011;29:191–8.
15. Manolova V, Flace A, Bauer M, Schwarz K, Saudan P, Bachmann MF. Nanoparticles target distinct dendritic cell populations according to their size. Eur J Immunol. 2008;38:1404–13.
16. Kim H, Uto T, Akagi T, Baba M, Akashi M. Amphiphilic poly(amino acid) nanoparticles induce size-dependent dendritic cell maturation. Adv Funct Mater. 2010;20:3925–31.

17. Foged C, Brodin B, Frokjaer S, Sundblad A. Particle size and surface charge affect particle uptake by human dendritic cells in an in vitro model. Int J Pharm. 2005;298:315–22.
18. Bilati U, Allémann E, Doelker E. Poly(D,L-lactide-co-glycolide) protein-loaded nanoparticles prepared by the double emulsion method—processing and formulation issues for enhanced entrapment efficiency. J Microencapsul. 2005;22:205–14.
19. Li X, Deng X, Yuan M, Xiong C, Huang Z, Zhang Y, *et al.* Investigation on process parameters involved in preparation of poly-dl-lactide-poly(ethylene glycol) microspheres containing Leptospira Interrogans antigens. Int J Pharm. 1999;178:245–55.
20. Sanad R, Abdel Malak N, El-Bayoomy T, Badawi AA. Preparation and characterization of oxybenzone-loaded solid lipid nanoparticles (SLNs) with enhanced safety and sunscreening efficacy: SPF and UVA-PF. Drug Discov Ther. 2010;4:472–83.
21. Stevanovic M, Uskokovic D. Poly(lactide-co-glycolide)-based micro and nanoparticles for the controlled drug delivery of vitamins. Curr Nanosci. 2009;5:1–14.
22. Li H-Y, Seville PC, Williamson IJ, Birchall JC. The use of amino acids to enhance the aerosolization of spray-dried powders for pulmonary gene therapy. J Gene Med. 2005;7:343–53.
23. Seville PC, Learoyd TP, Li H-Y, Williamson IJ, Birchall JC. Amino acid-modified spray-dried powders with enhanced aerosolization properties for pulmonary drug delivery. Powder Technol. 2007;178:40–50.
24. Bosquillon C, Lombry C, Préat V, Vanbever R. Influence of formulation excipients and physical characteristics of inhalation dry powders on their aerosolization performance. J Control Release. 2001;70:329–39.
25. Al-fagih IM, Alanazi FK, Hutcheon GA, Saleem I. Recent advances using supercritical fluid techniques for pulmonary administration of macromolecules via dry powder formulations. Drug Deliv Lett. 2011;1:128–34.
26. Bailey MM, Berkland CJ. Nanoparticle formulations in pulmonary drug delivery. Med Res Rev. 2009;29:196–212.
27. Soppimath KS, Aminabhavi TM, Kulkarni AR, Rudzinski WE. Biodegradable polymeric nanoparticles as drug delivery devices. J Control Release. 2001;70:1–20.
28. Thompson CJ, Hansford D, Higgins S, Hutcheon GA, Rostron C, Munday DL. Enzymatic synthesis and evaluation of new novel ω-pentadecalactone polymers for the production of biodegradable microspheres. J Microencapsul. 2006;23:213–26.
29. Pinto Reis C, Neufeld RJ, Ribeiro AJ, Veiga F. Nanoencapsulation I. Methods for preparation of drug-loaded polymeric nanoparticles. Nanomedicine: NBM. 2006;2:8–21.
30. Do KK, Kim SH, Kim HT. Applying the Taguchi method to the optimization for the synthesis of TiO2 nanoparticles by hydrolysis of TEOT in micelles. Colloids Surf A Physicochem Eng Asp. 2005;254:99–105.
31. Greenfield NJ. Using circular dichroism spectra to estimate protein secondary structure. Nat Protoc. 2007;1:2876–90.
32. Henzler Wildman KA, Lee D-K, Ramamoorthy A. Mechanism of lipid bilayer disruption by the human antimicrobial peptide, LL-37†. Biochemistry. 2003;42:6545–58.
33. Whitmore L, Woollett B, Miles AJ, Janes RW, Wallace BA. The protein circular dichroism data bank, a web-based site for access to circular dichroism spectroscopic data. Structure (Lond Engl 1993). 2010;18:1267–9.
34. Whitmore L, Wallace BA. Protein secondary structure analyses from circular dichroism spectroscopy: methods and reference databases. Biopolymers. 2008;89:392–400.
35. Whitmore L, Wallace BA. DICHROWEB, an online server for protein secondary structure analyses from circular dichroism spectroscopic data. Nucleic Acids Res. 2004;32:W668–73.
36. Abbate V, Kong X, Bansal SS. Photocrosslinked bovine serum albumin hydrogels with partial retention of esterase activity. Enzym Microb Technol. 2012;50:130–6.
37. Zhang J, Ma X, Guo Y, Yang L, Shen Q, Wang H, *et al.* Size-controllable preparation of bovine serum albumin-conjugated PbS nanoparticles. Mater Chem Phys. 2010;119:112–7.
38. Douglas SJ, Illum L, Davis SS. Particle size and size distribution of poly(butyl 2-cyanoacrylate) nanoparticles. II. Influence of stabilizers. J Colloid Interface Sci. 1985;103:154–63.
39. Mitra A, Lin S. Effect of surfactant on fabrication and characterization of paclitaxel-loaded polybutylcyanoacrylate nanoparticulate delivery systems. J Pharm Pharmacol. 2003;55:895–902.
40. Jalil R, Nixon JR. Microencapsulation using poly (L-lactic acid) III: effect of polymer molecular weight on the microcapsule properties. J Microencapsul. 1990;7:41–52.
41. Mittal G, Sahana DK, Bhardwaj V, Ravi Kumar MN V. Estradiol loaded PLGA nanoparticles for oral administration: effect of polymer molecular weight and copolymer composition on release behavior in vitro and in vivo. J Control Release. 2007;119:77–85.
42. Joshi V, Geary S, Salem A. Biodegradable particles as vaccine delivery systems: size matters. AAPS J. 2013;15:85–94.
43. Sloat BR, Sandoval MA, Hau AM, He Y, Cui Z. Strong antibody responses induced by protein antigens conjugated onto the surface of lecithin-based nanoparticles. J Control Release. 2010;141:93–100.
44. Yoon J-Y, Kim J-H, Kim W-S. The relationship of interaction forces in the protein adsorption onto polymeric microspheres. Colloids Surf A Physicochem Eng Asp. 1999;153:413–9.
45. Regev O, Khalfin R, Zussman E, Cohen Y. About the albumin structure in solution and related electro-spinnability issues. Int J Biol Macromol. 2010;47:261–5.
46. Li H-Y, Neill H, Innocent R, Seville P, Williamson I, Birchall JC. Enhanced dispersibility and deposition of spray-dried powders for pulmonary gene therapy. J Drug Target. 2003;11:425–32.
47. Sou T, Kaminskas LM, Nguyen T-H, Carlberg R, McIntosh MP, Morton DA V. The effect of amino acid excipients on morphology and solid-state properties of multi-component spray-dried formulations for pulmonary delivery of biomacromolecules. Eur J Pharm Biopharm. 2013;83:234–43.
48. Yang L, Guo Y, Ma X, Hu Z, Zhu S, Zhang X, *et al.* Cooperativity between pepsin and crystallization of calcium carbonate in distilled water. J Inorg Biochem. 2003;93:197–203.
49. Tildon JT, Ogilvie JW. The esterase activity of bovine mercaptalbumin. The reaction of the protein with p-nitrophenyl acetate. J Biol Chem. 1972;247:1265–71.
50. Córdova J, Ryan JD, Boonyaratanakornkit BB, Clark DS. Esterase activity of bovine serum albumin up to 160°C: a new benchmark for biocatalysis. Enzym Microb Technol. 2008;42:278–83.
51. Feng AL, Boraey MA, Gwin MA, Finlay PR, Kuehl PJ, Vehring R. Mechanistic models facilitate efficient development of leucine containing microparticles for pulmonary drug delivery. Int J Pharm. 2011;409:156–63.
52. Najafabadi AR, Gilani K, Barghi M, Rafiee-Tehrani M. The effect of vehicle on physical properties and aerosolization behaviour of disodium cromoglycate microparticles spray dried alone or with l-leucine. Int J Pharm. 2004;285:97–108.
53. Todoroff J, Ucakar B, Inglese M, Vandermarliere S, Fillee C, Renauld J-C, *et al.* Targeting the deep lungs, poloxamer 407 and a CpG oligonucleotide optimize immune responses to mycobacterium tuberculosis antigen 85A following pulmonary delivery. Eur J Pharm Biopharm. 2013;84(1):40–8.
54. Menzel M, Muellinger B, Weber N, Haeussinger K, Ziegler-Heitbrock L. Inhalative vaccination with pneumococcal polysaccharide in healthy volunteers. Vaccine. 2005;23:5113–9.